Volume 3 September 2013 ISSN 1883-3608

EANET Science Bulletin

Bach Ma National Park, Vietnam

Acid Deposition Monitoring Network in East Asia (EANET)

http://www.eanet.asia

Acid Deposition Monitoring Network in East Asia

(EANET)

Objectives

- *Create a common understanding of the state of acid deposition in East Asia.*

- *Provide useful inputs for decision making at local, national and regional levels with the aim of preventing or reducing adverse impacts on the environment caused by acid deposition.*

- *Contribute to cooperation on issues related to acid deposition among the participating countries.*

EANET Science Bulletin

Volume 3

The EANET Science Bulletin is published by the Network Center for EANET once every two years. The Network Center is located at the Asia Center for Air Pollution Research (ACAP) in Niigata, Japan.

Endorsed at the Thirteenth Session of the Scientific Advisory Committee of EANET

Preface

The EANET Science Bulletin Volume 3

This is the EANET Science Bulletin Volume 3 of the Acid Deposition Monitoring Network in East Asia. The contents are comprised of the report of the EANET research fellowship program (2010-2012), joints projects of EANET with participating countries and scientific and technological research papers from participating countries. This science bulletin is followed the Medium Term Plan (MTP) for the EANET (2011-2015) that adopted by the Twelfth Session of the Intergovernmental Meeting (IG12) in 2010. The EANET science bulletin is the activity No. 15 of the MTP which is the biennial publication in order to promote of the research studies, particularly, on the applicability of various methodologies for measurement of the air concentration in East Asia. The Fourteenth Session of the Intergovernmental Meeting (IG14) in 2012 also approved the budget for printing in according to the work program and budget plan of the EANET in 2013. Therefore, these research activities will be the great importance to achieve a better understanding of the atmospheric pollutants and impacts on the environment of the East Asian region which is the fastest economic growth in the world. Research results are very important and necessary for improving the situation of the scientific and technical matters of our EANET community. Therefore, we would like to thanks all authors that contributed and supported the EANET research papers on this EANET science bulletin volume 3. Without all of you, it wouldn't be possible to obtain these such valuable results. Hence, we would like to thank all of you on this occasion.

Dr. Hajime Akimoto

Director General

Asia Center for Air Pollution (ACAP)

Network Center for the EANET

September 2013

Contents

Message from the Editor

This is a message to all participating countries of the EANET in order to convince all concerns to contribute the research papers for the EANET Science Bulletin. Therefore, this article raises some important current issues of the EANET that aims at achieving at present and in the future for our participating countries of the EANET to consider implementing them.

Recent Information of the EANET Network Center from the Editor

Jesada Luangjame

Deputy Director General of ACAP, in charge of the EANET Network Center
E-mail: jesada@acap.asia

1. Preamble

The EANET Science Bulletin is actually the biennial issue of the Acid Deposition Monitoring Network in East Asia (EANET). The first publication volume 1 was issued in 2008. The aims of the bulletin are to serve the resulted researches from the researchers of the EANET participating countries that the EANET implemented the fellowship program since 2005. The EANET Science Bulletin volume 2 was issued in early 2011 which was approved by the Tenth Session of Scientific Advisory Committee (SAC10) in 2010 as schedule as biennial bulletin. However, the bulletin volume 3 should be issued in 2012 which is followed the Medium Term Plan (MTP) for the EANET (2011-2015) that adopted by the Twelfth Session of the Intergovernmental Meeting (IG12) in 2010. But, unfortunately, research papers were not enough to publish in 2012, therefore, the Network Center called for papers from the National Focal Points (NFPs) and SAC to contribute more papers, hence, the EANET Science Bulletin Volume 3 has to postpone to issue at the end of the year 2013. The editor is very grateful to all of the NFPs and authors who contributed the research papers for the bulletin. I would also like to request all of the NFPs and SAC to provide for the next volume of the science bulletin in the next two years (2015) as well. All of you may be aware that the sciences will be led for the policymakers for making decision on environmental issues. Without science results would be unreliable measures for policymakers and having uncertainty to solve the environmental problems and human health which are very important issues for the civilized world. This message, therefore, would convince all of you to pay attention to contribute the research results for the next EANET Science Bulletin.

For this article, I would like to raise some important current issues of the EANET that aims at achieving at present and in the future for our participating countries of the EANET to consider as below.

2. Strengthening cooperation for the EANET participating countries

The EANET had already 12 out of 13 participating countries signed the Instrument for strengthening the EANET cooperation in 2012. We hoped that it will be completed 13 countries in the near future as well as two more from the Southeast Asian countries; Brunei Darussalam and Singapore come to join as the EANET

members. As the Instrument, it was already implemented since January 1, 2012. It was emphasized on the importance of appropriate financial arrangement for the sound operation of the EANET with a view of sustaining the development of the EANET, strengthening the financial mechanism of the EANET and providing a sound basis for financial contribution to the EANET and enhancing capacity building of acid deposition monitoring for all the participating countries of the EANET, the efficiency of the EANET activities has been looking forwards to achieving it.

3. Expansion of the scope of the EANET

The expansion of the scope of the EANET was appeared in the Item 2 "Objectives and Scope" of the Instrument which stated that "the scope of this Instrument may be extended, as decided by the Intergovernmental Meeting (IG)". In line with this provision, the Terms of Reference (TOR) of the Working Group on Future Development of the EANET (WGFD) in 2011-2012 decided by the IG12 included the "Discussion on the issues of expansion of the scope of the EANET", and the Medium Term Plan for the EANET (2011-2015) also included this issue as one of the agenda to be discussed during the five-year strategy plan.

The major point of discussion at the WGFD11 in August 2012 was suggested that the Secretariat and the NC should provide further information in order that the participating countries could share the common understanding of the current scope of the expansion of the EANET.

In order to discuss the future development of the EANET, it is important to recognize present actual situation surrounding the EANET and to have common understanding among the participating countries. Air pollution problems have been highlighted as either a domestic, regional, or hemispherical problems. Ozone and $PM_{2.5}$ are now emphasized as high priority air pollution species in some countries. Intercontinental transport of ozone and aerosols has been recognized/identified as priority species such as the point of hemispherical air pollution in the Task Force on Hemispheric Transport of Air Pollution (TF HTAP) under the Convention on Long-range Transboundary Air Pollution (CLRTAP).

More recently, integrated approach for mitigating air pollution and climate change has attracted much attention internationally, and the United Nations Environment Programme (UNEP) has published a couple of reports in 2011 on the short-lived climate forcers (SLCF) in supporting co-benefits/co-control approach. Some governments of the EANET participating countries have expressed their interest in joining international initiatives promoting such co-benefits/co-control approach.

The participating countries may wish to share the understanding on the above situation. Discussions should be started for the future development of the EANET although in principle, the expansion of the EANET scope should be based on a step-by-step approach on which the development of the EANET has been based.

Concerning the discussion of expansion of the scope of the EANET, it is worthwhile that all the participating countries have common recognition of the present scope of the EANET, ozone and PM_{10}/$PM_{2.5}$, impacts on human health, and modeling and emission inventories are briefly reviewed as based on the past formal documents of the EANET. It is recommended to confirm that human health impacts of monitoring species are included within the present scope of the EANET. Modeling and emission inventories are also included as research activities as well as public awareness activities.

Enhancement of policy relevance of the activities including policy advice based on sound scientific

assessment is encouraged in accordance with the recently recognized importance of so called "science and policy interface". In this connection, new expertise associated with mitigation measures may need to be addressed under the EANET, which will require the expansion of the scope as well as institutional reform in some countries.

Moreover, to facilitate our discussion on research activities of the EANET and to seek for new direction of the EANET, it has been decided by the SAC11 with the guidance of the IG13 to review the status of air pollution in East Asia. The review will be done by a "Reviewing Committee on the Status of Air Pollution in East Asia (Reviewing Committee)" under the Task Force on Research Coordination (TFRC).

4. Co-benefits/co-control

As the expansion of the scope of the EANET, co-benefits and co-control are to be considered. Therefore, it has to explore the following approaches; definition, scope and trends of co-benefits.

4.1 Defining Co-Benefits

From the Asian context, the concept of a "co-benefits strategy" or a "co-control measure" is that a single activity or policy can generate multiple benefits across different sectors or fields of study. The co-benefits approach emerges as an important tool for bridging various environment and development issues.

From the Intergovernmental Panel on Climate Change (IPCC), co-benefits are the benefits from policy options implemented for various reasons at the same time, term of the co-benefits reflects that most policies designed to address Greenhouse Gas (GHG) mitigation also have other, often at least equally important, rationales involved at the inception of these policies, e.g., related to objectives of development, sustainability and equity.

The United States Environmental Protection Agency (US EPA) Integrated Environmental Strategies (IES) Program offers a less restrictive definition of "co-benefits" by not distinguishing between impacts that are explicitly taken into account and those that are not. The term co-benefits is used to refer to two or more benefits that are derived together from a single measure or set of measures. Co-benefits are generally 1) the health and economic benefits that result from reducing local air pollution, and 2) the GHG reductions associated with reducing ambient emissions.

Institute of Global Environmental Strategies (IGES) promotes a simple definition of co-benefits as potential benefits of climate change mitigation actions in other field or areas not covered by climate change or United Nations Framework Convention on Climate Change (UNFCCC).

The Clean Air Initiative for Asian Cities (CAI-Asia) interpretation of co-benefits is a hybrid that regards "co-benefits" as those derived from the intentional decision to address air pollution, energy demand, and climate change in an integrated manner, but also considers the other unspecified benefits that may arise such as improved transport and urban planning, reduced health and agricultural impacts, improved economy or reduced overall policy implementation cost.

Outside of Asia, the European Environment Agency (EEA) follows the IPCC definition, highlighting the efficient use of resources of co-control strategies particularly for air pollution and climate change. The United Kingdom (UK) Department for the Environment, Food and Rural Affairs (DEFRA) in a major study on air quality and climate change also focus on "win-win" measures across different time scales.

Currently, urbanization is increasing in Asia. There are one billion people living in Asia's urban areas and this number is growing at an average of 4% every year. Gross domestic product (GDP) growth leads to even stronger growth in energy consumption. Together, China and India will account for 80% growth in world coal demand from 2004-2030 as compared to the 10% for the Organisation for Economic Co-operation and Development (OECD) countries and 10% for the rest of the world. Although the initiatives to use cleaner energy sources and tap the renewable energy potential are growing in Asia, these are still insufficient to substantially lower the carbon footprint of the region. Rising incomes are accompanied by the increased demand for mobility and vehicle ownership. Three of the top ten countries with the highest future private-vehicle demand, namely China, India and Indonesia, are in Asia. Therefore, co-benefits/co-control strategies are very important to monitor.

Of the many environmental challenges besetting the region, the link between urban air quality and climate change emerges as one of the most researched. However, despite evidence that regional climate in Asia may already be changing, climate change is still of lesser priority for most developing countries in Asia compared to issues like poverty, lack of livelihood opportunities, water and food security, and natural disasters. Thus, the co-benefits approach to climate change and development is crucial for optimizing scarce resources, harmonizing policies across different sectors and among different levels of governance, and ensuring a more holistic approach to problem-solving.

4.2 Scope of Co-benefits

In terms of applicable scope, the basic premise of the co-benefits paradigm makes it flexible and adaptable to different fields. Dominant fields or issues being linked to GHG reduction/climate change mitigation are air quality, health, energy, and transport. Currently, most policymakers in Asia seem more focused on ambient air pollution and its associated health impacts as areas of co-benefits analysis. Although comparatively little focus is given to climate change as an immediate development issue in Asia, experts expect a likely expansion of the co-benefits approach to other areas particularly energy due to its significance in the policy agenda of most countries. Emerging linkages include economics (industry competitiveness, income distribution), social issues (e.g. enhanced stakeholder participation), agriculture and forestry, biodiversity, and land use/urban planning. Actions in these sectors outside of energy and transport appear are taken in lesser extent owing perhaps to the immaturity of quantifying methodologies. The co-benefits paradigm may be applied to adaptation as well as to climate change mitigation. For adaptation, it would be referred to the co-benefits with disaster risk management as well as with sustainable development in general since vulnerability to climate change is conditioned by very social, economic, political and environmental factors that determine development.

4.3 Co-benefits Trends

There were many research projects and studies that linked to air quality and climate change which related to contribute to the co-benefits/co-control since 2004 that could be improved for understanding of the trends. Therefore, the co-benefits approach is increasingly being adopted in the developed world. Related research projects in Asia show that projects tackle both climate change mitigation and air quality management as resembling as co-benefits approach in general. However, in the Asian region in past, it would suggest that the concept is still developing as a paradigm for problem solving and policy formulation. The review is based on web-based research as well on a questionnaire survey. The general trends of co-benefits initiatives in this region as grouped according to type of activity or output on scientific research, methods and tools. The increasing in the available scientific research is recognized on establishing linkages between climate change mitigation and other fields. In the field of urban air quality management, a sector emerging in this study's literature as most researched, recent studies have shown the need for mitigation to look beyond the six GHGs (e.g., CO_2, CH_4, SF_6, N_2O, PFCs, HFCs) of the Kyoto Protocol because other pollutants particularly aerosols and particulate matter, are found to affect climate as well. Recent research also lends credence to the proposition that climate change also affects air quality. In the transport and fuels sectors, studies reflect that the issues of land use and urban planning are also inextricably linked to GHG emissions in that these factors determine the modes of transportation. In addition, while the concept of co-benefits has yet to fully make its way into current cost-benefits analysis framework, empirical studies are increasing in such sectors as energy, agriculture, and economics.

5. Short-Lived Climate Pollutants (SLCPs)

The term of short-lived climate pollutants (SLCPs) is used recently. Before that it was used short-lived climate forcers (SLCFs) which pollutants have positive radioactive forcing to enhance global warming and climate change. However, SLCP is replaced SLCF which is more easily to the public thought for the climate pollutants. SLCPs are agents that have relatively short lifetime in the atmosphere, a few days to a few decades and a warming influence on climate. The main SLCPs are black carbon (BC), methane (CH_4) and tropospheric ozone (O_3), which are the most important contributors to the human enhancement of the global greenhouse effect after CO_2. These SLCPs are also dangerous air pollutants, with various detrimental impacts on human health, agriculture and ecosystems. Other SLCPs include some hydrofluorocarbons (HFCs). While HFCs are currently present in small quantity in the atmosphere their contribution to climate forcing is projected to climb to as much as 19% of global CO_2 emissions by 2050.

SLCPs are impacting public health, food, water and economic security of large populations, both directly through their impacts on human health, agriculture and ecosystems, and indirectly through their effects on climate. SLCPs have become a major development issue that calls for quick and significant worldwide action.

Many regions are already suffering from accelerated climate change. Over the world glaciers are melting, weather patterns changing and sea levels rising while the threat of overshooting the 2ºC "safety" target

is looming. Due to their short lifetimes, compared to CO_2 which remains in the atmosphere for approximately a century, actions to reduce emissions of the SLCPs will quickly lower their atmospheric concentrations, yielding a relatively rapid climate response. Fast action to reduce SLCPs, especially CH_4 and BC, has the potential to slow down the warming expected by 2050 by as much as 0.5ºC. However, if mitigating SLCPs will help to reduce the rate of global warming and avoid exceeding the 2°C target over the near term, long-term climate protection requires deep and rapid cut in carbon dioxide emissions. At the same time, by 2030, such action can prevent millions of premature deaths, while also avoiding the annual loss of more than 30 million tons of crops. Moreover, many of these benefits can be achieved at low cost and with significant energy savings.

In USA, to response on SLCPs, Secretary of State Hillary Rodham Clinton announced the Climate and Clean Air Coalition to Reduce SLCPs, a new global initiative to seize the opportunity of realizing concrete benefits on climate, health, food and energy resulting from reducing SLCPs. The coalition will focus efforts on reducing BC, HFCs, and CH_4. The founding coalition partners are Bangladesh, Canada, Ghana, Mexico, Sweden, and the United States, together with the UN Environment Programme. The new coalition is the first effort to treat these pollutants together, as a collective challenge. The coalition will reduce SLCPs by driving the development of national action plans and the adoption of policy priorities; building capacity among developing countries; mobilizing public and private funds for action; raising awareness globally; fostering regional and international cooperation, and; improving scientific understanding of the pollutant impacts and mitigation. The United States is already actively engaged in efforts to reduce these pollutants on the national and international levels. The U.S. Environment Protection Agency addresses these pollutants through robust programs that protect public health and the environment.

The pollutants targeted by this initiative remain in the atmosphere for only a few days to a few years after they are emitted. This is very short when compared to CO_2, which remains in the atmosphere for approximately a century. This “shorter” atmospheric lifetime means that actions to reduce emissions will quickly lower atmospheric concentrations of these pollutants, yielding a relatively rapid climate response. Of the pollutants that will be targeted by this initiative, CH_4 and BC stand out for their significant contribution to climate change, while HFCs are a rapidly increasing climate threat.

5.1 Methane (CH_4)

Methane (CH_4) is a greenhouse gas that is more than 20 times more potent than CO_2, and has an atmospheric lifetime of about 12 years. It is produced through natural processes (i.e. the decomposition of plant and animal waste), but is also emitted from many man-made sources, including coal mines, natural gas and oil systems, and landfills. In addition to the climate benefits, reducing CH_4 emissions has other important public health and agricultural benefits. Reducing CH_4 emissions can avoid the health effects and premature deaths associated with unhealthy O_3 levels. CH_4 also is the primary component of natural gas. Thus, capturing and utilizing methane as clean-burning natural gas can promote sustainable development and energy security.

5.2 Tropospheric ozone (O_3) and methane (CH_4)

O_3 is a reactive gas which, when in the stratosphere, absorbs dangerous ultraviolet radiation; however, lower atmosphere (tropospheric) O_3 is a major air and climate pollutant which is harmful to human health and

crop production. Its impacts on plant include not only lower crop yields but also a reduced ability to absorb CO_2. Tropospheric O_3 is not emitted directly but instead forms from reactions between precursor gases, both human-produced and natural. These precursor gases include CO_2, oxides of nitrogen (NOx), and volatile organic compounds (VOCs) which include CH_4. Globally increased CH_4 emissions are responsible for approximately two-thirds of the rise in tropospheric O_3. Reducing emissions of CH_4 will lead to significant reductions in tropospheric O_3 and its damaging effects. CH_4 is a powerful greenhouse gases with a 100-year global warming potential 21 times that of CO_2 and an atmospheric lifetime of approximately 12 years. The main sources of anthropogenic CH_4 emissions are oil and gas systems, enteric fermentation, landfills, manure management, wastewater treatment, rice cultivation, and emissions from coal mines. According to a Primer on SLCPs, recent UNEP assessment, anthropogenic CH_4 emissions are expected to grow 25% over 2005 levels by 2030, driven by increased production from coal mining, oil and gas production, and growth in agricultural and municipal waste emissions.

5.3 Black Carbon (BC)

Black carbon (BC) is a potent climate-forcing aerosol that remains in the atmosphere for only a few days or weeks. BC is a component of soot and is a product of the incomplete combustion of fossil fuels, biofuels, and biomass. BC contributes to climate change in several ways. It warms the atmosphere directly by absorbing solar radiation and emitting it as heat. It contributes to melting by darkening the surfaces of ice and snow when it is deposited on them. It can also affect the microphysical properties of clouds in a manner than can perturb precipitation patterns. Estimates of BC's radiative forcing indicate that it may be the second or third leading cause of global warming after CO_2 and CH_4.

The main sources of BC are open burning of biomass, diesel engines, and the residential burning of solid fuels such as coal, wood, dung, and agricultural residues. In 2000 global emissions of BC were estimated at approximately 8.4 million tons. Thanks to modern pollution controls and fuel switching, BC emissions in North America and Europe were significantly curbed in the early 1900s. However, mobile sources, particularly diesel vehicles, continue to be a major source category for these regions. BC sources in developing countries are significantly different from those in North America and Europe. In developing countries, a much larger proportion of BC emissions come from residential heating and cooking, and industry. According to UNEP, global emissions of BC are expected to remain relatively stable through 2030, with continuing reductions in North America and Europe largely offset by continued growth in other parts of the world.

Of the three pollutant types, BC remains in the atmosphere for the shortest amount of time, depositing on the ground only days to weeks after it is emitted. Reducing BC will have an important impact on air quality and public health. The World Health Organization (WHO) estimates that currently more than 3 million premature deaths each year can be attributed to the effects of urban outdoor air pollution and indoor air pollution. Fine particles, which include BC, contribute significantly to these adverse impacts.

5.4 Hydrofluorocarbons (HFCs)

HFCs are man-made greenhouse gases (factory-made chemicals) used in air conditioning, refrigeration, solvents, foam blowing agents, and aerosols. They have a warming effect hundreds to thousands of times more

powerful than CO_2. The average lifetime of the mix of HFCs, weighted by usage, is 15 years. HFCs are the fastest growing greenhouse gases in many countries, including the U.S., where emissions grew nearly 9% between 2009 and 2010 compared to 3.6% for CO_2. Globally, HFC emissions are growing 10 to 15% per year and are expected to double by 2020. Without fast action to limit their growth, by 2050 the annual climate forcing of HFCs could equal nearly 20% of the forcing from CO_2 emissions in a business as usual (BAU) scenario, and up to 40% of the forcing from CO_2 emissions under a scenario where CO_2 concentrations have been limited to 450 parts per million (ppm).

5.5 Summary on SLCPs

Carbon dioxide (CO_2) emissions are responsible for 55-60% of anthropogenic radiative forcing. Fast and aggressive CO_2 mitigation is therefore essential to combat the resulting climate change. But this is not enough. CO_2 mitigation must be combined with fast and aggressive reductions of the pollutants causing the other 40-45% of warming. These pollutants include BC, tropospheric O_3, CH_4, and HFCs. Because these pollutants have atmospheric lifetimes of only days to a decade and a half, they are referred to as SLCPs. Reducing SLCPs is critical for slowing the rate of climate change over the next several decades and for protecting the people and regions most vulnerable to near-term climate impacts. Although we have known about SLCPs for more than 35 years, the following scientific developments have catapulted them to the front lines in the battle against climate change.

- *First* is the recognition that we have already added enough greenhouse gases to warm the planet by 2.4°C or more during this century. Much of this warming has been offset by cooling aerosols, primarily sulphates, which are being reduced under current air pollution policies. These reductions are important, but will contribute to near-term warming. Without fast-action mitigation to cut SLCPs, warming may cross the 1.5° to 2°C threshold by midcentury. Reducing SLCPs is the most effective strategy for constraining warming in the near term, since most of their warming effect disappears within weeks to a decade and a half after reductions.
- *Second* is the recognition that in addition to being climate forcers, three of the four SLCPs are also harmful air pollutants. Reducing them will prevent millions of premature deaths every year, protect tens of millions of tonnes of crops, and contribute to sustainable development.
- *Third* is the recognition that the benefits for health, crops, and sustainable development will accrue primarily in the nations or regions that take action to mitigate these pollutants, due to the stronger impacts BC and tropospheric O_3 have near their emissions sources.
- *Fourth* is the recognition that there are practical and proven ways to reduce all four of these pollutants and that existing laws and institutions are often available to support the reductions. Reducing three of the SLCPs, BC, tropospheric O_3, and CH_4 has the potential to avoid ~0.5°C global average warming by 2050 and 0.84°C in the Arctic by 2070. This would cut the current rate of global warming by half, the rate of warming in the Arctic by two-thirds, and the rate of warming over the elevated regions of the Himalayas and Tibet by at least half.

Reducing SLCPs will in turn:

- Help stabilize regional climate systems and reduce heat waves, fires, droughts, floods and hurricanes in mid-latitudes, and slow shifts in monsoons, expansion of desertification, and increases in cyclones in the tropics.
- Slow the melting of glaciers and Arctic sea ice and the rate of sea-level rise.
- Slow the pace of climate impacts and provide critical time to adapt to large climate changes.

The primary direct local benefits for developing countries from reducing SLCPs include:

- Saving millions of lives a year and significantly reducing other illnesses.
- Improving food security.
- Expanding energy access for the billion forced to depend on solid biomass.

6. Human Health Impacts

Air pollution has been recognized as a major health issue for citizens and local communities for several hundred years. It has long been recognized as both a national and regional challenge with a historical focus on the highly industrialized parts of the world.

A new systematic analysis of all major global health risks has found that outdoor air pollution in the form of fine particles is a much more significant public health risk than previously known. It is contributing annually to over 3.2 million premature deaths worldwide and over 74 million years of healthy life lost. It now ranks among the top global health risk burdens.

Health impacts combined with environmental impacts of air pollution results in significant economic costs. Current air pollution in Asian cities is linked to the economic development model followed in Asia. The lack of environmentally sustainability of the past developmental model has been pointed out in different international reports and Asian countries have committed themselves to a more sustainable developmental model.

Air pollution, both indoors and outdoors, is a major environmental health problem affecting everyone in developed and developing countries alike. The 2005 *WHO Air quality guidelines* (AQGs) are designed to offer global guidance on reducing the health impacts of air pollution. They recommend revised limits for the concentration of selected air pollutants, particulate matter (PM), ozone (O_3), nitrogen dioxide (NO_2) and sulphur dioxide (SO_2), applicable across all WHO regions.

Air Quality Guidelines are as follows.

- There are serious risks to health from exposure to PM and O_3 in many cities of developed and developing countries. It is possible to derive a quantitative relationship between the pollution levels and specific health outcomes (increased mortality or morbidity). This allows invaluable insights into the health improvements that could be expected if air pollution is reduced.
- Even relatively low concentrations of air pollutants have been related to a range of adverse health effects.
- Poor indoor air quality may pose a risk to the health of over half of the world's population. In

homes where biomass fuels and coal are used for cooking and heating, PM levels may be 10–50 times higher than the guideline values.

- Significant reduction of exposure to air pollution can be achieved through lowering the concentrations of several of the most common air pollutants emitted during the combustion of fossil fuels. Such measures will also reduce greenhouse gases and contribute to the mitigation of global warming.

In addition to guideline values, the AQGs give interim targets related to outdoor air pollution, for each air pollutant, aimed at promoting a gradual shift from high to lower concentrations. If these targets were to be achieved, significant reductions in risks for acute and chronic health effects from air pollution can be expected.

6.1 WHO guideline values

Species	Annual mean	Hour mean	Minute mean
$PM_{2.5}$	10 μg m^{-3} annual mean	25 μg m^{-3} 24-hour mean	-
PM_{10}	20 μg m^{-3} annual mean	50 μg m^{-3} 24-hour mean	-
O_3	-	100 μg/m^3 8-hour mean	-
NO_2	40 μg m^{-3} annual mean	200 μg m^{-3} 1-hour mean	-
SO_2	-	20 μg m^{-3} 24-hour mean	500 μg m^{-3} 10-minute mean

6.2 PM

PM affects more people than any other pollutant. The major components of PM are sulphate, nitrates, ammonia, sodium chloride, carbon, mineral dust and water. It consists of a complex mixture of solid and liquid particles of organic and inorganic substances suspended in the air. The particles are identified according to their aerodynamic diameter, as either PM_{10} (particles with an aerodynamic diameter smaller than 10 μm) or $PM_{2.5}$ (aerodynamic diameter smaller than 2.5 μm). The latter are more dangerous since, when inhaled, they may reach the peripheral regions of the bronchioles, and interfere with gas exchange inside the lungs.

The effects of PM on health occur at levels of exposure currently being experienced by most urban and rural populations in both developed and developing countries. Chronic exposure to particles contributes to the risk of developing cardiovascular and respiratory diseases as well as of lung cancer. In developing countries, exposure to pollutants from indoor combustion of solid fuels on open fires or traditional stoves increases the risk of acute lower respiratory infections and associated mortality among young children; indoor air pollution from solid fuel use is also a major risk factor for chronic obstructive pulmonary disease and lung cancer among adults. The mortality in cities with high levels of pollution exceeds that observed in relatively cleaner cities by 15–20%. Even in the EU, average life expectancy is 8.6 months lower due to exposure to $PM_{2.5}$ produced by human activities.

6.3 O_3

O_3 at ground level, do not to be confused with the O_3 layer in the upper atmosphere. O_3 ground level is one of the major constituents of photochemical smog. It is formed by the reaction with sunlight (photochemical reaction) of pollutants such as nitrogen oxides (NO_x) from vehicle and industry emissions and volatile organic

compounds (VOCs) emitted by vehicles, solvents and industry. The highest levels of O_3 pollution occur during periods of sunny weather.

Excessive O_3 in the air can have a marked effect on human health. It can cause breathing problems, trigger asthma, reduce lung function and cause lung diseases. In Europe it is currently one of the air pollutants of most concern. Several European studies have reported that the daily mortality rises by 0.3% and that for heart diseases by 0.4 %, per 10 μg m^{-3} increase in O_3 exposure.

6.4 NO_2

As an air pollutant, NO_2 has several correlated activities.

- At short-term concentrations exceeding 200 μg m^{-3}, it is a toxic gas which causes significant inflammation of the airways.
- NO_2 is the main source of nitrate aerosols, which form an important fraction of $PM_{2.5}$ and, in the presence of ultraviolet light of O_3.

The major sources of anthropogenic emissions of NO_2 are combustion processes (heating, power generation, and engines in vehicles and ships).

Epidemiological studies have shown that symptoms of bronchitis in asthmatic children increase in association with long-term exposure to NO_2. Reduced lung function growth is also linked to NO_2 at concentrations currently measured (or observed) in cities of Europe and North America.

6.5 SO_2

SO_2 is a colourless gas with a sharp odour. It is produced from the burning of fossil fuels (coal and oil) and the smelting of mineral ores that contain sulphur. The main anthropogenic source of SO_2 is the burning of sulphur-containing fossil fuels for domestic heating, power generation and motor vehicles.

SO_2 can affect the respiratory system and the functions of the lungs, and causes irritation of the eyes. Inflammation of the respiratory tract causes coughing, mucus secretion, aggravation of asthma and chronic bronchitis and makes people more prone to infections of the respiratory tract. Hospital admissions for cardiac disease and mortality increase on days with higher SO_2 levels. When SO_2 combines with water, it forms sulphuric acid; this is the main component of acid rain which is a cause of deforestation.

7. Transboundary air pollution

The scientific-political conclusion was that no single country could solve the problem of long-range transboundary air pollution on its own.

The arguments against transboundary pollution were gradually undermined by additional scientific observations but the negotiations in Geneva were often complicated by the political differences between the two Blocs. Finland, Norway and Sweden pushed for firm obligations while the opponents tried to weaken them and wanted to have blunt provisions in the instrument. Canada and the United States took a sideline position. The USSR and its allies supported the Nordic countries against EEC countries. Striking a compromise, negotiators agreed that the instrument should be a framework convention with clear statements of its ultimate goal and that

it should contain provisions for subsequent negotiations for the reduction of emissions of sulphur and other substances, based on scientific studies of transboundary air pollution. Compilations for this purpose were to be carried out by the existing European Monitoring and Evaluation Programme (EMEP).

Over recent decades growing concern of the Acid Deposition Monitoring Network in East Asia (EANET) has also emerged over the widespread damage caused by long-range transboundary, and even intercontinental air pollution. This was underlined in 1972 at the United Nations Stockholm Conference on the Human Environment where a decision was also taken to establish the United Nations Environment Programme (UNEP). Transboundary air pollution was further highlighted in the 1975 Conference on Security and Cooperation in Europe (CSCE). Improving science and increasingly reliable monitoring led to a political agreement in the United Nations Economic Commission for Europe (UNECE) on the control and reduction of long-range transboundary air pollution within Europe and North America. The Convention on Long-range Transboundary Air Pollution (CLRTAP) was agreed in 1979 followed by eight specific legally-binding Protocols between 1984 and 1999. These developments have been mirrored in Asia. In East Asia, the EANET has been established and in South Asia, a network under the "Malé Declaration on Control and Prevention of Air Pollution and its Likely Transboundary Effects for South Asia" is in operation. The Association of Southeast Asian Nations (ASEAN) countries have established the "ASEAN Agreement on Transboundary Haze Pollution" which aims to prevent and monitor transboundary haze pollution.

Despite these agreements, air pollution continues to rise in many parts of the world with increasing problems for developing countries and regions. Increasingly it is being seen as not just a human health challenge but an economic one with costs to agriculture, important ecosystems such as forests and the productivity of coastal waters. Improving global and regional cooperation to cut air pollution is thus an environmental but also a social and economic imperative. It is necessary to provide insight into the scientific and technical aspects of the multilateral cooperation and negotiations as well as guidance on practical science-based development of regional environmental law with the aim of assisting negotiations.

It highlights the achievements of existing conventions, protocols and agreements and offers guidance on how to adapt this experience and tailor it to specific regional circumstances. The linkages also underline between air pollution and climate change, economic development and poverty outlining the multiple, Green Economy benefits of integrating air pollution programmes with those of greenhouse gases.

However the overall conclusion on implementation must be that it is highly successful regimes that have to think other things or recognize of:

- precautionary principle
- sustainable development
- integration of science with policy
- special circumstances of developing countries
- international cooperation to solve transboundary environmental problems
- common but differentiated responsibility among Parties
- flexibility to respond to scientific and technological developments over time

Furthermore, the newly discovered inter-linkage to climate change poses a novel challenge to further progress.

A reasonable conclusion is that the more sophisticated an agreement, the more technical and scientific support it will require and probably also a longer period of execution. The proper balance will be linked to the realistic ambition level of the negotiators and timetable, work plan and method of work will be set accordingly.

Science and monitoring will continue to produce data indefinitely which might be taken as a reason to postpone the conclusion of negotiations. The fact that experience has shown that the benefits of action on air pollution widely outweigh the costs, must speak in favour of the substantial investments for the conclusion and implementation of multilateral agreements to mitigate emissions of air pollution.

8. Asia Science Panel on Air Quality and Climate (ASPAC)

It is well known that air pollution has negative impacts on human health and ecosystems and control strategies are clearly a priority for reducing disease and mortality. The science behind most air pollution impacts and air quality management systems is now reasonably well established; monitoring networks are widespread, much is known about sources and emission inventories are available. The rapid economic growth, emissions of air pollutants in the Asian continent have also exceeded those of European and North American continents after the year 2000, and even those in East Asia (Northeast and Southeast Asia) alone are comparable to the other continents as of 2005. This situation prompted concerns about Asian air pollution locally, regionally, hemispherically and globally from the standpoint of air toxicants such as photochemical oxidants and particulate matter ($PM_{2.5}$), biogeochemically active species such as acidic and nitrogenous compounds as well as SLCPs such as BC and tropospheric O_3. An emerging issue to seriously consider is the link between air pollution and climate change, especially regarding SLCPs and effects of SO_2 reduction on climate change.

There is a need to consider such issues from a scientific viewpoint and make suggestions to policy makers to take action. However, the situation in Asia is different from Europe and North America where regional cooperation on air pollution mitigation based on scientific knowledge has been well developed under the CLRTAP; Asia does not have an adequate framework for scientific discussion for atmospheric management.

On the basis of the above considerations, a Japanese team conducted research on possible regional framework to strengthen atmospheric management and the science-policy interface to send timely and appropriate messages from the scientific community to policy makers. This team proposes an Asia Science Panel on Air Quality and Climate (ASPAC) aiming to synthesize scientific knowledge on air pollution in the Asian region to reach a common understanding among scientists and policy makers, and to develop an international initiative for an integrated approach to air pollution and climate change reflecting the views of Asian scientists.

ASPAC would be constituted of scientists related to air pollution research. It would review the existing latest scientific knowledge, prepare reports and “Summary for Policy Makers” based on a consensus of major research scientists on the issues of air pollution and its relation to climate change in Asian region.

9. Catchment analysis in the EANET participating countries

Currently, the EANET has been monitoring the catchment analysis projects in 3 participating countries, i.e. Japan (2002), Thailand (2005) and Malaysia (2008). The Philippines is now processing to monitor. The case studies have been implemented by the NC and scientists in the EANET participating countries in Thailand at the Sakaerat Silvicultural Research Station (SRS) site, Royal Forest Department, in Malaysia at the Danum Valley site in Sabah and Japan at the Kajikawa study site. The regular catchment-scale monitoring has also started in the Lake Ijira catchment in Japan, where acidification mechanisms of the catchment area are being clarified gradually by the catchment-scale analysis. For deposition processes, particulate SO_4^{2-} and EC were also studied in the Japanese cedar forest in Kajikawa, Niigata Prefecture, Japan, and in a dry evergreen forest and a dry deciduous forest in Sakaerat, Nakhon Ratchasima province, Thailand. The SO_4^{2-} fluxes attributed to rainfall outside the forest canopy (RF), throughfall (TF), and stemflow (SF) showed distinct seasonalities at both sites.

The catchment-scale monitoring may allow more practical discussion on relationship between seasonal or annual changes in stream water chemistry (concentrations or material/elemental fluxes) and those in atmospheric deposition. Material/elemental input-output budget in the catchment can be calculated based on the atmospheric deposition chemistry, stream water chemistry, and water balance. Moreover, based on the catchment-scale dataset, the simulation model on biogeochemical cycles is expected to be developed.

9.1 Objectives of the catchment-scale monitoring

- To evaluate effects of atmospheric deposition on ecosystems qualitatively and quantitatively on a catchment scale.
- To interpret seasonal or annual changes in the stream water chemistry based on atmospheric deposition and possible biogeochemical processes in a catchment**.**
- To discuss impacts of atmospheric deposition based on the input-output budget of materials/elements on a catchment scale.
- To provide necessary dataset to the catchment-scale simulation model for understanding the current status and making future projection of the material/elemental cycles in the catchment due to the changing environment.

9.2 Selection of monitoring sites

- A forest catchment with a stream should be selected, while the size of the catchment may depend on each situation.
- The catchment, where the water budget has been estimated, is preferable.
- Sensitivity of soil or bedrock geology to atmospheric deposition should be considered for site selection.
- If possible, the site should be in vicinity of the EANET acid deposition site to estimate atmospheric deposition amounts precisely.
- Other ecological information from nearby sites is valuable.

9.3 Monitoring items

The total deposition as an input and the discharge from the stream as an output should be estimated as minimum requirements. For mandatory, precipitation amount, wet deposition, total depositions (wet and dry included throughfall and stemflow measurements), water discharge with weir, stream water chemistry, and chemical discharge are monitored, while dry deposition may be optional. Most of items have been measured or proposed for deposition monitoring or ecological monitoring.

In addition to the input and output, items for biogeochemical processes should be monitored to discuss material/elemental cycles in the catchment. Possible items to be monitored for this purpose are soil and vegetation. Soil chemical properties and plant growth are mandatory. While other items may be considered depending on targets or optional, e.g., soil solution, moisture, physical properties and gas emission. For optional of vegetation, they are species composition, liter trap for elemental contents as well as water balance of the evapotranspiration.

9.4 Recommendations for the input items

- Spatial variability of the precipitation amount should be considered in mountainous area if the catchment area is relatively large.
- The throughfall-stemflow (TF-SF) method is useful to estimate total (wet and dry) atmospheric deposition amounts for certain constituents, such as SO_4^{2-}, whose canopy interaction can be negligible.
- Dry deposition flux should be estimated by appropriate methods other than the TF-SF method to estimate total deposition precisely, especially for nitrogen compounds, taking canopy interactions such as uptake or consumption into account.
- The deposition and meteorological data collected in the nearest EANET station should be utilized if available. The total deposition can be estimated by using the data of the filter-pack method and the wet-only sampler at the EANET station.
- In particular in tropical region, wet deposition of nitrogen should be estimated by appropriate methods since microbial consumption of nitrogen is large during the storage in the sampling field. The ion-exchange-resin sampler may be applicable in forest area for long-term collection (for several months).

9.5 Recommendations for the output items

- The water year should be decided based on hydrological cycle in each catchment taking precipitation and discharge patterns into account.
- Evapotranspiration should be estimated if possible, for precise water balance, especially in tropical region.
- Cooperation with hydrologists may be helpful to understand hydrological processes in the catchment in detail.

9.6 Recommendations for items of biogeochemical processes

- Plant growth should be measured in the catchment area. Tree ring analysis may be useful to estimate

the previous growth rate for the long-term analysis. At least, some information on plant growth should be compiled through a literature study.

- Soil samples should be collected for analysis taking a spatial variation of soil chemical properties in the catchment.

9.7 Chemical parameters to be measured

Major chemical parameters of the rainwater and stream water to be measured for the respective items are Cations: NH_4^+, Ca^{2+}, Mg^{2+}, Na^+, and K^+, Anions: SO_4^{2-}, NO_3^-, and Cl^-, and Electric conductivity (EC) and pH as a mandatory as well as air concentration (filter pack) and soil properties. For optional, they are soil solution and gasses as well as litter and leaf element samples.

9.8 Measurement frequency

Proposed frequencies for measurement of the respective items are as follows: precipitation amount collects continuously or daily, wet deposition (daily or weekly for wet only samplers and weekly or biweekly for bulk sampling), dry deposition (weekly for filter pack method, continuously for automatic monitor and biweekly or monthly for passive sampling method), total deposition (biweekly, or monthly for calculation of wet and dry), water discharge (continuously or biweekly), stream water chemistry (weekly or biweekly but for intensive sampling (1-2 hour interval) during heavy-rain or snow-melting events), soil chemical properties (once for several years or twice a year in case of tropical seasonal forest), and for plant growth and species composition (once for several years).

9.9 Recommendations for the measurement frequency

- Stream water samples should be collected at the outlet of the catchment periodically, hopefully at 2-week interval (or twice a month).
- Intensive sampling of the stream water should be conducted during heavy-rain or snow-melting events if possible.
- Seasonal variation of soil chemical properties should also be considered for some parameters, such as pH (H_2O), especially in tropical seasonal forest.

9.10 Quality assurance/quality control (QA/QC)

Data quality should be controlled and assured according to the EANET QA/QC program. Basically, protocols on sampling and chemical analysis can be standardized referring the existing EANET technical documents. The following fundamental matters should also be noted in the catchment-scale monitoring.

- Clear assignment of responsibility (personnel in charge of each activity)
- Standard operating procedures (SOPs) for each activity
- Documentation of activities

9.11 Evaluation

The data should be evaluated on a catchment scale. The input-output budget should be calculated based on the atmospheric deposition chemistry, stream water chemistry, and water balance to outline the material/elemental cycles in the catchment. The standard units should be used for the input and output. Recommended basic units for evaluation is as follows:

- Water flux (precipitation amount and stream water discharge): mm
- Chemical concentration: $mol_c\ L^{-1}$ (ex. $\mu mol_c\ L^{-1}$ or $mmol_c\ L^{-1}$)
- Ion flux (deposition, discharge or soil/vegetation flux): $mol_c\ ha^{-1}$ or $mol_c\ m^{-2}$
- Elemental flux for N and S: $kg\ ha^{-1}\ y^{-1}$ or $g\ m^{-2}\ y^{-1}$

Based on the compiled data with the standard units on a water-year basis, initial evaluations should be done for the following items:

- Water balance on a catchment-scale: input, output and possible evapotranspiration
- Material/elemental balance on a catchment-scale: input-output budget

9.12 Summary on catchment analysis

In general, the forest catchment in the East Asian region is largely influenced by seasonal changes caused by the monsoons. Seasonal changes of atmospheric deposition were very clear in Thailand. Moreover, the stream water chemistry may depend on soil characteristics and nutrient fluxes in the ecosystem. Experience gained through the project suggested that new technical issues should be considered in catchment-scale monitoring. For example, it may be necessary to consider spatial and seasonal variation in soil pH and mineral-nitrogen fluxes in the tropical seasonal forest. The information will be compiled and utilized for preparation of the guidelines for the future catchment-scale monitoring in EANET. Collaboration with biogeochemical model simulation is also planned in the new Global Environment Research Fund (GERF) projects. Therefore, more comprehensive outcomes will be obtained.

10. Conclusions

The editor would like to convince the EANET participating countries to have wider the EANET's attention on strengthening cooperation for the EANET participating countries, expansion of the scope of the EANET, co-benefits/co-control, short-lived climate pollutants (SLCPs, human health impacts, transboundary air pollution, Asia science panel on air quality and climate (ASPAC) and catchment analysis in the EANET participating countries that they are being implemented in order to achieve the human well-being, food security, alleviate the ecological degradation, energy, governance across scales and poverty alleviation and of course, pollutant thresholds.

In the near future, particle issues, we may concentrate on nanoparticles instead of PM_{10} and $PM_{2.5}$. There are numerous studies have shown that exposure to microparticle emissions increases the probability of heart attacks, asthma attacks, and hospital visits among at-risk individuals. However, while many studies have already focused on measurements of ambient nanoparticles because the potential of these pollutants increased exposure dramatically.

From motor vehicle emission studies, ambient nanoparticles were found to consist mostly of C, O, N, and S. Many particles also contained silicon (Si). The elemental compositions were apportioned into molecular species that are commonly found in ambient aerosol: sulphate (SO_4^{2-}), nitrate (NO_3^-), ammonium (NH_4^+), carbonaceous matter, and when present, silicon dioxide (SiO_2). Correlating the nano aerosol mass spectrometer

(NAMS) chemical-composition measurements with spike contributions allowed for the development of a chemical profile representing motor vehicle emissions, which could be used to apportion their total contribution to the ambient nanoparticle mass. Particles originating from motor vehicles had compositions dominated by unoxidized carbonaceous matter, whereas non–motor vehicle particles consisted mostly of SO_4^{2-}, NO_3^-, and oxidized carbonaceous matter. Motor vehicles were found to contribute up to 48% and 60% of the nanoparticle mass and number concentrations, respectively.

Ambient nanoparticles, particularly those 100 nm in diameter or less, are an important focus of research on the health effects of air pollution. Effects of ultrafine dimensions as nanoparticles, mainly penetrate the body via inhalation and deposited in the lungs, brain, cardiovascular system and etc. Due to their small size, nanoparticles can translocate from these entry portals into the circulatory and lymphatic systems, and ultimately to body tissues and organs. Some nanoparticles, depending on their composition and size, can produce irreversible damage to cells by oxidative stress or/and organelle injury. Scientists have hypothesized that these particles will be more toxic than $PM_{2.5}$ in aerodynamic diameter because of their physical characteristics and composition. To better identify human exposures and potential health effects associated with nanoparticles, a clearer understanding is needed of sources, atmospheric transport and chemical reactions, concentrations, and composition at the point of exposure.

Henceforth the National Focal Points should prepare the national plans for the future monitoring on all above mentioned issues. These issues are included to cover the status of the national policies and measures to deal with air quality, and proposals for steps to be taken in a regional action plan. The regional cooperation in response to a pollution emergency would be appropriate for joint activities in the future as well.

11. Bibliographies

Aitken, R.J., Creely, K.S. and Tran, C.L. 2004. Nanoparticles: An occupational hygiene review. Research report 274. Institute of Occupational Medicine. Research Park North, Riccarton, Edinburgh. 113 p.

Buzea, C., Blandino, I.I.P. and Robbie, K. 2007. Nanomaterials and nanoparticles: Sources and toxicity. Biointerphases. 2(4): MR17-MR172.

CAI-Asia. 2010. Air quality in Asia: status and trends. Pasig City, the Philippines. 20 p.

Castillo, C.K.G., Sanqui, D.C., Ajero, M. and Huizenga, C. 2007. The Co-Benefits of Responding to Climate Change: Status in Asia. United States Environmental Protection Agency (US EPA)/ Manila Observatory (MO)/ Clean Air Initiative for Asian Cities (CAI-Asia). 64 p.

HEI. 2013. Detection and characterization of nanoparticles from motor vehicles. Statement: Synopsis of Research Report 173. 2 p.

Hofmann, H. 2009. Nanomaterials. Power Technology Laboratory IMX EPFL Version 1 Sept 2009. 270 p.

http://www.malvern.com/labeng/industry/nanotechnology/nanoparticles_definition.htm.What are nanoparticles?

Institute for Governance & Sustainable Development (IGSD). 2013. Primer on Short-Lived Climate Pollutants: Slowing the rate of global warming over the near term by cutting short-lived climate pollutants to

complement carbon dioxide reductions for the long term. IGSD. Washington, DC, USA. 59 p.

Intergovernmental Panel on Climate Change (IPCC). 2001. Mitigation: contribution of Working Group III to the Third Assessment Report (TAR) to the Intergovernmental Panel on Climate Change. (http://www.grida.no/climate/ipcc_tar/wg3/index.htm).

IRSST. 2006. Health effects of nanoparticles. Studies and research projects report. The Institut de recherche Robert-Sauvé en santé et en sécurité du travail (IRSST). Quebec. Canada. 57 p.

Johnson, M.V., Klems, J.P., Zordan, C.A., Pennington, M.R. and Smith, J.N. 2013. Selective detection and characterization of nanoparticles from motor vehicles. Research Report 173, Health Effects Institute (HEI). Boston, Massachusetts. 60 p.

Luangjame, J., Garivait, H., Sase, H., Yamashita, N., Ohta, S., Leong, C.P. & Takahashi, M. 2009. Recommendations for preparation of a guideline on the future catchment monitoring in the EANET participating countries. Second Meeting for the Task Force on Soil and Vegetation Monitoring of EANET.

Sase, H., Matsuda, K., Visaratana, T., Garivait, H., Yamashita, N., Kietvuttinon, B., Hongthong, B., Luangjame, J., Khummongkol, P., Shindo, J., Endo, T., Sato, K., Uchiyama, S., Miyazawa, M., Nakata, M. and Lenggoro, W. 2012. Deposition process of sulphate and elemental carbon in Japanese and Thai forests. Asian Journal of Atmospheric Environment. 6(4): 246-258.

Sase, H., Takahashi, A., Sato, M., Kobayashi, H., Nakata, M. & Totsuka, T. 2008. Seasonal variation in the atmospheric deposition of inorganic constituents and canopy interactions in a Japanese cedar forest. Environmental Pollution 152: 1-10.

UNEP. 2010. Air pollution: Promoting regional cooperation. Bangkok, Thailand. 167 p.

UNEP. 2011. Near-term climate protection and clean air benefits: Action for controlling short-lived climate forcers. A UNEP Synthesis Report. UNEP. 58 p.

UNEP/WMO. 2011. Integrated Assessment of Black Carbon and Tropospheric Ozone. Summary for decision makers. UNEP. 31 p.

USEPA. 2012. Reducing black carbon emissions in South Asia: low cost opportunities. Office of International and Tribal Affairs. U.S. Environmental Protection Agency. 83 p.

Valavanidis, A. and Vlachogianni, T. 2010. Nanomaterials and nanoparticles in the aquatic environment: Toxicological and ecotoxicological risks. *Science advances on Environment, Toxicology & Ecotoxicology issues.* Department of Chemistry, University of Athens, University Campus Zografou, 15784 Athens, Greece. 10 p.

WHO. 2011. Air quality and health. Fact sheet No 313. 6 p.

Reports of the EANET Research Fellowship Program (2010-2012)

The EANET Science Bulletin is issued every two-year period. While the Research Fellowships are obtained every year, sometimes, there was a person or two persons per year that was depended on budget availability. Therefore, the reports of two-year programs are included in the bulletin. This bulletin is the EANET Science Bulletin Volume 3 that collected the research results of the year 2010-2012 programs.

Assessment of Long-range Transport Contribution on Haze Episode in Northern Thailand, Year 2007

Sopittaporn Sillapapiromsuk[1], Keiichi Sato[2] and Somporn Chantara[3]

[1]Environmental Science Program, Faculty of Science, Chiang Mai University, Chiang Mai, 50200, Thailand.
E-mail: s.sopittaporn@gmail.com
[2] Atmospheric Research Department, Asia Center for Air Pollution Research (ACAP). 1182 Sowa, Niigata, 950-2144, Japan
E-mail: ksato@acap.asia
[3]Environmental Chemistry Research Laboratory, Department of Chemistry, Faculty of Science, Chiang Mai University, Chiang Mai, 50200, Thailand.
E-mail: sp_chan@chiangmai.ac.th

Abstract

The haze episode over northern Thailand has been an almost yearly occurrence and becomes severe during the prolonged dry period with elevated PM_{10} concentrations. This study aims to assess contribution of long-range transport on occurrence of haze episode in Northern Thailand. PM_{10} concentrations and hotspot data as well as meteorological conditions of Chiang Mai station during 2004-2007 were analyzed. It was found that the PM_{10} concentrations were positively correlated with number of hotspots. On the other hand the PM_{10} concentrations were found to have negatively correlation with wind speed, especially in 2004 (r = -0.476), 2007 (r = -0.442) and 2009 (r = -0.445). The 3-day backward trajectories of air mass arriving at Chiang Mai in year 2007 were analyzed using hybrid single particle langrangian integrated trajectory (HYSPLIT) model and grouped by cluster analysis. The air mass for whole year (335 days; 100%) was classified into 4 groups. A major direction came from western continents of Thailand, in which 64% was found to be associated with air mass trajectories during the haze episode (February to April). At this period (86 days, 100%), air mass was classified into 6 groups, and the major direction still originated from western side (75%). Dry season in Thailand normally ranges from November to April. In this study, air mass data of January-April and November-December 2007 (170 days, 100%) were clustered into 6 groups. The origin of backward trajectories during these periods was mainly local (57%). The air masses in wet season (165 days) were also classified and most of data (55%) mainly started from the Indian Ocean because of southwest monsoon influence. The results revealed that haze episode in Upper-Northern Thailand mainly originated from the western continent in association with local activities. Therefore, potential sources of air pollution in that area should be considered.

Keywords: Long-range transport; Back trajectory; Cluster analysis; Air pollution; PM_{10}

1. Introduction

Air pollution is one of the most important environmental issues which are still to be solved and has far-reaching impacts on the sustainable development of the terrestrial biosphere and exposure to polluted air causes adverse human health effects. Previous studies have linked elevated levels of air pollutants to many human health problems such as low birth weight and birth defects, infant mortality, child asthma, increased hospital admittance, increased allergy cases, lung disease, respiratory and cardiovascular disease and mortality displacement. Therefore, characterizing air pollution distribution and understanding its causes and variations in megacities has become an urgent issue for policy makers (Wang *et al*., 2004). Particulate matter (PM) is still a major problem in almost all Asian countries with concentrations exceeding 300 $\mu g.m^{-3}$ in many cities (Baldasano *et al*., 2003)

Meteorological factors may affect visibility in several ways. Sunlight, for example, significantly affects visibility by promoting secondary aerosol formation. Atmospheric photochemistry produces the major visibility-reducing aerosols, i.e. suphfates, nitrates, and oxyhydrocarbons. Wind speed and atmospheric stability affect visibility because they determine atmospheric dispersion and therefore concentrations of aerosol particles. In general, as the wind speed increases, visibility improves, as the wind-induced atmospheric mixing results in lower aerosol concentrations. During periods of atmospheric stagnation (associated with slowly moving high pressure systems), vertical mixing is suppressed, aerosol concentrations increase, and visibility is reduced. The resultant haze may cover hundreds of thousands of square kilometers. It is not uncommon to have a major portion of the Midwest, Southeast, or the East Coast covered by a "blanket of haze" (Godish, 1997).

Smoke haze due to forest fires and agricultural burning is a recurring environmental problem in Southeast Asia. Thailand has experienced one of its worst hazes in March 2007, 8 provinces in northern Thailand have been blanketed in smoke and dust for two weeks after forest fires and agricultural burning in northern Thailand and neighboring Myanmar and Laos. On the 14th of March, the province of Chiang Rai was declared a disaster zone, while the nearby province of Chiang Mai, the largest city in northern Thailand reported hazardous levels of air pollution (Bangkok (AFP), 2007).

Air quality has become a big problem and has been steadily deteriorating over the past ten years of Chiang Mai. Airborne fine particles in recent years have increased and started to exceed the national ambient air quality standards (NAAQS) (120 $\mu g.m^{-3}$ for 24-hr average of PM_{10}) in all monitoring stations in the dry season (February to March) (PCD, 2009). The geographical features of Chiang Mai City's located in the Chiang Mai–Lamphun intermontane basin and is surrounded by high mountain ranges that results in the same air being re-circulated, accumulate more pollutants every time. Therefore, sources of air pollutants are also needed to be identified. Kim Oanh and Leelasakultum (2011) reported that an emission inventory (EI) conducted by the Pollution Control Department, Thailand for Muang district of Chiang Mai (not include the surrounding area of Chiang Mai province) evaluated the total particulate matter emission to be 700 tones of which 89% came from

forest fires, 5.4% from solid waste burning and 2.3% from agriculture residue field burning. Point sources (industry) contributed only 0.08%, mobile sources 2.6% and other sources 0.56%.

Without evidence to the contrary it was widely believed that once polluted air was transported for some distance downwind, the enormity of the atmosphere and dilution processes associated with it reduced pollutants to background levels. However, elevated levels of pollutants may occur hundreds to thousands of kilometers downwind of large point sources and areas producing urban plumes. This phenomenon is known as long-range transport (Godish, 1997). The knowledge of possible long-range transport contribution will help shed understanding on the nature of air pollution at a location, in order to formulate optimal abatement strategies. However, difficulties may arise when attempting to quantify this long-range transport contribution and to identify its source regions (Pongkiatkul *et al.*, 2007). A simple back-trajectory model is normally applied to track the origin of air masses (Stein et al., 2000; Zeng et al., 2003). The Hybrid Single-Particle Langrangian Integrated Trajectory model Version 4 (HYSPLIT4) is a useful air trajectory model, which is widely applied for long-range transport studies (Draxler and Hess, 1997).

2. Methods

2.1 PM_{10} data and Air Quality Monitoring station

Data of 24 hr-PM_{10} concentrations monitored at the Air Quality Monitoring (AQM) stations in Chiang Mai province (City Hall (CH) and Yupparaj Wittayalai School (YP) stations) and Nakhonsawan province (Nakhonsawan station (NS) as control site) was obtained from Pollution Control Department (PCD), Thailand. The locations of these stations are shown in Figure 1. The YP station was situated at a city center of Chiang Mai. It was surrounded by diverse urban facilities (e.g. public transport, school, grocery and government office) and has high population density as well as high traffic volume (1,532-2,308 vehicles per hours) (Na Nongkhai, 2004). This site was classified as a roadside based on Pollution Control Department (PCD) criteria. The CH station was located northwest of the city, approximately 6 km from the YP station. Community and traffic density was less dense in comparison with the inner city. The NS station was situated in Nakhonsawan Technical College surrounded by residential area. PM_{10} concentrations were measured continuously using 1400a Taper Element Oscillating Microbalance (TEOM) (Rupprecht & Patashnick, USA) at 3 m height in range 0 – 1000 $\mu g.m^{-3}$. TEOM mass detectors or microbalances utilize an inertial mass weighing principle. A TEOM detector consists of a substrate (usually a filter cartridge) placed on the end of a hollow tapered tube. The tube with the filter on the free end is oscillated in a clamped-free mode at its resonant frequency. This frequency depends on the physical characteristics of the tube and the mass on its free end. A particle laden air steam is drawn through the filter where the particles deposit and then through the hollow tube. The frequency of oscillation was measured and recorded by the microprocessor; the change in frequency was used to calculate the mass of particulate matter deposited on the filter (Teflon coated with glass fiber filter surface). The air flow rate at 16.67 L min^{-1} is sampled through the sampling head and divided between the filter flow (3 L min^{-1}) and an auxiliary flow (13.67 L min^{-1}). The filter flow is sent to the instrument's mass transducer, which contains the

analyze fraction of particulate. The inlet is heated to 50°C prior to particles being deposited onto the filter in order to eliminate the effect of condensation or evaporation of particle water (Washington State Department of Ecology Air Quality Program, 2004; Patashnick *et al*., 2002).

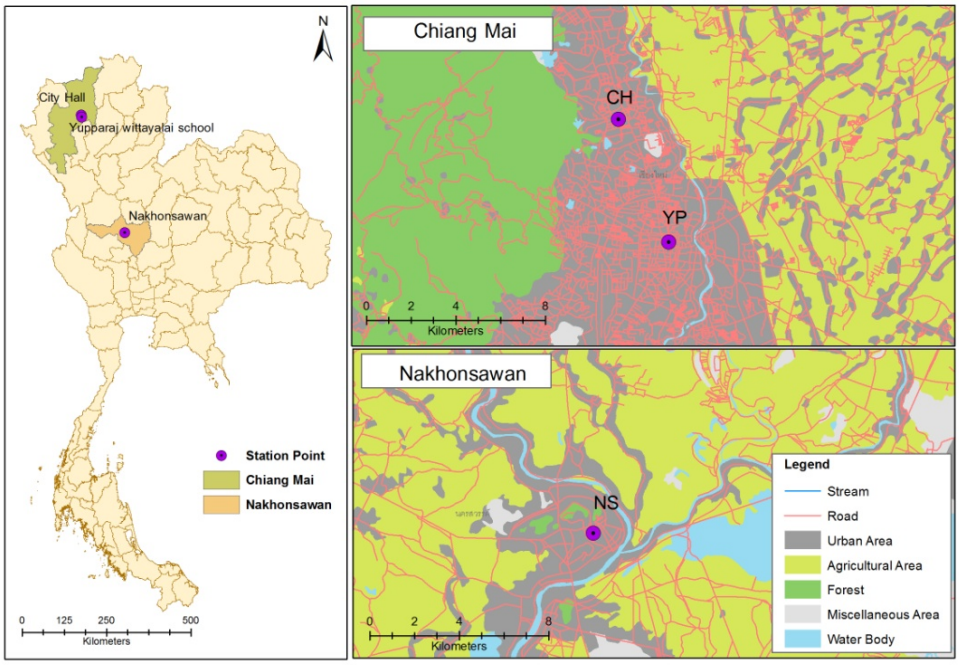

Figure 1. Location of the air quality monitoring stations; CH and YP in CM province and NS in Nakhonsawan province.

2.2 Hotspot data

The hotspot data are provided by Fire Information for Resource Management System (FIRMS) (Domain; minX: 77.368, minY: 6.782, maxX: 122.193, maxY: 29.107). FIRMS integrates remote sensing and GIS technologies to deliver global MODIS (or Moderate Resolution Imaging Spectroradiometer) hotspot/active fire locations to natural resource managers and other stakeholders around the World. FIRMS was developed by the University of Maryland with funds from NASA. The hotspot/fires are detected using data from the MODIS instrument, on board NASA's Aqua and Terra satellites, using a specific fire detection algorithm that makes use of the thermal band detection characteristics of the sensor. Each hotspot/active fire location represents the center of a 1km pixel (approximately) flagged as containing one or more actively burning hotspot/fires within that pixel. (NASA/University of Maryland, 2002)

2.3 Meteorological data

Thai Meteorological Department (TMD) provided data on rain precipitation, wind speed and wind direction used in this study. Most of the data were daily averages. Three meteorological factors were used as input data for cluster analysis.

The climate of Thailand is under the influence of monsoon winds of seasonal character i.e. southwest monsoon and northeast monsoon. The southwest monsoon which starts in May brings a stream of warm moist air from the Indian Ocean towards Thailand causing abundant rain over the country, especially the windward

side of the mountains. Rainfall during this period is not only caused by the southwest monsoon but also by the Inter Tropical Convergence Zone (ITCZ) and tropical cyclones which produce a large amount of rainfall. May is the period of first arrival of the ITCZ to the Southern Part. It moves northwards rapidly and lies across southern China around June to early July that is the reason of dry spell over upper Thailand. The ITCZ then moves southerly direction to lie over the Northern and Northeastern Parts of Thailand in August and later over the Central and Southern Part in September and October, respectively. The northeast monsoon which starts in October brings the cold and dry air from the anticyclone in China mainland over major parts of Thailand, especially the Northern and Northeastern Parts which is higher latitude areas. In the Southern Part, this monsoon causes mild weather and abundant rain along the eastern coast of the part. The onset of monsoons varies to some extent. Southwest monsoon usually starts in mid-May and ends in mid-October while northeast monsoon normally starts in mid-October and ends in mid-February.

2.4 Trajectory analysis

Backward trajectories arriving at the receptor were calculated using the hybrid single particle langrangian integrated trajectory (HYSPLIT) model. The 3-day backward trajectories were available online at http://ready.arl.noaa.gov/HYSPLIT.php. To minimize the fraction effect from the Earth's surface and to represent wind in the lower boundary layer (Begum et al., 2005), the air masses arriving at 1000 m above ground level (AGL) were chosen. The results from preliminary study on the effects of different starting levels in Thailand indicated that the air masses trajectories obtained for the start level of 1000 m agreed with those obtained for the 500 m start level on 70% of the days during the period from January 2002 to December 2004. It means that the air masses arriving levels may be at least considered to be within a layer of 500–1000 m (Pongkiatkul and Kim Oanh, 2007). The input data to HYSPLIT available 4 times a day (0, 6, 12, and 18 UTC), for total of 358 days during the period from January to December 2007.

2.5 Statistical analysis

The Pearson correlation of seasonal hotspot number and daily PM_{10} concentrations in year 2007 was calculated. Air mass trajectories from each day were clustered to determine the main trajectories direction arriving to receptor using hierarchical clustering method. SPSS package version 17 was used for all data analysis.

3. Results and discussion

3.1 PM_{10} concentrations during 2004-2009

PM_{10} concentrations of the three AQM stations; CH, YP and NS, from 2004 to 2009 were analyzed. In this work the whole year season was basically divided into dry (6 months) and wet seasons (6 months). Dry season includes 2 periods (January-April and November-December), while wet season starts from May to October.

Monthly rainfalls recorded at Chiang Mai meteorological station in years 2004-2009 together with PM_{10} concentrations measured at the AQM stations were plotted in Figure 2. Patterns of PM_{10} levels were

almost the same for every year. In dry season the PM_{10} concentrations were obviously higher than those in wet season. Remarkably in March 2004 and 2007, the levels of PM_{10} at Chiang Mai stations were higher than those of other years. Amount of rain precipitation obviously affected to ambient PM_{10} concentrations, which were high in dry season and low in wet season. Noticeably, the PM_{10} concentrations increased at the beginning of dry season (November) and became highest in March before decreasing by the end of April. Their patterns were almost the same for all stations.

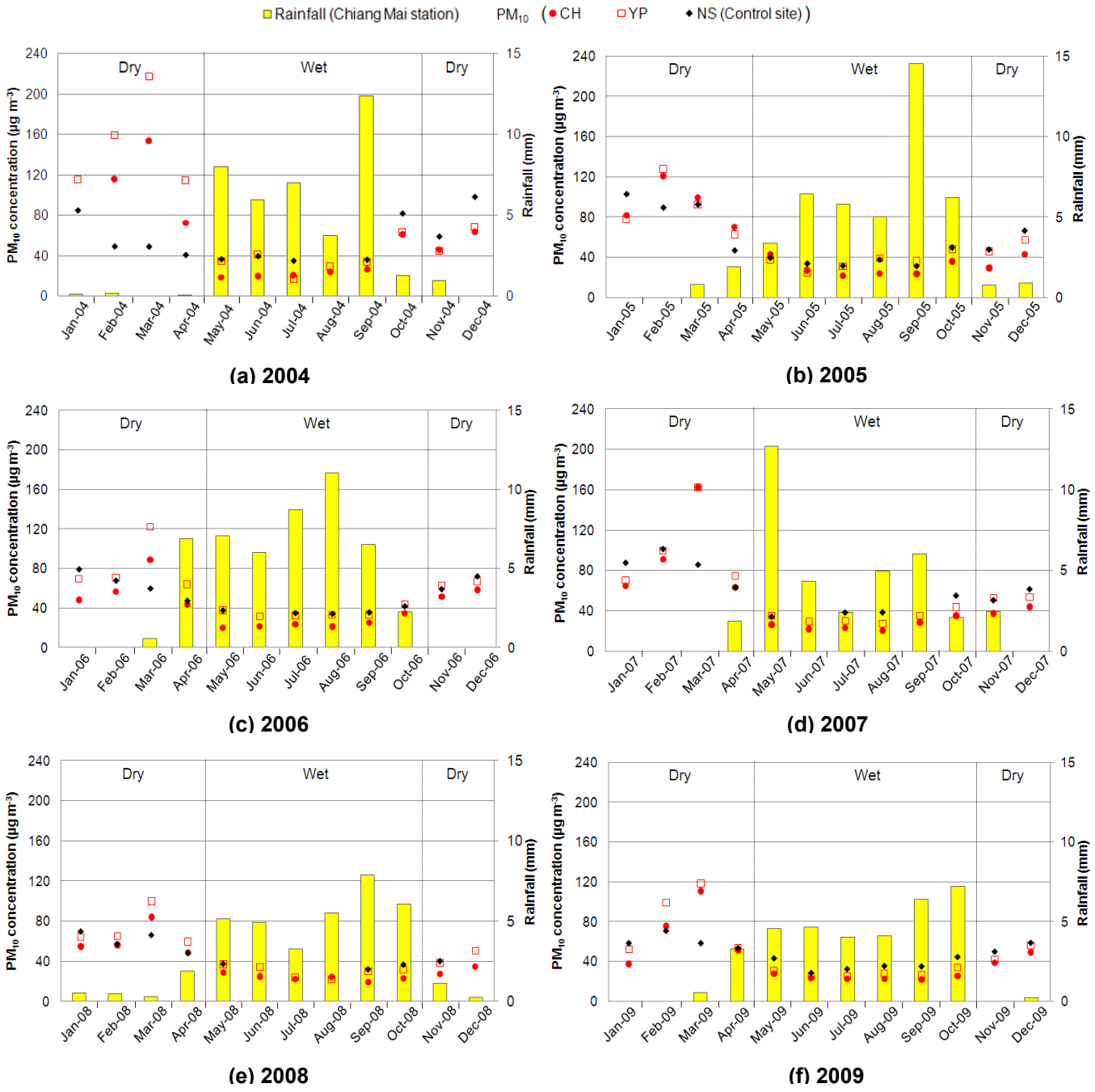

Figure 2. Monthly average PM_{10} variation and rainfall in Chiang Mai, 2004-2009.

Haze episode in northern Thailand often occurred from February to April. It was found to associate with high levels of PM_{10} concentrations. From the plots (Figure 3), PM_{10} concentrations were high in March. The highest PM_{10} concentrations were found in year 2007 (396.4 µg m^{-3} at YP station and 317 µg m^{-3} at CH station).

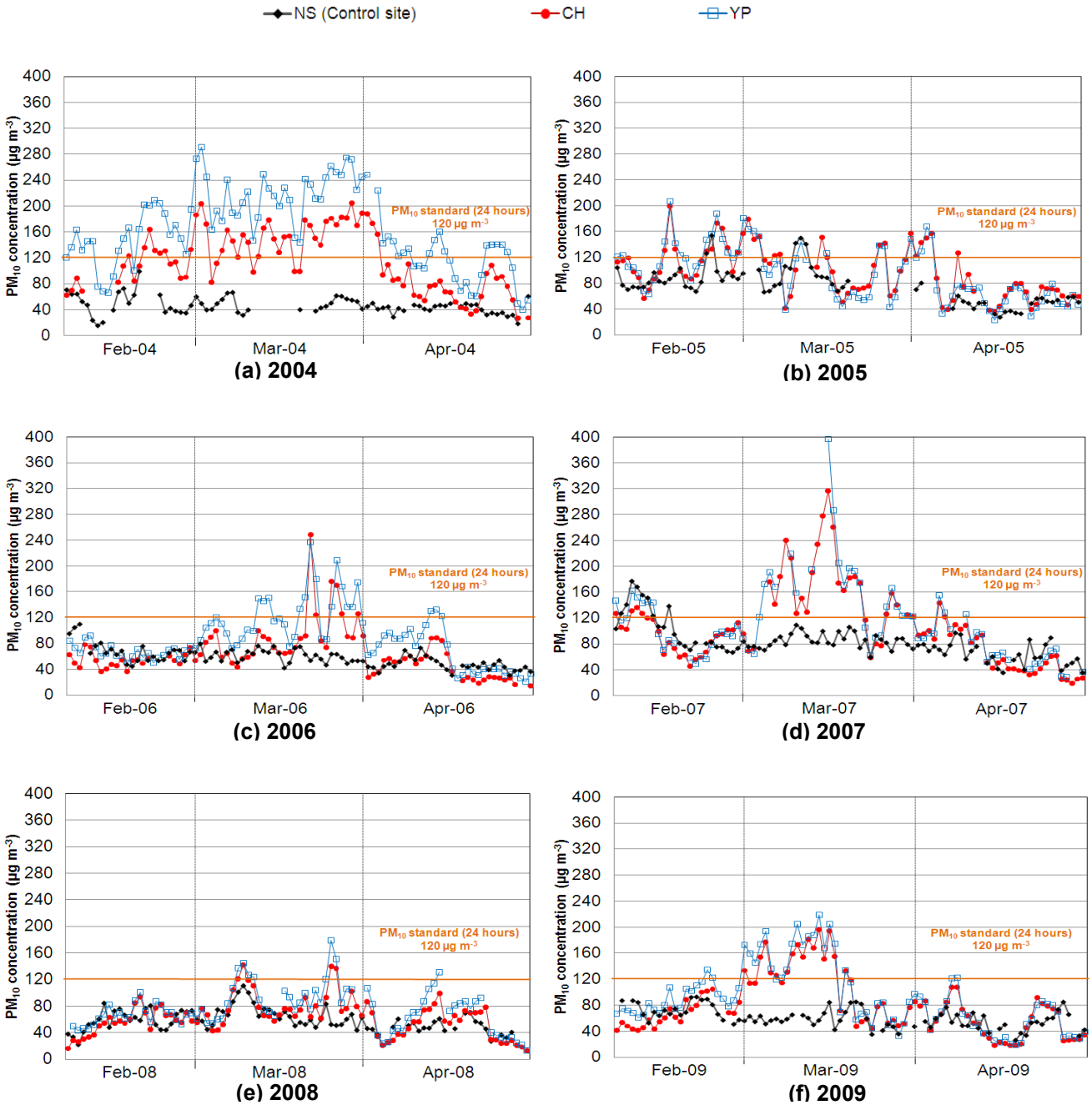

Figure 3. 24 hr-PM_{10} variation during February-April, 2004-2009 obtained from 3 AQM stations; NS, CH and YP.

Numbers of days those PM_{10} concentrations exceeded 24 hr national standard (120 μg m^{-3}) at CH and YP stations are plotted in Figure 4. As described, PM_{10} concentrations were high in March of every year, consequently high numbers of days were found in this month. Exception was found in year 2005, in which February presented the highest values for both stations. At the CH station in March, the numbers of days those PM_{10} concentrations exceeded the standard in a descending order were 2004 (27 days, 87%) > 2007 (23 days, 74%) > 2009 (14 days, 45%) > 2005 (8 days, 26%) > 2006 (6 days, 19%) > 2008 (4 days, 13%) while those at YP station were 2004 (30 days, 97%) > 2007 (19 days, 61%) > 2009 = 2006 (14 days, 45%) > 2008 (7 days, 22%) > 2005 (6 days, 19%). The highest percentage of numbers of days for both CH and YP stations were in March 2004 as presented in Figure 4. The PM_{10} data was found to relate with burnt forest area in northern region, which was also highest in 2004. (Department of National Parks, Wildlife and Plant Conservation, Thailand). However, the cumulative percent of PM_{10} concentrations at these two stations were highest in year 2007 (Figure 5). High PM_{10} concentrations in March obviously affected to cumulative percent of PM_{10}. Kim Oanh and Leelasakultum (2011) reported that weak wind and strong inversion, was most associated with haze episodes with the highest daily PM_{10} concentrations in Chiang Mai during 2001–2008. These meteorological conditions dominated during the severe haze episode in March 2007. Local sources including open biomass burning were also highest during March 2007 while the traffic emission presented stable pollutant emission for whole year. Therefore, year 2007 was selected for analysis of contribution of long-range transport on haze episode in Upper Northern Thailand.

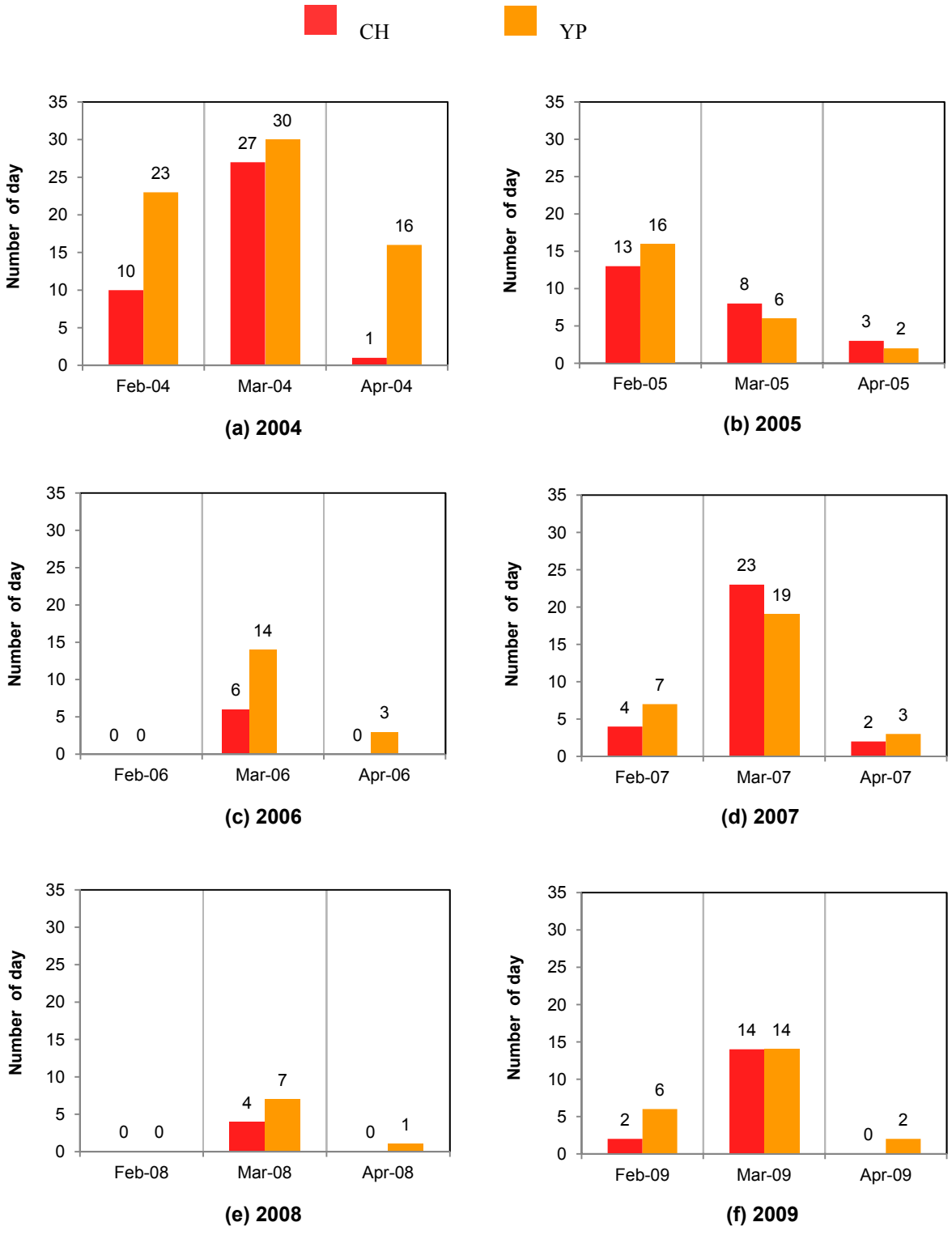

Figure 4. Numbers of days that PM_{10} concentrations higher than the Thailand's standard (24 hr.) in Chiang Mai, 2004-2009.

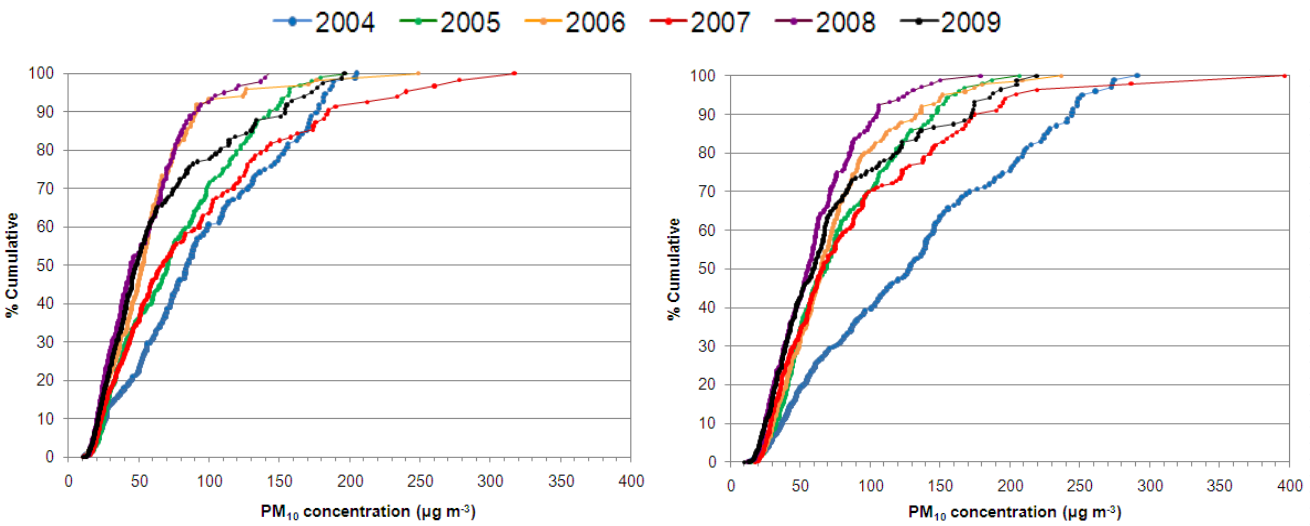

(a) CH **(b) YP**

Figure 5. The cumulative percent of PM_{10} concentrations in Chiang Mai, 2004-2009.

3.2 PM_{10} levels and wind speed

Wind speed and PM_{10} concentrations at the CH station during February to April, 2004-2009 were analyzed to find out their correlations (Figure 6). It was found that the correlations between wind speed and PM_{10} concentrations were all negative. Moreover, those correlations were stronger in year 2004 (r = -0.476) than those in 2007 (r = -0.442) and 2009 (r = -0.445). The values were almost the same with the study in Athens, Greece, which reported the correlation of -0.43 (Chaloulakou *et al.*, 2003). This observation demonstrated clear relationship between PM_{10} concentrations and wind speed. The strong negative correlation implied that wind speed is an important factor of PM_{10} concentrations. Strong wind flushes pollutants out of the Chiang Mai basin, while calm wind allows air pollutants to accumulate in the basin.

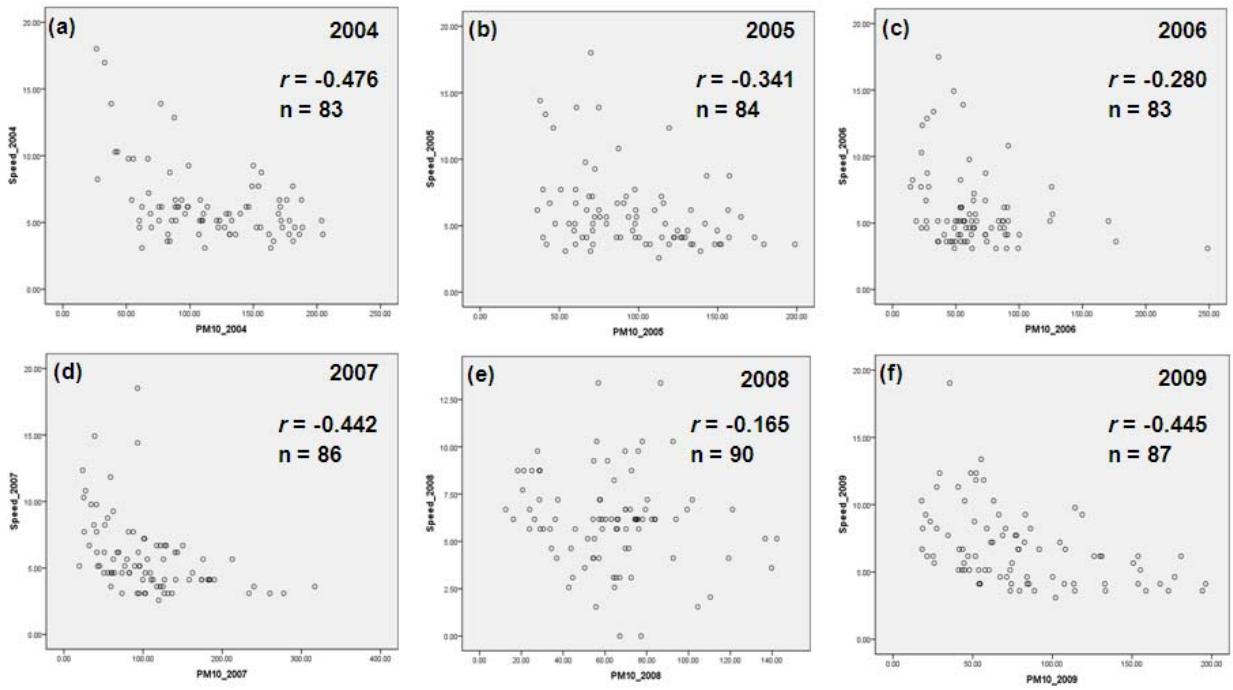

Figure 6. The correlation between wind speed and PM_{10} concentrations in Chiang Mai during February-April, 2004-2009.

3.3 Relationship between PM_{10} and hotspot number

In order to assess the contribution of long-range transport on haze episode in this area, the CH station was selected as a representative of Chiang Mai province. The location is more appropriate due to less effect from local sources such as traffic and communities. Therefore, its PM_{10} data was analyzed for further detail.

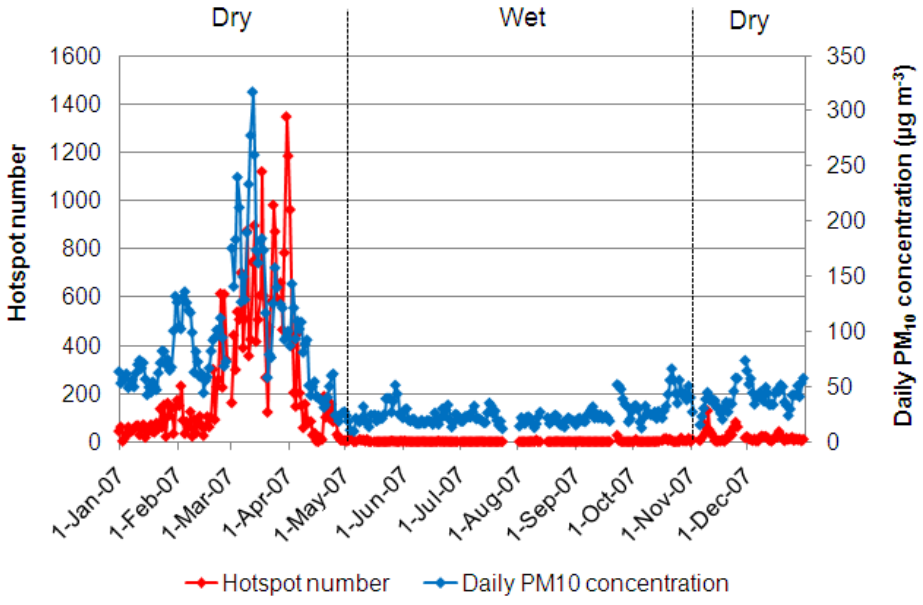

Figure 7. Variation between hotspot number and daily PM_{10} concentrations2007 .

PM_{10} concentrations obtained from the CH station as well as hotspot data in 2007 were plotted as shown in Figure 7. The results revealed that those data series were much higher in dry season than those in wet season. Both hotspot number and daily PM_{10} concentrations were high during January to April and they were highest in March. In dry period, fires are set for the most part in northern Thailand to clear land for subsequent cultivation by burning of agricultural waste. In addition, topography of northern Thailand in association with high number of open burning and meteorological conditions (temperature inversion) in dry season, air pollutants are accumulated in the mountain valleys and can be hardly escaped. Therefore, high concentrations of particulate matter and other harmful substances are reached.

Moreover, numbers of hotspot and PM_{10} concentrations were analyzed to find out correlation of each period (Table 1). The analysis showed that their correlations were positive. The whole year data were well correlated (r = 0.722). The correlations in dry season were relatively strong (0.532-0.659) while in the wet season it was relatively low (r = 0.330).

Table 1. Pearson correlations of hotspot number and PM_{10} concentrations, Year 2007.

Periods		Number of days (N)	Pearson correlation (*r*)
Whole year	Jan-Dec	337	0.722
Dry season	Jan-Apr, Nov-Dec	172	0.659
	Feb-Apr	86	0.532
Wet season	May-Oct	165	0.330

3.4 Classification of air mass trajectories

The 3-day backward trajectories of air masses arriving at Chiang Mai from January to December 2007 were determined. Classification of air mass trajectories were performed for whole year (2007) and also for each season: wet season (May-October) and dry season (January-April and November-December). Moreover, those of haze episode (February-April) were mainly considered.

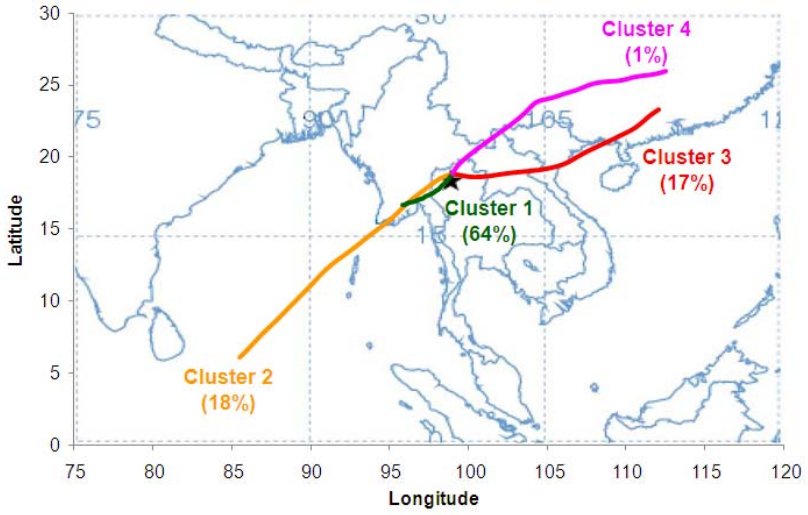

Figure 8. 3-day backward trajectories of clusters for whole year 2007.

The data for whole year (335 days; 100%) were analyzed by cluster analysis. Air mass trajectory can be classified into 4 clusters and percent of data in cluster 1, 2, 3 and 4 were 64%, 18%, 17% and 1%, respectively (Figure 8). The trajectory directions of all clusters were found to be in almost the same direction, which were southwest and northeast of the receptor. The 1st cluster (southwest of the receptor) was a major direction of air mass. The origin of trajectory in cluster 1 was in southern Myanmar continent and directly move northeast arrived the receptor. The cluster 2, 3 and 4 were similar in terms of length. For cluster 2, the trajectory started from Indian Ocean and entered inland at the south of Myanmar before arriving Chiang Mai in the same direction with cluster 1. Air mass of cluster 3 originated from the south of China passing the Pacific Ocean, entered inland at the northeast of Vietnam and move through Laos and the receptor in the east. The last cluster started from the south of China and moves southwest through northern part of Laos to reach Thailand.

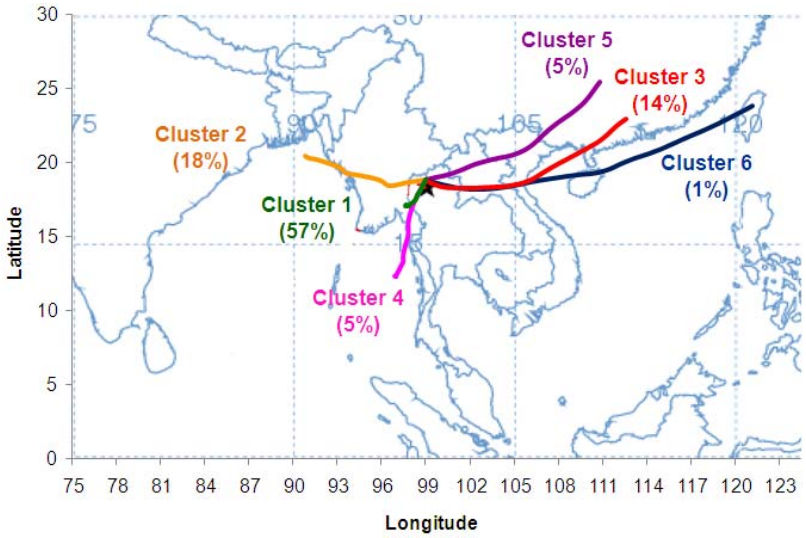

Figure 9. 3-day backward trajectories of clusters for dry season 2007 (January-April and November-December).

Back trajectories of the data of dry season (170 days including January-April and November-December) were grouped into 6 clusters as shown in Figure 9. 57% of the data were in cluster 1 (local area). Cluster 2, 3, 4, 5 and 6 contain 18%, 14%, 5%, 5% and 1%, respectively. The cluster 2 came from Indian Ocean and entered inland at southern Myanmar before arriving Chiang Mai. Air mass of cluster 4 started from Indian Ocean and arrived at the receptor in the south. Directions of air mass of cluster 3, 5 and 6 were the same as northeast monsoon direction. Cluster 3 and 5 originated at the south of China through Vietnam and Laos. Direction of cluster 6 was closed to cluster 3 but with longer pathways over the Pacific Ocean with clean air mass.

Air mass trajectories during haze episode (February to April) were run again to analyze pattern of air mass direction. They can be clustered into 6 groups as shown in Figure 10. All of air mass trajectories were presented distinct difference in terms of both direction and origin area. The frequency of all backward trajectories (86 days; 100%) were highest in the cluster 1 (75%) which came from southern Myanmar, while the

cluster 2 still originated from Myanmar at the southeast (15%). Moreover, the wind direction (Figure 11) during this period was well associated with this result which mostly started from western Thailand. The percent of air mass trajectories in cluster 3, 4, 5 and 6 were 4%, 2%, 2% and 2%, respectively. The air mass of cluster 3 started over Pacific Ocean through Vietnam and Laos arriving to Thailand. Cluster 4 originated over Indian Ocean and travel over Myanmar to the receptor while cluster 5 still started from Indian Ocean but entered inland at the south of Myanmar to Thailand. The last cluster started at the south of China through Vietnam and passing Laos before arriving to Thailand.

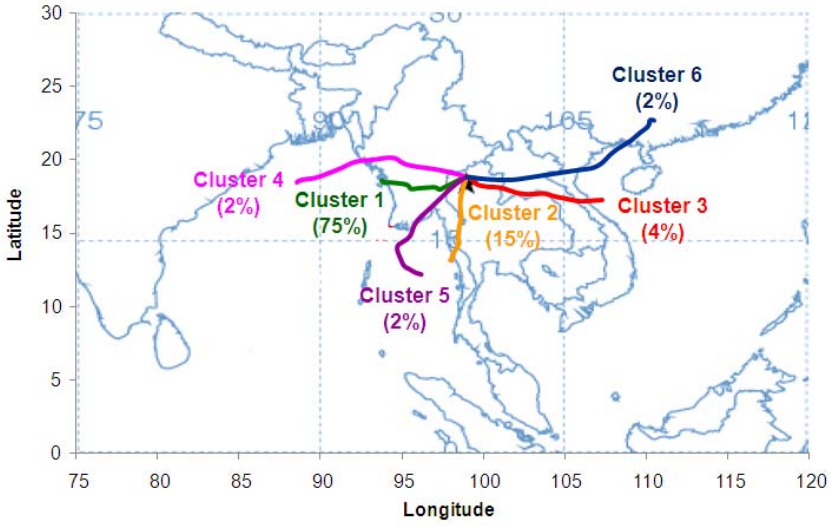

Figure 10. 3-day backward trajectories of clusters for dry season (February-April) 2007.

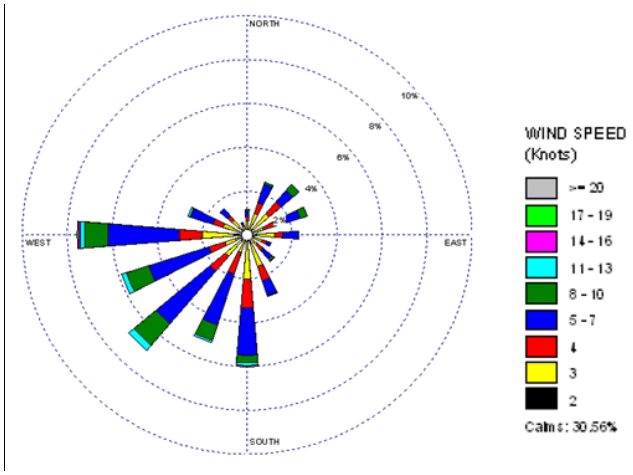

Figure 11. The windrose during February-April 2007.

The clustering of air mass in wet season (165 days) was grouped into 4 clusters (Figure 12). The trajectory of air mass in cluster 1 (55%) and cluster 3 (3%) originated from the Indian Ocean because of southwest monsoon through Myanmar and northern part of Thailand. The percent of data in cluster 2 were 41%. The air mass of cluster 2 started in the boundary of Vietnam and travel over Laos before arriving at the receptor

in the east while for cluster 4 (1%) came from China and directly move to northern Laos before arriving at Thailand.

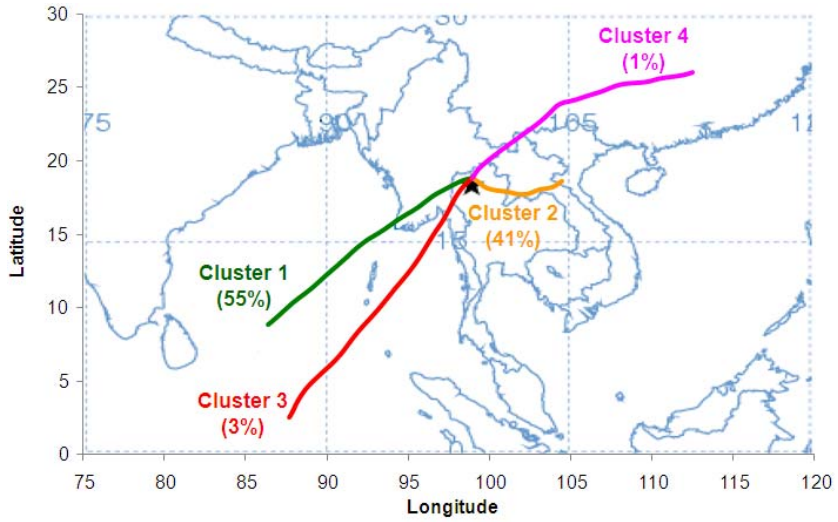

Figure 12. 3-day backward trajectories of clusters for wet season (May-October) 2007.

4. Conclusions

Haze episode in northern Thailand during March to April of almost every year was found to associate with the levels of daily PM_{10} in Chiang Mai. During 2004-2009, PM_{10} concentrations were high in dry season especially in March 2004 and 2007, which coincided with the strong correlation of hotspot number and daily PM_{10} concentrations. On the other hand, PM_{10} concentrations and wind speed were negatively correlated.

From cluster analysis, air mass trajectory mainly originated from western continent of Thailand during February to April 2007, while air mass trajectory in overall dry season (January-April and November-December) mainly came from local. In conclusion, major air masses in dry season came from the western continent of Thailand as well as local, which indicated potential sources of aerosols and pollutants to northern Thailand during haze period. However, more data in other years i.e. 2004 (episode year) and 2008 (background year) should also be applied to assess long-range transport contribution to air pollution in Chiang Mai to compare and confirm these results.

5. Acknowledgements

Financial supports from the Network Center for the Acid Deposition Monitoring Network in East Asia (EANET), Asia Center for Air Pollution Research (ACAP) and the Graduate School of Chiang Mai University are gratefully acknowledged. We also thank Pollution Control Department (PCD), Thailand, Fire Information for Resource Management System (FIRMS) and Thai Meteorological Department (TMD) for providing observation data and the NOAA Air Resources Laboratory (ARL) for the HYSPLIT dispersion model.

6. References

Baldasano, J.M., Valera, E. and Jimenez, P. 2003. Air quality data from large cities. The Science of the Total Environment. 307: 141–165.

Bangkok (AFP). 2007. Disaster zone declared as Thai haze reaches dangerous levels, http://www.channelnewsasia.com/stories/afp_asiapacific/view/263903/1/.html.

Begum, B.A., Kim, E., Jeong, C.H., Lee, D.W. and Hopke, P.K. 2005. Evaluation of the potential source contribution function using the 2002 Quebec forest fire episode. Atmospheric Environment. 39: 3719-3724.

Chaloulakou, A., Kassomenos, P., Spyrellis, N., Demokritou, P. and Koutrakis, P. 2003. Measurements of PM_{10} and $PM_{2.5}$ particle concentrations in Athens, Greece. Atmospheric Environment. 37: 649-660.

Department of National Parks, Wildlife and Plant Conservation, Thailand, Retrieved from http://www.dnp.go.th.

Draxler, R.R. and Hess, G.D. 1997. Description of the HYSPLIT 4 modelling system. NOAA Technical Memorandum, ERL ARL-224. http://www.arl.noaa.gov/data/web/models/hysplit4/win95/arl-224.pdf.

Godish, T. 1997. Air Quality. Third Edition. Lewis Publishers, New York.

Kim Oanh, N.T. and Leelasakultum, K. 2011. Analysis of meteorology and emission in haze episode prevalence over mountain-bounded region for early warning. Science of the Total Environment. 409: 2261-2271.

Na Nongkhai, K. 2004. Prediction of noise level due to traffic in Chiang Mai urban area. M.S. Thesis, Chiang Mai University.

NASA/University of Maryland. 2002. MODIS Hotspot / Active Fire Detections. Data set. MODIS Rapid Response Project, NASA/GSFC [producer], University of Maryland, Fire Information for Resource Management System [distributors]. Available on-line [http://maps.geog.umd.edu].

Stein, A.F., Lam, D. and Draxler, R.R. 2000. Incorporation of detailed chemistry into a three-dimensional Lagrangian–Eulerian hybrid model: application to regional tropospheric ozone. Atmospheric Environment. 34: 4361–4372.

Patashnick H., Meyer M. and Rogers B. 2002. Tapered element oscillating microbalance technology. Proceedings of the North American/Ninth U.S. Mine Ventilation Symposium. pp 625-631.

Pongkiatkul, P. and Kim Oanh, N.T. 2007. Assessment of potential long-range transport of particulate air pollution using trajectory modeling and monitoring data. Atmospheric Research. 85: 3–17.

Wang, K.Y., Shallcross, D.E., Hadjinicolaou, P. and Giannakopoulos, C. 2004. Ambient vehicular pollutions in the urban area of Taipei: Comparing normal with anomalous vehicle emissions. Water, Air and Soil Pollution. 156: 29-55.

Washington State Department of Ecology Air Quality Program. 2004. PM_{10} Tapered Element Oscillating Microbalance Operating Procedure. Air Quality Program.

Zeng, J., Tohjima, Y., Fujinuma, Y., Mukai, H. and Katsumoto, M. 2003. A study of trajectory quality using methane measurements from Hateruma Island. Atmospheric Environment. 37: 1911–1919.

Study on Model Simulation of Meteorological Parameters and Air Concentrations in South East Asia by using WRF and CMAQ

Pham Van Sy[1]* and Keiichi Sato[2]

[1]Center for Environmental Research, Vietnam Institute of Meteorology Hydrology and Environment, Vietnam.
*Contact address: 5/62 Nguyen Chi Thanh, Hanoi, Vietnam.
E-mail: phamsymt@gmail.com
[2]Asia Center for Air Pollution Research, Japan.
E-mail: ksato@acap.asia

Abstract

The model simulation study was performed for Southeast Asian region in which a few modeling study has been conducted. Meteorological parameters simulated by Weather Forecast and Research Model (WRF) and air quality data simulated by Community Multi-scale Air Quality (CMAQ) modeling system were compared by the monitoring data in Vietnam, China and Thailand. Temperature, relative humidity and wind field were relatively well reproduced by the model, whereas there large discrepancy from the observed rainfall data. The air quality simulation of some air pollutants such as SO_2, NOx, O_3 are generally agreed with daily concentrations. However, in some cases, there is large discrepancy, which implies that more elaboration of WRF and CMAQ model is necessary. The model results showed concentrations of SO_2 and NO_2 are high in urban area in Vietnam, China and Thailand.

1. Introduction

Many recent researches and observed data from satellite and air quality monitoring stations have demonstrated severe air pollution in East Asia, and total emission of Asian area has been being highly greater than that of Europe and America. Because this increasing trend is continuing, air pollution in East Asian region will be a big problem in the future. It will have significantly negative effect on lives and health of not only people in this region but also other continents.

The atmospheric modeling analysis is helpful to analyze the temporal and spatial variation of air pollutants and coverall the status of air pollution in the region. There are a number of modeling study in

Northeast Asia such as MICS Asia project (Carmichael, 2007), whereas there is a few of modeling study in Southeast Asian region (Engart and Leong, 2001) because of occasional heavy squall and equatorial convection. In this research, simulation results of meteorological parameters obtained by Weather Research and Forecasting (WRF) model and air concentrations (air quality) by Community Multiscale Air Quality (CMAQ) model were compared with observation data. Then, the feasibility of model simulation was discussed based on comparison results.

2. Model description

2.1. CMAQ modeling

The Community Multiscale Air Quality (CMAQ) model (Byun and Chere, 2006) developed by U.S. Environmental Protection Agency is a three-dimensional eulerian atmospheric chemistry and transport modeling system that simulates gaseous species, acid deposition, fine particulate matter, etc. in the troposphere. Designed as a one-atmosphere model, CMAQ can address the complex couplings among several air quality issues simultaneously across spatial scales ranging from local to hemispheric. The CMAQ source code is highly transparent and modular to facilitate extensibility through community development.

CMAQ is a third-generation air quality model that is designed for applications ranging from regulatory and policy analysis to understanding the complex interactions of atmospheric chemistry and physics. First-generation air quality models simulated air quality using simple chemistry at local scales, and Gaussian plume formulation was the basis for prediction. Second-generation models covered a broader range of scales (local, urban, regional) and pollutants, addressing each scale with a separate model that often focused on a single pollutant (e.g., ozone). Third-generation models, like CMAQ, treat multiple pollutants simultaneously up to continental or larger scales, often incorporating feedback between chemical and meteorological components. The Model-3/CMAQ system was first released to public in July 1998 and had a recent update release in October 2006.

In this research, CMAQ version used is 4.6, carbon mechanism IV (CBM-IV). The domain has the same horizontal size as WRF (as described in I.1 section), but different in vertical size with only 6 layers because of limited technical capability when creating emission files.

In order to make comparison between CMAQ results and observed data, the simulated data is interpolated by 4 nearest grid points at co-ordinate which is the same location of air quality monitoring station, and these length of distances are weighted factors. The simulated data is extracted and compared in daily, weekly or monthly depending on data feature of observing station such as frequency, available data. The result of pollutants simulation from CMAQ depend on much REAS emission data, therefore, this research just assess, but not analyze deeply the reasons.

2.2. WRF model and model domain

Weather Forecast and Research Model (WRF) is developed with co-operation of many organizations over the world such as NCAR/MMM, NOAA/NCEP, AFWA. WRF is open source code with many preeminent

features. Therefore, as its first appearance it has been received significant interest and widely applied in professional weather forecast as well as researches in many countries. It is regularly updated with the latest version 3.2.1, which is employed in this research.

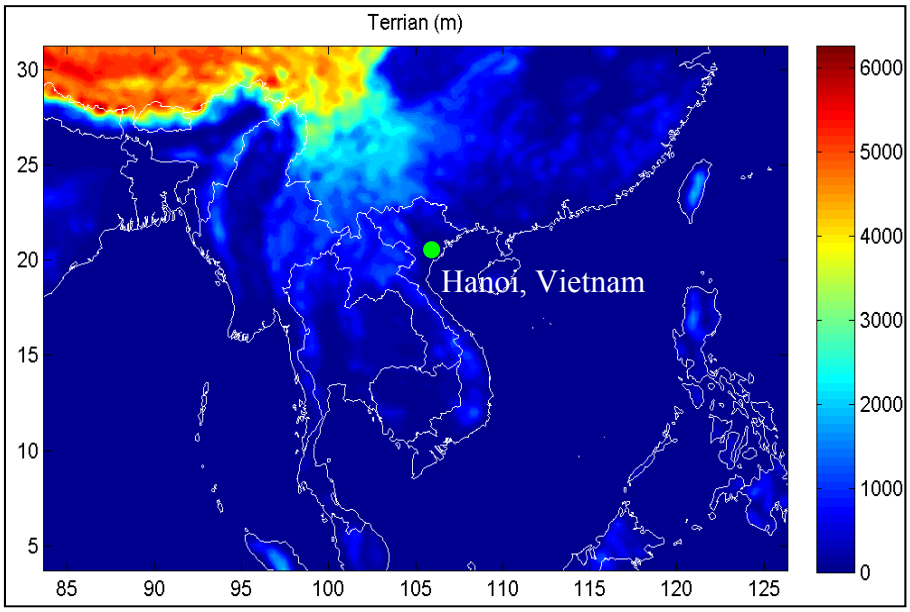

Figure 1. Map of model domain.

WRF model was run with Mercator projection centered at 18º N and 105º E. Terrain data derived from the US. Geological Survey (Figure 1) and global 25-category data of vegetation type and land-use data, with a resolution of 20 second. The WRF domain fixed in the research includes 158 x 108 grid cells, with the resolution of 30 x 30 km, extended from 0º N to 360º N and 87º E to 123º E. Horizontal resolution applied was the same in both WRF and CMAQ, but different in vertical resolution, whereas WRF has 28 vertical layers, CMAQ just has 6 layers in the sigma co-ordinate system, up to 500 hPa in height.

The input meteorological data used for WRF initialization are global reanalysis data with 6 hours on average with the period from December, 2008 to December, 2009. The WRF output files were processed by Meteorology Chemistry Interface Processor version 3.4 (MCIP 3.4) for subsequent chemical transport simulation by CMAQ. In order to minimize initial errors, WRF model was run 10 days before the modeling period.

2.3. Emission inventory

(a) Anthropogenic emission

Anthropogenic emission used in the research were obtained from Regional Emission Inventory in Asia (REAS) including some species: CH_4, CO, NH_3, NOx, and VOC for whole Asian from December, 2008 to December, 2009, they are annual data with 0.50º x 0.50º in resolution . They were extracted and interpolated into decided domain for the research area, besides they were also converted to suitable format for requirement of CMAQ model (Figure 2).

(b) Biogenic emission

Biogenic emission were obtained from Global Inventory for Chemistry-Climate Studies (GICC) for global area from 1997 – 2005, including CO, NOx, SO_2, and VOCs. They are monthly data with 10º x 10º in resolution (Figure 3). They were calculated based on product of SPOT-vegetation satellite and ATSR. Ratio factors were separately applied for forecast ecosystem and grassland to ensure continuous data in some periods, and month average data were considered seasonal inventory factors in whole period.

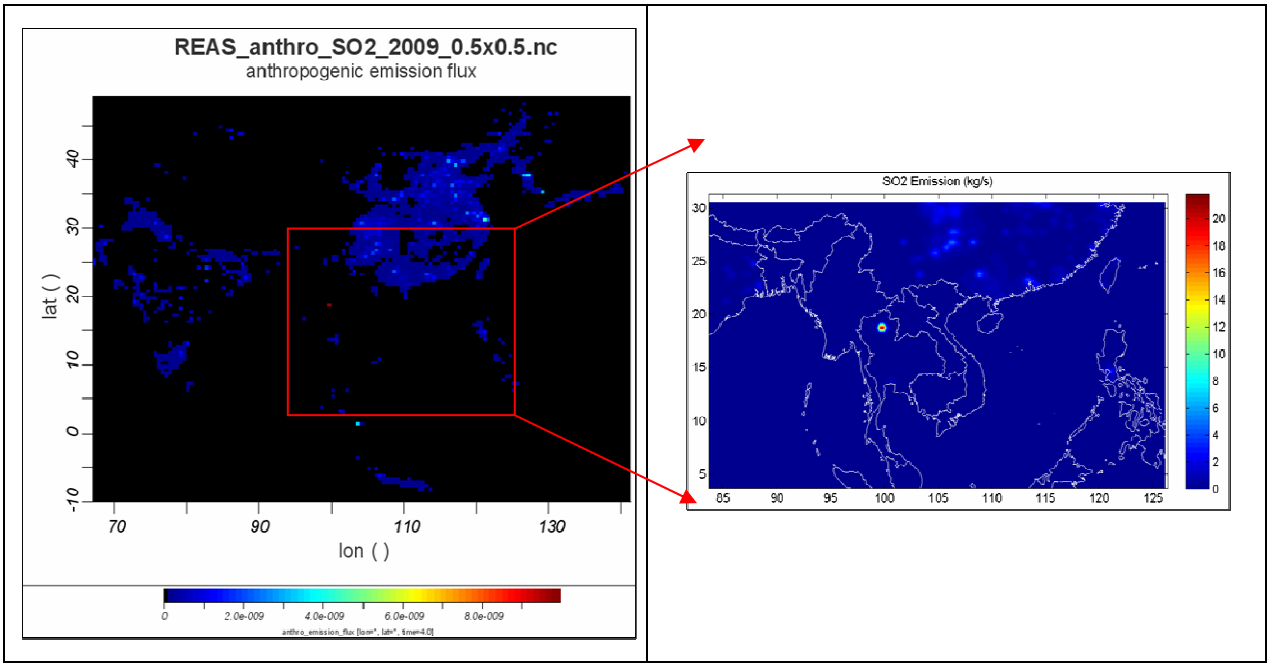

Figure 2. Map of SO_2 anthropogenic contribution in the research area interpolated from emission inventory of Asian area in 2009.

As the same as anthropogenic emission, biogenic emission data was extracted and interpolated into researching domain. Due to biogenic emission data is just from 1997 to 2005, whereas year simulated is 2009, therefore it is calculated as follow: (i) Calculating increase/decrease rate of monthly biogenic emission at each grid point in whole the period, (ii) Multiplying them with 2005 biogenic emission to make 2009 biogenic emission.

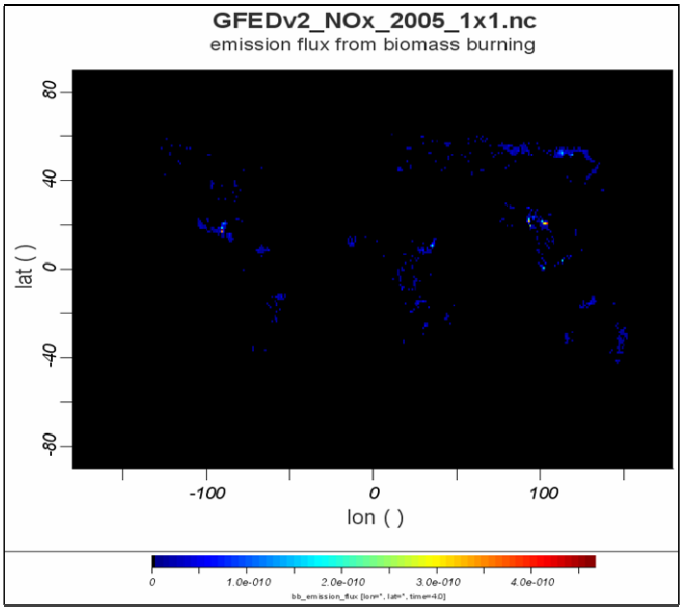

Figure 3. Map of global biogenic emission of NOx, 10ºx10º resolution in 2005.

3. Results and discussion

3.1. Simulation of Meteorological Parameters over South-East Asia

For assessing the simulation results of meteorological parameters, the time series of their simulation data were extracted at co-ordinate which is the same as location of weather monitoring stations employed 4 nearest grid points – interpolated method with distance lengths considered for weighted coefficients (Figure 4).

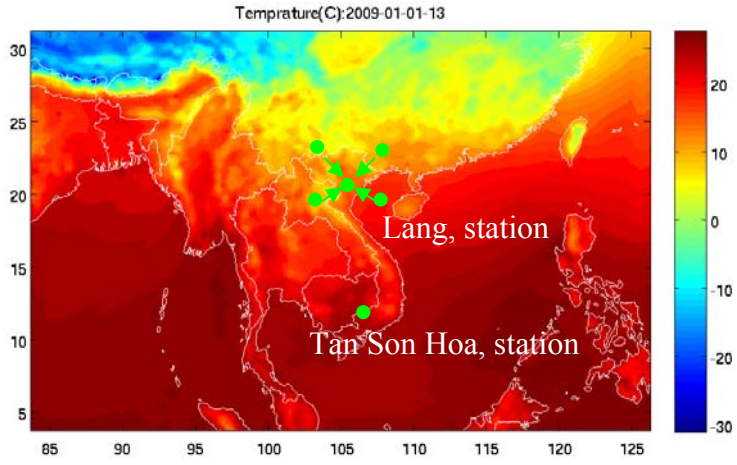

Figure 4. Map of temperature distribution in the model domain on January 1, 2009.

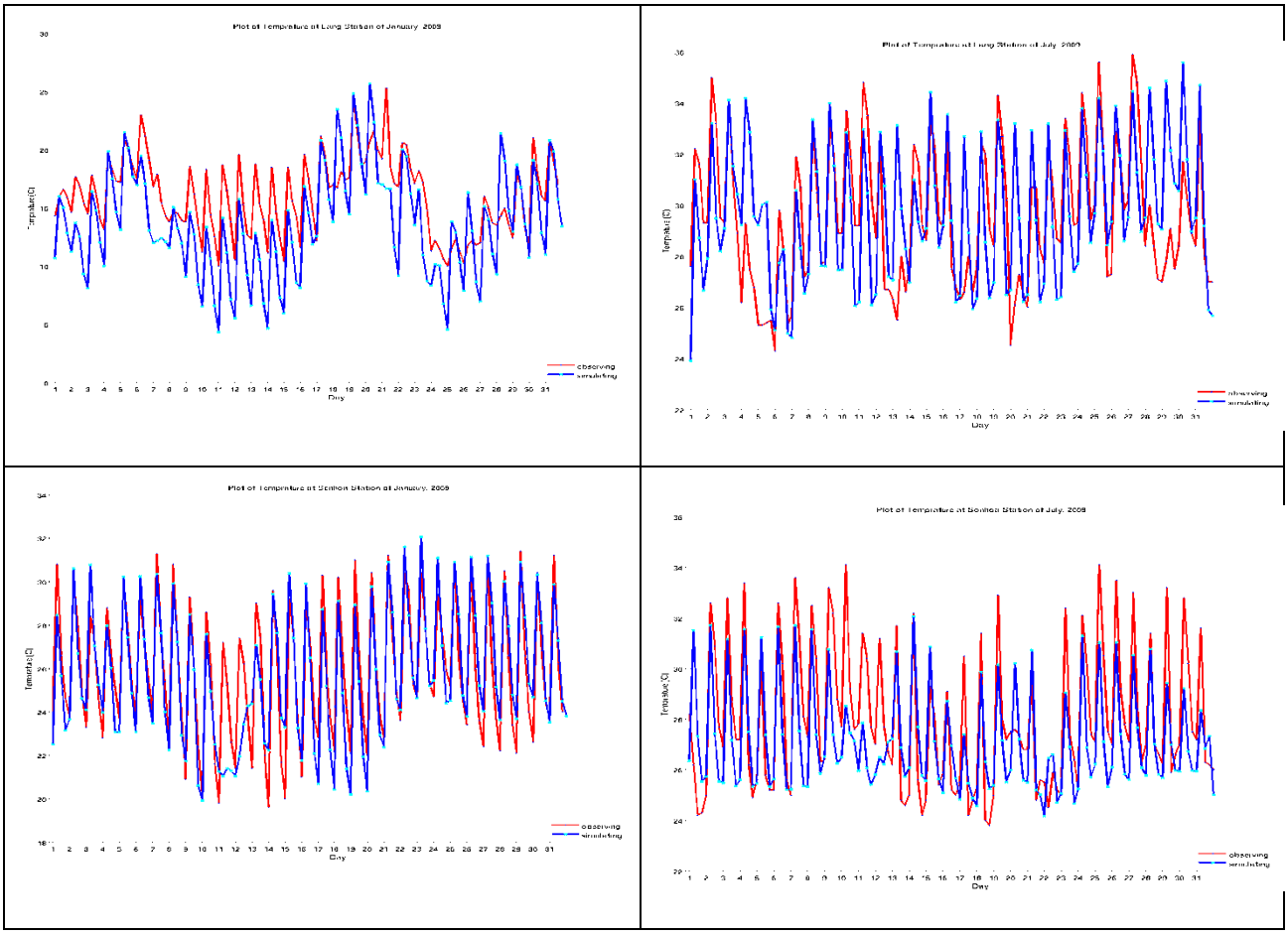

Figure 5. Comparison of modeled (blue) and observed (red) temperature in January (on the left) and July (on the right) at Lang station (above) and Tan Son Hoa station (below).

The comparing results at two stations show that, temperature simulation showed generally good reproduction in the research region, most time profiles comparison perform high coincidence. However, in some points, temperature simulating value is not still high accurate, it is sometimes higher and lower than observed data, and slight dephasing (Figure 5).

Due to just have absolute humidity from WRF output files; therefore, relative humidity is calculated based on some other weather parameters such as absolute humidity, temperature, pressure. The conversion formula as describing below:

$$E_s = 6.11 * 10^{\frac{7.5*T}{237.3+T}} \quad (1)$$

$$E_p = -\frac{(H * M_{\text{air}} * P_{\text{air}} - 1)}{H * M_{\text{air}} - M_{water}} \quad (2)$$

$$RH = \frac{E_p * 100}{E_s} \quad (3)$$

in which:

Es, Ep : Saturate water vapor pressure and water vapor pressure;

T : Air temperature;

H, RH : Are absolute humidity and relative humidity respectively;

M_{air}, M_{water} : Air density and water density respectively.

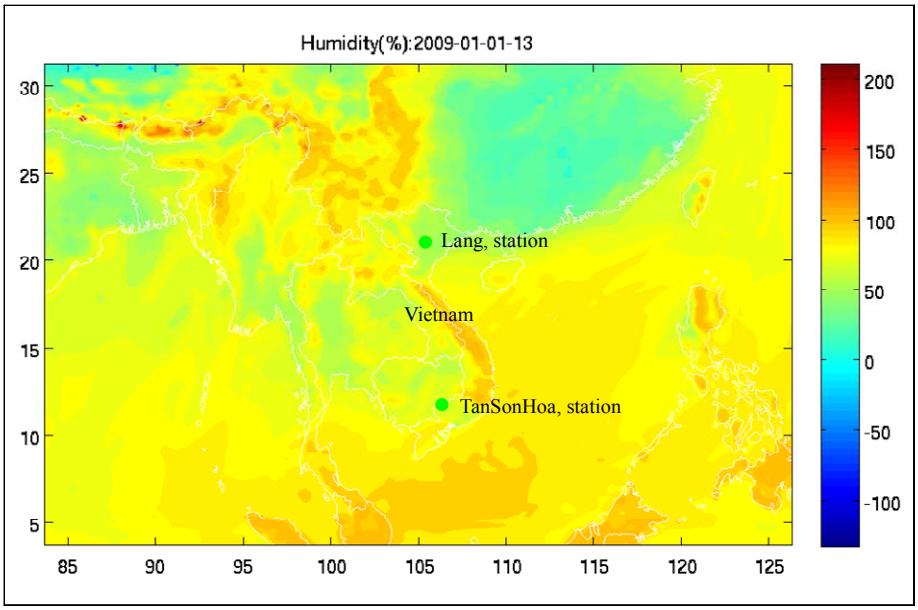

Figure 6. Map of relative humidity distribution in the model domain on January 1, 2009.

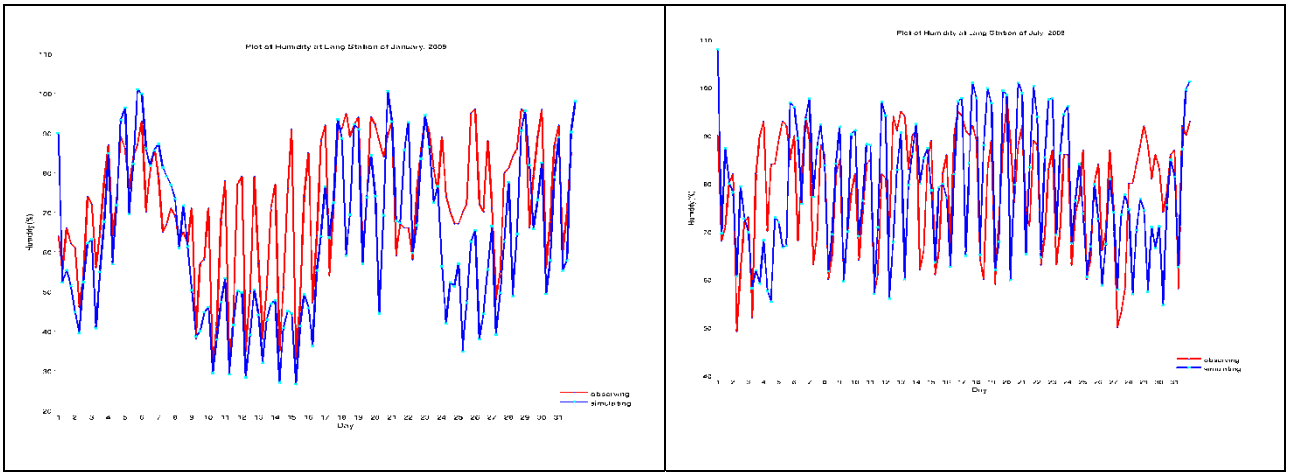

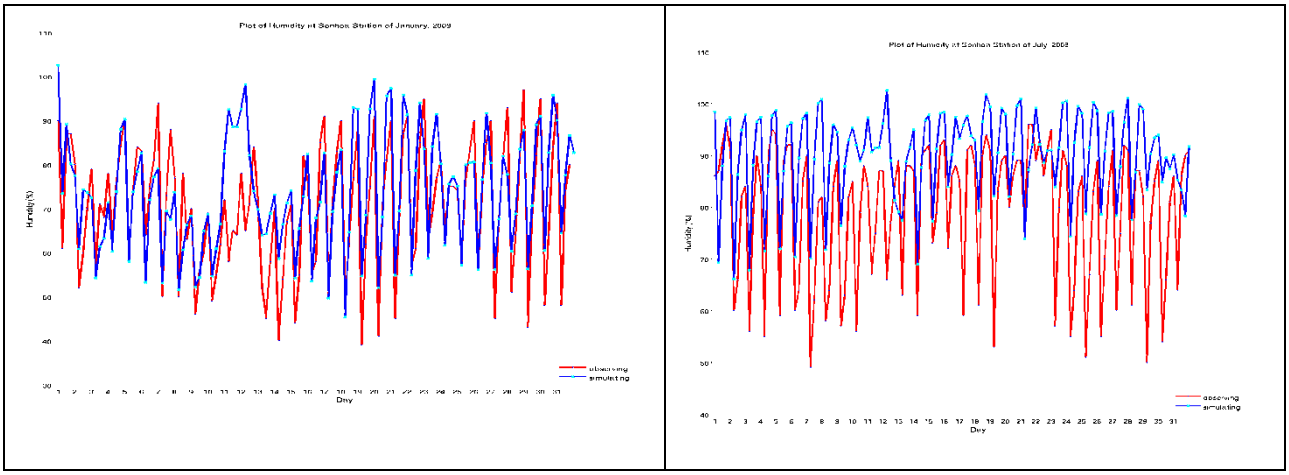

Figure 7. Comparison of modeled (blue) and observed (red) relative humidity in January (on the left) and July (on the right) at Lang station (above) and Tan Son Hoa station (below).

Figure 6 illustrates relative humidity distribution in the model domain on January 1, 2009, and Figure 7 shows comparison of modeled and observed relative humidity 2 stations in Vietnam. The comparison indicates that WRF simulated relative humidity fairly well in general, the simulated and observed time profile are concurrent. However, the same as temperature simulation, the WRF value is higher than observed data in some period of time, especially; most simulated value is 5–15% higher than observed data at Tan Son Hoa station in July.

Figure 8 illustrates wind field in the model domain on January 1, 2009, and Figure 9 shows comparison of modeled and observed wind velocity at 2 stations in Vietnam. WRF did not reproduce wind field well in both time profile and amplitude. The reasons of this discrepancy may be as follows: (i) WRF is not probably good in simulation with such coarse resolution (30 x 30 km) because of terrain affect; (ii) The wind around weather monitoring station is influenced by local obstacle such as: high building, trees, mountain; (iii) Sensitiveness of wind measuring devices do not meet small reflective changes of wind in the short time.

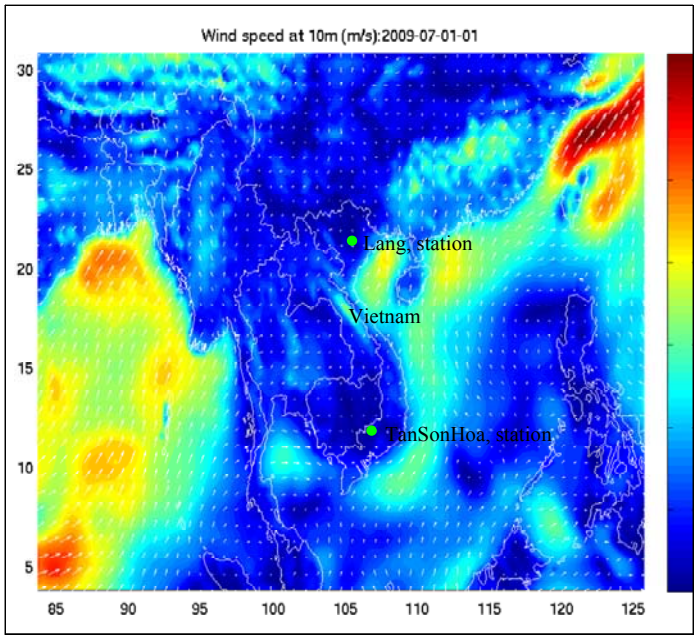

Figure 8. Map of wind field in the model domain on July 1, 2009.

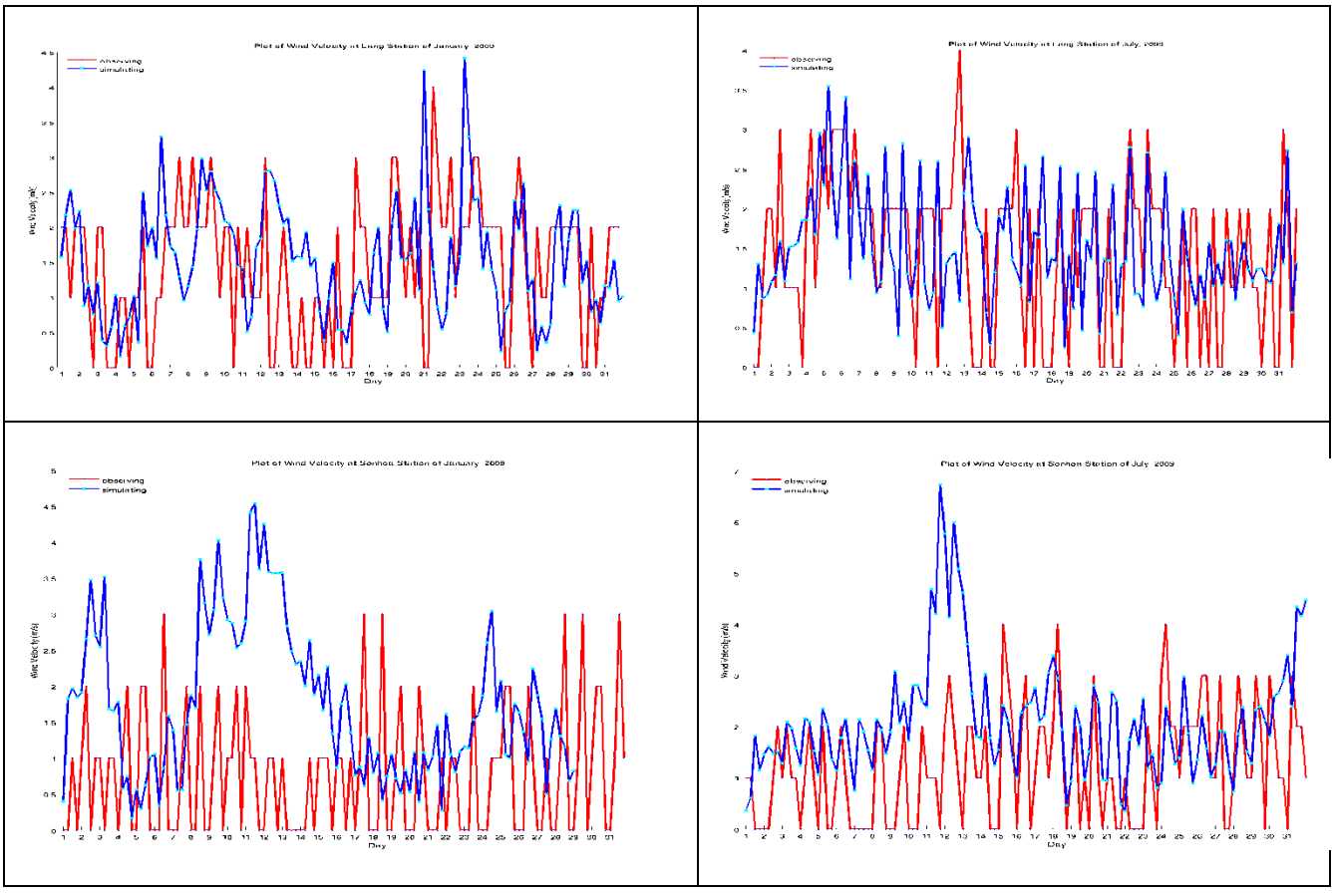

Figure 9. Comparison of modeled (blue) and observed (red) wind velocity in January (on the left) and July (on the right) at Lang station (above) and Tan Son Hoa station (below).

Comparison of rainfall at two stations Lang (in the north of Vietnam) and Tan Son Hoa (in the south of Vietnam) indicates that rainfall simulation was not so good (Figure 10, 11 and 12). At Lang station, its value is lower than observed value, whereas rainfall simulation is much higher than measured data about 5–15 mm at Tan Son Hoa station. However, when making comparison of rainfall on whole domain, it shows high resemblance between WRF rainfall simulation and satellite observed data, especially in periods which heavy rainfall occurs. These reasons can be explained as follow: (i) Humid diagram of WRF model is not able to perform well for local humid convection at coarse resolution 30 x 30 km. (ii) Extracted simulating data which is the same as site of weather monitoring stations was interpolated 4 nearest grid points, therefore, it perhaps get error from the impacts of other areas.

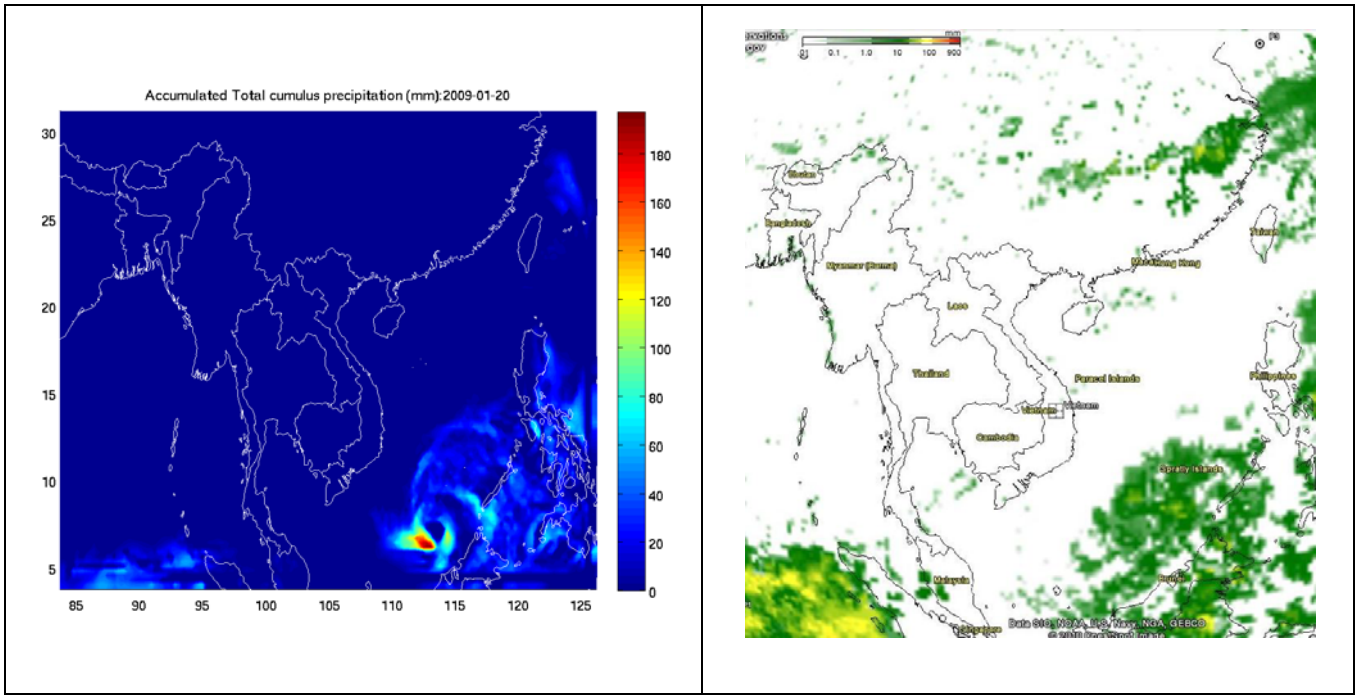

Figure 10. Comparison of rainfall contribution in research area between modeled result (left) and satellite observed data by NASA (right) on January 20, 2009.

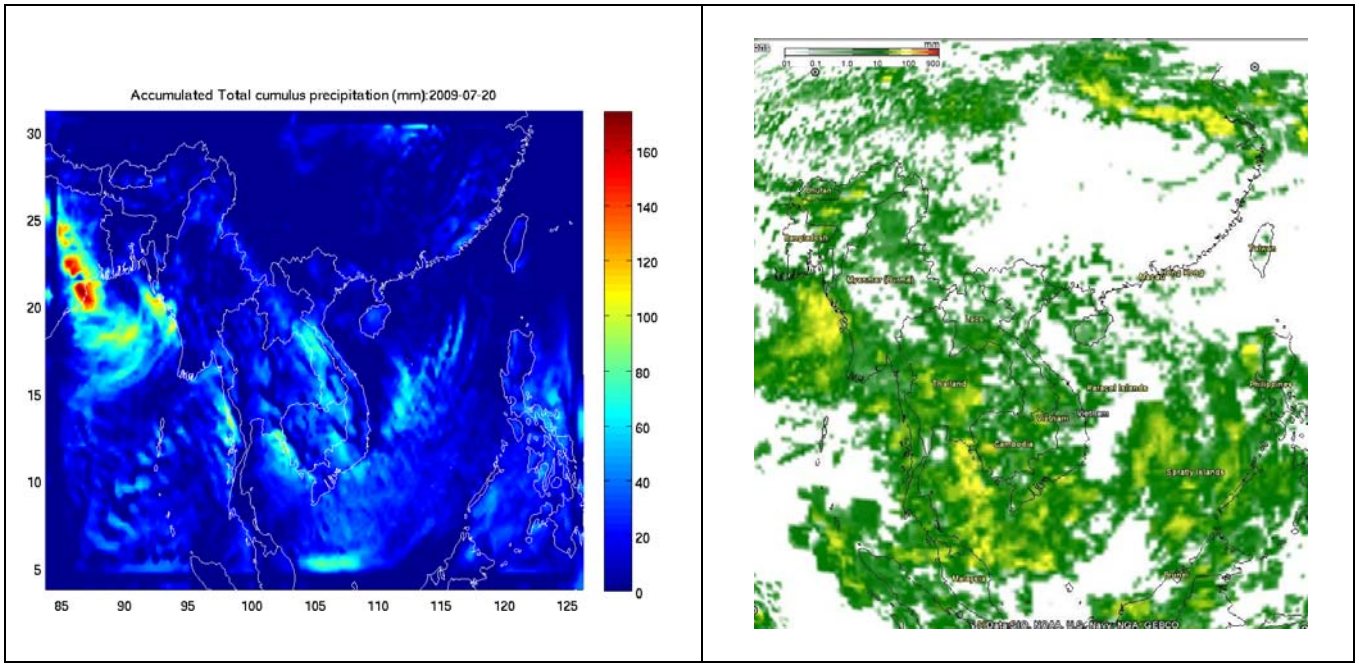

Figure 11. Comparison of rainfall contribution in research area between modeled result (left) and satellite observed data by NASA (right) on July 20, 2009.

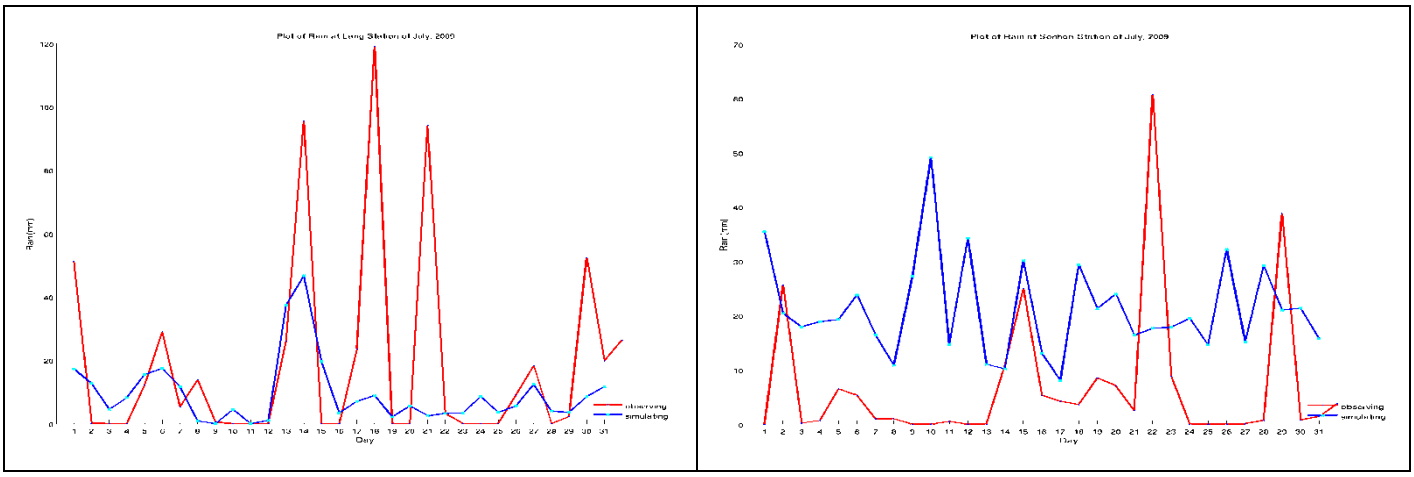

Figure 12. Comparison of rainfall at Lang station (on the left) and Tan Son Hoa station (on the right) in July 2009.

3.2. Simulation of Air Quality in South-East Asia

According to simulation of meteorological parameters, rainfall could not reproduce observation data. Because wet deposition is a major deposition process during rainy season in Southeast Asian region, it was hard to perform model simulation of atmospheric deposition. Therefore, in this study, only simulation of air pollutant concentrations (air quality) in South-East Asia was performed.

Figure 13 illustrates hourly SO_2 concentration distribution in the model domain at midnight on January 1, 2009, and Figures 14 and 15 show comparison of modeled and observed daily SO_2 concentration at 3 stations in Vietnam, China and Thailand. Simulated result showed that, the value of SO_2 concentration was higher in

some regions of south central China, fluctuating from 50 μg/m^3 to 170 μg/m^3, the highest value was showed at Chiang Mai, Thailand up to 450 μg/m^3. At Lang station in Vietnam, the simulated SO_2 concentration was generally agreed with the observed data in view of both value and time profile in January and July. On the other hand, the comparisons at Hongwen and Bangkok were not good; the simulated value is much greater than observed data, about 20 to 60 μg/m^3. The reason of this discrepancy was not clear, but local variability could be one of the reasons.

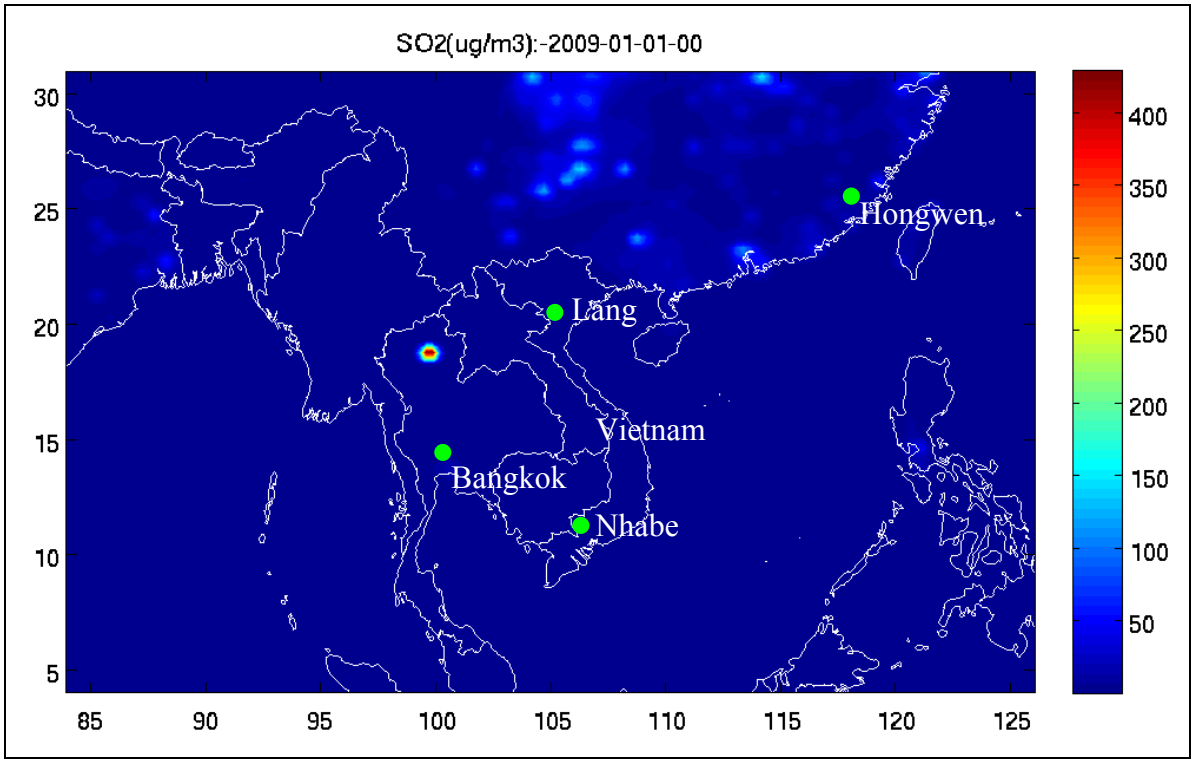

Figure 13. Distribution map of SO_2 concentration in the model domain at 0h on January 1, 2009.

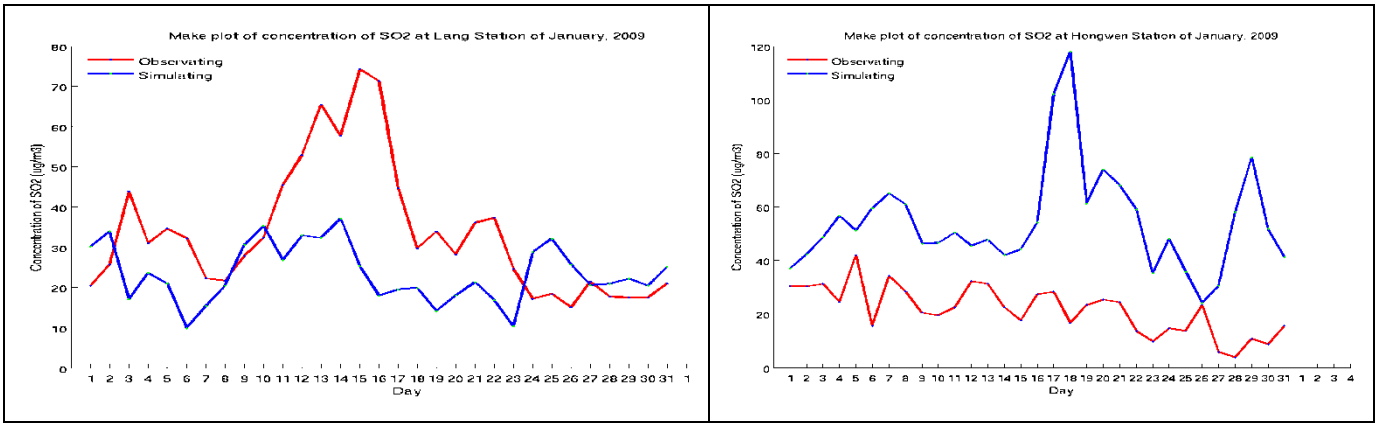

Figure 14. Comparison of modeled (blue) and observed (red) SO_2 daily concentration in January, 2009 at Lang station, Vietnam (on the left) and Hongwen station and China (on the right).

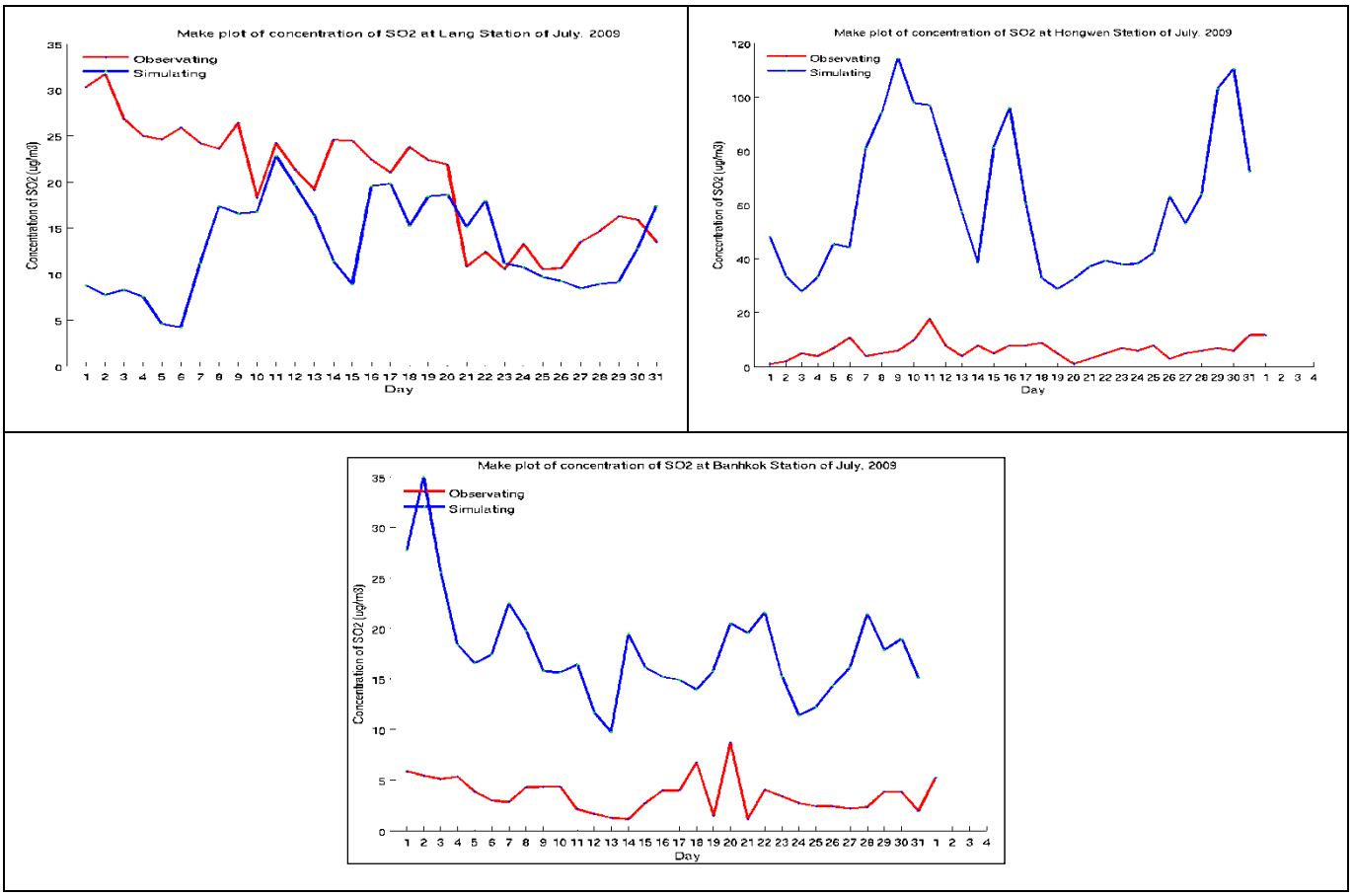

Figure 15. Comparison of modeled (blue) and observed (red) SO_2 daily concentration in July, 2009 at Lang station, Vietnam (on the above left) and Hongwen station, China (on the above right) and Bangkok station, Thailand (below).

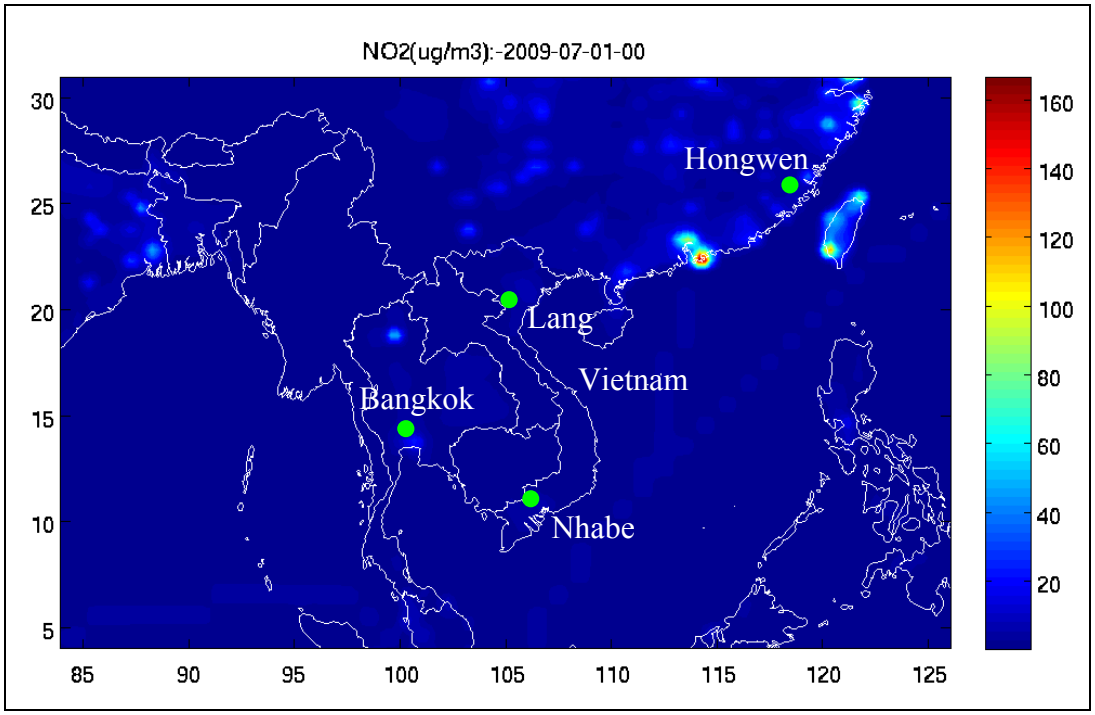

Figure 16. Distribution map of NO_2 concentration in the model domain at 0h on July 1, 2009.

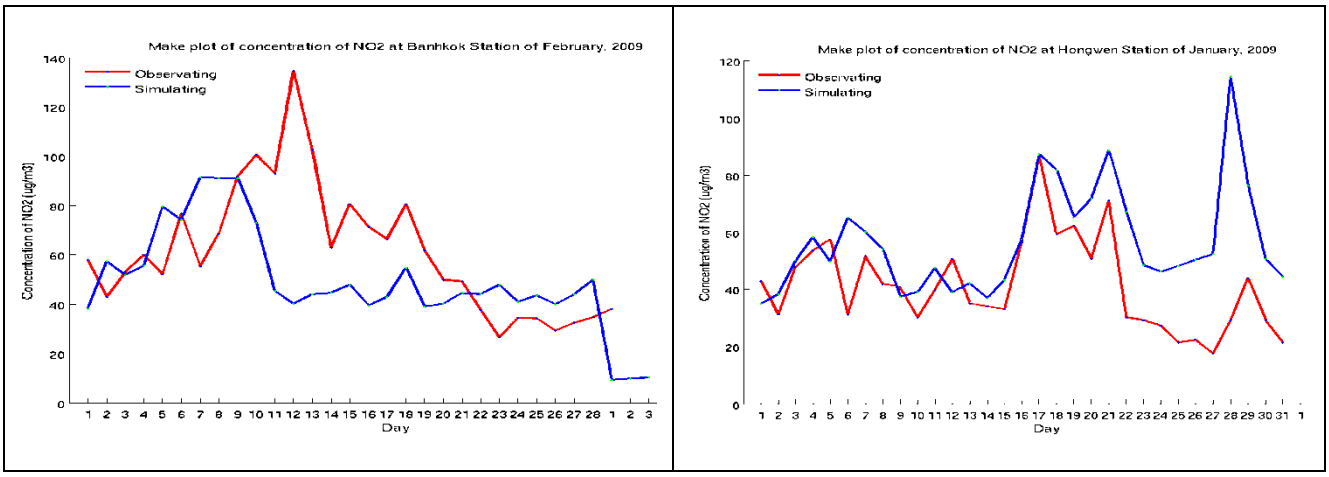

Figure 17. Comparison of modeled (blue) and observed (red) NO_2 daily concentration at Bangkok station, Thailand (left) in February, 2009 and Hongwen station, China (right) in January, 2009.

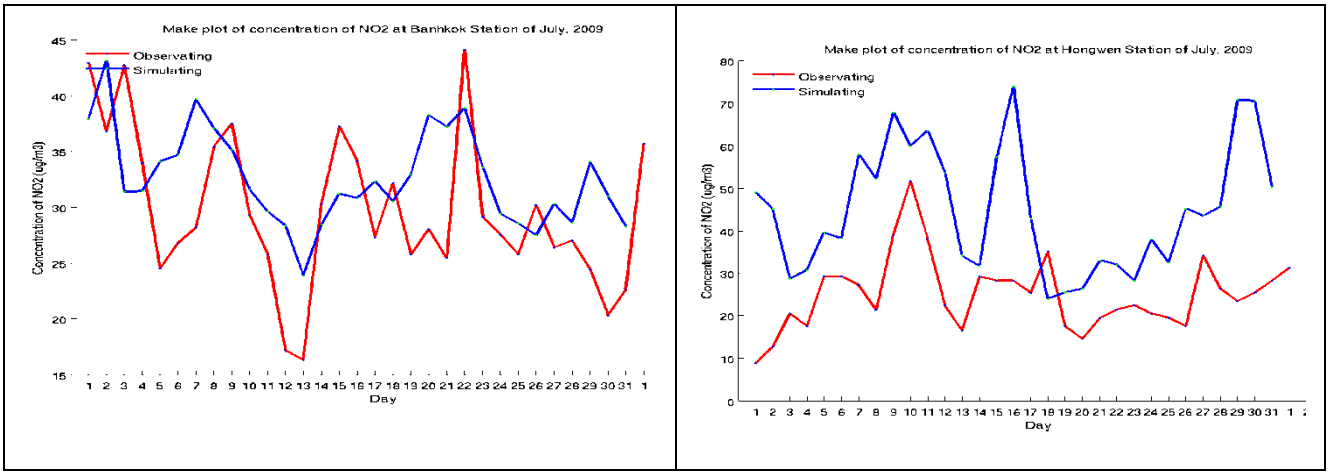

Figure 18. Comparison of modeled (blue) and observed (red) NO_2 daily concentration at Bangkok station, Thailand (left) and Hongwen station, China (right) in July, 2009.

Figure 16 illustrates hourly NO_2 concentration distribution in the model domain at midnight on July 1, 2009, and Figures 17 and 18 show comparison of modeled and observed daily NO_2 concentration at 2 stations in China and Thailand. Simulated result showed NO_2 concentration was high value at a coastal line in the South China sea and in some large city which include considerable traffic activities. The comparison at Bangkok station and Hongwen station indicated the relatively good performance of CMAQ model in both value and time profile of NO_2. On the other hand, there are some differences in some periods. Reproduction of local photochemical production of NO_2 should be elaborated.

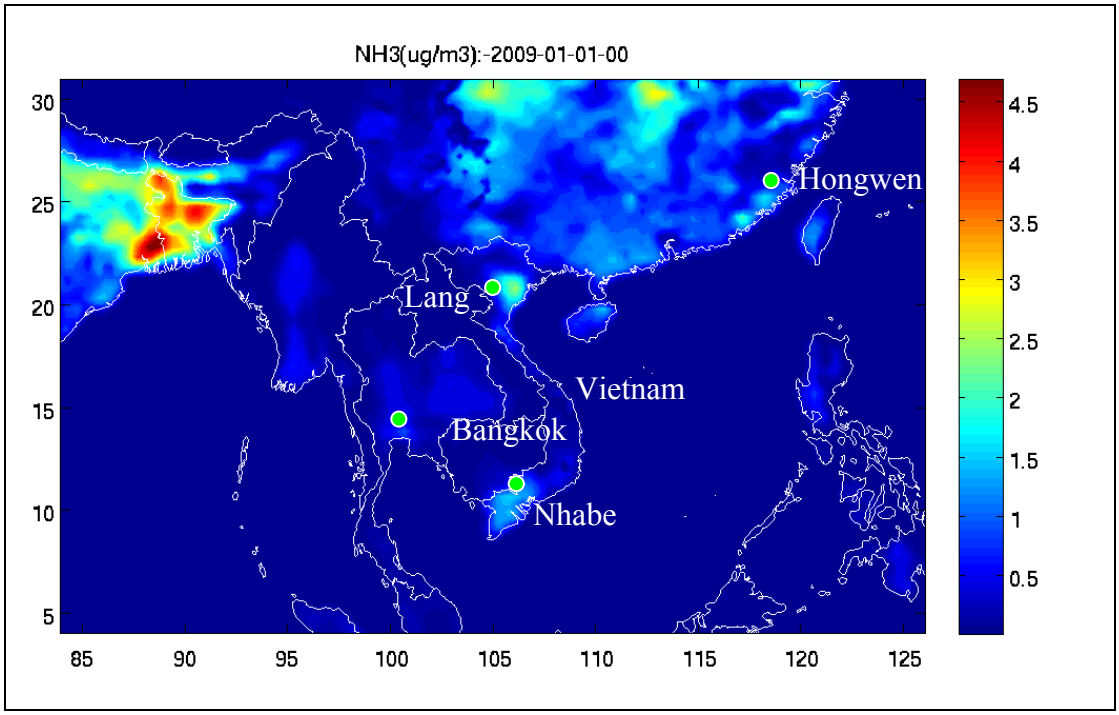

Figure 19. Distribution map of NH_3 concentration in the model domain at 0 h on January 1, 2009.

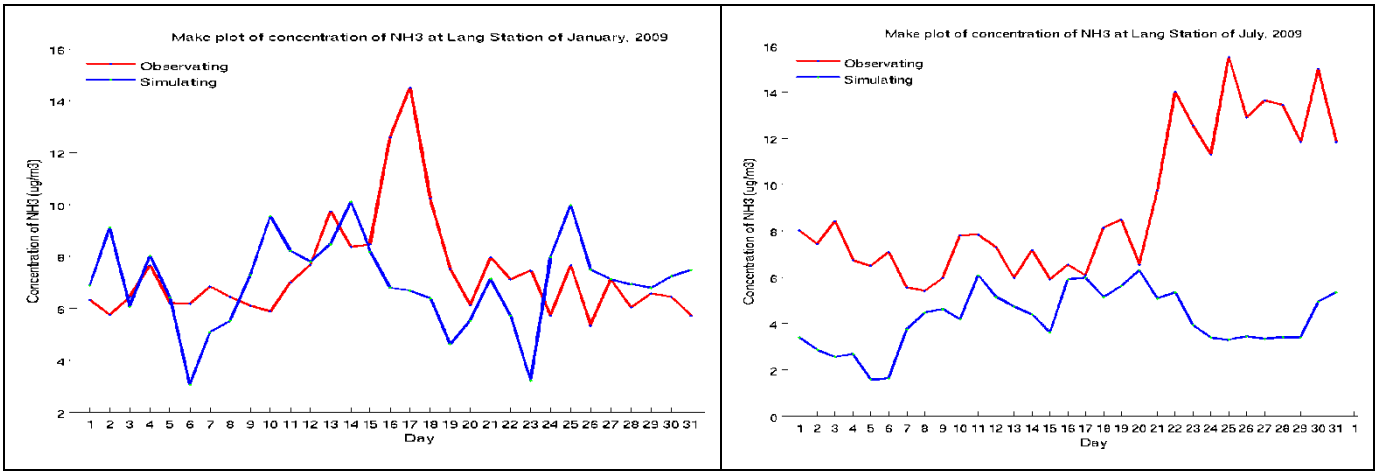

Figure 20. Comparison of modeled (blue) and observed (red) NH_3 daily concentration at Lang station, Vietnam in January (left) and July (right), 2009.

Figure 19 illustrates hourly NH_3 concentration distribution in the model domain at midnight on January 1, 2009, and Figure 20 show comparison of modeled and observed daily NH_3 concentration at the Lang station in Vietnam. The result of NH_3 simulation can clearly suggest that, the NH_3 concentration is high value in areas which have high livestock and cultivate activities, especially in some regions of India, China, north and south of Vietnam. Due to the limited observation data, the comparison was made only at the Lang station, Vietnam. It showed that CMAQ model performed well NH_3 in January, whereas in July the NH_3 simulation did not well reproduced, especially at the end of July the observed NH_3 concentration showed increasing tendency, whereas the simulated result showed decreasing trend. The reason of large discrepancy in summer may be attributable to gas-aerosol interaction of ammonia.

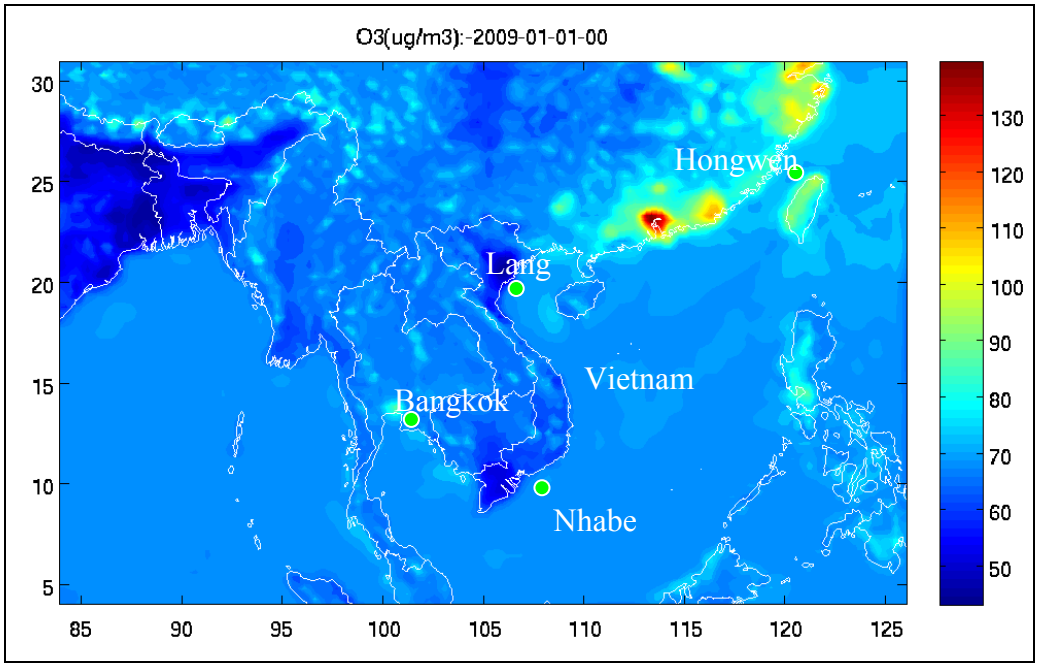

Figure 21. Distribution map of O_3 concentration in the model domain at 0h on January 1, 2009.

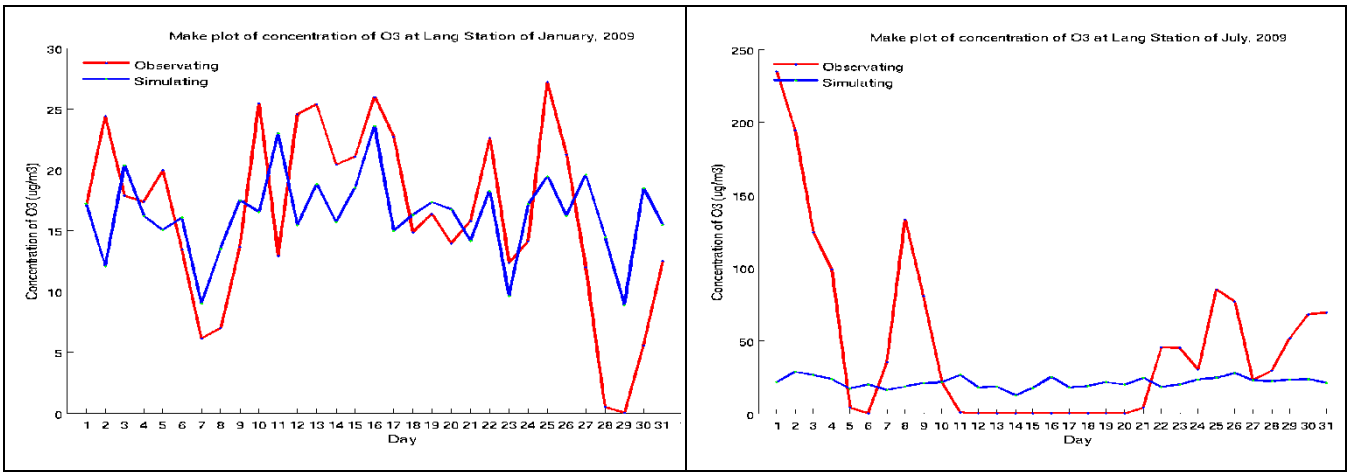

Figure 22. Comparison of modeled (blue) and observed (red) O_3 daily concentration at Lang station, Vietnam in January (left) and July (right), 2009.

Figure 21 illustrates hourly O_3 concentration distribution in the model domain at midnight on January 1, 2009, and Figure 22 show comparison of modeled and observed daily O_3 concentration at the Lang station in Vietnam. O_3 concentration was high in most areas of China such as Shanghai and Guangzhou, whereas it showed low value in both north and south of Vietnam, just about 50 $\mu g/m^3$. Due to the limited observation data, the comparison of O_3 was made at only the Lang station, Vietnam. Figure 20 clearly showed that CMAQ reproduced well O_3 concentration in January, but there is quite large discrepancy in July. The reason is probably attributable to technical problems of O_3 monitoring device. Comparison in summer should be further considered when the observation data are available at the other site.

4. Conclusions

The research shows that, meteorological parameter obtained from the WRF model, which is used in the CMAQ model to simulate air quality over Southeast Asia in 2009 is generally reliable. Emission data obtained from REAS inventory is acceptable, however it need more elaboration in some specific areas. The air quality simulation of some air pollutants such as SO_2, NOx, O_3 based on REAS emission inventory are generally agreed with daily concentrations by means of comparison of observation data of these species in January and July, 2009 at some air quality monitoring stations in Vietnam, China and Thailand. However, in some cases, there is large discrepancy. In order to perform better reproduction, elaboration of WRF and CMAQ model is necessary. Concentrations of SO_2 and NO_2 are high in some regions, cities of China such as Shanghai and Guangzhou and Bangkok, Chiang Mai in Thailand, Hanoi, and Ho Chi Minh in Vietnam. These results suggest that air quality in large cities is important issues now and future.

5. Acknowledgements

The author wish above thank to the Network Center (NC) which sponsored as well as gave me an opportunity to effectuate idea of researching acid deposition over South-east Asia in the EANET Research Fellowship program in 2010. I also thank to Dr. Keiichi Sato who always supported, gave useful advices in the research success from beginning to end. ACAP staff, too, deserve my thanks for creating the most convenient conditions both in material and spirit for me during 4 months studied in ACAP.

6. References

Byun, D.W. and Schere, K.L. 2006. Review of the governing equations, computational algorithms, and other components of the Model-3 Community Multi-scale Air Quality (CMAQ) modeling system. Applied Mechanics Review. 59: 51-77.

Carmichael, G.R., Sakurai, T., Streets, D., Hozumi, Y., Ueda, H., Park, S.U., Fung, C., Han, Z., Kajino, M., Engardt, M., Bennet, C., Hayami, H., Sartelet, K., Holloway, T., Wang, Z., Kannari, A., Fu, J., Matsuda, K., Thongboonchoo, N. and Amann, M. 2007. MICS-Asia II: the model inter-comparison study for Asia phase II methodology and overview of findings. Atmospheric Environment. 42: 3468-3490.

Engart, M. and Leong, C.P. 2001. Regional modelling of anthropogenic sulphur in Southeast Asia. Atmospheric Environment. 34: 5935-5947.

EANET Research Fellowship Program 2011

Effect of Simulated Acid Rain on Leachate Characteristics and Soil pH

Susilawati, K.[1]*, H. Sase[2], N. Yamashita[2], O.H. Ahmed[1] and N.M.N. Majid[3]

[1]Department of Crop Science, Faculty of Agriculture and Food Science, Universiti Putra Malaysia Bintulu Campus, Sarawak, 97008 Bintulu, Sarawak, Malaysia.
E-mail: susilawatikasim@gmail.com
[2]Asia Center for Air Pollution Research
1182 Sowa, Nishi-Ku, Niigata-shi, 950-2144, Japan
[3]Department of Forest Management, Faculty of Forestry, Universiti Putra Malaysia, 43400 UPM Serdang, Selangor, Malaysia.

Abstract

In Malaysia, studies on acid rain are still at the early stage and the effect of acid rain on organic soil is not well covered by scientists. Thus, a study was conducted to investigate the effect of simulated acid rain on organic (*Saprists*) and mineral soil (*Oxisols*) of Malaysia. Four levels of acid rain (pH 3 to 6) were tested in laboratory experiment for about 27 days with constant temperature, 27^{o}C. Soil and leachate were sampled in every 3 and 9 days, respectively. Leachate and soil samples were analyzed for their chemical characteristics by using recommended procedure by EANET. Application of SAR caused the increased of pH and decreased of cations (K^+, Ca^{2+}, Mg^{2+}, Na^+ and NH_4^+) content inorganic soil leachate, while increasing and decreasing trends were observed for SO_4^{2-} and NO_3^- contents, respectively. For mineral soil, SAR pH of 3 caused the increased of SO_4^{2-} content and no obvious changes of cations or NO_3^- content were observed. The amount of Cl^- in mineral soil leachate was decreased as the soil received SAR but no effect has been given by organic soil. Both soils recorded obvious changes of their chemical characteristics at the upper soil part (0 to 10 cm) when they received SAR pH of 3. For other SAR levels (pH 4, 5 and 6), the effect was more serious at the lower part (10 to 20 cm). High CEC of organic soil and the buffering capacity of mineral soil could be the reason for the findings, besides the other possible chemical reactions which occurred in the soil system. As a conclusion, application of SAR caused the changes of leachate properties of either mineral or organic soil. Since this study is not really comprehensive, detailed study is recommended to be carried out by using the same method and approach to validate the findings.

Keywords: acid rain, Oxisols, Saprists, leachate.

1. Introduction

Acid rain could give a serious effect to the soil and leachate properties. According to researchers application of acid rain decreased the pH of a soil especially at the top layer, and reduces its exchangeable cations (Ishiguro and Nakajima, 2000; McColl and Firestone, 1991; Reuss and Johnson, 1986). The decrease in soil pH is related to accumulation of Al^{3+} and H^+ in the soil water system (Bini and Bresolin, 1998). However, addition of SO_4^{2-}, H^+, NO_3^- and NH_4^+ leads to the occurrence of leaching and acidification processes which in turn increase the potential of cations loss (Lee and Weber, 1982; Drohan and Sharpe, 1997). Leaching process occurs when acidic water moves into the soil profiles and then promotes the replacement of H^+ at the soil surface. This will cause cation movement from the upper to the lower soil profile (Guicharnaud and Paton, 2006; Farr *et al.,* 2009). Al mobilization in acidic soils increased its quantity up to 90% of effective exchangeable cations (ECEC). These reactions caused Al-Ca antagonisms to occur and make nutrients less available (Etherington, 1975; Larssen and Carmichael, 2000). Presence of acidic sources such as H^+, SO_4^{2-}, $NO_3^-$and so on accelerate acidification process. Continuous addition of H^+ and increase in anion movement make the soil to undergo acidification. In this case, most of the negative charges are filled with H^+ (Chen *et al.,* 2011; Bini and Bresolin, 1998). The acidity caused by addition of acid rain reduced organic molecules solubility and indirectly reduced organic matter decomposition and production of organic acids (Reuss and Johnson, 1986). Low pH altered the chemical and biological reactions such as hydrolysis, oxidation-reduction, carbonation and so on, and produced toxic ions such as Zn, Cu, Mn and so on (Guicharnoud and Paton, 2006). In addition, excessive amounts of soluble heavy metals are toxic to most living things especially microorganisms to carry on their activities (Wilcke and Kaupenjohann, 1998). Due to this significant effect caused by acid rain on soil properties either organic or mineral, a study was conducted to investigate the effect of acid rain on soil pH and leachate characteristics.

2. Methods

Mineral (*Oxisols–Typicpaleuudults*) and organic (peat) soils (*Saprists*) were selected to be used in this study. Mineral soil was collected from undisturbed area at Universiti Putra Malaysia Bintulu Campus Sarawak while organic soil was collected at disturbed area in Mukah Sarawak, Malaysia. The soils were air-dried and pulverized to pass through 2 mm sieve. Soils were then stored at room temperature to be used later in leaching experiment. Simulated acid rain (SAR) was first prepared by mixing sulphuric and nitric acids at 3:2 ratio (SO_4^{2-}:NO_3^-) to obtain SAR of pH 3. Afterwards SAR solution was diluted accordingly to obtain SAR at pH 4, 5 and 6. The prepared SAR solutions were then stored at 0 to 5^oC. Leaching column was prepared by combining 2 parts of 50 mL syringe. Plastic tube was then attached at the bottom of the leaching column and 50mL plastic bottles were then placed underneath to collect the leachate. Afterwards, 20 cm thick soils were placed inside the leaching column. About 160 g of mineral and 60g of organic soils were used in this study. Soil depth was then divided into two parts which were 0 to 10cm and 10 to 20 cm. Glasswool was used to filter the water from the

soils. Leaching columns were randomly arranged in stainless steel rack. These were then placed in the incubator at 27^{o}C for homogenization purposes. Different SAR solutions were then slowly applied on the soils surface. SAR was applied twice a week with the total volume of 40 mL. Leachate and soil samples were collected at 3 and 9 days, respectively. Leachate samples were analyzed for pH, exchangeable cations (K^+, Ca^{2+}, Mg^{2+}, Na^+), NH_4^+, SO_4^{2-}, NO_3^- and Cl^-while soil samples were analyzed for pH, exchangeable cations (K^+, Ca^{2+}, Mg^{2+}, Na^+), NH_4^+, SO_4^{2-}, NO_3^-, exchangeable acidity, exchangeable H and exchangeable Al using standard procedures. All data were presented in figures and correlation test was done to analyze the relationship of the test parameters. The study was conducted in 27 days period with 3 and 9 intervals for soil and leachate sampling, respectively. The summary of materials and methods for this experiment is presented in Table 1(showed in appendices). The initial data of the mineral and organic soils used in this study is presented in Appendix Table 2.

3. Results

As shown in Figures 1 and 2, leachate pH changed when they were treated with different SAR levels. Application of different SAR levels to mineral soil did not give any effect to the leachate pH except at day 24 and 27 (Figure 1). Longer SAR application period may cause the leachate pH to decrease especially at SAR pH of 3. Different trend was observed for organic soils (Figure 2). Application of SAR generally increased the leachate pH. SAR at pH 3 caused the lowest increase of pH as compared to higher SAR pH (pH 4, 5 and 6). The increase of leachate pH for organic soil was observed after 12 days treated with SAR and the highest pH was recorded at day 27 for all SAR levels. Application of different SAR levels to mineral soils did not give any effect to the content of SO_4^{2-} in the leachate samples except for SAR pH of 3. SAR pH of 3 increased the SO_4^{2-} content in mineral soil leachate sample. After 27 days treated with SAR, the accumulation of $SO_4^{2-}$was observed for SAR pH 3 is higher than that of other SAR levels (pH 4, 5 and 6). However application of SAR to organic soils caused the sharp increase of SO_4^{2-} content in the leachate samples up to 15 day period, afterwards, a drastic decrease of SO_4^{2-} content was observed for all SAR levels. After 27 days, SAR at pH 3 and 4 showed higher amount of SO_4^{2-} content compared to pH 5 and 6. Application of SAR affects the content of NO_3^- in mineral soil leachate (Figure 5). Higher amount of NO_3^- were recorded at day 3, 12 and 15 while lower content was observed at day 6, 9, 18, 21, 24 and 27. Generally, SAR at pH 3 registered the lowest amount of NO_3^- content compared to SAR pH of 4, 5 and 6 (Figure 5). In the case of organic soil, the highest NO_3^- content was observed at day 15 for all SAR levels (Figure 6). All SAR levels recorded a sharp increase in NO_3^- content between days 12 to 15 before sharply decreasing at day 18. SAR pH of 3 recorded the highest amount of NO_3^-compared to pH of 4, 5 and 6 (Figure 6). Lower NO_3^- content was observed in mineral compared to organic soil leachate (Figures 5 and 6). Decreasing trend for Cl^- content was observed in mineral soil leachate samples when they were treated with different SAR levels (Figure 7). Generally, no clear differences were observed for the content of Cl^- except at day 27 when SAR at pH 5 recorded the highest value. Amount of SAR applied plays an important role in reducing Cl^- content in mineral soil leachate samples (Figure 7). The amount of $Cl^-$was stable after 12 days treated with different SAR levels. For organic soil leachate, the highest value was

recorded at day 9 and the lowest was at day 21 for all SAR levels (Figure 8). A sharp increase for Cl^- content was recorded from day 6 to 9 while the decreased was recorded after days 9 to 21. Generally SAR at pH 3 showed the highest value compared to pH 4, 5 and 6 within 27 days study period.

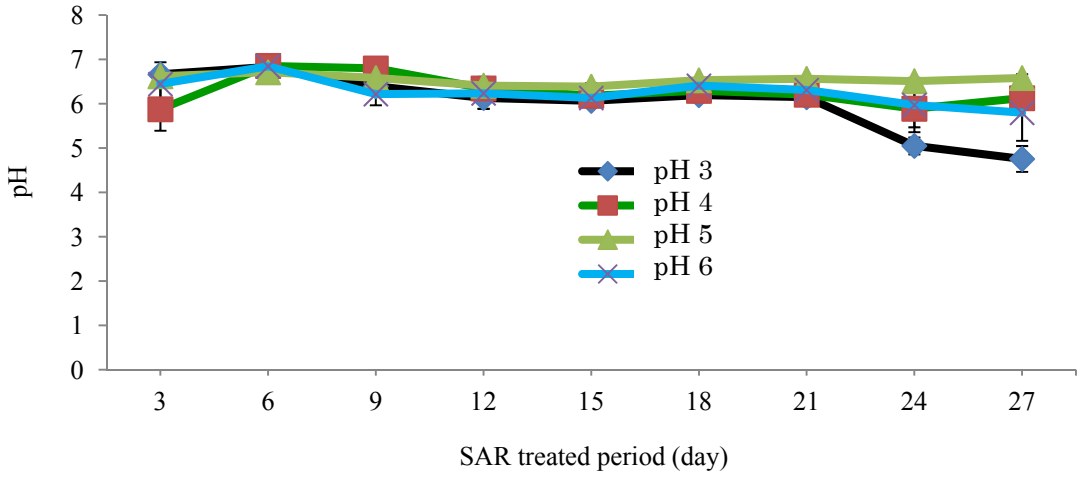

Figure 1. pH of mineral soil leachate over 27 days (after treatment with different SAR levels).

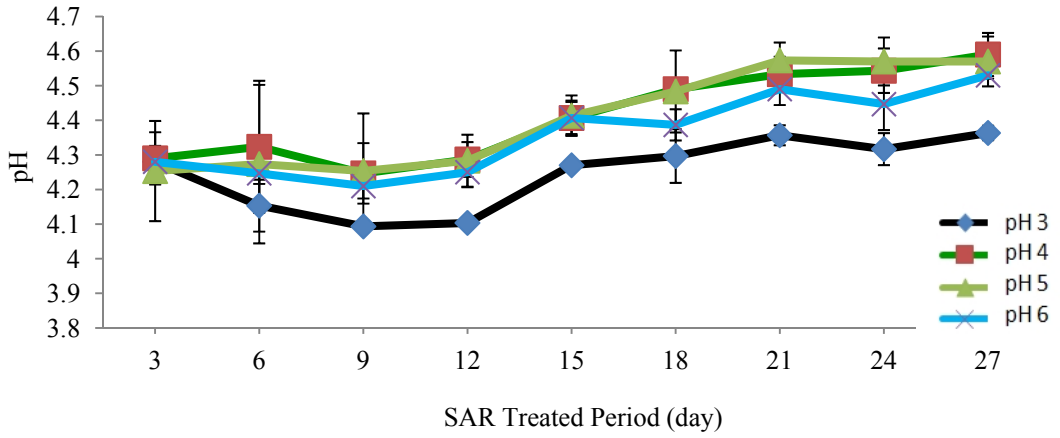

Figure 2. pH of organic soil leachate over 27 days (after treatment with different SAR levels).

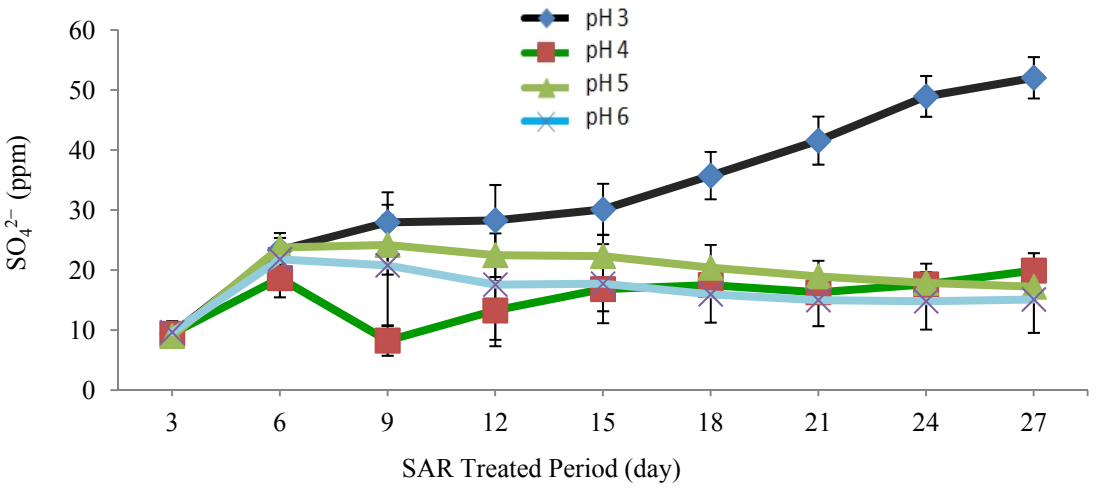

Figure 3. Sulphate content in mineral soil leachate over 27 days (after treatment with different SAR levels).

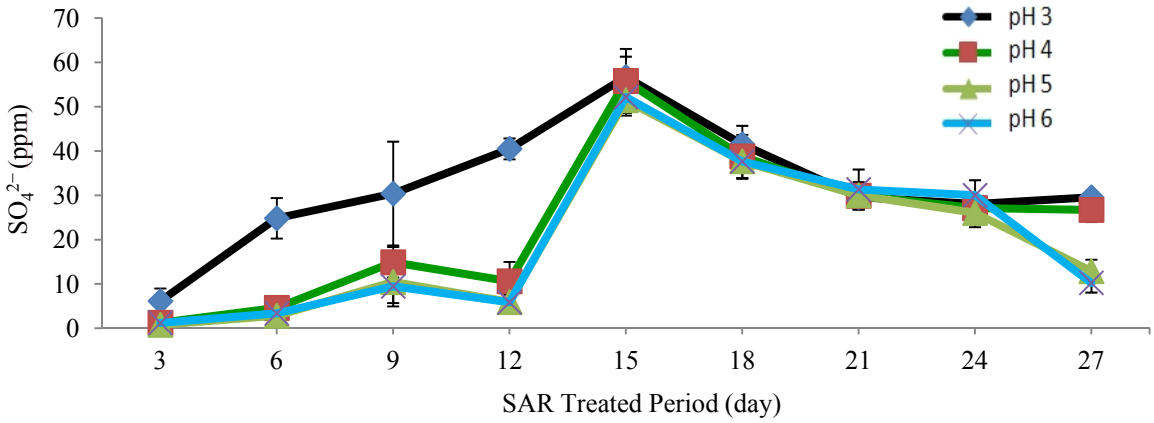

Figure 4. Sulphate content in organic soil leachate over 27 days (after treatment with different SAR levels).

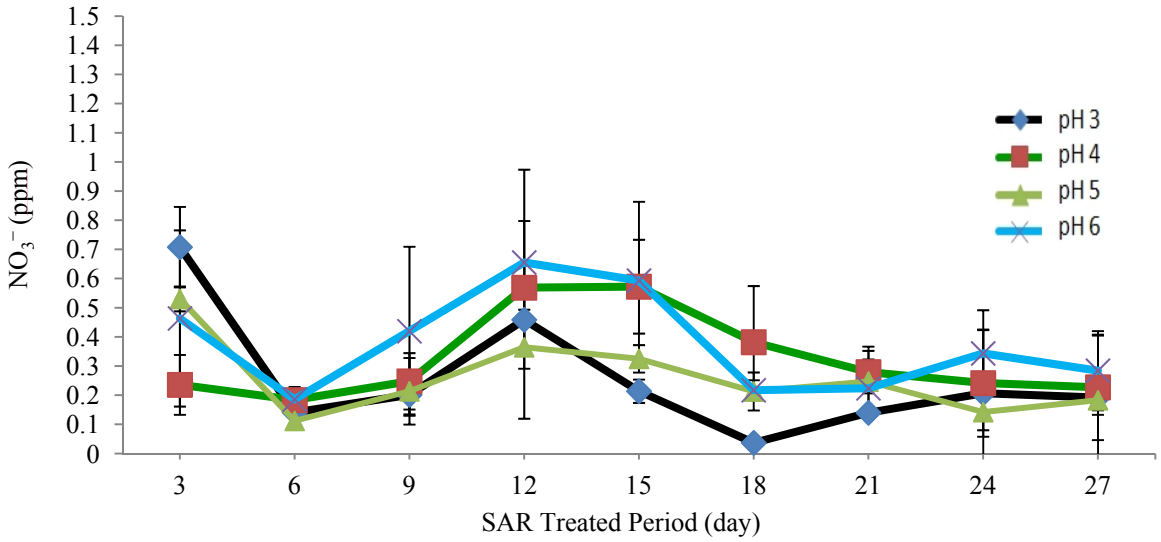

Figure 5. Nitrate content in mineral soil leachate over 27 days (after treatment with different SAR levels).

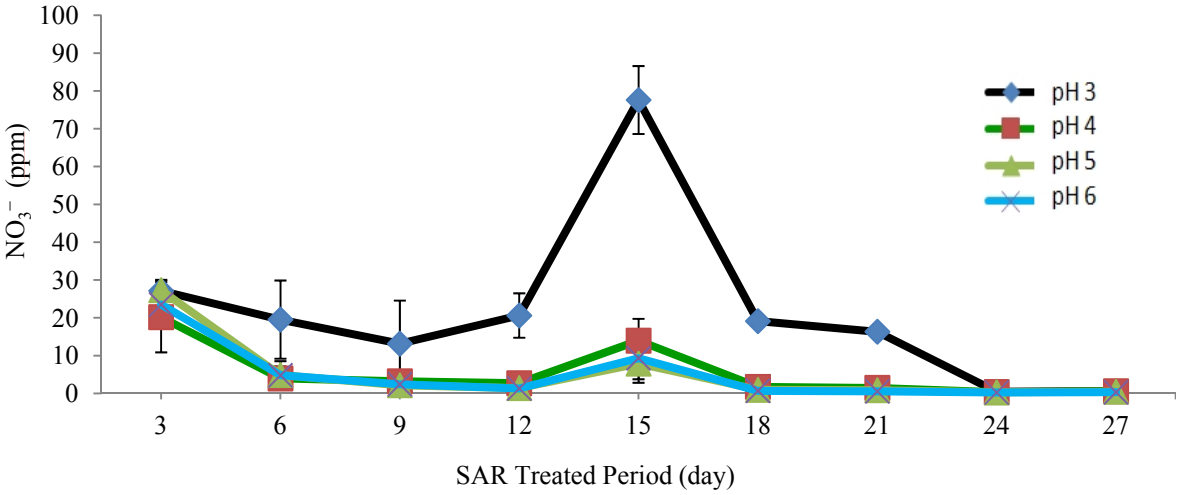

Figure 6. Nitrate content in organic soil leachate over 27 days (after treatment with different SAR levels).

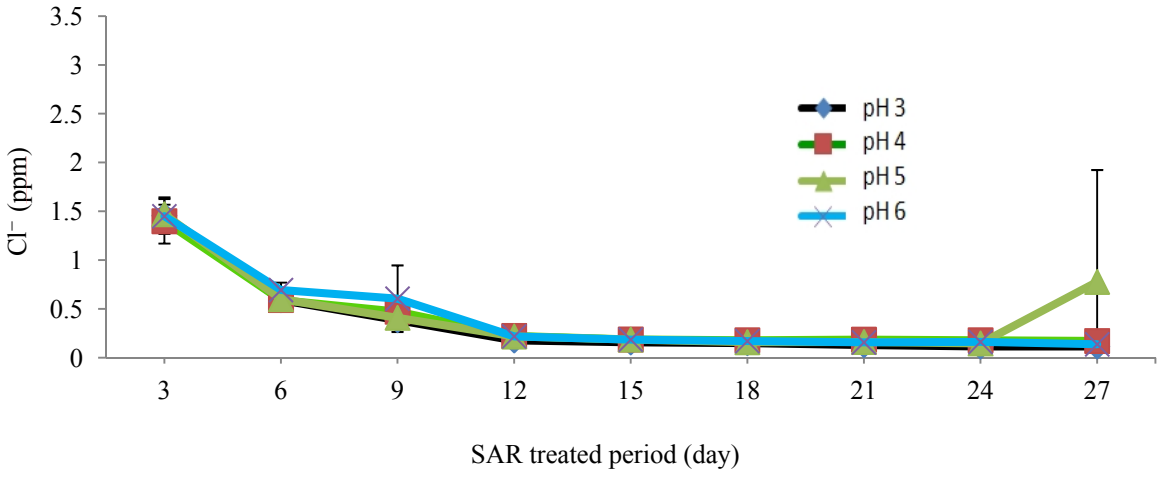

Figure 7. Chloride content in mineral soil leachate over 27 days (after treatment with different SAR levels).

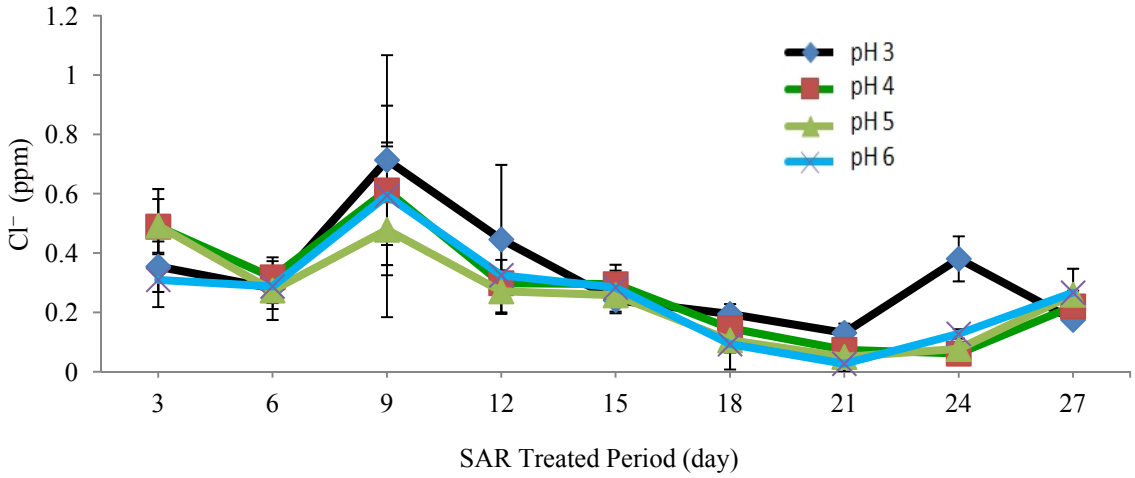

Figure 8. Chloride content in organic soil leachate over 27 days (after treatment with different SAR levels).

Slight increase of NH_4^+ content in mineral soil leachate was observed in this study (Figure 9). All SAR levels gave similar trend of NH_4^+ content except for SAR at pH 3 where it showed higher NH_4^+ as compared to other SAR levels. At day 27, SAR pH of 3 gave the highest amount of NH_4^+ and pH 5 was the lowest. The value for NH_4^+ at day 9 was the lowest within 27 days study period (Figure 9). As mineral and organic soils were compared, the amount of NH_4^+ in organic was extremely higher than that of mineral soils. For organic soil, application of SAR decreased the amount of NH_4^+ in the leachate sample (Figure 10). SAR pH of 3 showed the

highest amount of NH_4^+ compared to pH 4, 5, and 6. Application of SAR showed decreasing Na^+ content in both, organic and mineral soil leachates (Figures 11 and 12). Both soil leachates showed the lowest value at day 27 and the highest at day 3. The amount of Na^+ extracted or replaced by SAR on the exchange sites from both soils were of similar values. Similarly, application of SAR caused the decreased of K^+ content in both soil leachates (Figures 13 and 14). All SAR levels gave similar trend of K^+ reduction. In mineral soil leachate, K^+ content is stable after 9 day treatment with SAR while for organic soil, the K^+ content is continuously decreased with the study period. SAR at pH 3 did not show any clear difference in K^+ content compared to other SAR levels in mineral soil leachate (Figure 13). However, for organic soil, SAR at pH 3 caused the lowest decrease of K^+ as compared to other treatments (Figure 14). Higher K^+ values were observed in organic soil than mineral soil. Both soil recorded different trend for Ca^{2+} content (Figures 15 and 16). Application of different SAR levels caused increase and decrease of Ca^{2+} content in mineral soil leachate (Figure 15). Sharp decrease of Ca^{2+} content of mineral soil leachate was observed from days 3 to 9. At days 12 to 15, the amount of Ca^{2+} is stable before increasing again at day 15 to 27. SAR pH of 3 recorded higher amount of Ca^{2+} compared to other SAR levels while SAR at pH 5 was the lowest. A sharp decrease of Ca^{2+} content in organic soil is showed in Figure 16. At day 27, slightly higher amount of Ca^{2+} was noted at SAR pH 3 applications. Calcium contents from leachates for both soils were similar. Generally, SAR pH of 3 caused the higher amount of Mg^{2+} at day 27 as compared to other SAR levels (Figure 17). After 18 days of treatment with SAR, the amount of Mg^{2+} in all treated soil showed an increasing trend. For organic soil, a continued decreasing trend of Mg^{2+} was observed for all SAR levels (Figure 18). SAR at pH 3 caused slower decreased of Mg^{2+} compared to other SAR pH. All SAR levels recorded the highest value at day 3 and the lowest at day 27 for Mg^{2+} in organic soil leachate (Figure 18).

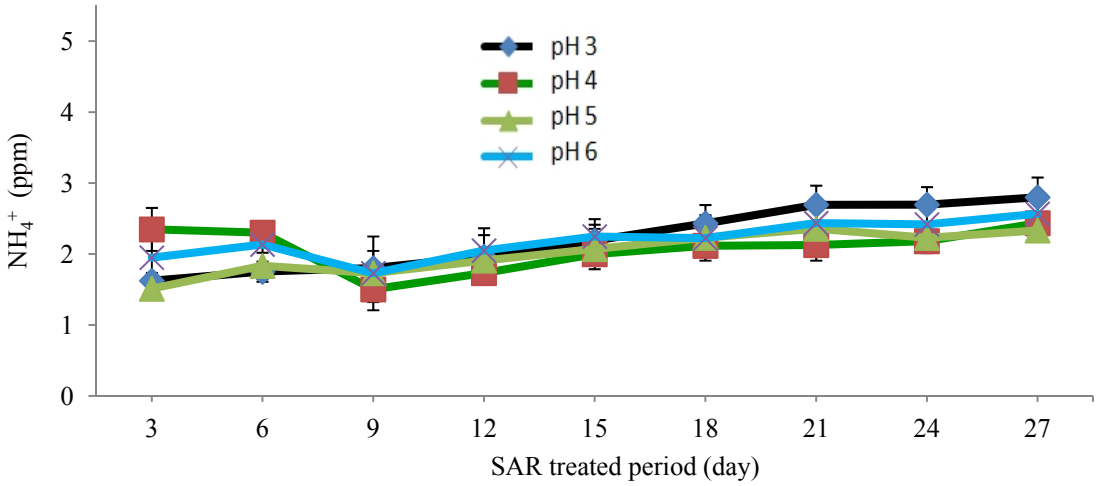

Figure 9. Ammonium content in mineral soil leachate over 27 days (after treatment with different SAR levels).

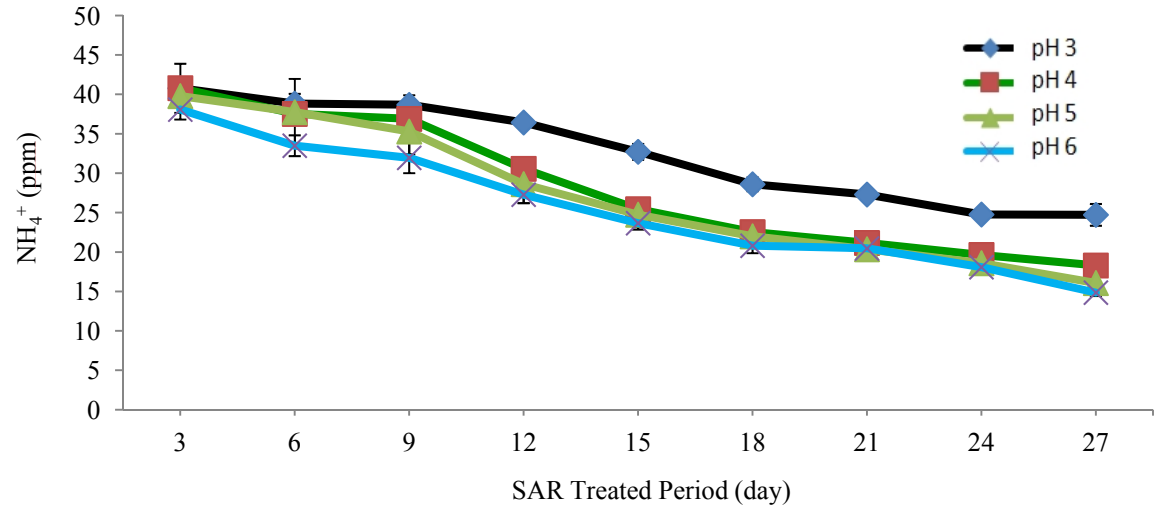

Figure 10. Ammonium content in organic soil leachate over 27 days (after treatment with different SAR levels).

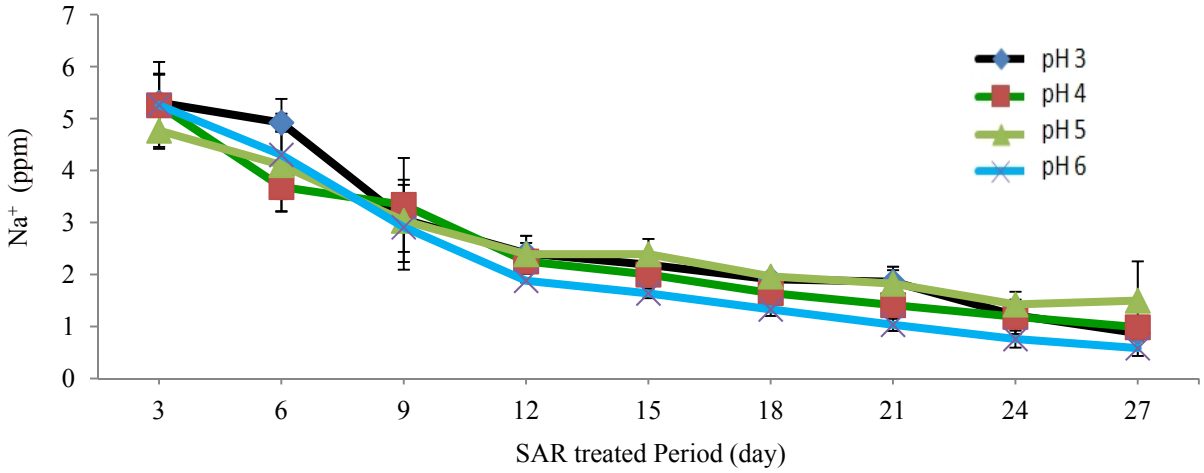

Figure 11. Sodium content in mineral soil leachate over 27 days (after treatment with different SAR levels).

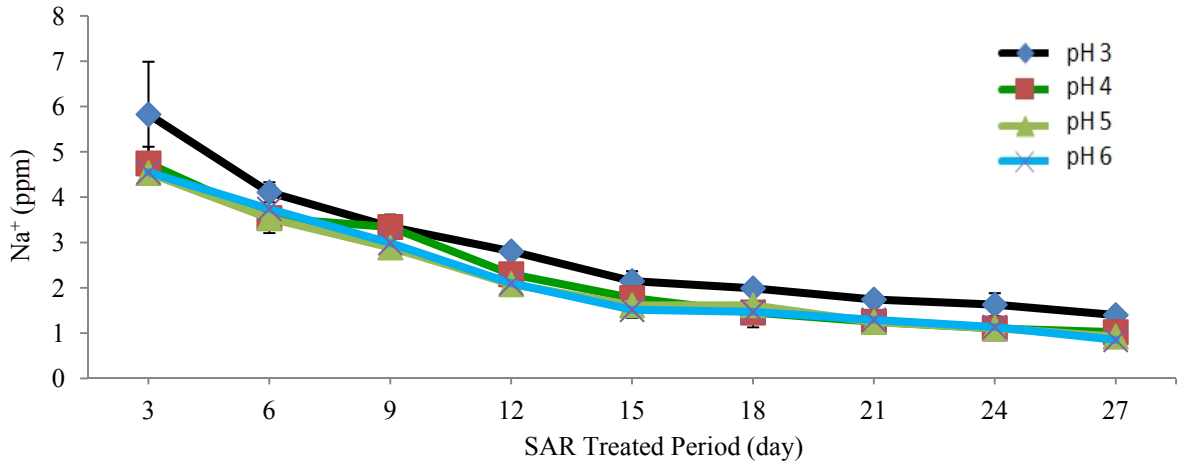

Figure 12. Sodium content in organic soil leachate over 27 days (after treatment with different SAR levels).

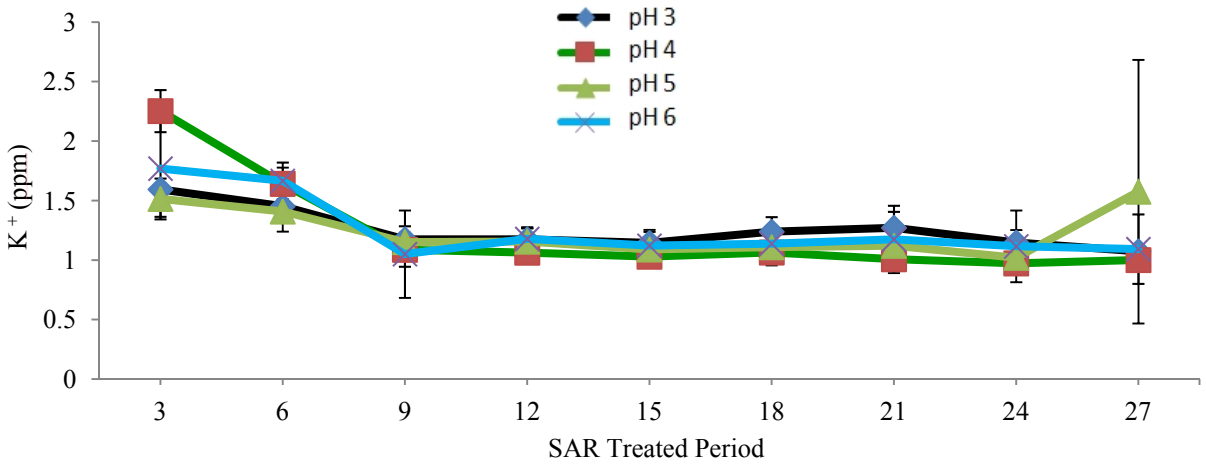

Figure 13. Potassium content in mineral soil leachate over 27 days (after treatment with different SAR levels).

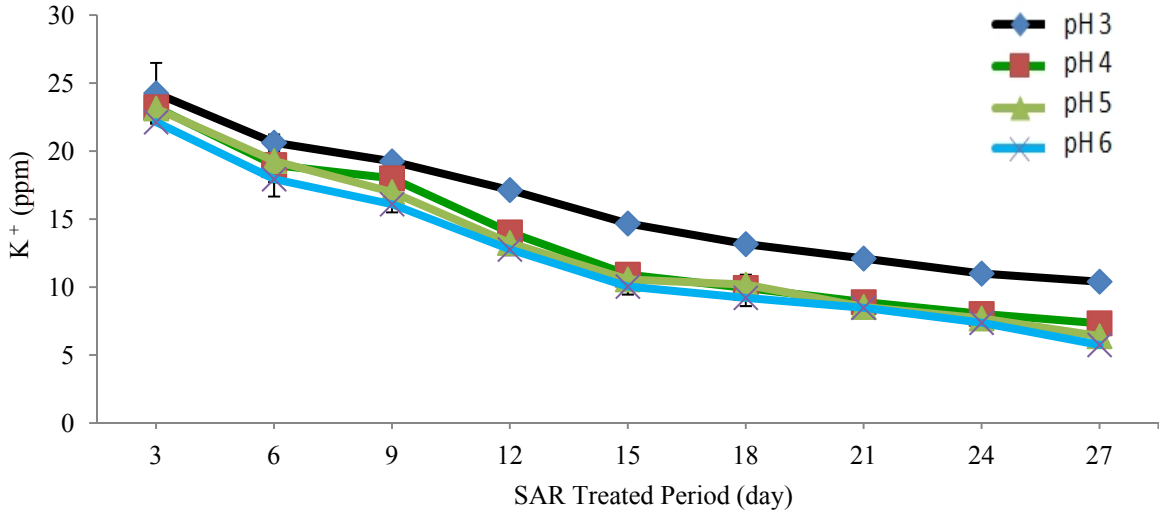

Figure 14. Potassium content in organic soil leachate over 27 days (after treatment with different SAR levels).

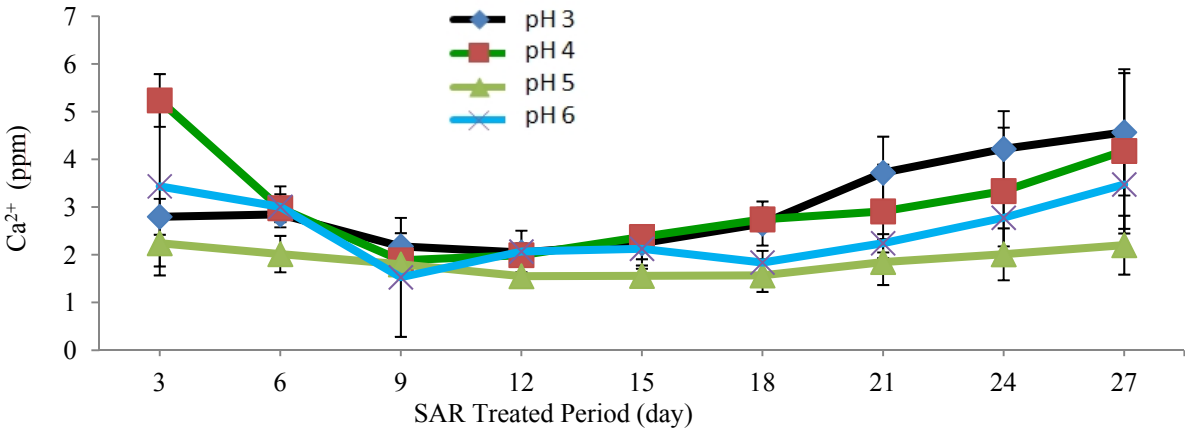

Figure 15. Calcium content in mineral soil leachate over 27 days (after treatment with different SAR levels).

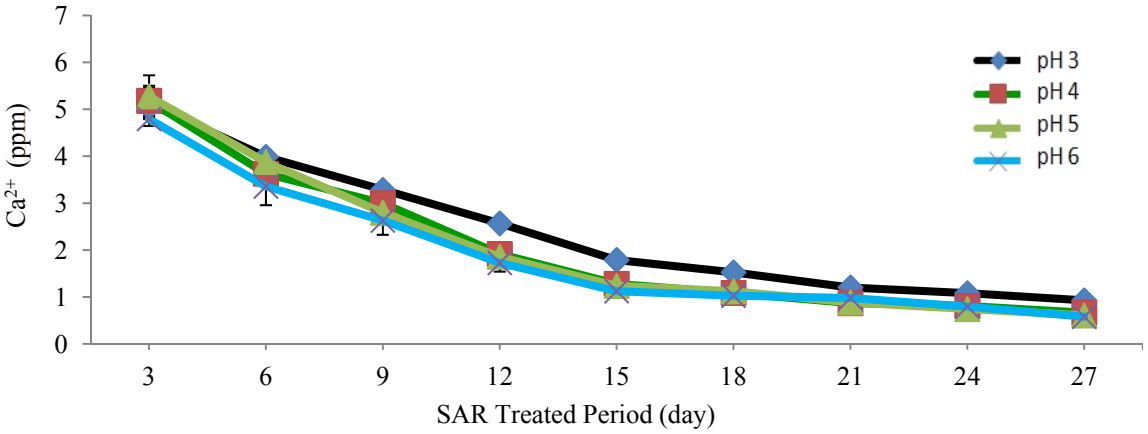

Figure 16. Calcium content in organic soil leachate over 27 days (after treatment with different SAR levels).

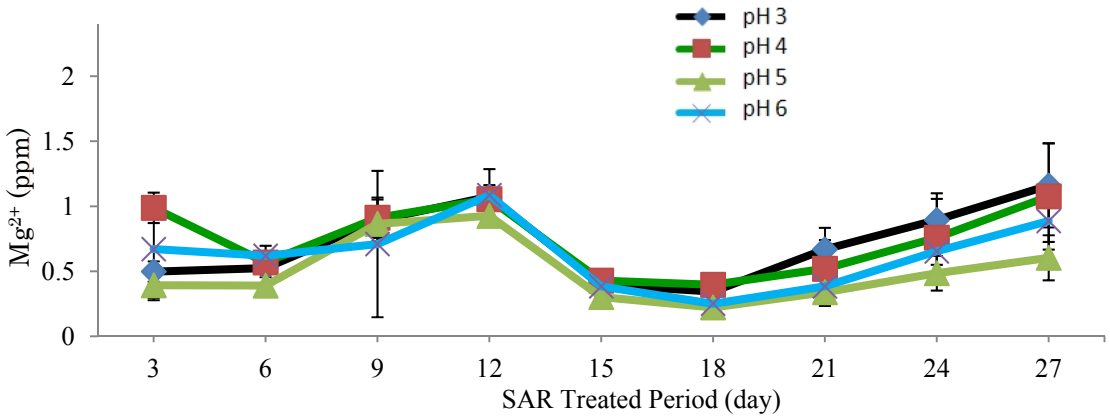

Figure 17. Magnesium content in mineral soil leachate over 27 days (after treatment with different SAR levels).

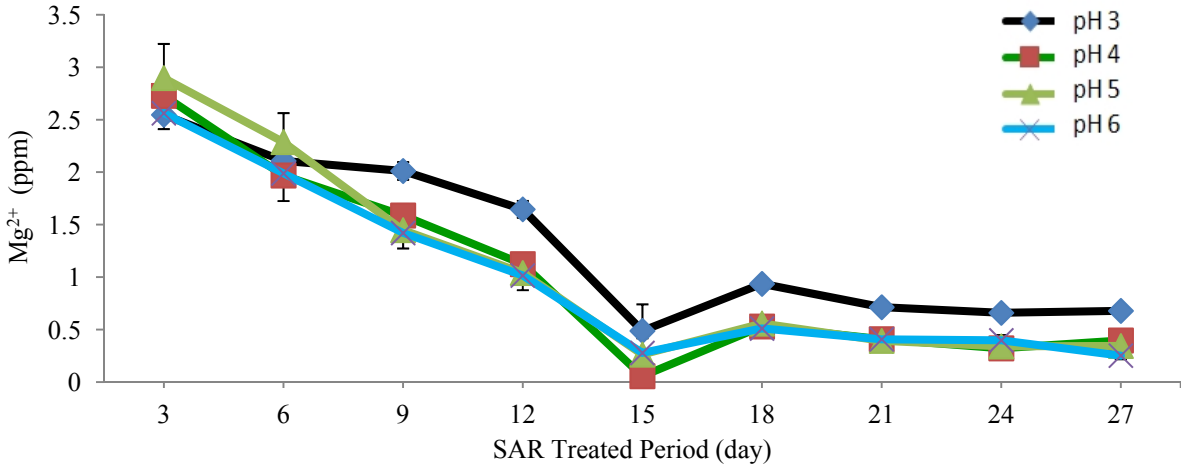

Figure 18. Magnesium content in organic soil leachate over 27 days (after treatment with different SAR levels).

Different soil depth pH was compared after they were treated with different SAR levels. SAR pH of 3 caused the decrease of pH at the upper part (0 to 10 cm) while SAR pH of 4, 5 and 6, caused the decrease at the lower soil part (10 to 20 cm) (Figure 19). Generally, higher soil pH is recorded at third sampling (after 27 days treatment with SAR) as compared to the first sampling (after 9 days treatment with SAR) (Figure 19). Similar trend was observed for organic soil (Figure 20). SAR at pH 4, 5, and 6 caused the increase of organic soil pH at both soil depths (Figure 20).

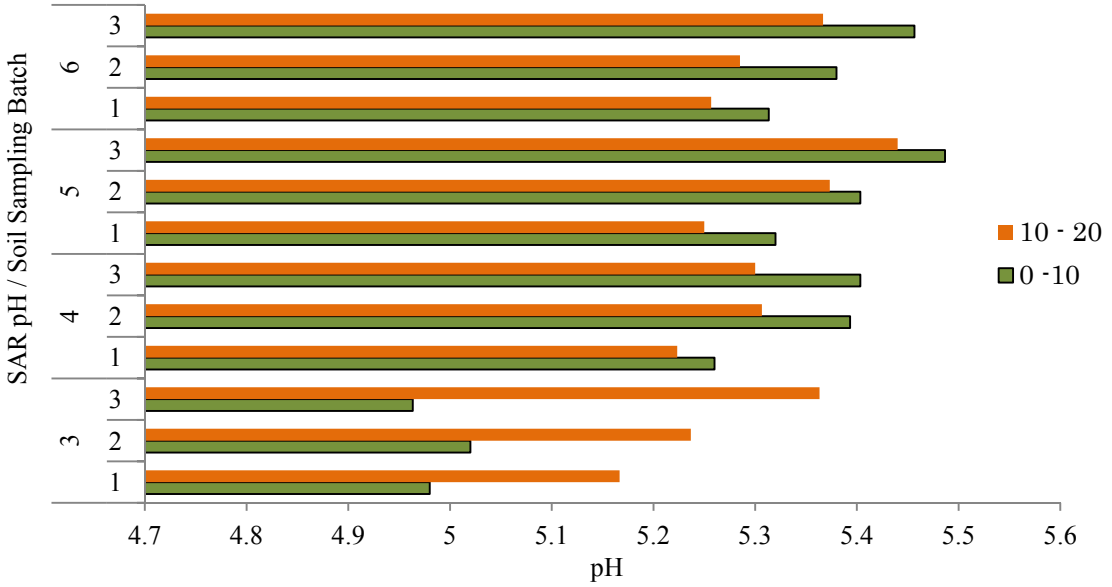

Figure 19. pH of mineral soil over 27 days period (after treatment applications).

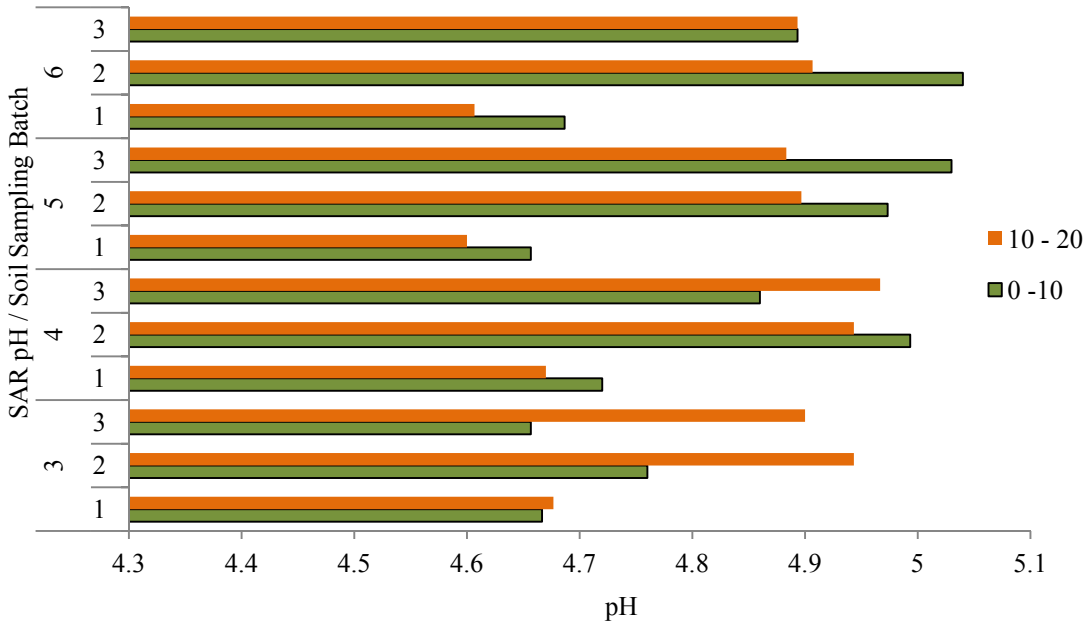

Figure 20. pH of organic soil over 27 days period (after treatment applications).

4. Discussion

Application of SAR did not change the pH of mineral soil leachate. This could be due to high buffering capacity of acidic mineral soil. Acidic mineral soil may have higher buffering capacity than that of alkaline soils which leads to small changes of their pH in response to acidic input (Wiklander, 1975). On the contrary, application of SAR caused the increase of pH in organic soil leachate. Type and properties of organic soil used could be the reason for this finding. Generally *saprists* soils contain huge amount of organic acids such as humic and fulvic acids (Stevenson, 1994). These acids have a large number of negative charges which functioned as the absorption site for H^+, NH_4^+, K^+, Ca^{2+}, Mg^{2+} and other nutrients (Tan, 2003). Furthermore, SAR contain huge amount of H^+ which can be exchanged either with NH_4^+, K^+, Ca^{2+}, Mg^{2+} and Na^+ and so on. This reactions could accumulates cations in the soil water system which in the long run could possibly react with anions (e.g. SO_4^{2-}, NO_3^-) to form chemical compounds [e.g. $(NH_4)_2SO_4$, NH_4NO_3 and so on]. The decrease of cations (Figures 10, 12, 14, 16, and 18) and anions (Figures 4, 6, and 8) could be the proof or reason for this assumption. Correlation analysis for peat soil leachate may also support this justification. However, more detailed studies are needed to confirm these findings. Application of SAR did not change the amount of NO_3^- in mineral soil leachate samples. Denitrification process could be the reason for this finding as this soil was left under anaerobic condition throughout the study period. Lack of O_2 supply favored denitrification process (Davidson and Swank, 1987). Although the pH of the soil is acidic, the effect of acidity to denitrification process is minor (Davidson and Kwank, 1987). According to Mosier *et al.* (2002), denitrification process is the important mechanism where N in the form of NO_3^- is released to the atmosphere as nitrogen gas.

Lower soil depth is more affected in terms of pH when both soils were treated with SAR at pH 4, 5 and 6 for both soils. However for SAR at pH 3, upper soil part is more affected. Concentration of H^+, SO_4^{2-}, and NO_3^- in different SAR levels could be reason for this finding. The mobility of these anions in the soil water system caused acidification to occur (Lee and Weber, 1982). This will lead to accumulation of H^+, Al oxides and organic acids in the system. At the same time, accumulation of H^+ and Al caused rapid increase in weak acids protonation which in turns reduced H^+ in the soil water system. Reduction of H^+ from this reaction could reduce its ability to be exchanged with exchangeable cations, thus caused less amount of mobile cations in the soil water system. Reduction in cations content in both soil leachate (Figures 10, 12, 14, 16, and 18) could be a possible proof for this justification. From these findings we assumed that the soils build immediate reaction after treatment with SAR at pH 3, while the reactions could take some times when SAR pH of 4, 5, and 6 were applied. However, detailed study needs to be conducted to validate these findings.

5. Conclusion

Application of SAR affects the characteristics of leachate and soil pH. The effect of SAR on mineral and organic soils was different, and details study is recommended to be conducted in the future experiment to confirm the findings.

6. References

Bini, C. and Bresolin, F. 1998. Soil acidification by acid rain in forest ecosystems: a case study in northern Italy. Sci. Total Environ. 222: 1-5.

Chen, N., Hong, H., Huang, Q., and Wu, J. 2011. Atmospheric nitrogen deposition and its long-term dynamics in a southeast China Coastal area. Journal of Environmental Management. 92: 1663-1667.

Drohan, J.R. and Sharpe, W.E. 1997. Long-term changes in forest soil acidity in Pennsylvania, USA. Water, Air, Soil Pollut. 95: 299-311.

Etherington, J.R. 1975. Environment and plant ecology. John Wiley and sons, London.347 p.

Guicharnaud, R. and Paton, G.I. 2006. An evaluation of acid deposition on cation leaching and weathering rates of an Andosol and a Cambisol. Journal of Geochemical Exploration. 88: 279-283.

Ishiguro, M. and Nakajima, T. 2000. Hydraulic conductivity of an allophonic Andisol leached with dilute acid solutions. Soil Science Society of America Journal. 64: 813-818.

Larssen, T. and Carmichael, G.R. 2000. Acid rain and acidification in China: the importance of base cation deposition. Environ. Pollut. 110: 89-102.

Lee, J.J. and Weber, D.E. 1982. Effect of sulphuric acid rain on major cation and sulphate concentration of water percolating through two model hardwood forests. J. Environ. Quality. 11: 57-64.

McColl, J.G. and Firestone, M.K. 1991. Soil chemical and microbial effects of simulated acid rain on clover and soft chess. Water, Air, and Soil Pollution. 60: 301-313.

Mosier, A.R., Doran, J.W., and Freney, J.R. 2002. Managing soil denitrification. Journal of soil and water conservation. 57(6): 505-512.

Reuss, J.O. and Johnson, D.W. 1986. Acid Deposition and the Acidification of Soils and Waters, Springer, New York. 119 p.

Stevenson, F.J. 1994. Humus chemistry: genesis, composition, reactions, 2nd edition. Wiley, New York. pp. 378-486.

Tan, K.H. 2003. Humic matter in soil and the environment: Principles and controversies. Marcel Dekker, Inc., New York. pp. 34-71.

Wilcke, W. And Kaupenjohann, M. 1998. Heavy metal distribution between soil aggregate core and surface fractions along gradients of deposition from the atmosphere. Geoderma. 83: 55-66.

Appendices

Appendix Table 1. Summary of materials and methods used for leaching study.

Item	Description
Soil Type	2 types - Organic (*Saprists*) - Mineral (*Oxisols - TypicPaleuudults*)
Simulated Acid Rain (SAR) levels	4 levels 1. pH 6 3. pH 4 2. pH 5 4. pH 3
Application of SAR	1. 40mL/week (2 x 20mL of application) 2. Applied in every 3 days (9x of application)
Sampling of soil	3 Times 1. 9 days after SAR applied 2. 18 days after SAR applied 3. 27 days after SAR applied
Sampling of Leachate	9 times (will be collected before 2nd, 3rd, 4th, 5th, 6th, 7th , 8th , 9th and last application of SAR)

Appendix Table 2. Physico-chemical Properties of Mineral and Organic Soils.

Parameter	Mineral	Organic
pH in water	4.84	ND
pH in KCl	3.58	ND
Exchangeable K^+ concentration (cmol/kg)	0.54	ND
Exchangeable Ca^{2+} concentration (cmol/kg)	2.25	ND
Exchangeable Mg^{2+} concentration (cmol/kg)	0.02	ND
Exchangeable Na^+ concentration (cmol/kg)	0.23	ND
Exchangeable Acidity (cmol/kg)	2.92	ND
Exchangeable Al (cmol/kg)	1.35	ND
Exchangeable H (cmol/kg)	1.95	608.7
Cation Exchange Capacity (cmol/kg)	10.2	ND

Exchangeable NH_4^+ (mg/kg)	49.04	ND
Available NO_3^- (mg/kg)	21.02	ND
Available P (mg/kg)	0.1	ND
Total N (%)	0.11	1.424
Bulk density (g cm^{-3})	1.2	ND
Total Organic Carbon (%)	6	55.91
Ash content (%)	94	44.09
Organic matter (%)	3.48	32.43
Soil texture (sandy clay loam)		
Sand (%)	65.48	ND
Clay (%)	21.25	ND
Silt (%)	13.00	ND
Humic acid yield (%)	ND	13.77

Quality Assurance and Quality Control Procedures for Ozone Monitoring in China

Baolin Chu[1], Yawed Yao[1], Xiaofeng Wu[1], Takuya Shiozaki[2], Keiichi Sato[2] and Qiang Fu[1,*]

[1]Quality Management Department, China National Environmental Monitoring Center (CNEMC), No.8 (B) Anwai Dayangfang, Beiyuan Road, Chaoyang District, Beijing 100012, P. R. China

E-mail: chubl@cnemc.cn

[2]Asia Center for Air Pollution Research (ACAP), 1182 Sowa, Niigata, 950-2144, Japan

*Correspondence: Dr. Qiang Fu, Head of Quality Management Department.

Abstract

The traceability system for ozone monitoring in China was proposed. Quality assurance and quality control (QA/QC) procedures for ozone monitoring were described. Acceptance testing and calibration of 49i were conducted by 49i-PS. It was revealed that the analyzers could meet the technical specifications for acceptance. The initial verification was also successfully implemented.

Key words: ozone monitoring, calibration, standard transfer, acceptance testing.

1. Introduction

1.1 Background

In China, the newly revised *Ambient Air Quality Standard (GB 3095-2012)* has been jointly issued by Ministry of Environmental Protection (MEP) and General Administration of Quality Supervision, Inspection and Quarantine (AQSIQ) on Feb. 29, 2012 and will be implemented on Jan. 1, 2016. The new standard had adjustments, additions, stricter limits and new contents. 8-hour average concentration limit of ozone (O_3) was added.

It is required that any major cities on prevention and control of air pollution failing to meet the standard shall develop and implement the plan for meeting the air quality standard according to the Law of the People's Republic of China on the Prevention and Control of Atmospheric Pollution. The goal of National Ambient Air Automated Monitoring Network is to measure concentrations and spatial and temporal trends of selected air pollutants (O_3 included) at 661 sites located in 113 key environmental protection cities throughout China. The

ozone monitoring including QA/QC procedures are in urgent for the implementation of the new standard in China.

The traceability is an important part in QA/QC system. Basically, all physical and chemical measurements should be traceable to SI unit. Calibration by Standard Reference Photometer (SRP) or transfer standard is widely used because of high precision and long term stability. However, this type of calibration is not SI traceable. Occasional check by SI traceable method (such as gas phase titration by NO gas) should be performed.

There are ozone primary standards (Model 49i-PS) and ozone analyzers (Model 49i) currently in Quality Management Dept., CNEMC. The ozone traceability system of ambient ozone monitoring in China could be established based on these transfer standards and SRP located in China.

1.2 Calibration traceability

Considering the purpose of achieving higher O_3 standard, CNEMC should maintain as direct a path as possible between its standards and National Institute of Standards and Technology (NIST). It also follows the general rule of thumb that monitoring organizations should always seek to minimize the use of additional levels of transfer standards.

As shown in Figure 1, four (4) ozone primary standards (Model 49i-PS) and six (6) ozone analyzers (Model 49i) should be calibrated by Level 1 O_3 standard (SRP). The O_3 transfer standards of provincial environmental monitoring centers should be calibrated by 49i-PS or 49i. The O_3 analyzers of municipal environmental monitoring centers should be calibrated by O_3 transfer standards of provincial environmental monitoring centers.

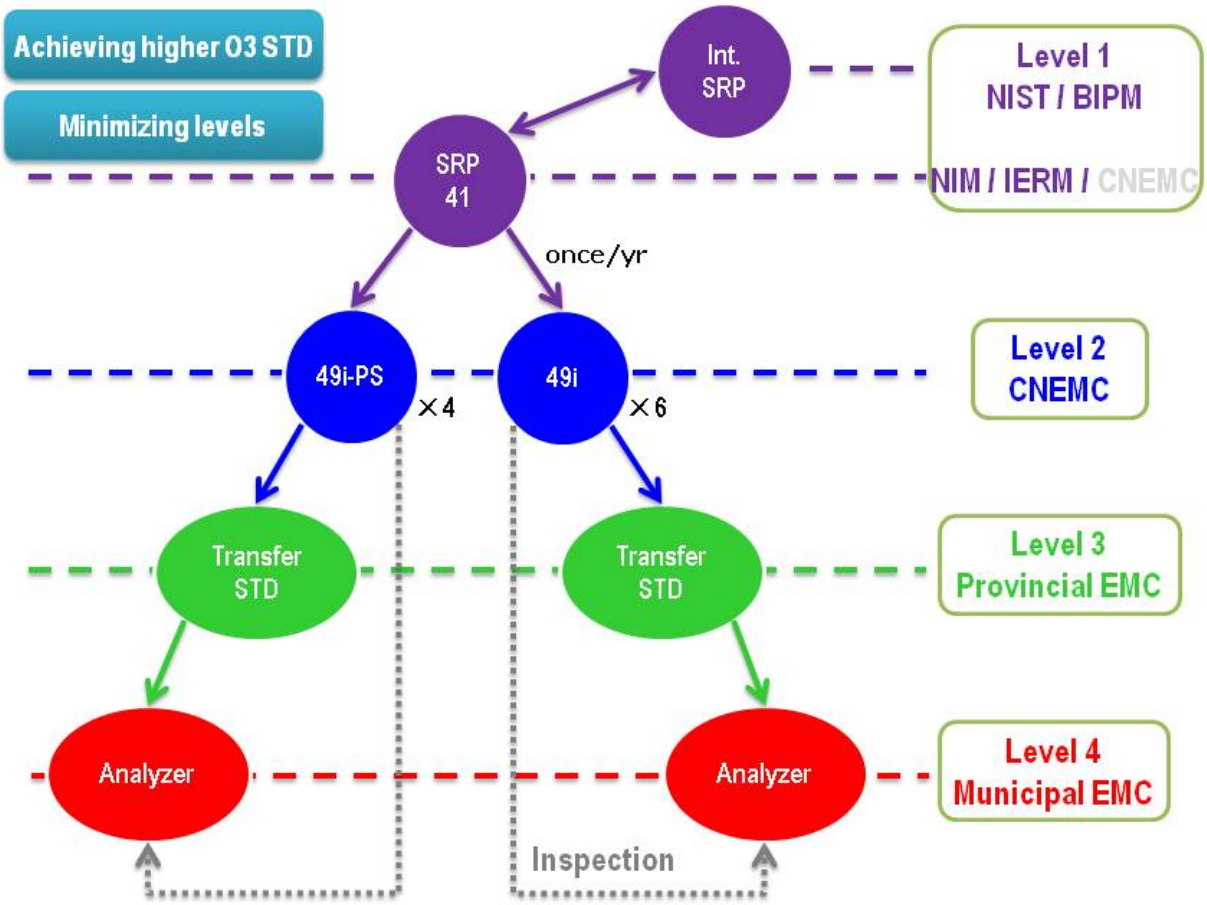

Figure 1. O_3 traceability scheme in China.

Verification of O_3 analyzers of municipal environmental monitoring centers by CNEMC could be carried out as inspection for the QA/QC performance of provincial environmental monitoring centers. A new verification rather than reverification should be implemented for this purpose because different standards will be used in this case. However, the calibration should be carried out by provincial environmental monitoring centers after the verification if necessary. The acceptance criteria for the verification of O_3 analyzers of municipal environmental monitoring centers to the Level 2 standard could be different from that for the verification of O_3 analyzers of municipal environmental monitoring centers to the Level 3 standard.

Thus, Level 2 O_3 transfer standards, Level 3 O_3 transfer standard, and Level 4 O_3 standard are maintained and operated by CNEMC, provincial environmental monitoring centers, and municipal environmental monitoring centers, respectively, as shown in Table 1.

As suggested in EPA-454/B-10-001, Level-3 standards are, at a minimum, a photometer. The level 3 standard can be a photometer and generator but should not be just a generator. There are four types of calibration of Level 3 standard using Level 2 standard in CNEMC, as tabulated in Table 2.

Table 1. Different level of ozone standards in environmental monitoring organizations of China.

Organization	Standard	Standard level	Type
NIM/IERM	SRP	1	Stationary
CNEMC	49i-PS × 4	2	Stationary
	49i × 6	2	Stationary
Provincial environmental monitoring center	O_3 transfer standard	3	Traveling
Municipal environmental monitoring center	O_3 monitor	4	On-site

Note: Level-2 standard is distinguished as the standard that is transported to SRP for comparison once a year.

Table 2. Instrument configuration for four types of calibration.

Level 2 O_3 STD	Level 3 O_3 STD	Ancillary equipment
Model 49i-PS (photometer and O_3 generator)	Photometer	Zero air generator
	Photometer and O_3 generator	Zero air generator
Model 49i (photometer)	Photometer	Zero air generator, O_3 generator
	Photometer and O_3 generator	Zero air generator

1.3 Scope

The fellowship study was conducted in particular for the following scope:

- Acceptance testing procedures for new O_3 standards and analyzers.
- Calibration procedures for O_3 standards and analyzers. This study mainly focused on the calibration by SRP or transfer standard.

2. Methods

2.1 Instrument

In this study, the O_3 transfer standard 49i-PS (Thermo Scientific, USA) and O_3 analyzers 49i (Thermo Scientific, USA) were utilized. 49i-PS was used as the standard gas generator.

The instrument model appears in the article does not mean that it is the authors' recommendation.

2.2 Acceptance procedures

For commercially available analytical instruments, some or all of the testing may be carried out by the manufacturer. However, the user should assume a skeptical attitude, in view of manufacturing tolerances and possible defective components, and carry out at least some minimal tests to verify that each unit is acceptable. Moreover, qualifying new instruments can help ensure the instruments will perform under various field conditions that might not get observed during a traditional verification processes described.

The acceptance testing for ozone analyzers was conducted according to the content of Appendix B in *Ambient Air Quality Automatic Monitoring Technical Specifications (HJ 193-2005)*.

The testing methods are as follows.

2.2.1 Zero drift

The zero point was calibrated after the instrument power was on. Zero gas was continuously supplied for 24 hr and the zero drift was recorded.

2.2.2 Span drift

Span calibration (400 ppb, full scale 500 ppb) was conducted. Standard gas of 400 ppb was continuously supplied for 24 hr and the span drift was recorded.

2.2.3 Precision

Standard gas of 400 ppb was continuously supplied for more than 15 min and the data of the 15th minute was recorded. The test was repeated for 5 times. The maximum deviation was recorded.

2.2.4 Response time

Standard gas of 400 ppb was supplied and the averaging time was set to 10 sec. The time from the beginning of the data change to 360 ppb (90% of the gas concentration) was recorded. The testing was repeated for 3 times. The average time was recorded. After the instruments passed the acceptance testing discussed above, the instruments could be used for further study.

2.3 Calibration procedures

2.3.1 Initial verification

Prior to use, an O_3 transfer standard must be verified by establishing a quantitative verification relationship between the transfer standard and the higher level O_3 concentrations obtained by the UV calibration procedure as specified in *Appendix D of 40 CFR, Part 50 (EPA 1979)*. The O_3 analyzers also should be verified by establishing a quantitative verification relationship between the analyzer and the higher level O_3 standard. The verification procedures are as follows.

The verification relationship shall consist of the average of 6 individual comparisons of the transfer standard to a higher level UV O_3 standard. Each comparison must cover the full range of O_3 concentrations and is to be carried out on a different day to a primary standard.

Each comparison shall consist of at least 6 comparison points at concentrations approximately evenly spaced over the concentration range of the transfer standard, including 0 and (90 ± 5%) of the upper range limit of the transfer standard. For the 6 or more comparison points of each comparison, compute the slope and intercept by the least squares linear regression of the transfer standard output (either a generated O_3 concentration or a concentration assay) and the UV authoritative O_3 standard.

When 6 comparisons have been completed, compute the average slope ($\bar{m}$):

$$\bar{m} = \frac{1}{6}\sum_{i=1}^{6} m_i \qquad \text{(Eq. 1)}$$

and the average intercepts ($\bar{I}$):

$$\bar{I} = \frac{1}{6}\sum_{i=1}^{6} I_i \qquad \text{(Eq. 2)}$$

where m_i and I_i are the individual slopes and intercepts, respectively, of each comparison regression.

Compute the relative standard deviation of the 6 slopes, (s_m):

$$s_m = \frac{100}{\bar{m}}\sqrt{\frac{1}{5}\left[\sum_{i=1}^{6}(m_i)^2 - \frac{1}{6}(\sum_{i=1}^{6} m_i)^2\right]}\,\% \qquad \text{(Eq. 3)}$$

and the standard deviation s_I defined in Equation 4 for the 6 intercepts:

$$s_I = \sqrt{\frac{1}{5}\left[\sum_{i=1}^{6}(I_i)^2 - \frac{1}{6}(\sum_{i=1}^{6} I_i)^2\right]} \qquad \text{(Eq. 4)}$$

The value of s_m must be ≤ 3.7%, and s_I must be ≤ 1.5 (ppb). If either of these specifications is exceeded, it indicates that the transfer standard or analyzer has too much variability and corrective action must be taken to reduce the variability before the transfer standard or analyzer may be certified.

If the transfer standard meets the specifications (s_m ≤ 3.7%, s_I ≤ 1.5 ppb), the verification relationship for the transfer standard consists of the average slope ($\bar{m}$) and the average intercept ($\bar{I}$) can be computed as shown in Equation 5.

$$\text{Std. } O_3 \text{ conc.} = \frac{1}{\bar{m}}(\text{Indicated } O_3 \text{ conc.} - \bar{I}) \qquad \text{(Eq. 5)}$$

2.3.2 Periodic reverification

A verified transfer standard of Level 3 and greater must be reverified at the beginning and end of the ozone season or at least every six months whichever is less. A transfer standard which loses its verification may cause the loss of ambient O_3 measurements made with ambient monitors that were calibrated with the transfer standard.

Consequently, more frequent reverification schedule will reduce the magnitude and risk of any such loss. If a transfer standard in only a generation device (no photometer) it is strongly suggested that more frequent reverifications occur. More frequent reverification may also provide better accuracy, particularly for transfer standards that show slow but steady change (drift) over long periods of time.

To maintain continuous verification, an O_3 transfer standard must be recertified as follows.

The first step in the reverification procedure is to carry out a comparison of the transfer standard to an authoritative standard as specified in 2.3.1.

The linear regression slope of the new comparison (m) must be within the interval $\bar{m} \pm 0.05\bar{m}$ (i.e., the average slope of the latest 6 comparisons).

If the new slope of transfer standard is within the ± 5% specification, compute a new average slope $\bar{m}$

and a new average intercept $\bar{I}$ as prescribed in 2.3.1 using the new comparison and the 5 most recent previous comparisons. Thus $\bar{m}$ and $\bar{I}$ are running or moving averages always based on the 6 most recent comparisons. Compute a new relative standard deviation of the slopes (s_m) and standard deviation (S_I) based on the new comparison and the 5 most recent previous comparisons.

The new s_m and S_I must again meet the respective 3.7% and 1.5 SD specifications. If all specifications are met, then a new verification relationship (based on the updated $\bar{m}$ and $\bar{I}$) is established.

If a certified transfer standard fails to meet one of the reverification specifications, it loses its verification. Reverification then requires 6 new comparisons according to the entire verification procedure described in section 2.3.1. This failure could be due to a malfunction, which obviously should be corrected before repeating the verification procedure. If a transfer standard has been repaired or serviced in a way which could affect its output, the complete verification procedure must also be repeated.

3. Results and discussion

3.1 Acceptance testing

3.1.1 Zero drift

The zero drift testing results were shown in Figure 2.

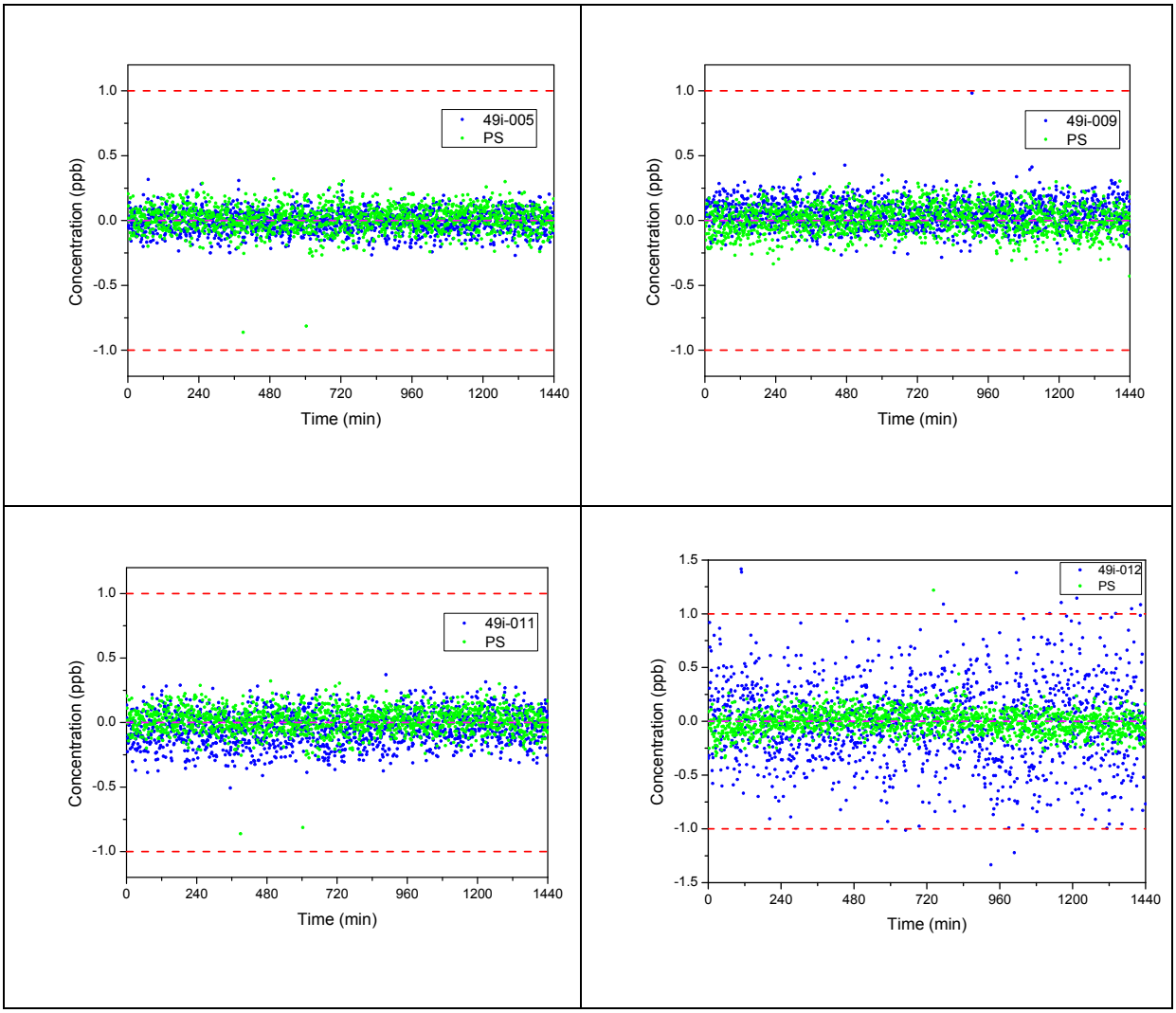

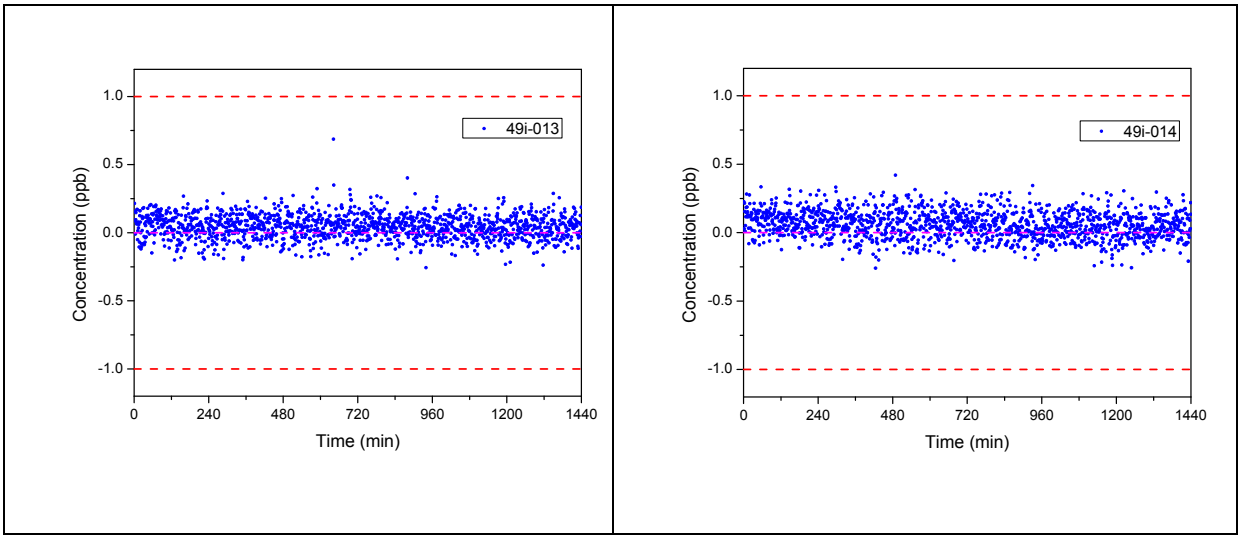

Figure 2. Zero drift graphs.

All the O_3 analyzers passed the testing except 49i-012. For 49i-012, some data was out of ±1ppb.

3.1.2 Span drift

The span drift testing results were shown in Figure 3.

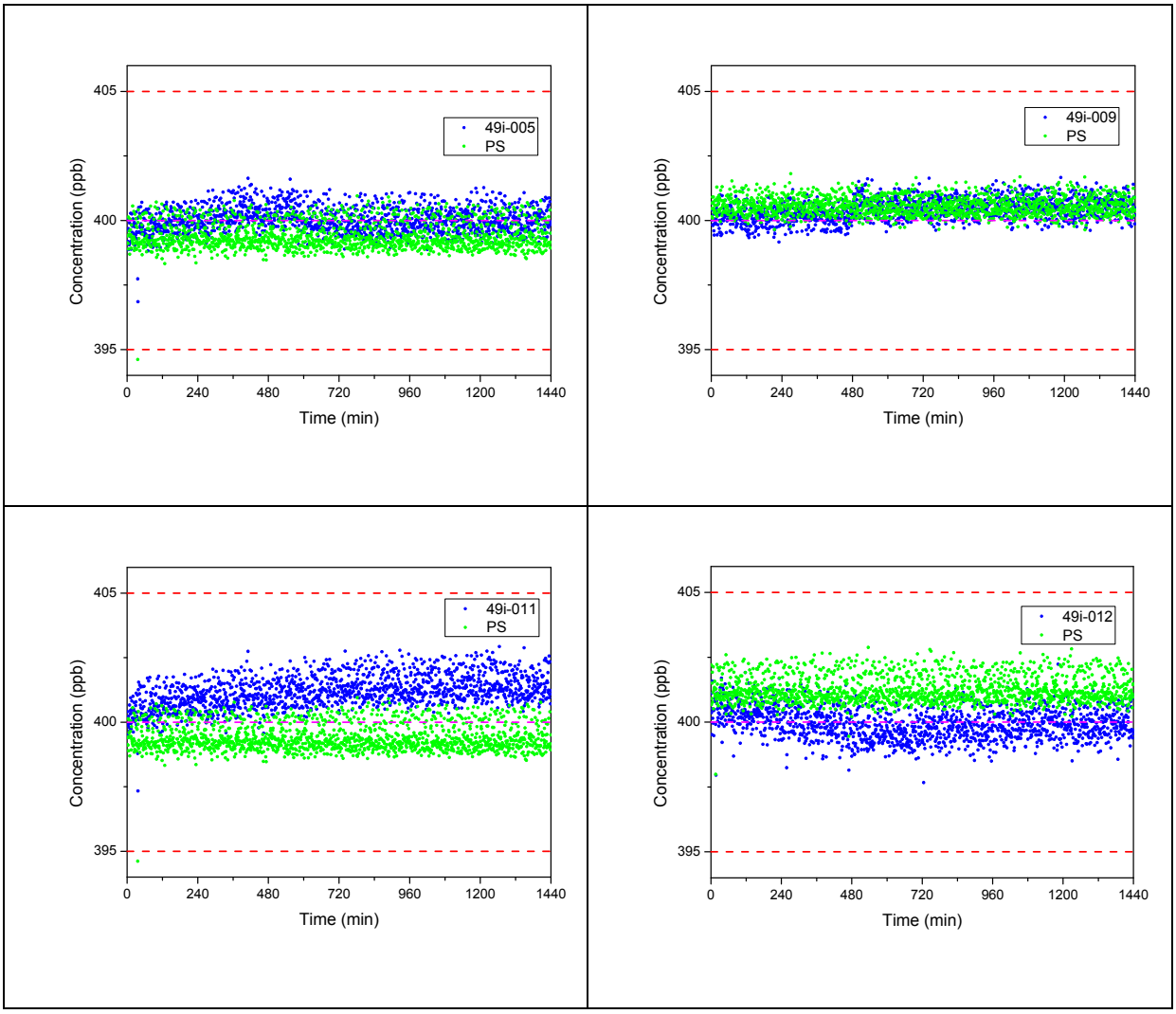

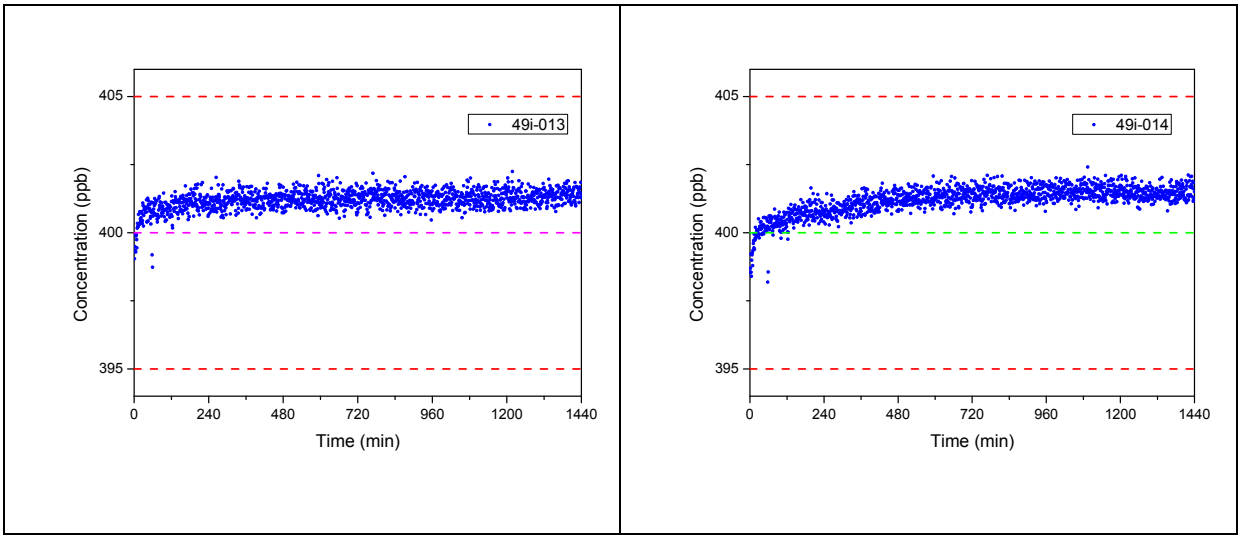

Figure 3. Span drift graphs.

All the analyzers met the span drift requirement.

3.1.3 Precision

The precisions were shown in Table 3.

Table 3 Precisions (gas of 400 ppb was used)

Instrument No.	**005**	**009**	**011**	**012**	**013**	**014**
Maximum deviation (ppb)	0.9226	0.5862	0.9276	1.2160	-0.9774	-0.6956

3.1.4 Response time

The precisions were shown in Table 4.

Table 4. Response time.

Instrument No.	**005**	**009**	**011**	**012**	**013**	**014**
Time (s)	13.06	16.92	16.47	16.72	10.09	9.96

All the data of acceptance testing were shown in Table 5.

Table 5. Acceptance testing data.

Instrument No.	**Zero drift (ppb, 24 hr)**		**Span drift (ppb, 24 hr)**		**Precision (ppb)**		**Response time (sec)**	
	Specification	**Test value**	**Specification**	**Test value**	**Specification**	**Test value**	**Specification**	**Test value**
005	< ±1	0.32	≤1%full scale (≤±5)	-3.15	≤1% reading (≤±4)	0.92	≤20	13.06
009		0.98		1.67		0.59		16.92
011		-0.51		2.93		0.93		16.47
012		-1.53		1.91		1.02		16.72
013		0.69		2.25		-0.98		10.09
014		0.42		2.41		-0.70		9.96

All the testing data met the technical specification except for the zero drift of 49i-012.

It was sent back to the manufacturer. Currently, it meets the technical specification after the adjustment.

3.2 Calibration

49i-012 was used in the calibration experiment. The data of 6-Day initial ozone verification and the linear regression were shown in Table 6.

Table 6. 6-Day initial ozone verification.

Date	**C_{PS} (X)/ ppb**	**C_{49i} (Y)/ ppb**	**Absolute deviation (ppb)**	**Relative deviation %**	**r**	**Slope (m_i)**	**Intercept (I_i)**
Day 1	0	0	0	-	1	0.987	-0.343

May 30, 2012	50	49	-1	-2.00			
	100	98	-2	-2.00			
	200	197	-3	-1.50			
	300	296	-4	-1.33			
	450	444	-6	-1.33			
	0	0	0	-			
	50	49	-1	-2.00			
Day 2	100	99	-1	-1.00			
May 31, 2012	200	197	-3	-1.50	1	0.987	-0.070
	300	296	-4	-1.33			
	450	444	-6	-1.33			
	0	0	0	-			
	50	49	-1	-2.00			
Day 3	100	99	-1	-1.00			
Jun. 1, 2012	200	197	-3	-1.50	1	0.989	-0.244
	300	296	-4	-1.33			
	450	445	-5	-1.11			
	0	0	0	-			
	50	49	-1	-2.00			
Day 4	100	98	-2	-2.00			
Jun. 4, 2012	200	197	-3	-1.50	1	0.989	-0.517
	300	296	-4	-1.33			
	450	445	-5	-1.11			
	0	0	0	-			
	50	49	-1	-2.00			
Day 5	100	99	-1	-1.00			
Jun. 5, 2012	200	198	-2	-1.00	1	0.990	-0.081
	300	297	-3	-1.00			
	450	445	-5	-1.11			
	0	0	0	-			
	50	49	-1	-2.00			
Day 6	100	99	-1	-1.00			
Jun. 6, 2012	200	198	-2	-1.00	1	0.990	-0.081
	300	297	-3	-1.00			
	450	445	-5	-1.11			
Average						**0.989**	**-0.223**

Standard deviation (ppb)							**0.182**
RSD%						**0.14**	

s_m was less than 3.7%, and sI was less than 1.5 ppb. The instrument after maintenance met the requirement for calibration.

Thus, the quantitative relationship was obtained as equation 6.

$$C_{49i} = 0.989 \times C_{PS} - 0.223 \qquad \textbf{(Eq. 6)}$$

The reverification would be carried out in the future study.

4. Conclusions

The ozone standard transfer scheme was depicted. The important QA/QC procedures including acceptance testing and calibration were illustrated. The analyzers used in this study could meet the technical specifications for acceptance. The zero drift was less than 1 ppb. The span drift was less than 3.15 ppb. The precision was less than 1.02 ppb. The response time was than 16.92 sec. The initial verification was also successfully implemented. s_m was 0.14%, and sI was 0.182 ppb. The quantitative relationship could be expressed as $C_{49i} = 0.989 \times C_{PS} - 0.223$.

5. Acknowledgements

The authors would like to thank the financial support provided by the Research Fellowship Program of EANET.

The authors would like to thank Mr. Shirai, Miss. Aoyagi and Mrs. Nakamura (Data Management Department, ACAP) for the informative discussion on the research subject.

The authors would like to thank Dr. Hajime Akimoto, Dr. Jesada Luangjame, Mr. Makoto Hayashi, Mr. Jiro Sato, Dr. Ken Yamashita, Mr. Shiro Toda, Mrs. Junko Fujita, Mrs. Kozue Kasahara, Mr. Takashi Sugita, Dr. Tsuyoshi Ohizumi, Dr. Mingqun Huo, Mr. Nobuhiro Nagai, Dr. Hiroyuki Sase, Dr. Naoyuki Yamashita and all staffs of ACAP for valuable suggestions and considerate help during the stay in Niigata, Japan.

6. References

CASTNET. 2010. Quality Assurance Project Plan (QAPP), Air Resource Specialists Standard Operating Procedures (SOP) and Calibration of ambient air quality analyzers. Clean Air Status and Trends

Network (CASTNET). Calibration and routine maintenance of thermo environmental instruments model and ozone analyzers (3100-2004).

EANET. 2001. Quality Assurance/Quality Control (QA/QC) Program for the Air Concentration Monitoring in East Asia. The First Session of the Scientific Advisory Committee (SAC1) on the Acid Deposition Monitoring Network in East Asia (EANET) in November 2001, Chiang Mai, Thailand. 29 p.

MEP. 2006. Automated methods for ambient air quality monitoring, standard HJ/T 193-2005. Ministry of Environmental Protection (MEP), the People's Republic of China, Xizhimennei Nanxiaojie, Beijing.

MEP. 2010. Ambient air - Determination of ozone – Ultraviolet photometric method, standard HJ 590-2010. Ministry of Environmental Protection (MEP), the People's Republic of China, Xizhimennei Nanxiaojie, Beijing.

UNEPA. 2010. Standards For The Calibration of Ambient Air Monitoring Analyzers For Ozone. Technical Assistance Document, EPA-454/B-10-001. U.S. Environmental Protection Agency, Office of Air Quality Planning and Standards, Air Quality Assessment Division, Research Triangle Park, North Carolina 27711. 68 p.

Identifying of Acid Deposition Potential Sources in Thailand using PMF Model and PCA Analysis

Ittipol Pawarmart[1] and Keiichi Sato[2]

[1]Pollution Control Department, Ministry of Natural Resources and Environment,
Bangkok 10400, Thailand.
E-mail: ittipol.p@pcd.go.th
[2]Asia center for Air Pollution Research (ACAP),
1182 Sowa, 950-2144, Niigata, Japan
E-mail: ksato@acap.asia

Abstract

Source apportionment of acid deposition has now become an increasingly important and significant tool for current perspectives of acid deposition situation since identification of various source characteristics of acid deposition is important and necessary for policy makers to implement further control strategies appropriately. This research study aims to compare the aerosol and rain water components monitoring dataset collected from different 4 monitoring stations in Thailand from 2001 to 2011 (1. urban site (Public Relation Department station in Bangkok) 2. rural site (Mae Hia station in Chiang Mai province) 3. industrial site (Chonburi station in Chonburi province) and 4. rural site (Sakaerat station in Nakhon Ratchasima province)). The statistical instruments which are the Principal Components Analysis (PCA) and the Positive Matrix Factorization (PMF) were applied for identifying potential source types and generate modeled source profiles of acid depositions. The findings of this study could help to comprehend the most potential sources of acid deposition and their characteristics in different monitoring stations and periods.

Keywords: aerosol, acid deposition, source profile, PCA, PMF

1. Introduction

As a national focal point of the Acid Deposition Monitoring Network in East Asia (EANET), Thailand by the Pollution Control Department (PCD) has established an acid deposition monitoring stations firstly since 2001 in order to monitor acid deposition situations in Thailand and collaborate with the acid deposition measurement networks across the 13 member countries in the East Asia region. Recently, 11 acid deposition monitoring stations totally have been operated in Thailand which 6 of those were designated for EANET and the

wet and dry depositions including precipitations data have been measured and collected. Those monitoring data are required and very important to evaluate acid deposition situations, to develop control programs, to evaluate risk to human health and to evaluate a success of those control strategies as well. However, analyzes and interpretations of the collected monitoring data are limited and lacking of skills and experience in Thailand. Therefore, applying and experience in analyze and interpretation techniques including statistic instruments are needed and required for the acid deposition evaluation, not only on the acid deposition situations but also identifying the potential sources of acid deposition in Thailand.

In recent years, factor analysis has become an important statistical instrument of investigation in modern science, being an adequate tool to investigate the principles of interaction of components and their integration into a system. Also, a higher level of data interpretations and analyzes techniques have been applied to acid deposition studies presently such as the Principal Components Analysis (PCA), Positive Matrix Factorization (PMF) and Chemical Mass Balance (CMB) receptor models. The use of statistical methods are different by types; however; one of the most important advantages of PMF is the inclusion of uncertainties in the model that allows us to apply different weights to different variables, taking into consideration the lack of precision of the analytical methods; thus it selects only rotated solutions with positive contributions from the sources. Other advantage is that PMF can identify potential sources of interested pollutants and provide the contribution of each source in absence of prior information on sources (Paatero *et al.*, 2005). Also PMF identifies and quantifies sources relatively faster than other models such as CMB and PCA. In particular, the PCA analysis has been applied previously to many research studies in Thailand to identify the potential sources of acid depositions and their characteristics in different areas. (Thepanondh, 2005; Panyakapo *et al*., 2007; Onchang and Sato, 2009 and Sillapapiromsuk *et al*., 2010)

This research study aims to compare the aerosol and rain water components monitoring dataset collected from different 4 monitoring stations in Thailand between 2004 to 2008 and to apply the statistical instruments which are the Principal Components Analysis (PCA) and the Positive Matrix Factorization (PMF) for identifying potential source types and generate modeled source profiles of acid depositions. Source apportionment of acid deposition has now become an increasingly important and significant tool for current perspectives of acid deposition situation since identification of various source characteristics of acid deposition is important and necessary for policy makers to implement further control strategies appropriately. The findings of this study could help to comprehend the most potential sources of acid deposition and their characteristics in different monitoring stations and periods.

2. Experimental Methods

2.1 Sampling sites

The monitoring dataset of aerosol and rain water components were collected from different 4 monitoring stations since 2001 to 2010 in Thailand which are 1) urban site (Public Relation Department station in Bangkok) 2) rural site (Mae Hia station in Chiang Mai province) 3) industrial site (Chonburi station in

Chonburi province) and 4) rural site (Sakaerat station in Nakhon Ratchasima province) (Figure 1). The aerosol and rain water components were measured following the EANET technical guidelines (EANET, 2003). The aerosol samples were sampling by filter pack as 10 days basis and the rain water samples were sampling as daily basis of the raining day in a year. The collected samples were analyzed for wet ionic species (nss-SO_4^{2-}, ss-SO_4^{2-}, NO_3^-, Cl^-, NH_4^+, Na^+, K^+, Mg^{2+}, nss-Ca^{2+}, ss-Ca^{2+} and H^+) and dry ionic species (nss-SO_4^{2-}, ss-SO_4^{2-}, NO_3^-, Cl^-, NH_4^+, Na^+, K^+, Mg^{2+} and Ca^{2+}) using ion chromatography. The data quality was also determined by checking ion balance using the principle of electro-neutrality in precipitation water (cation and anion balance, R1) and by comparing measured and calculated conductivities (R2) following the QA/QC criteria of EANET (EANET, 2000).

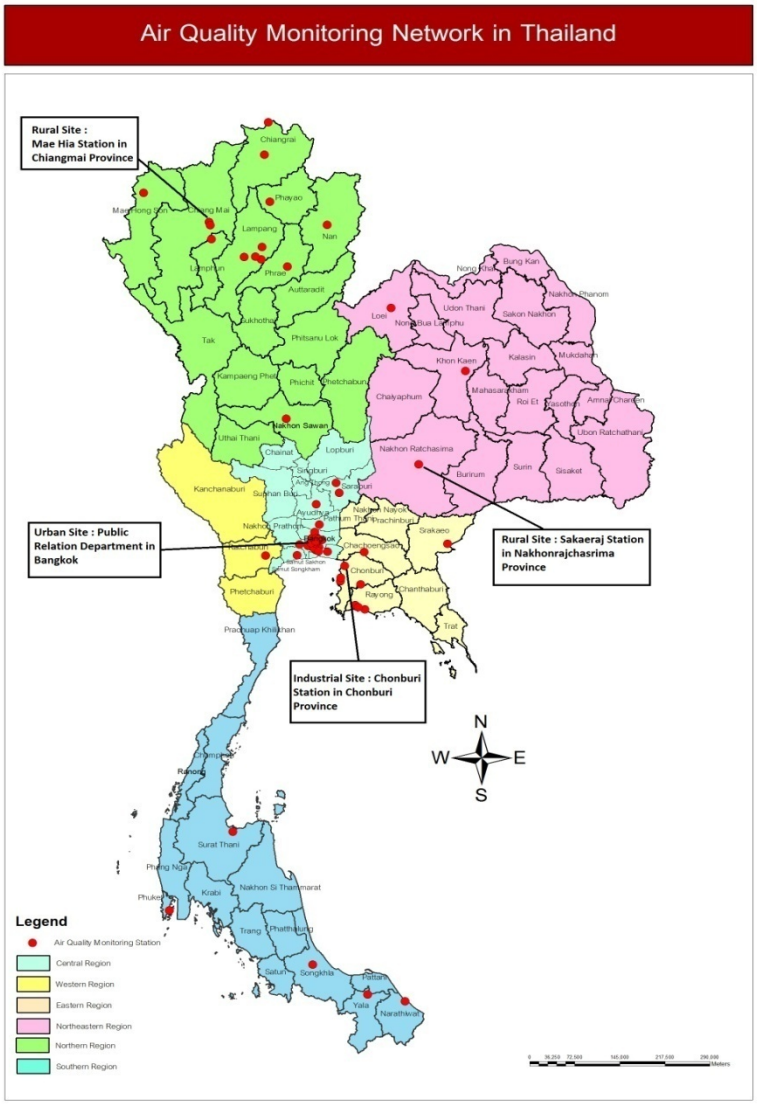

Figure 1. Location of selected aerosol and rain water compositions monitoring stations.

2.2 Positive Matrix Factorization Receptor Model (PMF)

In order to generate modeled source profiles, Positive Matrix Factorization (PMF) version 3.0 by US EPA was performed on the complete data sets of aerosol and rain water components collected in 2004 and 2008 from each of the four monitoring stations in Thailand. PMF is one of many solutions to the CMB equations and it uses time series of data to constrain the source profiles as well as the source contributions. A solution is selected as modeled factors are associated with source types based on a comparison of their dominant chemical components with measured source profiles (US EPA, 2008). The PMF assumes that concentrations at receptor sites are impacted by linear combinations of source emissions, which are derived as factors in the model. Thus, model supposes there are *p* sources impacting a receptor, and linear combinations of the impacts from the *p* sources give rise to the observed concentrations of the various species (Paatero *et al*., 2005).

Mathematically can be written as:

$$X_{ij} = \sum_{k=1}^{p} G_{ik} F_{kj} + E_{ij} \quad (1)$$

where Xij is the *(i x j)* matrix of ambient concentrations of j species on the i days, Gik is the *(i x k)* matrix of sources contributions of k factors on i days, Fkj is the *(k x j)* matrix of source profiles of k factors that is species j, and Eij is the *(i x j)* matrix of residuals not fitted by the model. The task of PMF model is to minimize the Q function using constrained, weighted least–squares. This function is defined as:

$$Q = \sum_{i=1}^{n} \sum_{j=1}^{m} \left(\frac{X_{ij} - \sum_{k=1}^{p} G_{ik} F_{kj}}{S_{ij}} \right)^2 \quad (2)$$

To perform the PMF model, a qualitative knowledge of the sources is only required, however PMF model also has limitations such as inability to clearly separate covariant sources. It is remarkable that PMF factors only reveal species temporally covary and thus the model will group them. However, temporal variability of a pollutant concentration is not solely determined by changes in emissions, as PMF model assumes, so we should not link the factors to source profiles directly, although many studies refer the PMF factors as sources. PMF requires two input files, one file with the concentrations and one with the uncertainties associated with those concentrations. The selection of modeling parameters and number of factors is not straightforward and is still largely affected by the experience of authors (Paatero *et al*., 2003).

The PMF Model has been widely used in previous studies to identify the number of possible sources having a major influence on air pollution problems in many countries. (For example: Troussier *et al*., 2007; Raman and Hope, 2007; Kitayama *et al*., 2008; Zhang, 2009; Thornhill *et al.*, 2010; Oh *et al.*, 2011; Pindado *et al.*, 2011).

2.3 Principle Component Analysis (PCA)

As a statistical instrument, Factor Analysis Multiple-Regression (FA-MR) is a receptor modeling technique employed to apportion the contributing sources to ambient pollution. One such technique of factor analysis is the principal component analysis (PCA). The objective of applying PCA is to derive a small number of components, which explain a maximum of the variance in the data. In this study, factor analysis PCA was applied to dataset of aerosol and rain water components data of dry and ionic species of the 4 monitoring stations in 2004 and 2008 to identify their potential sources and the different of their characteristics. Initial factors were extracted from a matrix of correlations. Factors with eigenvalues over than 1 were considered for varimax rotation to obtain the final factor matrix, retaining unities in the principal diagonal of the correlation matrix. A loading factor which greater than 0.70 was considered to be important in this study. Factor analysis was carried out by the principle component method using the statistical package – SPSS version 17 for Windows. This method has been widely used in previous studies to identify the number of possible sources having a major influence on air pollution problems (for example, Zunckel *et al.*, 2003; Thepanondh *et al.*, 2005; Seto *et al.*, 2007; Reff *et al*., 2007; Zhang *et al.,* 2007; Panyakapo and Onchang, 2008; Viana *et al.*, 2008; Oh et al., 2011).

2.4 Source Analysis of Major Ionic Compositions

In order to identify potential source types, the resolved sources profiles from the operation of PMF Model and the PCA analysis were compared with all known profiles obtained from previous research studies and the identification of sources was based on the presence of dominant ionic species to indicate the potential sources of ionic species in aerosol and rain water samples which are combustion process (nss-SO_4^{2-} and NO_3^-), marine contribution (ss-SO_4^{2-}, ss-Ca^{2+}, Na^+ and Cl^-), biomass burning (K^+) and crustal source (nss-Ca^{2+} and Mg^{2+}) (Fujita *et al*., 2000; Yamasoe *et al.*, 2000; Okay *et al*., 2002; Migliavacca, 2004; Panyakapo *et al.*, 2006; Sanmanee *et al.*, 2007). The combustion process was characterized by the presence of SO_4^{2-} and NO_3^- in high concentration (Sunder Raman and Hope, 2007). High concentration of ss-SO_4^{2-}, ss-Ca^{2+}, Na^+ and Cl^- indicates for marine contribution and K^+ might be also considered as a chemical signature of biomass burning since K^+ occurs usually in coarse particles in soil, while fine particles of K^+ resulted from the wood combustion. NH_4^+ has been indicated for the agricultural source. Also, nss-Ca^{2+} and Mg^{+2} have been best suited for soil dust source. The tracer associated with this profile clearly supports the existence of soil and dust re-suspension sources (Khare *et al*., 2004; Zunckel *et al*., 2003).

3. Results

In this research study, the dataset of the dry ionic species (9 species; nss-SO_4^{2-}, ss-SO_4^{2-}, NO_3^-, Cl^-, NH_4^+, Na^+, K^+, Mg^{2+} and Ca^{2+}) and the wet ionic species (11 species; nss-SO_4^{2-}, ss-SO_4^{2-}, NO_3^-, Cl^-, NH_4^+, Na^+, K^+, Mg^{2+}, nss-Ca^{2+}, ss-Ca^{2+} and H^+) collected from the different 4 acid deposition monitoring stations in 2004 and 2008 (only at Sakaerat station collected in 2006 and 2008) were computed by the PCA analysis and the PMF Model in order to compare the concentrations and to identify the potential sources and the different of their

characteristics in different periods. The number of factors or potential sources statistically determined is highly dependent on number of aerosol samples and rain water samples of each monitoring sites, number of ionic species, various local and regional environments and study scopes (Oh *et* al., 2011) In case of the PCA analysis, factors with eigenvalue greater than 1 were considered for varimax rotation to obtain the final factor matrix. After rotation of the factor-loading matrix, the factors were interpreted as origins or common sources assuming that the inter-correlations among the original variables were generated by a smaller number of unobserved factors. For the PMF Model, the number of factors was selected after evaluating the following steps: a) signal to noise of the input variable was carefully examined and values less than 0.2 were recorded as bad, 0.2 to 2 were recorded as weak and above 2 were recognize as strong, b) the goodness-of-fit parameters, i.e., *Q* (robust) and *Q* (true) were optimized changing the number of factors and compared with *Q* (theoretical) (US EPA, 2008).

3.1 Urban site: Public Relation Department station in Bangkok

The varimax-rotated PCA and PMF Model were performed using the dataset of the dry and wet ionic species collected at the Public Relation Station in Bangkok, compared between dataset in 2004 (dry ionic species, n = 20 and wet ionic species, n = 35) and in 2008 (dry ionic species, n = 72 and wet ionic species, n = 62). The obtained results of the PCA and the PMF Model operations are shown in Table 1 to Table 4 and in Figure 2 to Figure 5, respectively.

Table 1 shows the identification of 3 factors of the dry ionic species in 2004 computing by the PCA analysis, explaining about 89.5% of the data variance as well as loading greater than 0.7. The first factor displays high loading level, accounting for 50.07% of nss-SO_4^{2-}, NO_3^-, Cl^- and K^+ indicating of combustion process, biomass burning and marine contribution sources. Factor 2 explains 23.66% of the variance proving correlation of ss-SO_4^{2-} and Na^+ which represented for marine contribution source. The third factor contributes 15.77% of the variance and shows NH_4^+ and Ca^{2+} as significant. This significantly indicates cation distributions from crustal and agricultural activities. Figure 2 shows the results of the dry ionic species dataset in 2004 using the PMF Model, found 3 factors representing for 3 potential sources. The dominant species of the factor 1 were nss-SO_4^{2-}, Cl^- and K^+, respectively which indicated for combustion process, marine contribution and biomass burning sources. The factor 2 was composed of nss-SO_4^{2-}, Ca^{2+} and NH_4^+ proving ionic distribution from combustion process, crustal and agricultural activities. The factor 3 contributes for NO_3^- and Na^+ indicating for combustion process and marine contribution.

Table 1. Varimax-rotated PCA of dry ionic species at the Public Relation Department in Bangkok in 2004.

Component	Factor 1	Factor 2	Factor 3
nss-SO_4^{2-}	**0.763**		0.616
ss-SO_4^{2-}		**0.978**	
NO_3^-	**0.793**	0.270	0.218
Cl^-	**0.971**		
NH_4^+			**0.910**

Na^+		**0.978**	
K^+	**0.955**	0.257	
Mg^{2+}	0.481	0.676	
Ca^{2+}	0.247		**0.898**
Eigenvalue	4.506	2.130	1.420
Variance (%)	50.072	23.664	15.775
Cumulative (%)	50.072	73.736	89.511
Possible source	Combustion process Biomass burning Marine contribution	Marine contribution	Agricultural Crustal

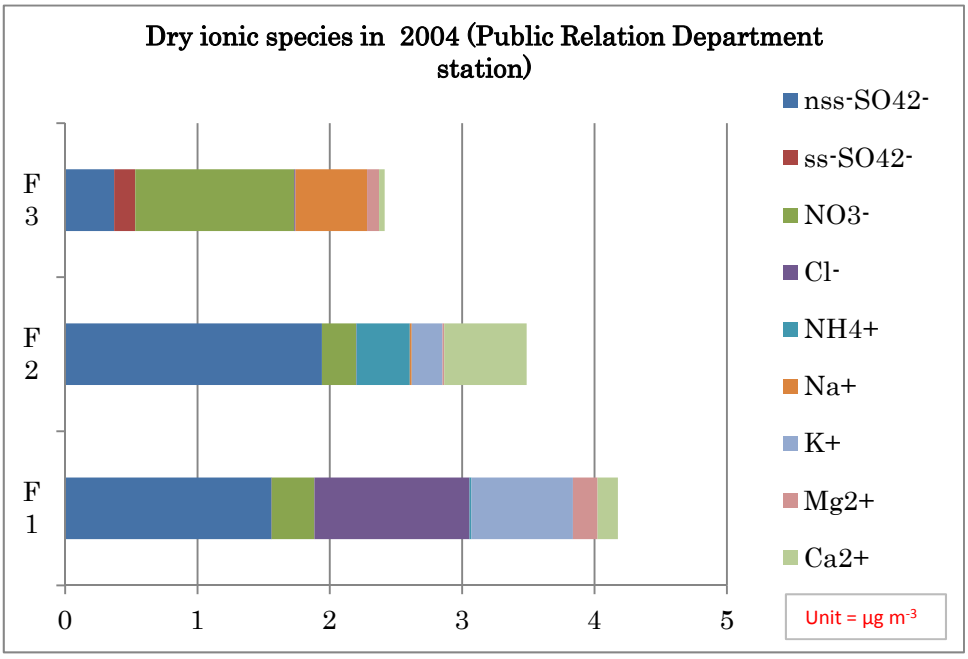

F1 = Combustion process/marine contribution/Biomass burning

F2 = Combustion process/crustal

F3 = Combustion process/marine contribution

Figure 2. Source profiles of dry ionic species at the Public Relation Department in Bangkok in 2004.

Table 2 shows the identification of 3 factors of the dry ionic species in 2008 computing by the PCA analysis, explaining about 88.01% of the data variance as well as loading greater than 0.7. The first factor displays high loading level, accounting for 59.19% of nss-SO_4^{2-}, NO_3^-, Ca^{2+} and K^+ indicating of combustion process, biomass burning, crustal and marine contribution sources. Factor 2 explains 16.91% of the variance

proving correlation of ss-SO_4^{2-}, Cl^- and Na^+ which represented for marine contribution. The third factor contributes 11.91% of the variance and shows NH_4^+ as significant. This significantly indicates cation distributions from agricultural activities. Figure 3 shows the results of the dry ionic species dataset in 2008 using the PMF Model, found 3 factors representing for 3 potential sources. The dominant species of the factor 1 were NO_3^- and Na^+, respectively which indicated for combustion process and marine contribution sources. The factor 2 was composed of nss-SO_4^{2-} NO_3^- and Ca^{2+} proving ionic distribution from combustion process and crustal. The factor 3 contributes for nss-SO_4^{2-}, NO_3^- and NH_4^+ indicating for combustion process and agricultural activities.

Table 2. Varimax-rotated PCA of dry ionic species at the Public Relation Department in Bangkok in 2008.

Component	Factor 1	Factor 2	Factor 3
nss-SO_4^{2-}	**0.922**		
ss-SO_4^{2-}	0.401	**0.891**	
NO_3^-	**0.774**	0.429	
Cl^-		**0.718**	0.547
NH_4^+			**0.955**
Na^+	0.401	**0.891**	
K^+	**0.847**	0.271	
Mg^{2+}	0.436	0.502	0.640
Ca^{2+}	**0.920**		0.231
Eigenvalue	5.327	1.522	1.072
Variance (%)	59.188	16.914	11.912
Cumulative (%)	59.188	76.101	88.013
Possible source	Combustion process Biomass burning Crustal	Marine contribution	Agricultural

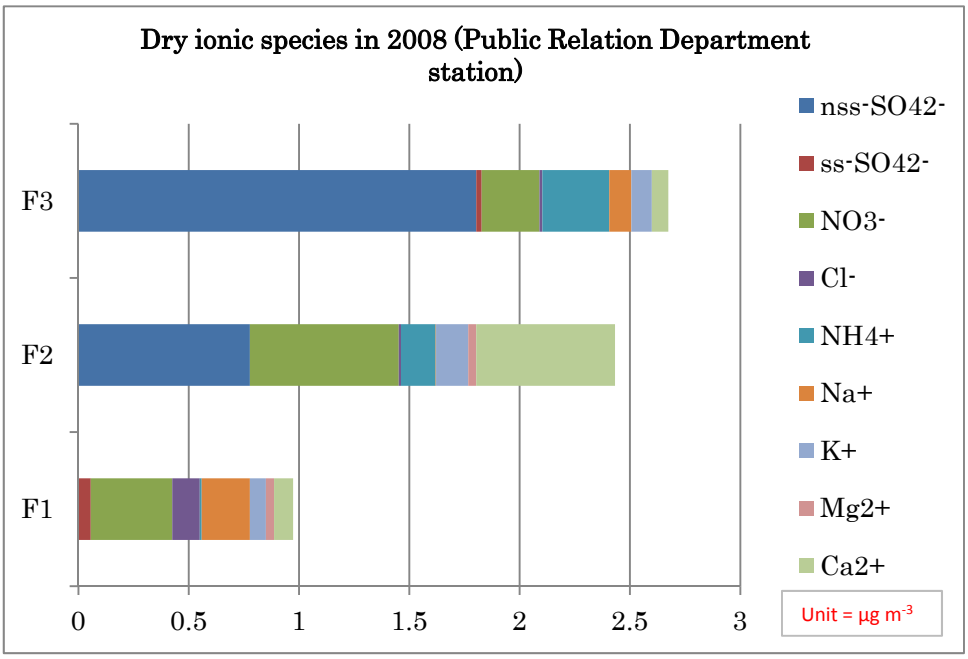

F1 = Combustion process/marine contribution

F2 = Combustion process/crustal

F3 = Combustion process/agricultural

Figure 3. Source profiles of dry ionic species at the Public Relation Department in Bangkok in 2008.

Table 3 shows the identification of 2 factors of the wet ionic species in 2004 computing by the PCA analysis, explaining about 89.10% of the data variance as well as loading greater than 0.7. The first factor displays high loading level, accounting for 71.80% of nss-SO_4^{2-}, NO_3^-, nss-Ca^{2+} NH_4^+, H^+ and K^+ indicating of combustion process, crustal ,agricultural activities, acid and biomass burning, respectively. Factor 2 explains 17.29% of the variance proving correlation of ss-SO_4^{2-}, Cl^-, Na^+, Mg^{2+} and ss-Ca^{2+} which represented for marine contribution and crustal. For the results of the PMF Model, Figure 4 shows the results of the wet ionic species dataset in 2004, found 3 factors representing for 3 potential sources. The dominant species of the factor 1 were nss-SO_4^{2-}, NO_3^-, NH_4^+ and nss-Ca^{2+}, respectively which indicated for combustion process ,agricultural activities and crustal. The factor 2 was composed of nss-SO_4^{2-} NO_3^-, NH_4^+ and K^+ proving ionic distribution from combustion process, agricultural activities and biomass burning. The factor 3 contributes for Cl^- and Na^+ indicating for marine contribution.

Table 3. Varimax-rotated PCA of wet ionic species at the Public Relation Department in Bangkok in 2004.

Component	Factor 1	Factor 2
nss-SO_4^{2-}	**0.912**	0.346
ss-SO_4^{2-}	0.269	**0.961**
NO_3^-	**0.906**	
Cl^-	0.305	**0.948**

NH_4^+	**0.852**	0.429
Na^+	0.269	**0.961**
K^+	**0.858**	0.376
Mg^{2+}	0.612	**0.733**
nss-Ca^{2+}	**0.851**	0.217
ss-Ca^{2+}	0.269	**0.961**
H^+	**0.714**	
Eigenvalue	7.899	1.903
Variance (%)	71.807	17.297
Cumulative (%)	71.807	89.104
Possible source	Combustion process Biomass burning Crustal Agricultural	Marine contribution

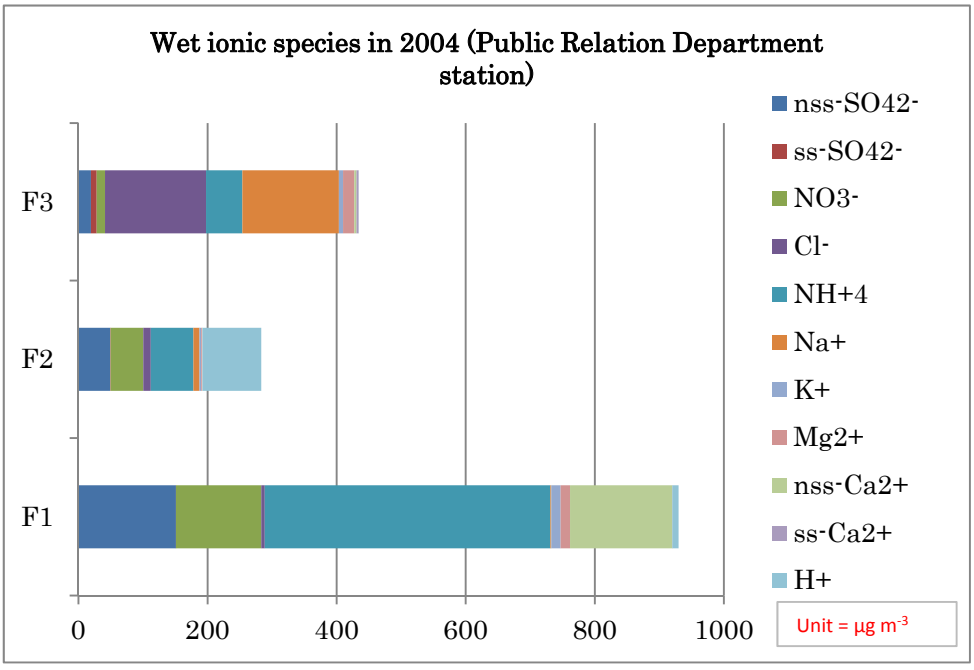

F1 = Combustion process/agricultural/crustal

F2 = Combustion process/agricultural/acid

F3 = Marine contribution

Figure 4. Source profiles of wet ionic species at the Public Relation Department in Bangkok in 2004.

Table 4 shows the identification of 2 factors of the wet ionic species in 2008,computing by the PCA analysis, explaining about 85.53% of the data variance as well as loading greater than 0.7. The first factor

displays high loading level, accounting for 68.59% of ss-SO_4^{2-}, Cl^-, Na^+, Mg^{2+}, nss-Ca^+ and ss-Ca^{2+} indicating of marine contribution and crustal, respectively. Factor 2 explains 16.94% of the variance proving correlation of nss-SO_4^{2-}, NO_3^-, NH_4^+, K^+ and H^+ which represented for combustion process, agricultural activities, biomass burning and acid.

For the results of the PMF Model, Figure 5 shows the results of the wet ionic species dataset in 2008, found 3 factors representing for 3 potential sources. The dominant species of the factor 1 were NH_4^+ and H^+, respectively which indicated for agricultural activities and acid. The factor 2 was composed of Cl^- and Na^+ proving ionic distribution from marine contribution. The factor 3 contributes for NH_4^+, NO_3^- and nss-SO_4^{2-} indicating for agricultural activities and combustion process.

Table 4. Varimax-rotated PCA of wet ionic species at the Public Relation Department in Bangkok in 2008.

Component	Factor 1	Factor 2
nss-SO_4^{2-}	0.446	**0.859**
ss-SO_4^{2-}	**0.954**	0.225
NO_3^-	0.328	**0.898**
Cl^-	**0.931**	0.287
NH_4^+	0.351	**0.831**
Na^+	**0.954**	0.225
K^+	0.459	**0.766**
Mg^{2+}	**0.887**	0.424
nss-Ca^{2+}	**0.797**	
ss-Ca^{2+}	**0.954**	0.225
H^+		**0.695**
Eigenvalue	7.545	1.864
Variance (%)	68.592	16.941
Cumulative (%)	68.592	85.533
Possible source	Marine contribution Crustal	Combustion process Biomass burning Agricultural Acid

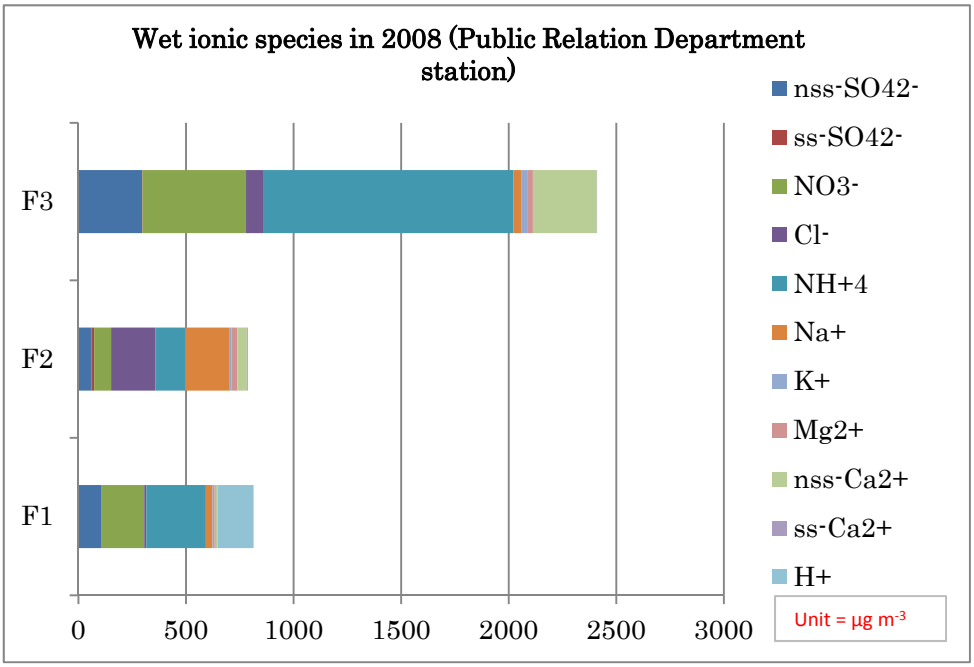

F1 = Combustion process/agricultural/acid

F2 = Marine contribution

F3 = Agricultural/combustion process/crustal

Figure 5. Source profiles of wet ionic species at the Public Relation Department in Bangkok in 2008.

The number of factor loading and potential source obtained from the computing of the PCA analysis and the PMF Model using the dry and wet ionic species in 2004 and 2008 were similar to research findings of the previous studies by Thepanondh *et al.*, 2005; King Mongkut's University of Technology Thonburi (KMUTT) that reported up to 2-4 factors for the potential sources of ionic species in Bangkok as a representative for urban area and the dominant source is mobile source. Also, 5 dominant potential sources have been found such as combustion process, marine contribution, agricultural activities, biomass burning and crustal. The dominant ionic species were nss-SO_4^{2-}, NO_3^- and NH_4^+, respectively which indicated for the contribution of mobile source and agricultural activities. The obtained results indicated a significantly contribution of a mixed potential sources and an independent source in Bangkok.

3.2 Rural site: Mae Hia station in Chiang Mai province

The varimax-rotated PCA and PMF Model were performed using the dataset of dry and wet ionic species collected at the Mae Hia station in Chiang Mai, compared between dataset in 2004 (dry ionic species, n = 31 and wet ionic species , n = 36) and in 2008 (dry ionic species, n = 110 and wet ionic species, n = 132). The obtained results of the PCA and the PMF Model operations are shown in Table 5 to Table 8 and in Figure 6 to Figure 9, respectively.

Table 5 shows the identification of 3 factors of the dry ionic species dataset in 2004, explaining about 91.25% of the data variance as well as loading greater than 0.7. The first factor displays high loading level, accounting for 43.02% of ss-SO_4^{2-}, Cl^-, Na^+ and K^+ indicating of marine contribution and biomass burning.

Factor 2 explains 30.37% of the variance proving correlation of NO_3^-, Mg^{2+} and Ca^{2+} which represented for combustion process and crustal. The third factor contributes 17.86% of the variance and shows nss-SO_4^{2-} and NH_4^+ as significant. This significantly indicates ionic distributions from combustion process and agricultural activities. Figure 6 shows the results of the dry ionic species dataset in 2004 computing by the PMF Model, found 3 factors representing for 3 potential sources. The dominant species of the factor 1 was NH_4^+ which indicated for agricultural activities. The factor 2 was composed of nss-SO_4^{2-}, proving ionic distribution from combustion process. The factor 3 contributes for nss-SO_4^{2-} and NO_3^- indicating for combustion process.

Table 5. Varimax-rotated PCA of dry ionic species at the Mae Hia station in Chiang Mai province in 2004.

Component	Factor 1	Factor 2	Factor 3
nss-SO_4^{2-}			**0.945**
ss-SO_4^{2-}	**0.992**		
NO_3^-		**0.877**	
Cl^-	**0.986**		
NH_4^+		0.218	**0.920**
Na^+	**0.992**		
K^+	**0.860**	0.420	
Mg^{2+}		**0.888**	
Ca^{2+}	0.250	**0.904**	0.265
Eigenvalue	3.872	2.734	1.608
Variance (%)	43.022	30.373	17.863
Cumulative (%)	43.022	73.395	91.259
Possible source	Marine contribution Biomass burning	Combustion process Crustal	Combustion process Agricultural

Table 6 shows the identification of 3 factors of the dry ionic species dataset in 2008, explaining about 79.57% of the data variance as well as loading greater than 0.7. The first factor displays high loading level, accounting for 43.88% of NO_3^-, Mg^{2+} and Ca^{2+}, Cl^-, Na^+ and K^+ indicating of combustion process and crustal. Factor 2 explains 22.90% of the variance proving correlation of nss-SO_4^{2-} which represented for combustion process. The third factor contributes 12.78% of the variance and shows ss-SO_4^{2-} and Na^+ as significant. This significantly indicates ionic distributions from marine contribution. Figure 7 shows the results of the dry ionic species dataset in 2008 computing by the PMF Model, found 3 factors representing for 3 potential sources. The dominant species of the factor 1 were NO_3^- and Ca^{2+}, respectively which indicated for combustion process and crustal. The factor 2 was composed of K^+ proving ionic distribution from biomass burning. The factor 3 contributes for nss-SO_4^{2-} and NH_4^+ indicating for combustion process and agricultural activities.

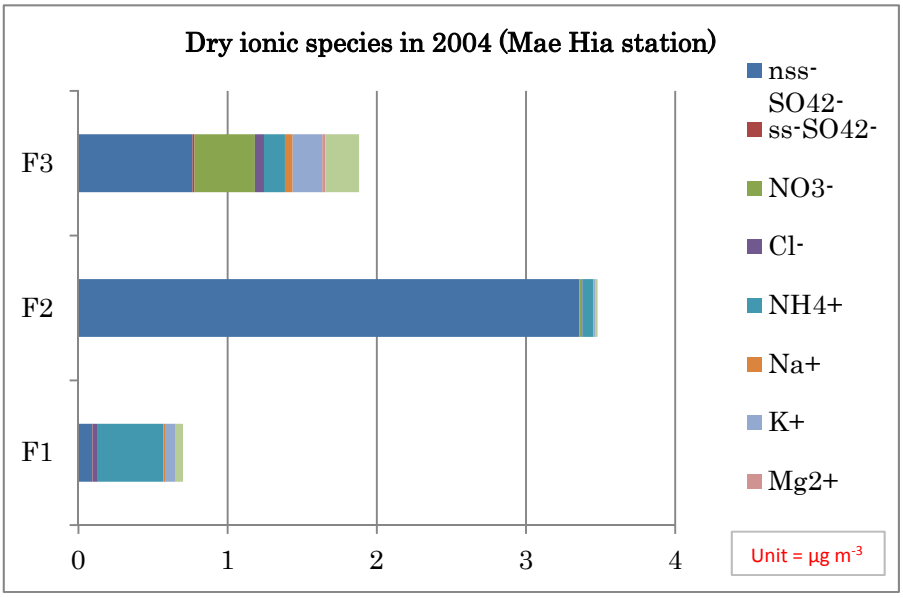

F1 = Agricultural

F2 = Combustion process

F3 = Combustion process/biomass burning/crustal

Figure 6. Source profiles of dry ionic species at the Mae Hia station in Chiang Mai province in 2004.

Table 6. Varimax-rotated PCA of dry ionic species at the Mae Hia station in Chiang Mai province in 2008.

Component	Factor 1	Factor 2	Factor 3
nss-SO_4^{2-}	0.418	**0.820**	
ss-SO_4^{2-}			**0.997**
NO_3^-	**0.833**		
Cl^-	0.394	0.523	
NH_4^+	0.341	0.626	
Na^+			**0.997**
K^+	0.492	0.671	
Mg^{2+}	**0.845**	0.273	
Ca^{2+}	**0.894**	0.245	
Eigenvalue	3.949	2.061	1.151
Variance (%)	43.882	22.900	12.787
Cumulative (%)	43.8822	66.783	79.570
Possible source	Combustion process Crustal	Combustion process	Marine contribution

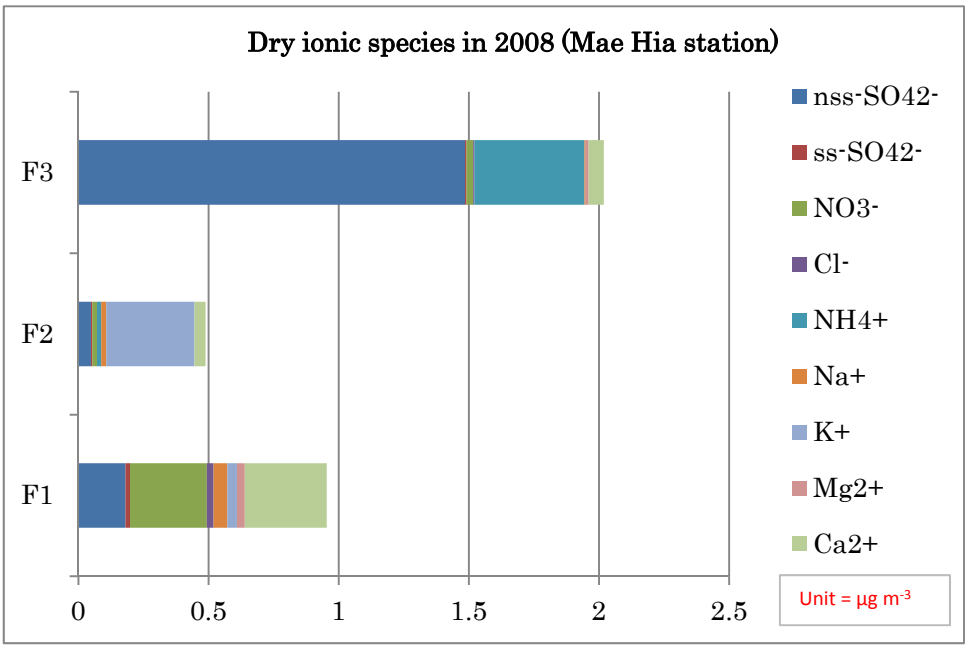

F1 = Combustion process/crustal

F2 = Biomass burning

F3 = Combustion process/agricultural

Figure 7. Source profiles of Dry ionic species at the Mae Hia station in Chiang Mai province in 2008.

Table 7 shows the identification of 2 factors of the wet ionic species dataset in 2004, explaining about 87.81% of the data variance as well as loading greater than 0.7. The first factor displays high loading level, accounting for 64.53% of ss-SO_4^{2-}, Na^+, K^+, Mg^{2+}, nss-Ca^{2+} and ss-Ca^{2+} indicating of marine contribution, biomass burning and crustal. Factor 2 explains 23.27% of the variance proving correlation of nss-SO_4^{2-}, NO_3^-, NH_4^+ and H^+ which represented for combustion process, agricultural activities and acid. Figure 8 shows the results of the wet ionic species dataset in 2004 computing by the PMF Model, found 3 factors representing for 3 potential sources. The dominant species of the factor 1 were NO_3^- and Cl^-, respectively which indicated for combustion process and marine contribution. The factor 2 was composed of Na^+ and nss-Ca^{2+} proving ionic distribution from marine contribution and crustal. The factor 3 contributes for NH_4^+, NO_3^- and nss-SO_4^{2-} indicating for agricultural activities and combustion process.

Table 7. Varimax-rotated PCA of wet ionic species at the Mae Hia station in Chiang Mai province in 2004.

Component	Factor 1	Factor 2
nss-SO_4^{2-}		**0.822**
ss-SO_4^{2-}	**0.979**	
NO_3^-	0.270	**0.897**
Cl^-	0.657	0.630

NH_4^+	0.361	**0.854**
Na^+	**0.979**	
K^+	**0.935**	
Mg^{2+}	**0.901**	0.335
nss-Ca^{2+}	**0.924**	
ss-Ca^{2+}	**0.979**	
H^+		**0.888**
Eigenvalue	7.099	2.561
Variance (%)	64.534	23.279
Cumulative (%)	64.534	87.813
Possible source	Marine contribution Biomass burning Crustal	Combustion process Agricultural

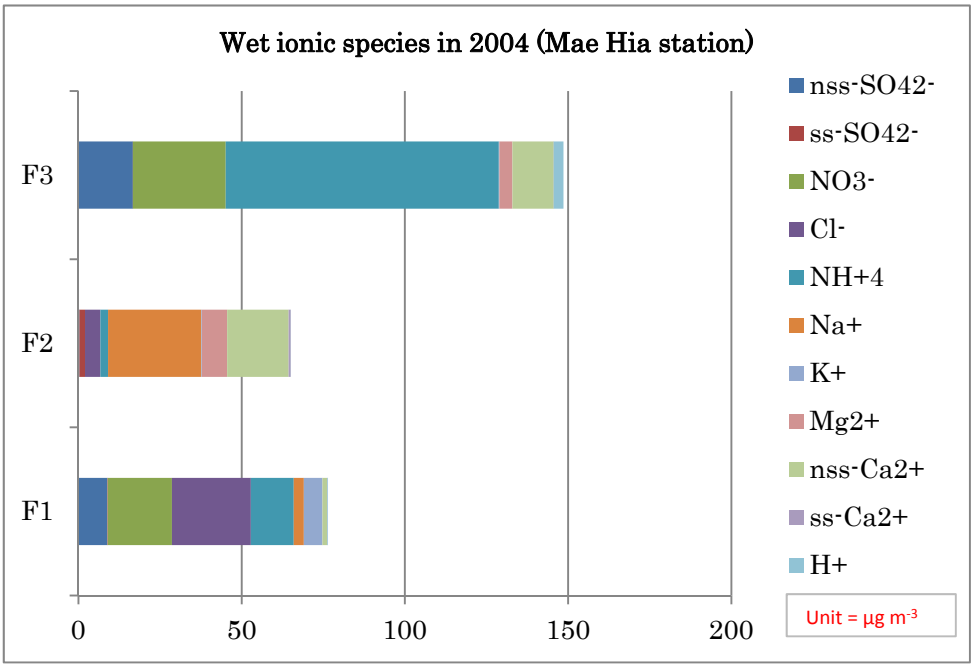

F1 = Combustion process/marine contribution/agricultural

F2 = Marine contribution/crustal

F3 = Agricultural/combustion process/crustal

Figure 8. Source profiles of wet ionic species at the Mae Hia station in Chiang Mai province in 2004.

Table 8 shows the identification of 2 factors of the wet ionic species dataset in 2008, explaining about 76.98% of the data variance as well as loading greater than 0.7. The first factor displays high loading level, accounting for 60.65% of ss-SO_4^{2-}, Na^+, K^+, Mg^{2+} and ss-Ca^{2+} indicating of marine contribution, biomass burning and crustal. Factor 2 explains 16.33% of the variance proving correlation of nss-SO_4^{2-}, NO_3^-, NH_4^+ and H^+ which represented for combustion process, agricultural activities and acid. Figure 9 shows the results of the wet ionic species dataset in 2008 computing by the PMF Model, found 3 factors representing for 3 potential sources. The dominant species of the factor 1 were K^+, Mg^{2+} and nss-Ca^{2+}, respectively which indicated for biomass burning and crustal. The factor 2 was composed of Cl^- and Na^+ proving ionics distribution from marine contribution. The factor 3 contributes for NH_4^+, NO_3^- and nss-Ca^{2+} indicating for agricultural activities, combustion process and crustal.

Table 8. Varimax-rotated PCA of wet ionic species at the Mae Hia station in Chiang Mai province in 2008.

Component	Factor 1	Factor 2
nss-SO_4^{2-}	0.209	**0.894**
ss-SO_4^{2-}	**0.901**	0.275
NO_3^-	0.331	**0.877**
Cl^-	0.572	0.571
NH_4^+	0.368	**0.763**
Na^+	**0.900**	0.273
K^+	**0.733**	
Mg^{2+}	**0.883**	
nss-Ca^{2+}	0.670	0.576
ss-Ca^{2+}	**0.901**	0.273
H^+		**0.722**
Eigenvalue	6.672	1.796
Variance (%)	60.651	16.331
Cumulative (%)	60.651	76.982
Possible source	Marine contribution Biomass burning Crustal	Combustion process Agricultural

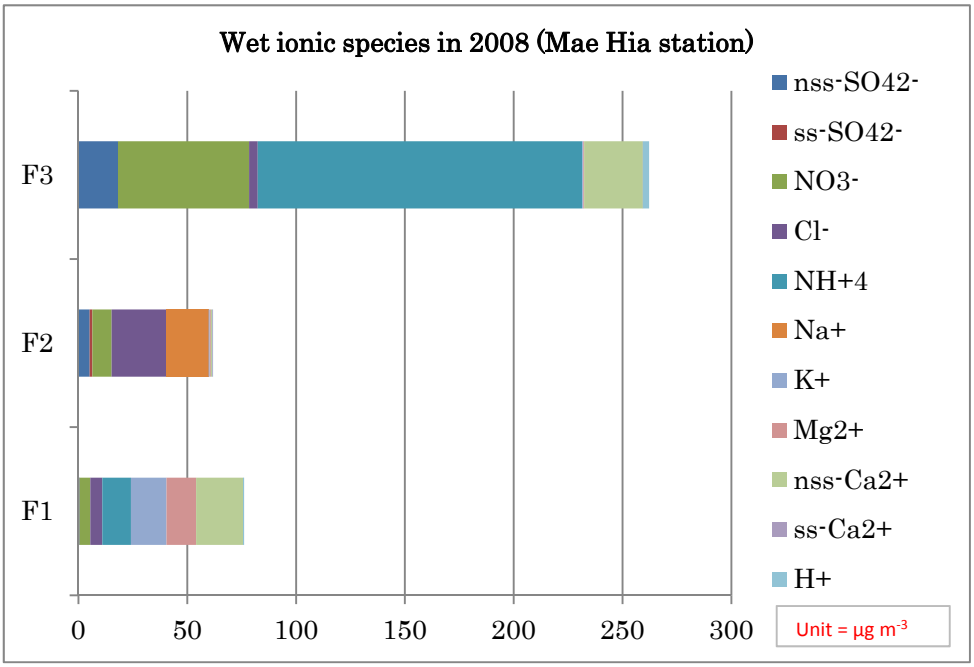

F1 = Crustal/biomass burning

F2 = Marine contribution

F3 = Agricultural/combustion process/crustal

Figure 9. Source profiles of wet ionic species at the Mae Hia station in Chiang Mai province in 2008.

The number of factor loading and potential source obtained from the computing of the PCA analysis and the PMF Model using the dry and wet ionic species in 2004 and 2008 were similar to research findings of the previous studies by Thepanondh *et al*., 2005; Onchang and Sato, 2009; Sillapapiromsuk *et al.*, 2010 that reported up to 2-4 factors for the potential sources of ionic species in Chiang Mai province as a representative for rural area. Also, 5 dominant potential sources were indicated such as combustion process, marine contribution, agricultural activities, biomass burning and crustal. The dominant ionic species were nss-SO_4^{2-}, NO_3^-, Cl^- and NH_4^+, respectively which indicated for the contribution of mobile source and agricultural activities. The obtained results indicated a significantly contribution of the mixed potential sources and an independent source in Chiang Mai province.

3.3 Industrial site: Chonburi station in Chonburi province

The varimax-rotated PCA and PMF Model were performed using the dataset of dry and wet ionic species collected at the Chonburi station in Chonburi province, compared between dataset in 2004 (dry ionic species, n = 30 and wet ionic species, n = 36) and in 2008 (dry ionic species, n = 79 and wet ionic species, n = 99). The obtained results of the PCA and the PMF Model operations are shown in Table 9 to Table 12 and Figure 10 to Figure 13, respectively.

Table 9 shows the identification of 2 factors of the dry ionic species dataset in 2004, explaining about 81.01% of the data variance as well as loading greater than 0.7. The first factor displays high loading level, accounting for 66.13% of nss-SO_4^{2-}, ss-SO_4^{2-}, Cl^-, Na^+, K^+, Mg^{2+} and Ca^{2+} indicating of combustion process ,

marine contribution, biomass burning and crustal. Factor 2 explains 14.88% of the variance proving correlation of NH_4^+ which represented for agricultural activities. Figure 10 shows the results of the dry ionic species dataset in 2004 computing by the PMF Model, found 3 factors representing for 3 potential sources. The dominant species of the factor 1 were Cl^- and Na^+, respectively which indicated for marine contribution. The factor 2 was composed of nss-SO_4^{2-} and K^+ proving ionic distribution from combustion process and biomass burning. The factor 3 contributes for nss-SO_4^{2-} indicating for combustion process.

Table 9. Varimax-rotated PCA of dry ionic species at the Chonburi station in Chonburi province in 2004.

Component	Factor 1	Factor 2
nss-SO_4^{2-}	**0.922**	
ss-SO_4^{2-}	**0.860**	0.280
NO_3^-	0.333	0.590
Cl^-	**0.911**	0.296
NH_4^+		**0.787**
Na^+	**0.860**	0.280
K^+	**0.949**	
Mg^{2+}	**0.890**	0.359
Ca^{2+}	**0.920**	0.273
Eigenvalue	5.952	1.339
Variance (%)	66.139	14.881
Cumulative (%)	66.139	81.019
Possible source	Combustion process Marine contribution Biomass burning	Agricultural

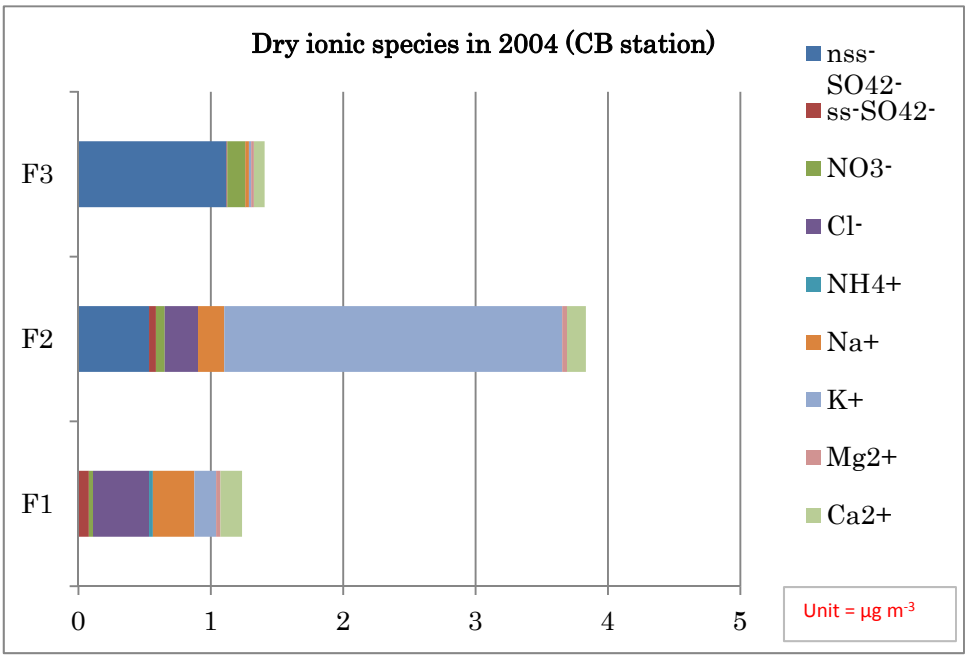

F1 = Marine contribution

F2 = Biomass burning

F3 = Combustion process

Figure 10. Source profiles of dry ionic species at the Chonburi station in Chonburi province in 2004.

Table 10 shows the identification of 3 factors of the dry ionic species dataset in 2008, explaining about 70.46% of the data variance as well as loading greater than 0.7. The first factor displays high loading level, accounting for 35.45% of nss-SO_4^{2-} and NO_3^- indicating of combustion process. Factor 2 explains 20.77% of the variance proving correlation of ss-SO_4^{2-} and Na^+ which represented for marine contribution. The third factor contributes 14.28% of the variance and shows Ca^{2+} as significant. This significantly indicates ionic distributions from crustal. Figure 11 shows the results of the dry ionic species dataset in 2008 computing by the PMF Model, found 3 factors representing for 3 potential sources. The dominant species of the factor 1 were nss-SO_4^{2-} , NO_3^- and Ca^{2+}, respectively which indicated for combustion process and crustal. The factor 2 was composed of Cl^- and NO_3^- proving ionic distribution from marine contribution and combustion process. The factor 3 contributes for NO_3^- and nss-SO_4^{2-} indicating for combustion process.

Table 10. Varimax-rotated PCA of dry ionic species at the Chonburi station in Chonburi province in 2008.

Component	Factor 1	Factor 2	Factor 3
nss-SO_4^{2-}	**0.882**		
ss-SO_4^{2-}		**0.987**	
NO_3^-	**0.956**		
Cl^-			0.686

NH_4^+	0.436		0.269
Na^+		**0.987**	
K^+	0.654	0.317	0.334
Mg^{2+}	0.418		0.688
Ca^{2+}		0.218	**0.737**
Eigenvalue	3.191	1.869	1.281
Variance (%)	35.456	20.771	14.287
Cumulative (%)	35.456	56.227	70.463
Possible source	Combustion process	Marine contribution	Crustal

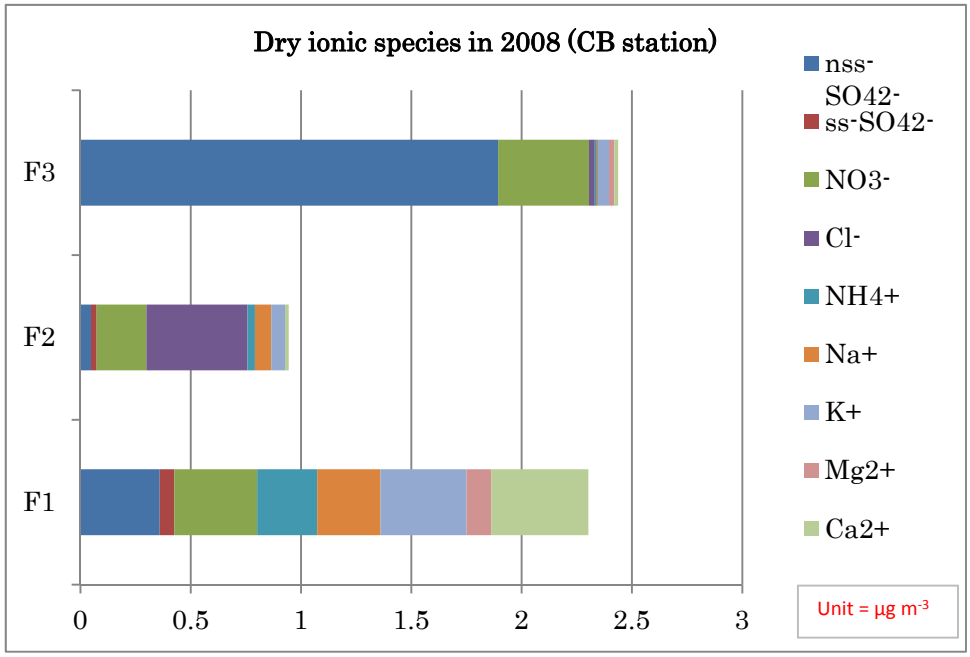

F1 = Combustion process/biomass burning/crustal

F2 = Marine contribution

F3 = Combustion process

Figure 11. Source profiles of dry ionic species at the Chonburi station in Chonburi province in 2008.

Table 11 shows the identification of 3 factors of the wet ionic species dataset in 2004, explaining about 77.62% of the data variance as well as loading greater than 0.7. The first factor displays high loading level, accounting for 46.86% of ss-SO_4^{2-}, Cl^-, Na^+ and ss-Ca^{2+} indicating of marine contribution and crustal. Factor 2 explains 21.61% of the variance proving correlation of nss-SO_4^{2-}, NO_3^-, NH_4^+ and H^+ which represented for combustion process, agricultural and acid. The third factor contributes 9.13% of the variance and shows K^+ as significant. This significantly indicates ionic distributions from biomass burning. Figure 12 shows the results of

the wet ionic species dataset in 2004 computing by the PMF Model, found 3 factors representing for 3 potential sources. The dominant species of the factor 1 were nss-SO_4^{2-} and Cl^-, respectively which indicated for combustion process and marine contribution. The factor 2 was composed of nss-SO_4^{2-}, NO_3^-, NH_4^+ and H^+ proving ionic distribution from combustion process, agricultural and acid. The factor 3 contributes for NO_3^-, NH_4^+ and Na^+ indicating for combustion process, agricultural activities and marine contribution.

Table 11. Varimax-rotated PCA of wet ionic species at the Chonburi station in Chonburi province in 2004.

Component	Factor 1	Factor 2	Factor 3
nss-SO_4^{2-}	0.236	**0.922**	
ss-SO_4^{2-}	**0.811**	0.264	
NO_3^-		**0.878**	
Cl^-	**0.845**		
NH_4^+	0.394	**0.736**	0.286
Na^+	**0.902**		0.318
K^+			**0.893**
Mg^{2+}	0.462	0.233	0.313
nss-Ca^{2+}	0.356	0.446	0.645
ss-Ca^{2+}	**0.856**		0.384
H^+		**0.925**	
Eigenvalue	5.156	2.378	1.005
Variance (%)	46.869	21.618	9.139
Cumulative (%)	46.869	68.487	77.626
Possible source	Marine contribution	Combustion process Agricultural Acid	Biomass burning

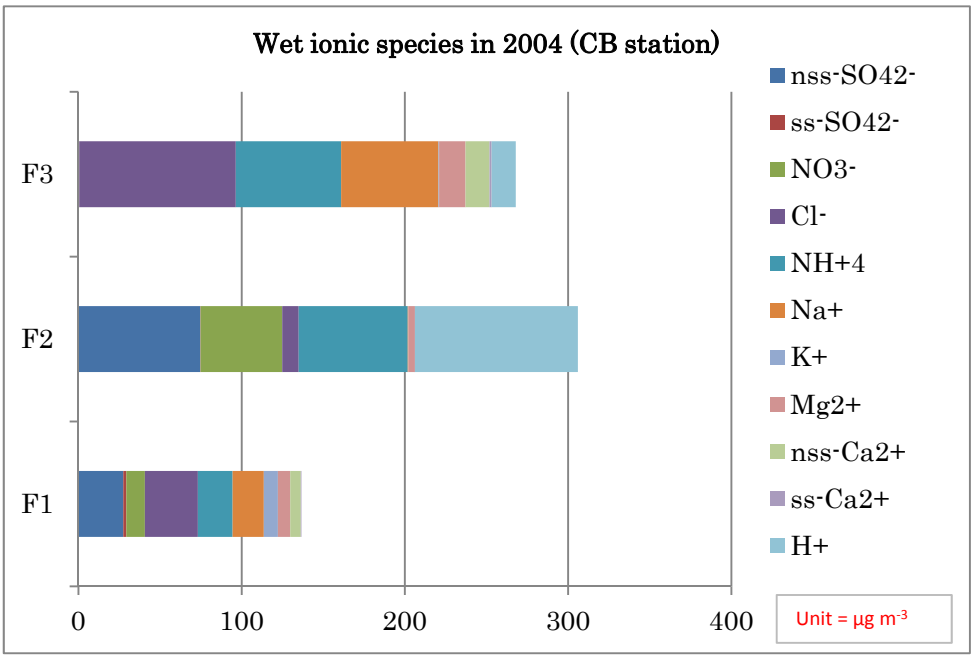

F1 = Marine contribution/combustion process

F2 = Acid/combustion process/agricultural

F3 = Marine contribution/agricultural

Figure 12. Source profiles of wet ionic species at the Chonburi station in Chonburi province in 2004.

Table 12 shows the identification of 2 factors of the wet ionic species dataset in 2008, explaining about 71.01% of the data variance as well as loading greater than 0.7. The first factor displays high loading level, accounting for 47.34% of ss-SO_4^{2-}, Cl^-, Na^+ and ss-Ca^{2+} indicating of marine contribution. Factor 2 explains 23.73% of the variance proving correlation of nss-SO_4^{2-}, NH_4^+ and H^+ which represented for combustion process, agricultural activities and acid. Figure 13 shows the results of the wet ionic species dataset in 2008 computing by the PMF Model, found 3 factors representing for 3 potential sources. The dominant species of the factor 1 were nss-SO_4^{2-}, NH_4^+ and H^+, respectively which indicated for combustion process, agricultural activities and acid. The factor 2 was composed of Cl^- and Na^+ proving ionic distribution from marine contribution. The factor 3 contributes for NO_3^-, NH_4^+, and nss-Ca^{2+} indicating for combustion process, agricultural activities and crustal.

Table 12. Varimax-rotated PCA of wet ionic species at the Chonburi station in Chonburi province in 2008.

Component	Factor 1	Factor 2
nss-SO_4^{2-}		**0.921**
ss-SO_4^{2-}	**0.963**	
NO_3^-	0.363	0.559
Cl^-	**0.912**	

NH_4^+		**0.881**
Na^+	**0.964**	
K^+		0.494
Mg^{2+}	0.555	0.655
nss-Ca^{2+}		0.678
ss-Ca^{2+}	**0.945**	
H^+		**0.774**
Eigenvalue	5.208	2.611
Variance (%)	47.345	23.733
Cumulative (%)	47.345	71.078
Possible source	Marine contribution	Combustion process Agricultural Acid

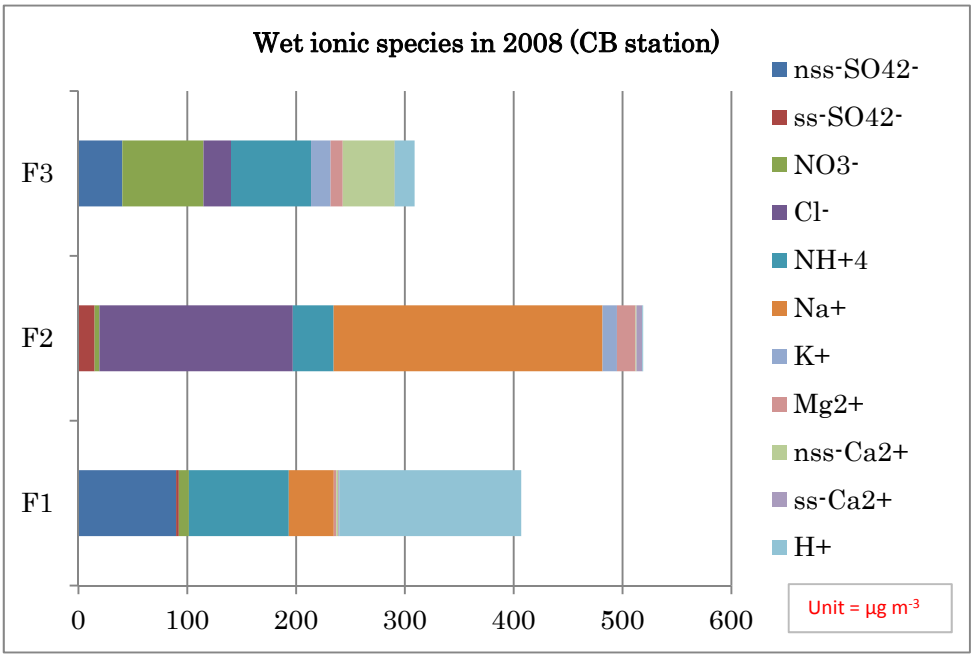

F1 = Acid/combustion process/agricultural

F2 = Marine contribution

F3 = Combustion process/agricultural/crustal

Figure 13. Source profiles of wet ionic species at the Chonburi station in Chonburi province in 2008.

The number of factor loading and potential source obtained from the computing of the PCA analysis and the PMF Model using the dry and wet ionic species in 2004 and 2008 were similar to research findings of the recent study by Kasetsart University (KU), 2012 that reported up to 2-4 factors for the potential sources of ionic species in Chonburi province as a representative for industrial area. Also, 6 dominant potential sources were indicated such as combustion process, marine contribution, agricultural activities, biomass burning, crustal and acid. The dominant ionic species were nss-SO_4^{2-}, Cl^-, Na^+, K^+ and H^+, respectively which indicated for the contribution of mobile source, marine contribution, biomass burning and acid. The obtained results indicated a significantly contribution of the mixed potential sources and an independent source in Chonburi province.

3.4 Rural site: Sakaerat station in Nakhon Ratchasima province

Since the Sakaerat station was first established in 2006, the varimax-rotated PCA and PMF Model were performed using the dataset of dry and wet ionic species collected at the Sakaerat station in Nakhon Ratchasima province, compared between dataset in 2006 (dry ionic species, n = 34 and wet ionic species, n = 36) and in 2008 (dry ionic species, n = 114 and wet ionic species, n = 124). The obtained results of the PCA and the PMF Model operations are shown in Table 13 to 16 and in Figure 14 to Figure 17, respectively.

Table 13 shows the identification of 4 factors of the dry ionic species dataset in 2006, explaining about 93.85% of the data variance as well as loading greater than 0.7. The first factor displays high loading level, accounting for 38.53% of K^+ and Mg^{2+} indicating of biomass burning and crustal. Factor 2 explains 26.73% of the variance proving correlation of ss-SO_4^{2-} and Na^+ which represented for marine contribution. The third factor contributes 17.02% of the variance and shows NO_3^- and Ca^{2+} as significant. This significantly indicates ionic distributions from combustion process and crustal. Factor 4 explains 11.55% of the variance proving correlation of nss-SO_4^{2-} and NH_4^+ which represented for combustion process and agricultural activities. Figure 14 shows the results of the dry ionic species dataset in 2006 computing by the PMF Model, found 3 factors representing for 3 potential sources. The dominant species of the factor 1 were nss-SO_4^{2-} and NH_4^+, respectively which indicated for combustion process and agricultural activities. The factor 2 was composed of nss-SO_4^{2-} and NO_3^- proving ionic distribution from combustion process. The factor 3 contributes for nss-SO_4^{2-}, NH_4^+ and K^+ indicating for combustion process , agricultural activities and biomass burning.

Table 13. Varimax-rotated PCA of dry ionic species at the Sakaerat station in 2006.

Component	Factor 1	Factor 2	Factor 3	Factor 4
nss-SO_4^{2-}		0.226		**0.966**
ss-SO_4^{2-}		**0.965**		
NO_3^-	0.221		**0.904**	
Cl^-	0.642		0.642	
NH_4^+				**0.993**
Na^+		**0.985**		
K^+	**0.923**	0.241		
Mg^{2+}	**0.953**			

Ca^{2+}		0.362	**0.861**	
Eigenvalue	3.468	2.406	1.532	1.040
Variance (%)	38.537	26.737	17.024	11.557
Cumulative (%)	38.537	65.233	82.293	93.855
Possible source	Biomass burning	Marine contribution	Combustion process Crustal	Combustion process Agricultural

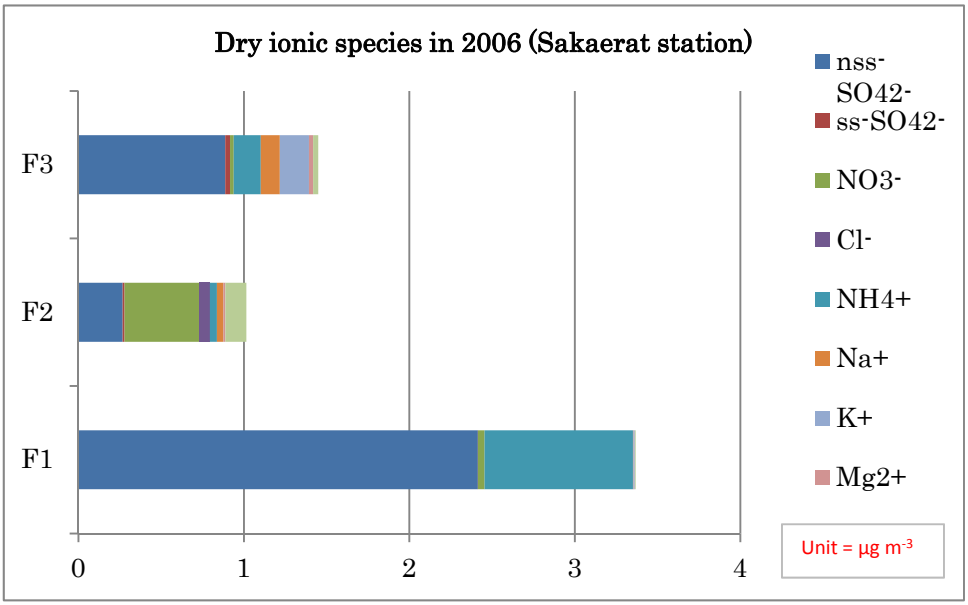

F1 = Combustion process/agricultural

F2 = Combustion process/crustal

F3 = Combustion process/biomass burning

Figure 14. Source profiles of dry ionic species at the Sakaerat station in 2006.

Table 14 shows the identification of 2 factors of the dry ionic species dataset in 2008, explaining about 77.50% of the data variance as well as loading greater than 0.7. The first factor displays high loading level, accounting for 52.20% of ss-SO_4^{2-}, NO_3^-, Na^+ and Mg^{2+} indicating of marine contribution, combustion process and crustal. Factor 2 explains 25.29% of the variance proving correlation of nss-SO_4^{2-}, NH_4^+ and K^+ which represented for combustion process ,agricultural activities and biomass burning. Figure 15 shows the results of the dry ionic species dataset in 2008 computing by the PMF Model, found 3 factors representing for 3 potential sources. The dominant species of the factor 1 were nss-SO_4^{2-} and NH_4^+, respectively which indicated for combustion process and agricultural activities. The factor 2 was composed of nss-SO_4^{2-}, NH_4^+ and K^+ proving ionic distribution from combustion process, agricultural and biomass burning. The factor 3 contributes for nss-SO_4^{2-} and NO_3^- indicating for combustion process.

Table 14. Varimax-rotated PCA of dry ionic species at the Sakaerat station in 2008.

Component	Factor 1	Factor 2
nss-SO_4^{2-}		**0.933**
ss-SO_4^{2-}	**0.824**	0.280
NO_3^-	**0.809**	0.233
Cl^-	0.550	0.549
NH_4^+		**0.945**
Na^+	**0.824**	0.280
K^+	0.304	**0.811**
Mg^{2+}	**0.857**	0.441
Ca^{2+}	0.695	0.405
Eigenvalue	4.699	2.277
Variance (%)	52.207	25.299
Cumulative (%)	52.207	77.505
Possible source	Marine contribution	Combustion process Agricultural Biomass burning

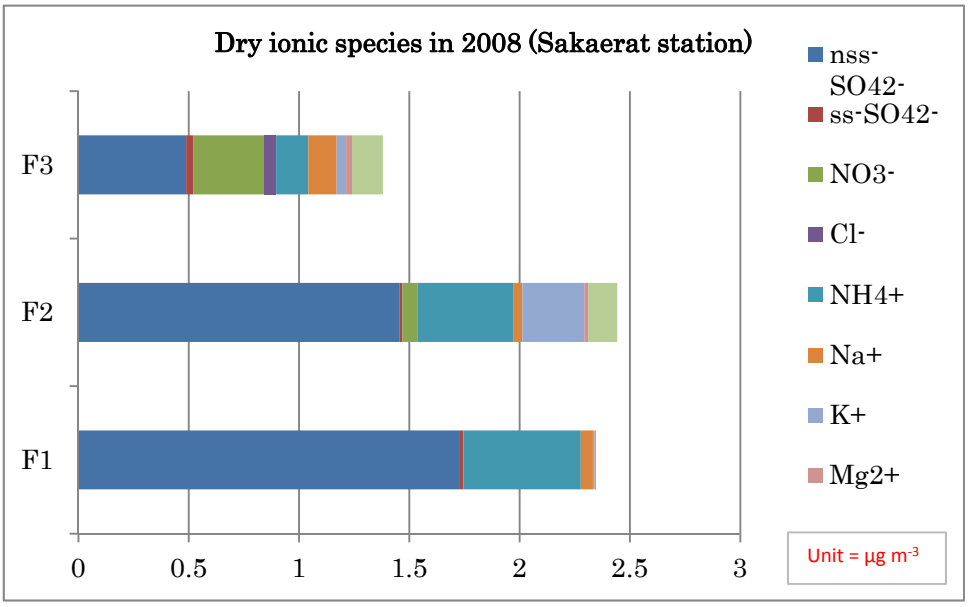

F1 = Combustion process/agricultural

F2 = Combustion process/agricultural/biomass burning

F3 = Combustion process/crustal

Figure 15. Source profiles of dry ionic species at the Sakaerat station in 2008.

Table 15 shows the identification of 3 factors of the wet ionic species dataset in 2006, explaining about 83.26% of the data variance as well as loading greater than 0.7. The first factor displays high loading level, accounting for 47.12% of ss-SO_4^{2-}, Cl^-, Na^+, Mg^{2+} and ss-Ca^{2+} indicating of marine contribution and crustal. Factor 2 explains 21.95% of the variance proving correlation of nss-SO_4^{2-}, NO_3^-, NH_4^+ and H^+ which represented for combustion process, agricultural and acid. The third factor contributes 14.17% of the variance and shows K^+ and nss-Ca^{2+} as significant. This significantly indicates ionic distributions from biomass burning and crustal. Figure 16 shows the results of the wet ionic species dataset in 2006 computing by the PMF Model, found 3 factors representing for 3 potential sources. The dominant species of the factor 1 were NO_3^- and NH_4^+ respectively which indicated for combustion process and agricultural activities. The factor 2 contributes Na^+, proving ionic distribution from marine contribution. The factor 3 was composed of nss-SO_4^{2-}, NO_3^- and H^+ indicating for combustion process and acid.

Table 15. Varimax-rotated PCA of wet ionic species at the Sakaerat station in 2006.

Component	Factor 1	Factor 2	Factor 3
nss-SO_4^{2-}	0.218	**0.904**	
ss-SO_4^{2-}	**0.982**		
NO_3^-	0.223	**0.839**	0.211
Cl^-	**0.841**	0.339	
NH_4^+		**0.603**	
Na^+	**0.982**		
K^+		0.257	**0.890**
Mg^{2+}	**0.752**		0.396
nss-Ca^{2+}			**0.934**
ss-Ca^{2+}	**0.982**		
H^+		**0.890**	
Eigenvalue	5.184	2.415	1.560
Variance (%)	47.126	21.957	14.179
Cumulative (%)	47.126	69.083	83.262
Possible source	Marine contribution	Combustion process Agricultural Acid	Biomass burning Crustal

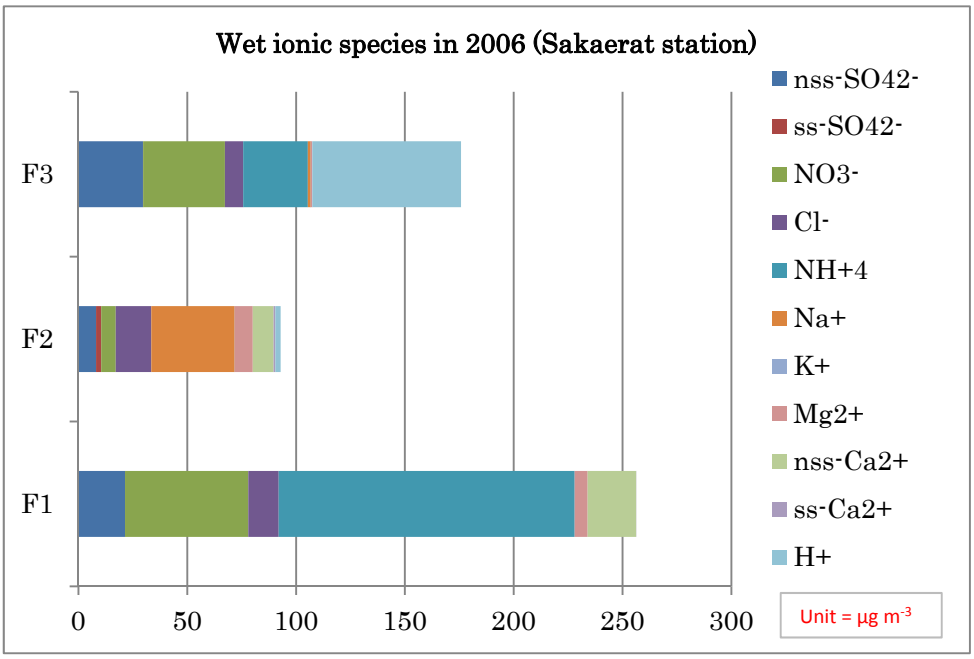

F1 = Agricultural/combustion process

F2 = Marine contribution

F3 = Acid/combustion process

Figure 16. Source profiles of wet ionic species at the Sakaerat station in 2006.

Table 16 shows the identification of 2 factors of the wet ionic species dataset in 2008, explaining about 86.87% of the data variance as well as loading greater than 0.7. The first factor displays high loading level, accounting for 74.18% of ss-SO_4^{2-}, Cl^-, Na^+, Mg^{2+}, nss-Ca^{2+} and ss-Ca^{2+} indicating of marine contribution and crustal. Factor 2 explains 12.48% of the variance proving correlation of nss-SO_4^{2-}, NO_3^-, NH_4^+ and H^+ which represented for combustion process ,agricultural activities and acid. Figure 17 shows the results of the wet ionic species dataset in 2008 computing by the PMF Model, found 3 factors representing for 3 potential sources. The dominant species of the factor 1 were Cl^- and Na^+, respectively which indicated for agricultural marine contribution. The factor 2 was composed of NO_3^- and NH_4^+ proving ionic distribution from combustion process and agricultural activities. The factor 3 contributes for nss-SO_4^{2-}, NO_3^- and H^+ indicating for combustion process and acid.

Table 16. Varimax-rotated PCA of wet ionic species at the Sakaerat station in 2008.

Component	Factor 1	Factor 2
nss-SO_4^{2-}	0.362	**0.883**
ss-SO_4^{2-}	**0.899**	0.359
NO_3^-	0.478	**0.823**
Cl^-	**0.717**	0.460
NH_4^+	0.458	**0.842**
Na^+	**0.899**	0.358

K^+	0.676	0.533
Mg^{2+}	**0.844**	0.393
nss-Ca^{2+}	**0.886**	
ss-Ca^{2+}	**0.899**	0.353
H^+		**0.914**
Eigenvalue	8.161	1.373
Variance (%)	74.188	12.485
Cumulative (%)	74.188	86.873
Possible source	Marine contribution Crustal	Combustion process Acid

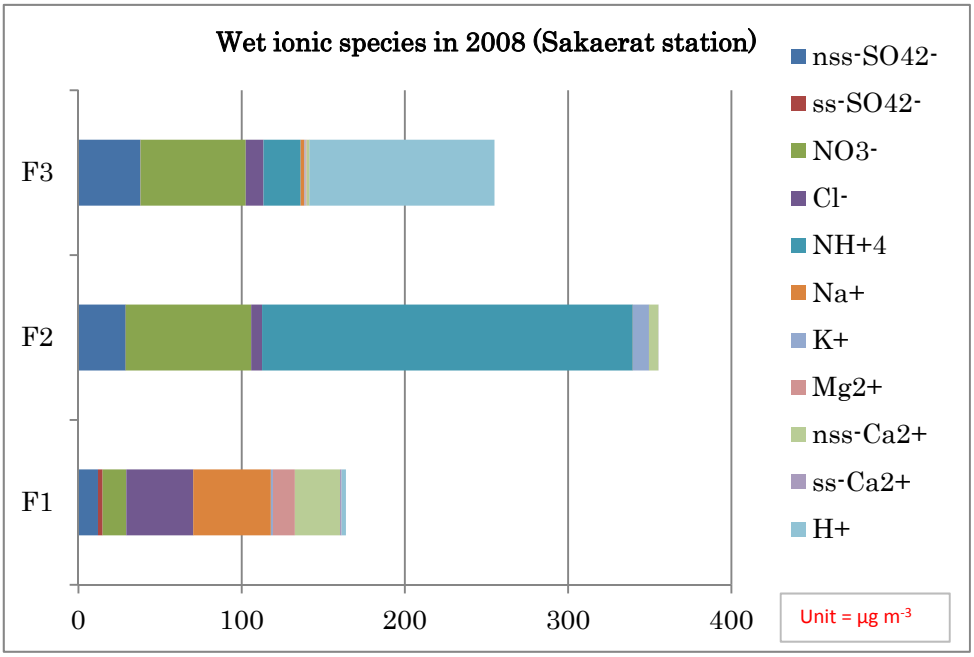

F1 = Marine contribution

F2 = Agricultural/combustion process

F3 = Acid/combustion process

Figure 17. Source profiles of wet ionic species at the Sakaerat station in 2008.

The number of factor loading and potential source obtained from the computing of the PCA analysis and the PMF Model using the dry and wet ionic species in 2004 and 2008 were similar to research findings of the recent study by Khon Kaen University (KKU), 2012 that reported up to 2-4 factors for the potential sources of ionic species in Nakhon Ratchasima province as a representative for rural area. Also, 5 dominant potential sources were indicated such as combustion process, marine contribution, agricultural activities, biomass burning and crustal. The dominant ionic species were nss-SO_4^{2-}, NH_4^+ and H^+, respectively which indicated for a contribution of combustion process, agricultural activities and acid. The obtained results indicated a

significantly contribution of the mixed potential sources and an independent source in Nakhon Ratchasima province.

4. Discussion

The computed results from both the PCA analysis and the PMF model found up to 2-4 factors similarity which are different by the monitoring stations especially the results using of the wet ionic specie dataset in all monitoring stations found 2 factors of the potential sources compared with the using of the dry ionic specie dataset which found up to 3- 4 factors. The factors represented for the potential sources of acid deposition classified by the dominant ionic species in the aerosol and rain water samples. The potential sources found commonly in combustion process (nss-SO_4^{2-} and NO_3^-), biomass burning (K^+), marine contribution (ss-SO_4^{2-}, Cl^-, Na^+ and ss-Ca^{2+}), agricultural activities (NH_4^+), crustal (Ca^{2+}, Mg^{2+} and nss-Ca^{2+}) and acid (H^+) which some of those were presented individually and the others were presented as mixed sources.

The dominant ionic species in this study found different by the monitoring stations and the potential sources; for example, the dominant ionic species of the combustion process was indicated by a good correlation between nss-SO_4^{2-} and NO_3^-, on the other hand the dominant ionic species of the marine contribution indicated by a good correlation of ss-SO_4^{2-}, Cl^-, Na^+ and ss-Ca^{2+} of the dataset collected in each monitoring stations and K^+ and NH_4^+ are the dominant ionic species of biomass burning and agricultural activities, respectively. Computed results using the PCA analysis and the PMF Model found very similar in the number of obtained factors of the potential sources and the dominant ionic species both the dataset of the dry and wet ionic species. The NH_4^+ and H^+ of wet ionic species were dominant ionic species which were different from the dry ionic species. The concentrations of ionic species computed by the PMF Model were found higher in the urban station than in the industrial station and rural station especially the nss-SO_4^{2-} and NO_3^- which represented for the mobile source. The concentrations of wet ionic species were found higher than the dry ionic species in all monitoring stations. The concentrations of ionic species in 2004 were lower than in 2008 because of the changing in the potential sources and environment.

5. Conclusions

The statistical instruments as the PCA and PMF Model have been applied to Thailand using the acid deposition monitoring dataset collected in 2004 and 2008 at the different 4 monitoring stations (1. urban site (Public Relation Department station in Bangkok) 2. rural site (Mae Hia station in Chiang Mai province) 3. Industrial site (Chonburi station in Chonburi province) and 4. Rural site (Sakaerat station in Nakhon Ratchasima province) to computing the concentrations and their characteristics of ionic species of aerosol and rain water components and to identify the potential sources of acid depositions in Thailand.

The computed results of both models found up to 2-4 factors of the potential sources in all monitoring stations which are combustion process (nss-SO_4^{2-} and NO_3^-), biomass burning (K^+), marine contribution

(ss-SO_4^{2-}, Cl^-, Na^+ and ss-Ca^{2+}), agricultural activities (NH_4^+), crustal (Ca^{2+} and Mg^{2+}) and acid (H^+). In some factors, independent potential source was presented clearly such as combustion process, marine contribution, biomass burning and agricultural activities and some others were found mixed sources between those potential sources in all monitoring stations. The dominant potential sources in urban area were combustion process, marine contribution and biomass burning. In the meantime the dominant potential sources of industrial area were mixed sources and marine contribution as similar as the rural area. The investigations found higher concentrations of ionic species in urban area than in industrial and rural areas, respectively. It was also significantly higher than the amount of NH_4^+ and H^+ wet ionic species in all monitoring station; on the other hand the dominant dry ionic species were nss-SO_4^{2-} and NO_3^-. The comparison between the PCA analysis and the PMF Model were found very similar in the number of obtained factors of the potential sources and the dominant ionic species both the dataset of the dry and wet ionic species. However, backward trajectory analysis should be concerned and conducted in further study in order to identify the relationship between the potential distance source areas and the pathways that give rise to the monitored aerosol and rain water components in the study areas.

6. Acknowledgements

The authors gratefully acknowledge the Asia Center for Air Pollution Research (ACAP) in Japan for providing observation data from EANET monitoring sites and giving an opportunity to conduct this research. We would like to express our thankfulness to Dr. Hajime Akimoto and Dr. Tsuyoshi Ohizumi for their valuable comments and suggestions to develop this paper. We thank Pollution Control Department of Thailand (PCD), especially, Mr. Pichaid Atipakya and Ms. Wassana Toruksa for their kind supports regarding air quality data.

7. References

Cao, Y.Z., Wang, S., Zhang, G., Luo, J. and Lu, S. 2009. Chemical characteristics of wet precipitation at an urban site of Guangzhou, South China. Atmospheric Research. 94:462-469.

Chakraborty, A. and Gupta, T. 2009. Chemical characterization of Submicron Aerosol in Kanpur Region: A Source apportionment Study, International Journal of civil and environmental engineering.

EANET. 2000. Technical Manual for Wet Deposition Monitoring in East Asia. The Second Interim Scientific Advisory Group Meeting of Acid Deposition Monitoring Network in East Asia. Acid Deposition Monitoring Network in East Asia (EANET).

EANET. 2003. Technical Document for Filter Pack Monitoring in East Asia. Third Session of the Science Advisory Committee (SAC3). Acid Deposition Monitoring Network in East Asia (EANET).

Fujita, S., Takahashi, A., Weng, J., Huang, L., Kim, H., Li, C., Huang, F. and Jeng, F. 2000. Precipitation chemistry in East Asia. Atmospheric Environment. 34: 525–537.

Kaplunovsky, A.S. 2005. Factor analysis in Environmental Studies. HAIT Journal of Science and Engineering. 2(1-2): 54-94.

Kasetsart University (KU). 2012. Report of Acid deposition in Eastern, Thailand. Pollution Control Department (PCD), Thailand.

Khare, P. Goel, A. Patel, D. and Behari, J. 2004. Chemical characterization of rainwater at a developing urban habitat of Northern India. Atmospheric Research. 69: 135–145.

Khon Kaen University (KKU). 2012. Report of Acid deposition in Northeastern, Thailand. Pollution Control Department (PCD), Thailand.

King Mongkut's University of Technology Thonburi (KMUTT). 2012. Report of Acid deposition in Northern, Thailand. Pollution Control Department (PCD), Thailand.

Kitayama, K., Murao, N. and Hara, H. 2008. PMF analysis of impacts of SO_2 from Miyakejima and Asian Continent on Precipitation Sulphate in Japan. Tokyo University of Agriculture and Technology.

Migliavacca, D. Teixeira, E.C., Pires, M., and Fachel, J. 2004. Study of chemical elements in atmospheric precipitation in South Brazil. Atmospheric Environment. 38: 1641–1656.

Oh, M.S., Lee, T.J. and Kim, D.S. 2011. Quantitative Source Apportionment of Size-segregated particulate Matter at Urbanized Local site in Korea. Aerosol and air Quality Research. 11: 247-264.

Okay, C. Akkoyunlu, B.O. and Tayanc¸ M. 2002. Composition of wet deposition in Kaynarca, Turkey. Environmental Pollution. 118: 401–410.

Onchang, R. and Sato, K. 2011. Effect of Haze Episodes on Chemical Composition of Wet and Dry Depositions at Monitoring sites in Thailand. EANET Research Fellowship Program 2009. EANET Science Bulletin Volume 2, January 2011, ISSN 1883-3608.

Paatero, P., Hopke, P.K., Begum, B.A. and Biswas, S.K. 2005. A graphical diagnostic method for assessing the rotation in factor analytical models of atmospheric pollution. Atmospheric Environment. 39: 193□201.

Paatero, P., Hopke, P.K., Song, X.H. and Ramadan, Z. 2002. Understanding and controlling rotations in factor analytic models. Chemometrics and Intelligent Laboratory Systems. 60: 253□264.

Panyakapo, M. and Bohuwech, D. 2006. Acid deposition in western Thailand 2005–2006. Department of Environmental Science, Research Report. Faculty of Science, Silpakorn University and Pollution Control Department, Bangkok.

Panyakapo, M. and Onchang, R. 2008. A four-year investigation on wet deposition in western Thailand. Journal of Environmental Sciences. 20: 441–448.

Pindado, O. and Perez, R.M. 2011. Source apportionment of particulate organic compounds in a rural area of Spain by positive matrix factorization. Atmosphere Pollution Research. 2: 492-505.

Raman, R.S. and Hopke, P.K. 2007. Source apportionment of fine particle utilizing partially speciated carbonaceous aerosol data at two rural locations in New York State. Atmospheric Environment. 41: 7923-7939.

Reff, A., Eberly, S.I. and Bhave, P.V. 2007. Receptor modeling of ambient particulate matter data using positive matrix factorization: review of existing methods. Journal of the Air and Waste Management Association. 57: 146-154.

Sanmanee, N., Swangjang, K., Areekijseree, M. and Panishkan, K. 2007. E_ects of organic matters on Ca, Zn, Pb, and Cu in two di_erent groups of agricultural soils, Thailand. International Conference on "Humic Substances in Ecosystems 7". Torun-Bachotek, Poland, 17–21 June 2007.

Seto, S., Sato, M., Tatano, T., Kusakari, T. and Hara, H. 2007. Spatial distribution and source identification of wet deposition at remote EANET sites in Japan. Atmospheric Environment. 41: 9386–9396

Thepanondh, S., Ayers, G. P. and Hooper, M. A. 2005. Analysis of precipitation chemistry in northern Thailand. Clean Air and Environmental Quality. 39: 43–47.

Thornhill, D.A., Williams, A.E., Onasch, T.B., Wood, E., Herndon, S.C., Kolb, C.E., Knighton, W.B., Zavala, M., Molina, L.T. and Marr, L.C. 2010. Application of positive matrix factorization to on-road measurement for source apportionment of diesel and gasoline-powered vehicle emission in Mexico City. Atmospheric Chemistry and Physics Journal. 10: 3629-3644.

Tiwari, S., Kulshrestha, U.C. and Padmanabhamurty, B. 2007. Monsoon Rain Chemistry and source apportionment using receptor modeling in and around National capital Region (NCR) of Delhi, India, Atmospheric Environment. 41(27): 5595-5604.

Troussier, F., Lecoge, N. and Galloo, J.C. 2007. Source apportionment of VOC in 3 French sites by CMB and PMF models and critical analysis.WIT Transactions on Ecology and the Environment, Vol. 101.

US EPA. 2008. EPA Positive Matrix Factorization (PMF) 3.0 fundamentals and user guide. http://www.epa. gov/heasd/products/pmf/pmf.html.

Viana, M., Kuhlbusch, T.A.J., Querol, X., Alastuey, A., Harrison, R.M., Hopke, P.K., Winiwarter, W., Vallius, A., Szidat, S., Prevot, A.S.H., Hueglin, C., Bloemen, H., Wahlin, P., Vecchi, R., Miranda, A.I., Kasper□Giebl, A., Maenhaut, W. and Hitzenberger, R. 2008. Source apportionment of particulate matter in Europe: a review of methods and results. Journal of Aerosol Science. 39: 827□849.

Yamasoe, M.A., Artaxo, P., Miguel, A.H. and Allen, A.G. 2000. Chemical composition of aerosol particles from direct emissions of vegetation fires in the Amazon Basin: water-soluble species and trace elements. Atmospheric Environment. 34: 1641– 1653.

Zhang, M., Wang, S., Wu, F., Yuan, X. and Zhang, Y. 2007. Chemical composition of wet precipitation and anthropogenic influence at a developing urban site in Southeastern China. Atmos. Res. 84: 311–322.

Zunckel, M., Saizar, C. and Zarauz, J. 2003. Rainwater composition in northeast Uruguay. Atmospheric Environment. 37: 1601–1611.

Joint Projects of the EANET with Participating Countries

EANET has also joint research projects with our participating countries on different activities, however, unfortunately, this bulletin is not available to obtain the completed results, because these projects are longer than two-year period, therefore, they are only progress reports involved included in this EANET Science Bulletin Volume 3.

Progress Report on Joint Research Project with Japan, Thailand and Malaysia on Catchment Analysis

Hiroyuki Sase[1*], Tsuyoshi Ohizumi[1], Naoyuki Yamashita[1], Thiti Visaratana[2], Bopit Kietvuttinon[2], Hathairatana Garivait[3]and Nik Muhamad Majid[4]

[1]Asia Center for Air Pollution Research (ACAP), [2]Royal Forest Department, Thailand.
[3]Environmental Research and Training Center, Department of Environmental Quality Promotion, Thailand, [4]Universiti Putra Malaysia.
*Corresponding Author: 1182 Sowa, Nishi-ku, Niigata 950-2144, Japan.
E-mail: sase@acap.asia

Abstract

Effect of sulphur deposition on terrestrial ecosystems is still one of the important issues to be investigated in East Asia. Based on a scientific community of Acid Deposition Monitoring Network in East Asia (EANET), dynamics of sulphur derived from atmospheric deposition are investigated in forest catchments in Niigata, Japan, Nakhon Ratchasima, Thailand, and Sabah and Sarawak, Malaysia. To clarify sulphur dynamics in the forest ecosystems, analysis of sulphur isotopic ratio is applied for rainwater, soil water and stream water in addition to measurement of the fluxes. The data obtained in the project will be informative for discussion on possible impacts of sulphur deposition on the forests. Since nitrogen deposition is also quite large in the region, its relation to acidification/eutrophication should also be discussed.

Keywords: forest catchment, sulphur isotope, Japanese cedar, dry evergreen forest, tropical rainforest, rehabilitated forest

1. Introduction

Atmospheric deposition of sulphur compounds may gradually decrease according to the recent emission inventories in East Asia (e.g. Lu *et al.,* 2010). However, the sulphur deposition level is still high and cumulative load of sulphur is quite large in the EANET region. Since sulphur deposited on ecosystems may be retained in soil and/or cycled in the soil-plant system, manifestation of its effect may be delayed (e.g. Mitchell and Likens 2011; Kobayashi *et al*., 2012). Moreover, several rivers/lakes for monitoring on inland aquatic environment in the East Asian countries showed pH-declining trend with SO_4^{2-}-increasing trend (EANET,

2011). Effect of sulphur deposition on terrestrial ecosystems is one of the important issues to be investigated in East Asia.

Scientists from the Network Center (NC) and the EANET countries have been promoting the catchment-scale analysis in different types of forests, namely in Kajikawa site, Niigata, Japan, in Sakaerat site, Nakhon Ratchasima, Thailand and in Danum Valley site, Sabah, Malaysia. Taking account of the background above, the research team made efforts to obtain a new grant to study sulphur dynamics in the forest catchments. Finally, the team has successfully obtained the research grant from the international research fund, Asia Pacific Network on Global Change Research (APN). Based on the existing catchment project, sulphur dynamics in the forest ecosystems are investigated. The surveys have been started in the existing three catchments above and also in a new site, Bintulu Rehabilitated Forest in Sarawak, Malaysia. In order to determine sulphur dynamics in the forest ecosystems, analysis of sulphur isotopic ratio is applied for rainwater, soil water and stream water in addition to measurement of the fluxes. The data obtained in the project will explain the possible impacts of sulphur deposition on the forests. Since nitrogen deposition is also quite high in the region, its relation to acidification/eutrophication should also be discussed. In this report, we will introduce recent progress on the catchment projects in Japan, Thailand and Malaysia, especially on the APN Project.

2. Methods

2.1. Site description

The study sites were established in four forest catchments in Japan, Thailand and Malaysia, as shown in Table 1. Fluxes of ions including SO_4^{2-} had been studied by previous projects since 2002, 2005 and 2008 in Kajikawa, Sakaerat and Danum Valley sites, respectively. However, the surveys in these sites were mostly finished in 2010/2011. In 2012, the study sites were reactivated for the APN project and the rehabilitated forest in Bintulu was added as a new site for the APN project.

Table 1. Study forest catchments in Japan, Thailand and Malaysia.

Site	Kajikawa	Sakaerat	Danum Valley	Bintulu
Country	Niigata, Japan	Nakhon Ratchasima, Thailand	Sabah, Malaysia	Sarawak, Malaysia
Forest type	Japanese cedar	Dry evergreen forest (DEF)	Tropical rainforest	Rehabilitated Forest
Start year	2002	2005	2008	2012

2.2. Project outline

Field surveys and data analysis are conducted in the selected forests to address the following issues:

i) Flux determination of sulphur and nitrogen.

ii) Analysis of sulphur isotope ratio of rainwater and stream water.

iii) Speciation of sulphur compounds in soil layer.

iv) Trial application of biogeochemical simulation model.

The data obtained from the topics i) to iii) will be utilized for a trial application of a biogeochemical simulation model. The outcomes from the project will be informative for evaluating possible impacts of sulphur deposition on the forests. Since nitrogen deposition is also quite high in the region, its relation to acidification/eutrophication would also be determined.

As for i) flux determination of sulphur and nitrogen, the fluxes by rainfall outside forest canopy (RF), throughfall (TF), soil solution (SS) and stream water (SW) have been measured by previous projects in Kajikawa, Sakaerat and Danum Valley sites. The existing data are utilized to summarize the fluxes in these sites, while RF, TF and SW are still measured in Kajikawa and Sakaerat sites. The data obtained from the resin samplers (Figure 1) for sulphur isotope analysis will also be used for this purpose. In the case of Bintulu site, the fluxes from SW may not be able to be estimated, since the stream is flowed not continuously but just seasonally.

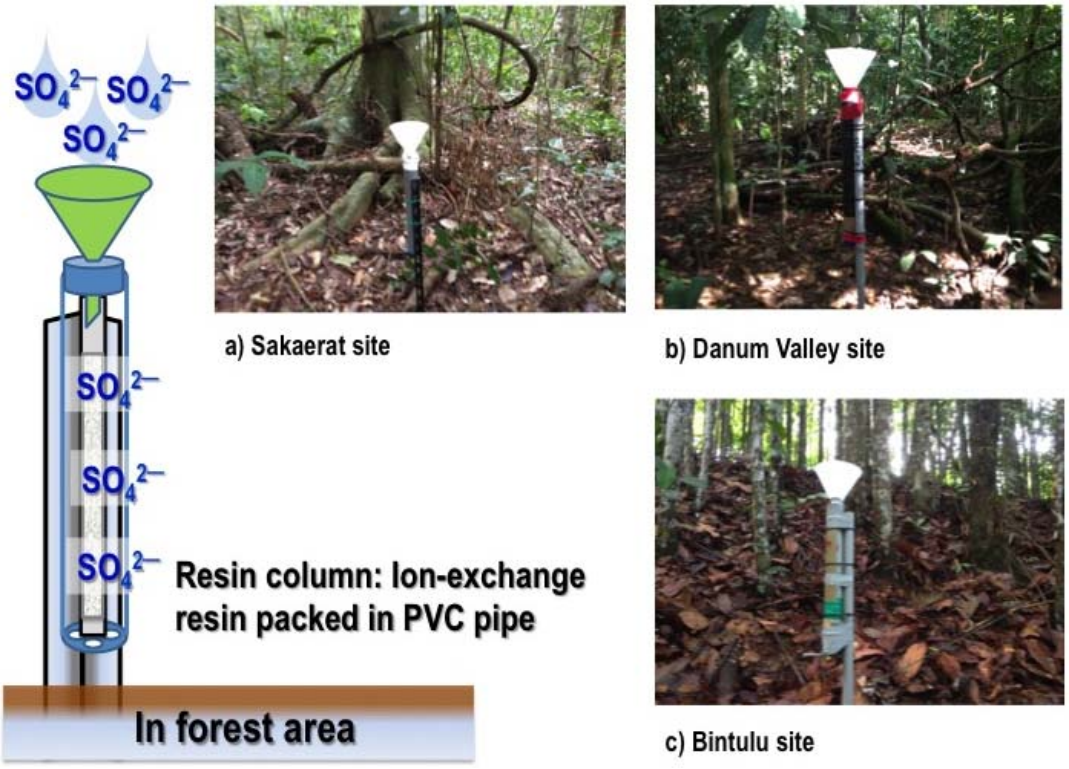

Figure 1. Resin samplers for sulphur isotope analysis.

As for ii) sulphur isotope analysis, we applied "resin sampling" in this project. In the case of rainwater, the resin column, in which an ion-exchange resin was packed, was installed with a plastic funnel to collect RF and TF below the canopy (Figure 1). The ion-exchange resin in the column can trap SO_4^{2-} in rainwater. The resin sampling is also applied for collection of SS and SW, for which plastic rings and mesh bags were used for packing the ion-exchange resin, respectively. The resin ring samplers for SS were installed in different depths in soil to collect SO_4^{2-} in water vertically flowed down from each depth. The resin samplers for rainwater and SS were installed in the fields for several months to obtain enough amounts of SO_4^{2-} for isotope analysis. The resin bags for SW were placed in the streams for several hours. In the case of Kajikawa site, water samples are also used for sulphur isotope analysis.

2.3. Sulphur isotope analysis

The SO_4^{2-} extracted from the resin samplers or in water samples are precipitated as $BaSO_4$ by using $BaCl_2$. The sulphur isotope ratio in the powdered $BaSO_4$ is analyzed by using the Elemental Analyzer (EA) - Mass Spectrometer (MS). Isotope ratio of sulphur compounds ($^{34}S/^{32}S$) may be changed by biological process (isotope fractionation). Sulphur isotope ratio of rainwater and SW is measured to discriminate origin of sulphur (atmospheric or biological origin) and to discuss retention time of sulphur in the ecosystems. Sulphur isotope ratio is expressed as:

$\delta^{34}S\ (‰) = \{(^{34}S/^{32}S)_{sample}/(^{34}S/^{32}S)_{CDT} - 1\} \times 1000$

where, $(^{34}S/^{32}S)_{sample}$ and $(^{34}S/^{32}S)_{CDT}$ were isotopic ratios of sample and Canyon Diablo troilite (standard substance), respectively.

3. Progress of the project

3.1. Flux determination of sulphur and nitrogen

Data analysis of the existing data is conducted, in particular for Kajikawa, Sakaerat and Danum Valley sites. In these sites, we have already accumulated the data on ion fluxes for 10, 6 and 4 years, respectively. Several research papers based on the previous surveys have been published in international journals. Figure 2 shows seasonal variation of SO_4^{2-} fluxes from RF and TF+SF in Kajikawa site and Sakaerat site based on the accumulated data (Sase *et al*., 2012). Clear seasonality can be seen in both sites. In Kajikawa site, the fluxes increased in winter due to seasonal west winds, which might be affected by a long-range transport from the Asian Continent. In Sakaerat site, the fluxes increased in the beginning and middle of wet season, which reflected the precipitation pattern. The high peaks in the beginning of wet season may also be affected by biomass burning during dry season. The monsoon characterizes the climatic regime in the East Asian region and this play a role in the deposition patterns in the region.

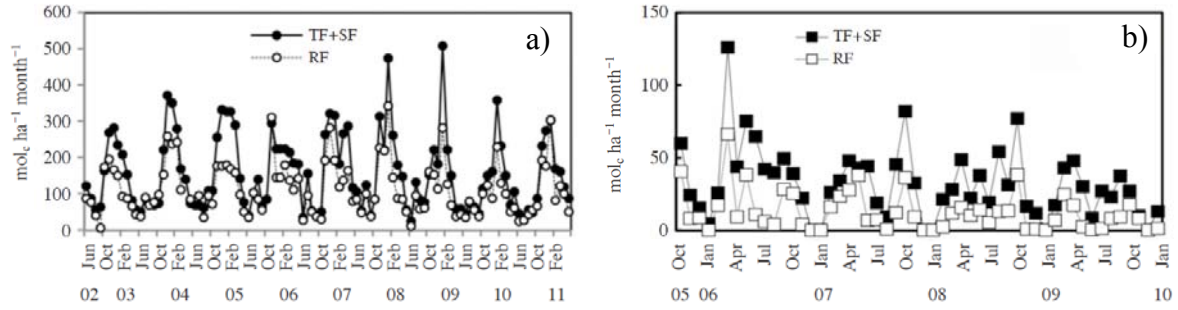

Figure 2. Seasonal variation of SO_4^{2-} fluxes from rainfall outside the canopy and the sum of throughfall and stemflow in (a) a Japanese cedar forest in Kajikawa, Japan, and (b) a dry evergreen forest in Sakaerat, Thailand. RF, rainfall outside the canopy; TF, throughfall; SF, stemflow. (Modified after Sase *et al*., 2012).

3.2. Analysis of sulphur isotope ratio of rainwater and stream water

Preliminary surveys for sulphur isotope analysis of rainwater and SW were started in Kajiakwa site in August 2012. Rainwater from RF and TF and SW were collected and their sulphur isotope ratio was measured by EA-MS. The resin samplers were also applied in Kajikawa site and comparability of the data to that from water samples was confirmed. Measurement of sulphur isotope ratio in SS was also attempted.

The resin samplers for RF, TF, SS and SW were installed in Sakaerat site in October 2012, while the samplers for RF, TF and SS were installed in Danum Valley and Bintulu sites in December 2012. The resin samplers for RF, TF and SS will be exchanged after several months. In Sakaerat site, the resin bag sampler will be exchanged periodically once or twice a month. In Danum Valley site and Bintulu site, water samples will basically be used for isotope analysis, while the resin sampling is also tried occasionally. The collection methods applied in each site for sulphur isotope analysis are shown in Table 2.

Table 2. Collection methods applied for sulphur isotope analysis

Media	Kajikawa	Sakaerat	Danum Valley	Bintulu
Rainfall	W/(R)	W/R	R	R
Throughfall	W	R	R	R
Soil solution	W/R	R	R	R
Stream	W/(R)	W/R	W/R	W/R

Note. W, water sample is used for sulphur isotope analysis; R, resin sampler is used for sulphur isotope analysis.

The first results on the sulphur isotope ratio in Kajikawa site were shown in Figure 3. The $\delta^{34}S$ of RF was similar to those previously reported in Niigata Prefecture (Ohizumi *et al.,* 2001). In Niigata Prefecture, it is well known that SO_4^{2-} is transported by seasonal northwest winds in winter, as shown in Figure 2. Changes in the isotope ratio should carefully be watched from autumn to winter. The isotope ratio of RF was clearly lower than those in soil and stream. This may suggest biological fractionation of sulphur isotope in the ecosystems. Geochemical processes in soil, such as absorption and desorption of SO_4^{2-}, may not change the isotope ratio.

Biological processes, such as decomposition of litter and sulphate reduction by microorganisms, may increase the isotope ratio in SS and SW.

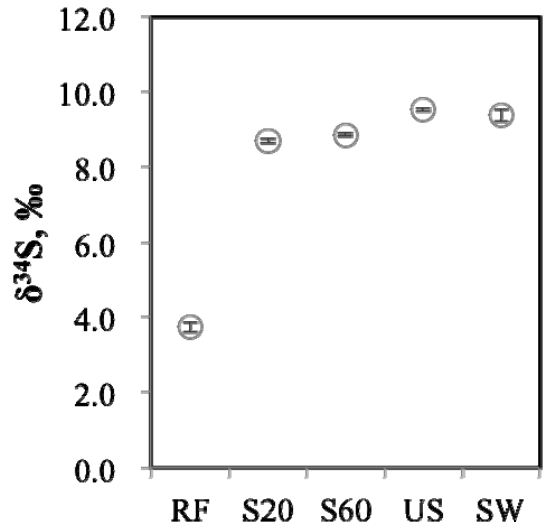

Figure 3. Sulphur isotope ratio ($\delta^{34}S$) of rainfall outside forest canopy (RF), soil solution collected at 20 cm depth (S20), soil solution collected at 60 cm depth, stream water collected at upstream point (US), and stream water collected at the outlet of the catchment (SW). Error bar shows standard deviation of triplicate analyses. Samples were collected in August 2012.

The method for pretreatment of $BaSO_4$ for the isotope analysis is also informed to the project members in Thailand and Malaysia. It was discussed that pretreatment of $BaSO_4$ would be carried out in each country, although the analysis by EA-MS will be carried out in Japan. It is expected that the information and knowledge of the sulphur isotope study will be shared among the members.

3.3. Speciation of sulphur compounds in soil layer

Soil samples in Bintulu were collected in cooperation with collaborators of UPM Bintulu Campus (UPMKB) in December 2012. Collection of soil samples is also planned in Kajikawa, Sakaerat and Danum Valley in 2013. It was decided that extractable sulphate by phosphate solution would be analyzed, since this portion mainly consists of water-soluble and adsorbed sulphate, which is recognized as plant available. Soil analysis will be conducted in UPMKB or ACAP.

3.4. Collaboration and cooperation with EANET and relevant agencies in each countries

Since the project is conducted based on the EANET community, the project leader attended a meeting with representatives of the EANET relevant agencies in Malaysia, including MMD, Ministry of Natural Resources and Environment (NRE), Department of Environment (DOE), Department of Chemistry (DOC), Universiti Teknologi Mara (UiTM) and UPM (Figure 3) and introduced the outcomes of the previous project in Danum Valley and the plan of the new APN project. It was agreed that a project workshop would be held in June 24, 2012 in Selangor, Malaysia to share outcomes/progress of the project with relevant agencies.

Figure 4. Meeting with EANET relevant agencies in Petaling Jaya, Malaysia in December 2012.

The project outline is introduced in the meeting of Task Force on Research Coordination of EANET and the 12th Session of Scientific Advisory Committee (SAC12) in November 2012.

4. Acknowledgements

The project above was supported by the Asia Pacific Network for Global Change Research (APN) (ARCP2012-18NMY-Sase). A part of the surveys in Sakaerat site and Bintulu site was financially supported by KAKENHI (20120012) from MEXT, Japan and Mitsubishi Corporation, Japan, respectively. Field surveys and laboratory analysis are supported by Y. Inomata, T. Saito, Duriya Staporn, Ahmed Osumanu Haruna, Seca Gandaseca, Jikos Gidiman, Toh Ying Ying, Leong Kok Peng, Maznorizan Mohamad, Nick Chappell and other collaborators. Authors thank them for their support and cooperation on the project.

5. References

Kobayashi, R., Sumarriani, Y., Yamashita, N., Ohta, T., Matsubara, H., Yagoh, H., Nakata, M., Sase, H. 2012. Seasonal variation of water chemistry and sulphur budget in an acid-sensitive river along the Sea of Japan. Limnology, 14: 195-209.

EANET 2011. The Second Periodic Report on State of Acid Deposition in East Asia. Network Center for EANET, Asia Center for Air Pollution Research, Niigata, Japan.

Lu, Z., Zhang, Q., Streets, D.G. 2011. Sulphur dioxide and primary carbonaceous aerosol emissions in China and India, 1996–2010. Atmos. Chem. Phys., 11, 9839–9864.

Mitchell, M.J., Likens, G.E. 2011. Watershed sulphur biogeochemistry: shift from atmospheric deposition dominance to climatic regulation. Environmental Science and Technology, 45: 5267–5271.

Ohizumi, T., Take, N., Moriyama, N., Suzuki, O., Kusakabe, M. 2001. Seasonal and spatial variations in the chemical and sulphur isotopic composition of acid deposition in Niigata Prefecture, Japan. Water, Air and Soil Pollution, 130: 1679–1684.

Sase, H, Matsuda, K, Visaratana, T, Garivait, H, Yamashita, N, Kietvuttinon, B, Hongthong, B, Luangjame, J, Khummongkol, P, Shindo, J, Endo, T, Sato, K, Uchiyama, S, Miyazawa, M, Nakata, M, Lenggoro, I.W. 2012. Deposition process of sulphate and elemental carbon in Japanese and Thai forests. Asian Journal of Atmospheric Environment, 6: 246-258.

Joint Research Project for Developing Low Cost Methodology on Gas Concentration Monitoring in East Asia

Ohizumi[1], T., Nagai[1], T., Golobokova[2], L., Toruksa[3], W. and Meng[4], X.

[1]Asia Center for Air Pollution Research, [2]Limnological Institute, Russian Academy of Sciences/Siberian Branch, Russia, [3]Air Quality and Noise Management Bureau, Pollution Control Department, Thailand, [4] Atmospheric Research Department, Chongqing Academy of Environment Sciences, China.

E-mail: ohizumi@acap.asia

1. Introduction

In order to evaluate the extent of acid deposition in East Asia spatially and temporally, a sufficiently long record of data on chemical composition of rainwater and concentration of air pollutants from a dense network of sites distributed over the region is usually required. However, the number of the EANET monitoring sites is limited and not well distributed. One of the reasons for the lack of air quality monitoring sites in some countries is the high cost of automatic instruments and recurrent costs of operating the instruments.

One of the possible ways to overcome this problem is to adopt the simpler and/or low cost methodologies such as filter-pack, passive sampler, and denuder methods in less accessible sites. These methodologies are used widely in monitoring networks and for field campaigns in Europe and North America. However, they have not been extensively tested in the East Asian region which may have different climate conditions and other unique factors.

The Strategy on EANET Development (2006-2010) included an activity to improve implementation of all required monitoring items with necessary data completeness and accuracy. One of the outputs expected from this activity is a recommendation on use of less expensive methods to reduce monitoring cost and increase the number of monitoring sites in the EANET network. According to the strategy, we had performed a project entitled “Joint research project for developing low cost methodology on gas concentration monitoring in East Asia” as a cooperative research project among China, Japan, Russia, and Thailand and its outcomes are summarized in this paper.

2. Objectives

The project has been carrying out with the following objectives:

- To evaluate the accuracy of measurements using passive samplers with those from the automatic

instruments and filter pack methods at selected sites in the participating countries of the EANET;

- To determine the suitability of applying the low cost methodologies for the EANET monitoring.

3. Methods

The measurements had been conducted at selected sites in the participating countries of the EANET by subjecting the samplers to a range of climate conditions to identify factors that could affect their performance and reliability. The following 4 countries having different climate conditions and concentration levels of the gaseous air pollutants were participating in the project, namely, China (Jinyunshan), Japan (Niigata-Maki), Russia (Mondy), and Thailand (Bangkok and Samutsakhon).

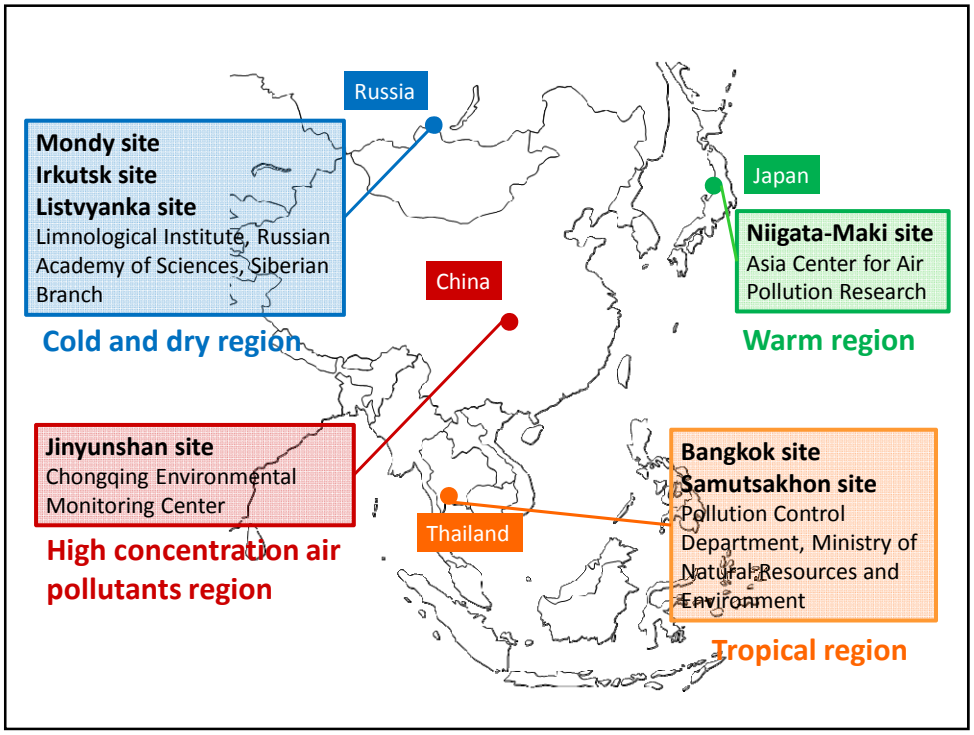

Figure 1. Location of monitoring sites and organizations in charge of the monitoring.

Passive sampler (hereafter referred as PS) method was performed by using the passive sampler manufactured by OGAWA Company. Sampling and analytical methods for PS monitoring were followed information provided by the company. Filter-pack (hereafter referred as FP) method was operated based on the manual established by EANET. Besides data of automatic air pollutant monitor (hereafter referred as AP) method operated by the national ambient air concentration monitoring manual in each country were collected as a reference data for evaluating PS and FP monitoring data. Instrument, parameters, sampling period, and analytical method were summarized here for each monitoring site.

Jinyunshan in China was selected as a site characterized by high concentration of air pollutants. The monitoring was implemented as following table:

Jinyunshan	PS method	FP method	AP method
Instrument	OGAWA passive sampler	4 stage filter pack	NO_X : Environment S.A AC 32M SO_2 : Environment S.A AF 22M O_3: Environment S.A O_3 42M
Parameters	NO_X, NO_2, SO_2, O_3, NH_3	SO_2, NH_3	NO_X, NO_2, SO_2, O_3
Sampling period	Bi-weekly 16 Dec. 2009 ～	Bi-weekly Expected to start from January 2011	Hourly Data available from Dec. 2009
Analytical method	Ion Chromatography	Ion Chromatography	NOx: Chemiluminescent SO_2: UV fluorescent O_3: UV photometric

Niigata-Maki in Japan was selected as a site in warm region. The monitoring was implemented as following table:

Niigata-Maki	PS method	FP method	AP method
Instrument	OGAWA passive sampler	4 stage filter pack	NO_X: HORIBA APNA-365 SO_2: HORIBA APSA-365 O_3: HORIBA APOA-370
Parameters	NO_X, NO_2, SO_2, O_3, NH_3	SO_2, NH_3	NO_X, NO_2, SO_2, O_3
Sampling period	Bi-weekly 4 Nov. 2009 ～	Bi-weekly 4 Nov. 2009 ～	Hourly Data available from 4 Nov. 2009
Analytical method	Ion Chromatography	Ion Chromatography	NOx: Chemiluminescent SO_2: UV fluorescent O_3: UV photometric

Mondy in Russia was selected as a site in cold and dry region. The monitoring was implemented as following table:

Russia	PS method	FP method	AP method
Instrument	OGAWA passive sampler		O_3: Dasibi Model 1007-AHJ
Parameters	O_3		O_3
Sampling period	Monthly Data available from Feb. 2009		Hourly Data available from Feb .2009
Analytical method	Ion Chromatography		O_3: UV photometric

Bangkok and Samutsakhon in Thailand were selected as sites in tropical region. The monitoring was implemented as following table:

Bangkok Samutsakhon	PS method	FP method	AP method
Instrument	OGAWA passive sampler	4 stage filter method	Bangkok; NO_X: Nippon Thermo Co., Ltd. SO_2: Nippon Thermo Co., Ltd. O_3: Nippon Thermo Co., Ltd. Samutsakhon; NO_X: API model 200 SO_2: API model 100 O_3: API model 400
Parameters	NO_X, NO_2, SO_2, O_3	SO_2, NH_3	NO_X, NO_2, SO_2, O_3
Sampling period	10 days 1 Jan. 2009 ～	10 days 1 Jan. 2009 ～	Hourly Data available from Jan .2009
Analytical method	Ion Chromatography	Ion Chromatography	NOx: Chemiluminescent SO_2: UV fluorescent O_3: UV photometric

4. Results and Discussion

The monitoring by using low cost methodologies such as PS method and FP method had been implemented in four regions mentioned above since 2009. Obtained data by those methodologies have been evaluated in the comparison with the results of AP method in each participating organization. A part of them was introduced for each item in this section.

1) Nitrogen dioxide

NO_2 concentration was monitored by two methods in four sites with different climate condition and concentration level (Figure 2).

Two sites in Thailand were characterized by high temperature, high humidity, and high concentration of NO_2. The NO_2 concentrations by PS method in both sites in Thailand showed good agreement with AP method throughout the study period.

The concentrations of NO_2 measured by PS method showed similar variation with the concentration measured by AP method in Niigata-Maki where was characterized by low concentration of NO_2.

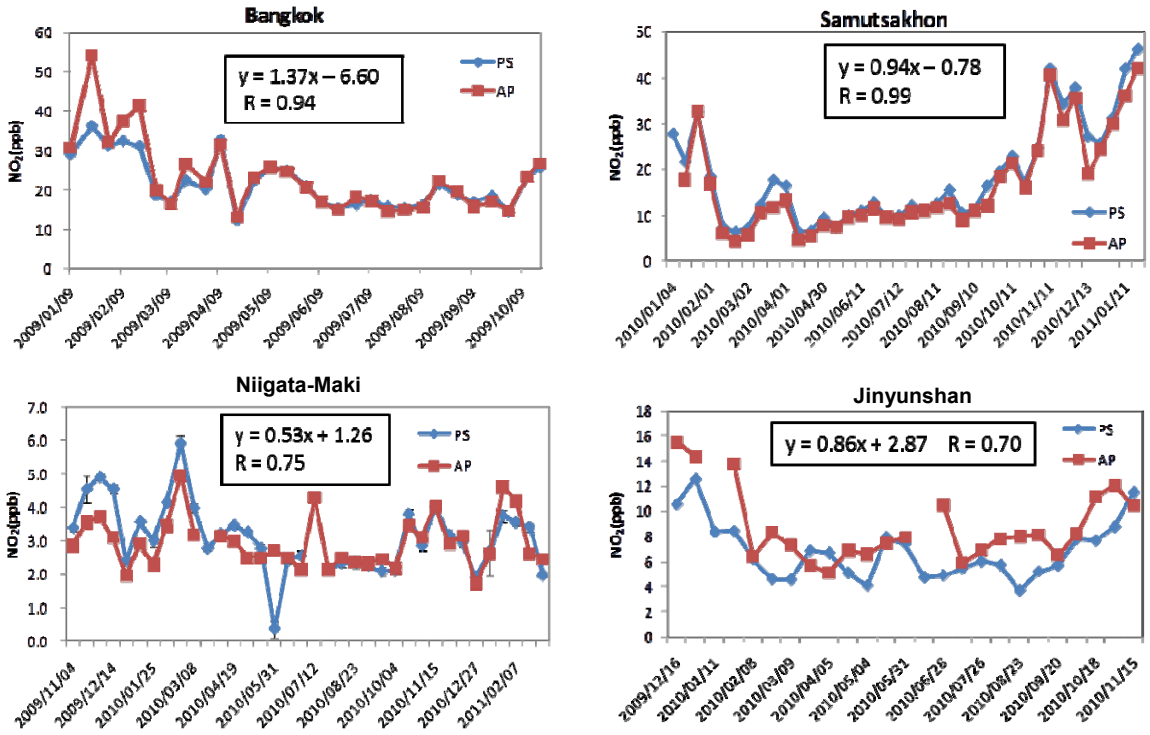

Figure 2. Comparison of nitrogen dioxide gas concentration monitored by Passive (PS) and Automatic Air Pollution Monitor (AP) methods in Bangkok, Samutsakhon, Niigata-Maki and Jinyunshan.

The concentrations of NO_2 measured by PS method were synchronized with the concentration measured by AP method in Jinyunshan.

In the comparison with AP method, it was confirmed that NO_2 concentration monitored by PS method is acceptable even in low concentration and tropical region.

2) Nitrogen oxides

The NOx concentrations measured by PS method in two sites in Thailand showed good agreement with the concentration of AP method throughout the study period (Figure 3).

The concentrations of NOx measured by PS method were synchronized well with the concentration measured by AP method in Niigata-Maki where was characterized by low concentration of NOx. However, PS

concentration was always slightly higher than that of AP method and same tendency was appeared in Bangkok. Although the reason couldn't be clarified here, that feature should be taken into account.

The concentrations of NOx measured by PS method were synchronized with the concentration measured by AP method in Jinyunshan.

In the comparison with AP method, it was confirmed that NOx concentration monitored by PS method was acceptable even in low concentration and tropical region.

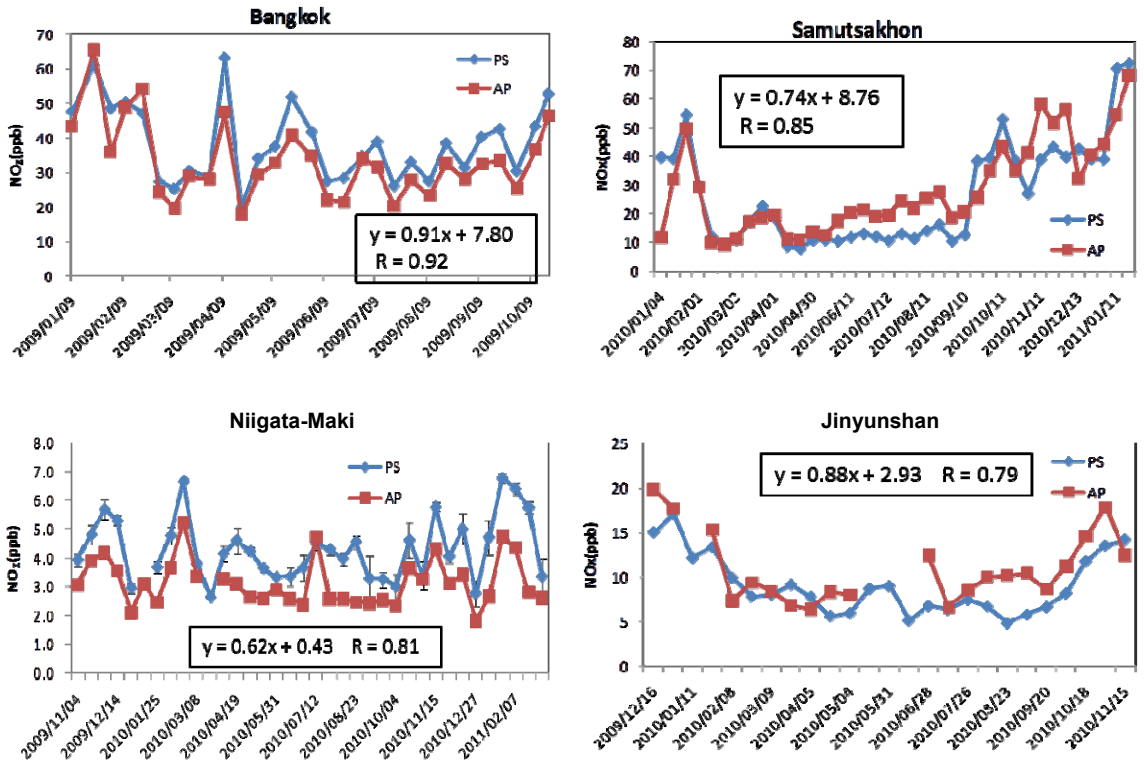

Figure 3. Comparison of nitrogen oxides gas concentration monitored by Passive (PS) and Automatic Air Pollution Monitor (AP) methods in Bangkok, Samutsakhon, Niigata-Maki, and Jinyunshan.

3) Sulphur dioxide

SO_2 concentration monitored by PS method was evaluated in the comparison with FP and AP methods in Bangkok and Niigata-Maki sites. SO_2 concentration by PS method in Samutsakhon and Jinyunshan sites was also compared with AP method. Those sites were selected as the sites representing different climate condition and concentration level shown in Figure1. Monitoring results were presented in Figure 4.

The results of three methods were comparable in 2010 in Bangkok except some periods. However, correlation among 3 methods is not so strong in Bangkok.

The results of two methods showed good agreement except in the period from July to September in Samutsakhon.

SO_2 concentration by PS method showed different fluctuation from the other two methods in Niigata-Maki in winter, especially in the periods from December 2009 to March 2010 and from November to

December 2010. The site was located in the area along the Sea of Japan and suffered strong northwest wind in winter time. As shown in Figure 4, large differences between PS and the other methods were observed mainly in the period when wind speed was more than 5 m/sec in average. At those periods, PS data tended to be higher than the other methods. From those reasons, it was seemed that strong wind from the sea might avoid theoretical sample collection of PS method. To prevent the effect of those strong wings, shape of sampling shelter should be improved.

The results of two methods agreed well even in SO_2 high concentration area in Jinyunshan.

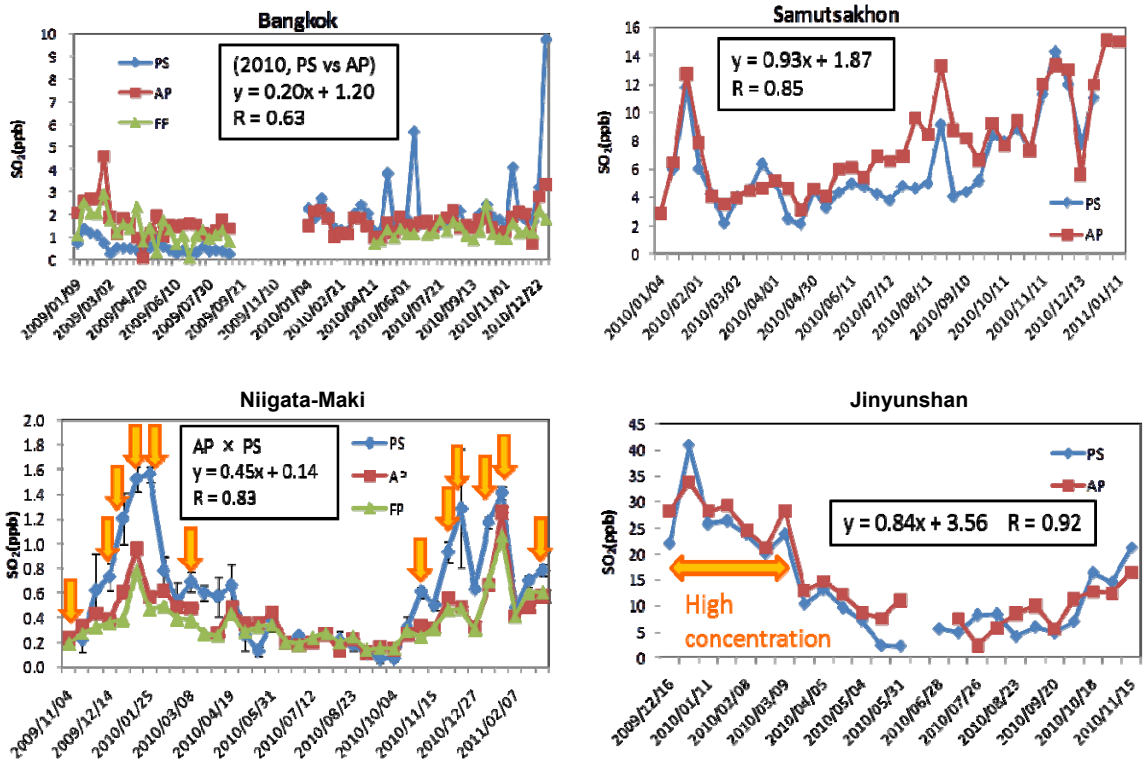

Figure 4. Comparison of sulphur dioxide gas concentration monitored by Passive (PS), Automatic Air Pollution Monitor (AP), and Filter-pack methods in Bangkok, Samutsakhon, Niigata-Maki, and Jinyunshan. Arrows in the figure of Niigata-Maki show the days when high wind velocity (>5 m/s) was observed.

4) Ozone

Parallel monitoring results between PS and AP methods were shown in Figure 5.

The results of two methods showed good agreement in the rain season in Thailand. But, before and after rain season, PS concentration was relatively higher than AP concentration.

O_3 concentration has a large difference between PS and AP methods in Niigata-Maki. Yellow arrow in Figure 5 indicated the sample collection periods when averaged wind speed was higher than 5 m/sec. At those periods, PS data tended to be higher than AP data. It was seemed that strong wind from the sea might avoid theoretical sample collection of PS method. As same as the case of SO_2, shape of sampling shelter should be improved to mitigate the effect of strong wind during sample collection. The results of two methods for O_3 agreed well in Jinyunshan.

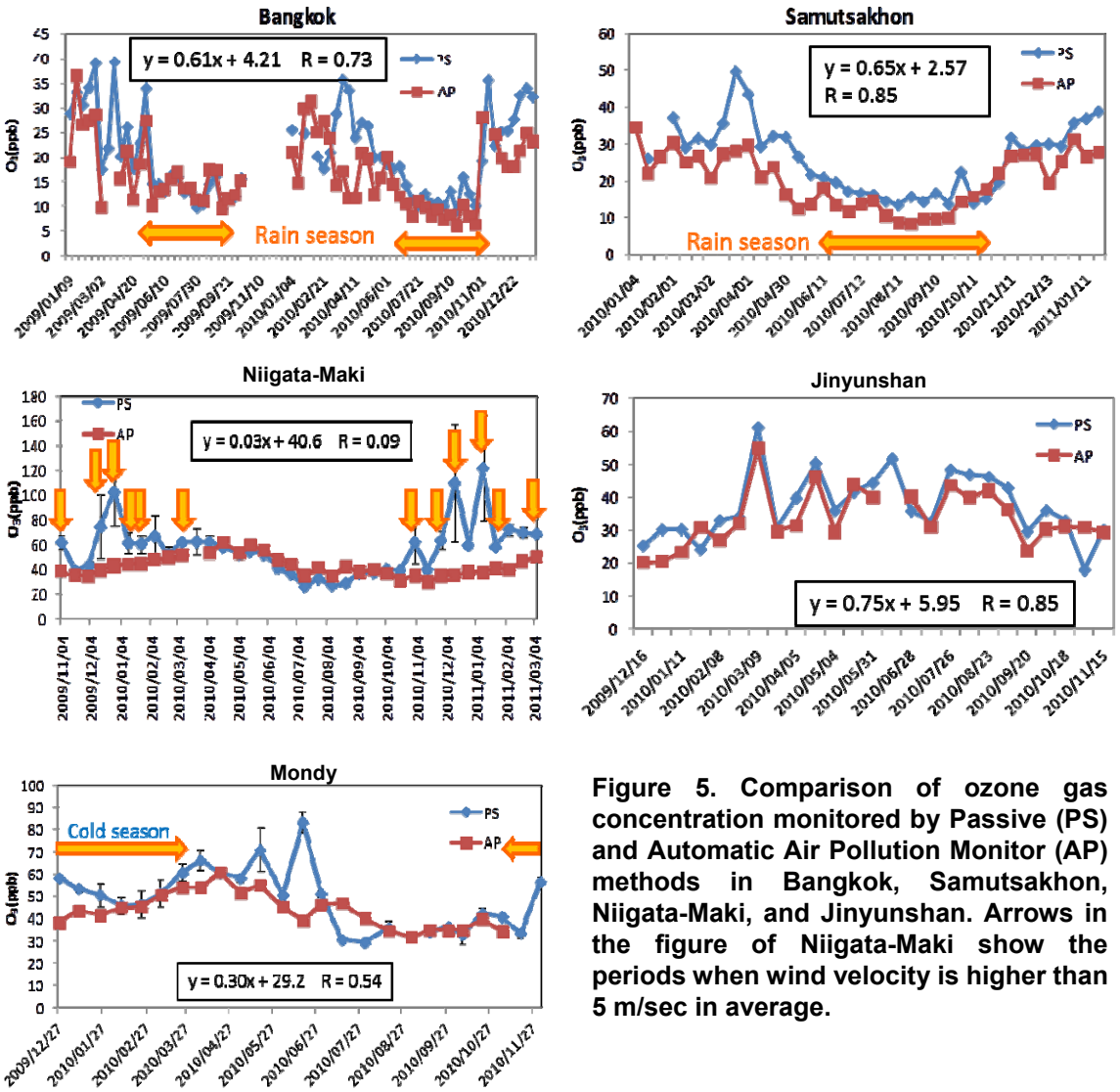

Figure 5. Comparison of ozone gas concentration monitored by Passive (PS) and Automatic Air Pollution Monitor (AP) methods in Bangkok, Samutsakhon, Niigata-Maki, and Jinyunshan. Arrows in the figure of Niigata-Maki show the periods when wind velocity is higher than 5 m/sec in average.

Measurement value and fluctuation of O_3 between PS and AP method corresponded well in the latter half of monitoring period in Mondy. Correlation analysis showed that the ozone concentrations at the site measured by PS and AP methods were closely related. The correlation coefficient between these values was about 0.9 in linear relationship. Measurement value and fluctuation between PS and AP methods showed agreement except for some periods. Though the temperature in Russia from November to March was much lower, PS method was applicable even in that hard condition.

5) Ammonia

Parallel monitoring results of ammonia gas concentration by PS and FP methods in Bangkok and Niigata-Maki were shown in Figure 6.

The concentration of NH_3 measured by PS method was synchronized with the concentration measured by FP method in Bangkok where NH_3 concentration ranged from 0-20 ppb. Although NH_3 concentration in Niigata-Maki was one tenth lower than that in Bangkok, the concentrations of NH_3 measured by PS method were also synchronized with the concentration measured by FP method.

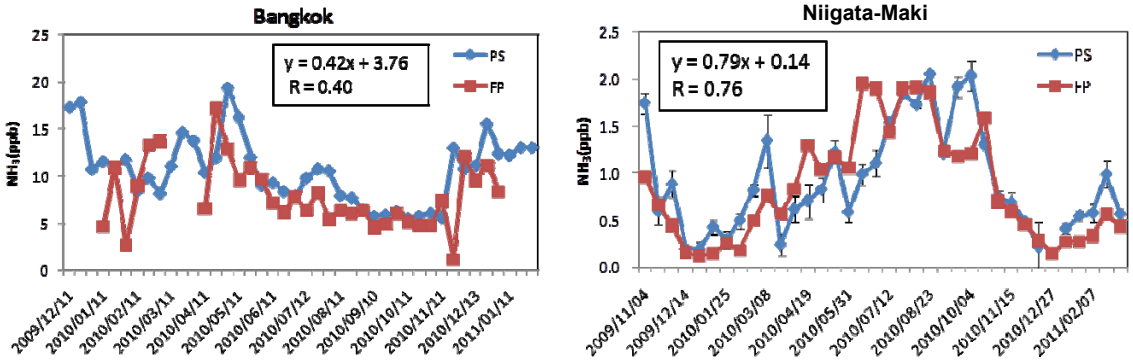

Figure 6. Comparison of ammonia gas concentration monitored by Passive (PS) and Filter-pack (FP) methods in Bangkok and Niigata-Maki.

5. Summary

We performed PS method by using Ogawa Passive Sampler in five sites of four regions representing various climate condition and concentration level of gaseous air pollutants. PS monitoring results were evaluated in the comparison with FP and AP methods which were operated simultaneously with PS method. Those results were summarized in Figure 7. Major outcomes for each air pollutant were the following.

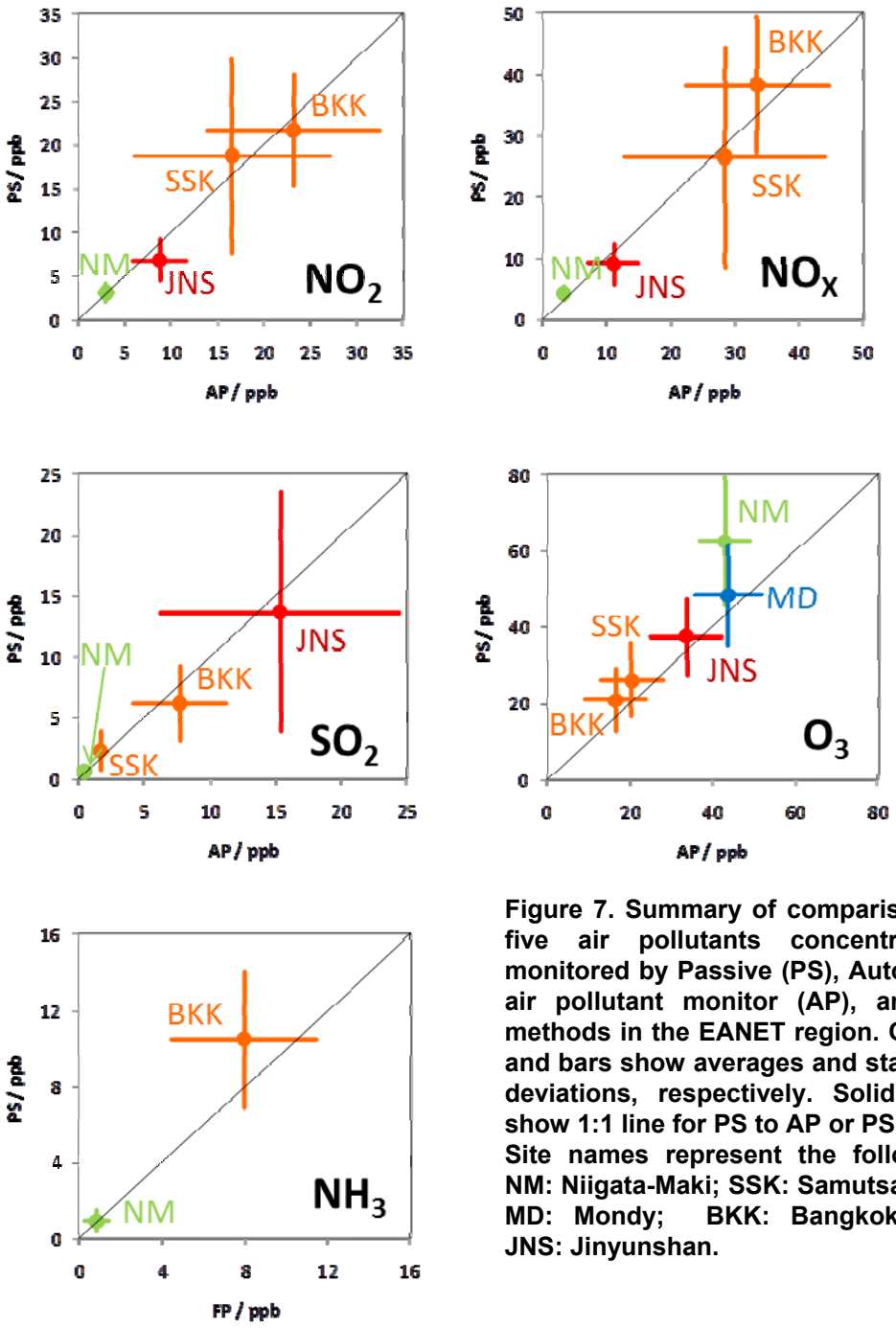

Figure 7. Summary of comparison on five air pollutants concentrations monitored by Passive (PS), Automatic air pollutant monitor (AP), and FP methods in the EANET region. Circles and bars show averages and standard deviations, respectively. Solid lines show 1:1 line for PS to AP or PS to FP. Site names represent the following; NM: Niigata-Maki; SSK: Samutsakhon; MD: Mondy; BKK: Bangkok; and JNS: Jinyunshan.

- NO_X, NO_2 and NH_3: PS showed good agreement with AP or FP in Jinyunshan, Niigata-Maki, Bangkok, and Samutsakhon. PS is applicable in warm and tropical region.
- O_3: PS is synchronized with AP in Mondy, Jinyunshan and a part of Niigata-Maki, Bangkok, and Samutsakhon. PS is applicable in most of the condition except in the period with strong wind and dry season in tropical region.
- SO_2: PS is synchronized with AP in Jinyunshan, Bangkok, Samutsakhon and a part of Niigata-Maki. PS for SO_2 is applicable in most of the condition except in strong wind period.

Monitored concentration by PS method was comparable with AP and FP methods except some cases, so that PS method was applicable for monitoring gaseous air pollutant concentration in the EANET region. Although PS method couldn't provide high time resolution data, that method was especially effective on clarification of spatial distribution of air pollution in a large area or as screening method for setting long term monitoring sites. In this project, parallel ozone monitoring by PS method was already performed in three EANET sites, Irkutsk, Listvyanka, and Mondy in Russia (Figure 8). The PS monitoring is expected to be expanded to a remote area which is difficult to access in a country having a vast land. Additionally, that method had obvious great advantage that the power supply was not needed in addition to being inexpensive. Taking those characteristics of PS method into account, it should be utilized in the future EANET activities.

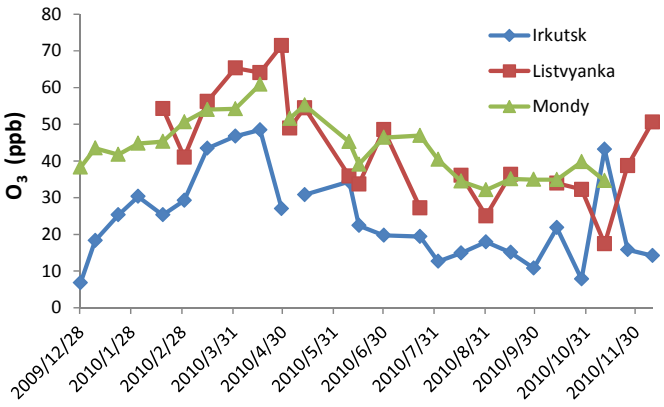

Figure 8. Parallel ozone monitoring by passive method in East Siberia, Russia.

6. References

World Meteorological Organization (WMO). 1988. Report on Passive Samplers for Atmospheric Chemistry Measurements and their Role in Global Atmospheric Watch (GAW). World Meteorological Organization Global Atmospheric Watch (WMO GAW) No. 122. (WMO TD No. 829).

Acid deposition Monitoring Network in East Asia (EANET). 2003. Technical Document for Filter Pack Method in East Asia, November 2003.

Joint Research Project with Republic of Korea on Aerosol Monitoring Methodology

Keiichi Sato[1], Mingqun Huo[1], Yayoi Inomata[1], Hiroaki Yagoh[1], Tsuyoshi Ohizumi[1], Joon-Young Ahn[2] and Lim-Seok Chang[2].

[1]Asia Center for Air Pollution Research, 1182 Sowa, Nishi-ku, Niigata 950-2144, Japan.

E-mail: ksato@acap.asia.

[2]Climate and Air Quality Research Department, National Institute of Environmental Research, Kyungseo-dong, Seo-gu, Incheon404-170, Republic of Korea.

1. Introduction

In the discussion at the Fourth Session of the Scientific Advisory Committee (SAC4) of the Acid Deposition Monitoring Network in East Asia (EANET) for the improvement of dry deposition monitoring methodologies, it was suggested that a study on PM_{10}, $PM_{2.5}$ and their components in the selected sites should be considered. In line with this suggestion, the project on aerosol monitoring was planned as a joint research between National Institute of Environmental Research (NIER), Ministry of the Environment, Republic of Korea and the Network Center (NC) of EANET. In order to evaluate aerosol sampling methodology and atmospheric behavior of fine particles in Japan and Republic of Korea, intensive monitoring was carried out at both the Korean and Japanese sites during 2005 and 2007. Several methods for aerosol monitoring including $PM_{2.5}$ and PM_{10} collections were implemented simultaneously in both sites. After compiling the monitoring results, the progress of the project and preliminary results from the intensive monitoring were discussed at the small data analysis workshop each year.

The main objectives of the previous joint study during 2005 and 2007 were to compare the 3-stage filter pack method with the 4-stage filter pack method, which is described in the Technical Document for Filter Pack Method in East Asia (EANET, 2003), in Korea and Japan, and to compare $PM_{2.5}$ (separated by a cyclone or a cascade impactor) with open face type of filter pack method in Korea and Japan. For the air concentrations monitoring of the EANET, there are 2 kinds of filter pack monitoring methods used. The Republic of Korea uses the 3-stage filter pack monitoring method and the other countries use the 4-stage filter pack monitoring method. In this context, this joint research project compares these 2 kinds of filter pack method with each other aiming at the improvement of the method of the filter pack monitoring. In addition, the behavior of $PM_{2.5}$ measured in Republic of Korea and Japan will be evaluated through this joint research project.

The target species of the previous joint project are nitrate, sulfate, and the other cation species which are designated as the priority dry deposition monitoring species in the EANET. Recently, atmospheric behaviors of carbonaceous aerosol were one of the most interested topics in the field of atmospheric sciences because carbonaceous aerosols include potentially harmful organic components and some types of aerosol such as black carbon may affect radiative forcing and climate change. Therefore, carbonaceous components should be included in the target species in the present joint research project. In this report, the results of parallel monitoring implemented from 2010 to 2012 and time variation of air concentrations during long range transportation of air pollutants are discussed.

2. Objectives

The project is being carried out with the aim of the following objectives:

1. To consider a new monitoring item of carbonaceous species as the supplemental data of sulfate and nitrate aerosol.
2. To compare 3-stage filter pack method with 4-stage filter pack method in Korea and Japan.
3. To compare $PM_{2.5}$ (cyclone and impactor) with open face type of filter pack method in Korea and Japan.

3. Monitoring and analytical methods

The intensive monitoring was conducted at Jeju in Korea and the ACAP (Asia Center for Air Pollution Research), Niigata in Japan in two seasons of spring (May) and autumn (October) from 2010 to 2012. Aerosol was observed by parallel measurement of the following 4 kinds of method summarized in Figure 1.

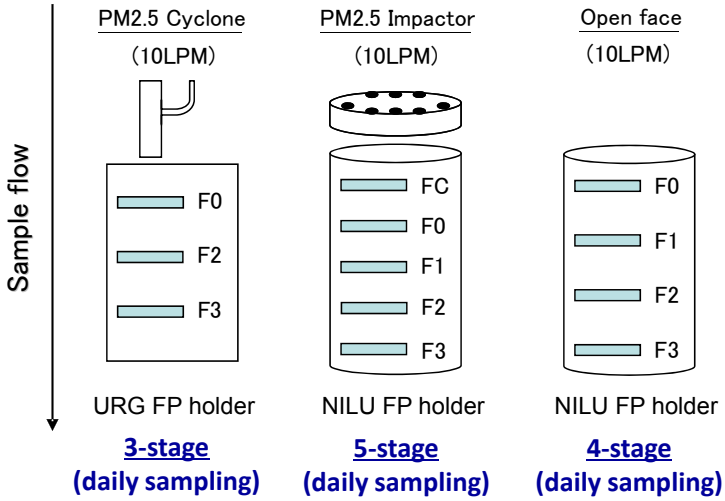

Figure 1. Summary of sampling methods of aerosol monitoring.

In the filter pack installed $PM_{2.5}$ cyclone, fine particle ($PM_{2.5}$) was collected on the F0 stage, and acidic gases and ammonia gas were collected on the F2 and F3 stages, respectively. In the filter pack installed $PM_{2.5}$ impactor, coarse and fine particle ($PM_{2.5}$) were collected on the FC and F0 stages, respectively, and gaseous substances were collected on the F1, F2 and F3 stages. In the 4 stage filter pack, total suspended particle were collected on the F0 stage, and gaseous substances were collected on the F1, F2 and F3 stages. To compare results of the cyclone method and the impactor method may clarify the difference between the different two aerosol separation methods. To compare results of gas concentrations measured by the impactor method and the 4 stage method may clarify the difference of total aerosol concentration between the different sampling methods. Each sampling should be implemented on the 24 hour sampling.

Gaseous species of SO_2, HNO_3, HCl and aerosol components of SO_4^{2+}, NO_3^-, Cl^-, Na^+, NH_4^+, K^+, Ca^{2+}, Mg^{2+}were determined by ion chromatography (EANET, 2003), and carbonaceous components in aerosol were determined by the Thermal/Optical Carbon Analysis method with IMPROVE protocol (Chow *et al*., 2004). Table 1 shows the list of carbon fraction and analytical conditions. Depending on combustion temperature and matrix gas, carbonaceous components were fractionated into OC1-OC4 (Organic carbon) and EC1-EC3 (Elemental carbon).

Table 1. List of carbon fraction and analytical conditions in IMPROVE protocol.

Carbon fraction	Analytical conditions	
	Temperature	Matrix gas
OC1	120ºC	He
OC2	240ºC	He
OC3	450ºC	He
OC4	550ºC	He
EC1	550ºC	98%He+2%O_2
EC2	700ºC	98%He+2%O_2
EC3	800ºC	98%He+2%O_2

4. Results and discussions

Figures 2-5 show time profiles of fractionated carbon concentrations in aerosol that sampled at the Niigata site in October 2010, and Figures 7-10 show time profiles of carbon concentrations in October 2011. Figures 6 and 11 illustrate daily back trajectories during the sampling period in 2010 and 2011, respectively. When carbon concentrations in TSP sampled by the 4 stage filter pack and the filter pack equipped with $PM_{2.5}$ impactor are compared, average difference of carbon concentration were approximately 10%. These results implied that there is no significant loss of carbonaceous aerosol deposited on $PM_{2.5}$ impactor. However, in some cases, the difference was more than double. The reason of these discrepancies should be carefully considered. When carbon concentrations in $PM_{2.5}$ sampled by the filter pack equipped with $PM_{2.5}$ cyclone and the filter pack equipped with $PM_{2.5}$ impactor are compared, the carbon concentrations by $PM_{2.5}$ tended to showed lower values

than those by $PM_{2.5}$ impactor. The average difference was 11.8%, and this tendency was remarkable when ambient carbon concentration was higher.

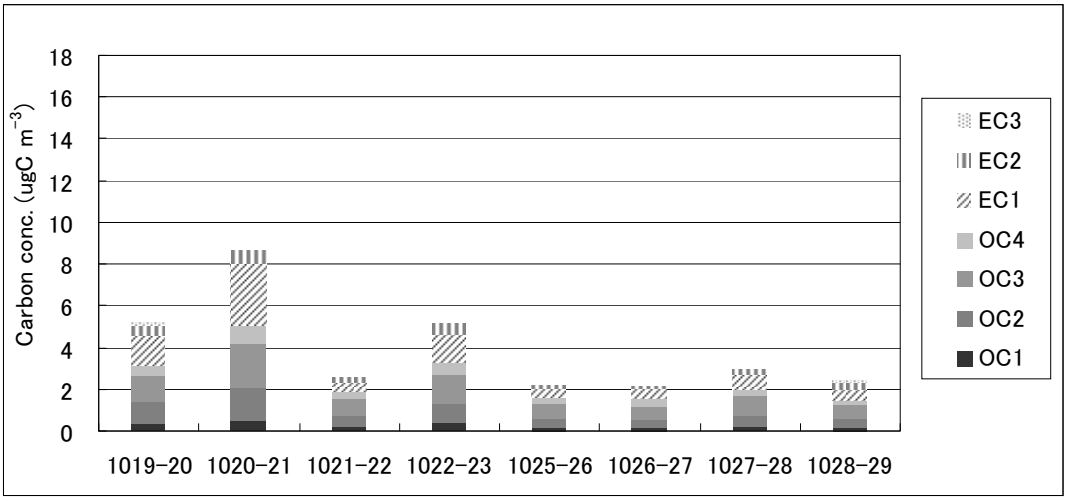

Figure 2. Carbon conc. in $PM_{2.5}$ sampled by $PM_{2.5}$ cyclone at Niigata (October 2010).

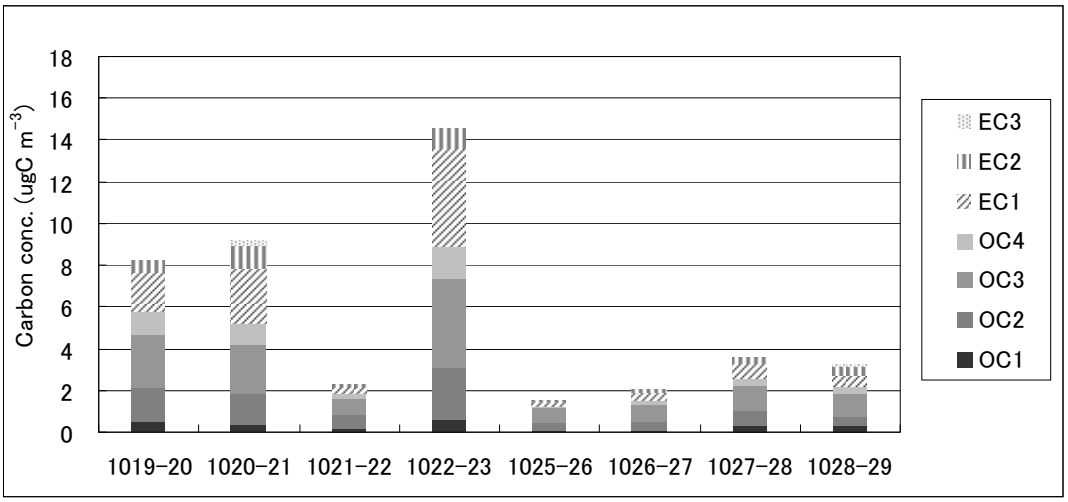

Figure 3. Carbon conc. in TSP sampled by 4 stage filter pack at Niigata (October 2010).

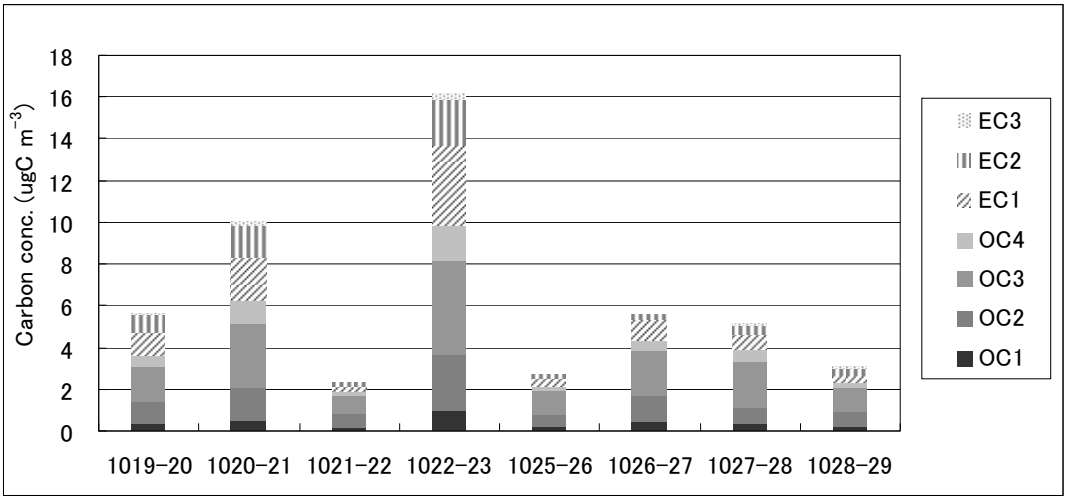

Figure 4. Carbon conc. in coarse PM sampled by $PM_{2.5}$ impactor at Niigata (October 2010).

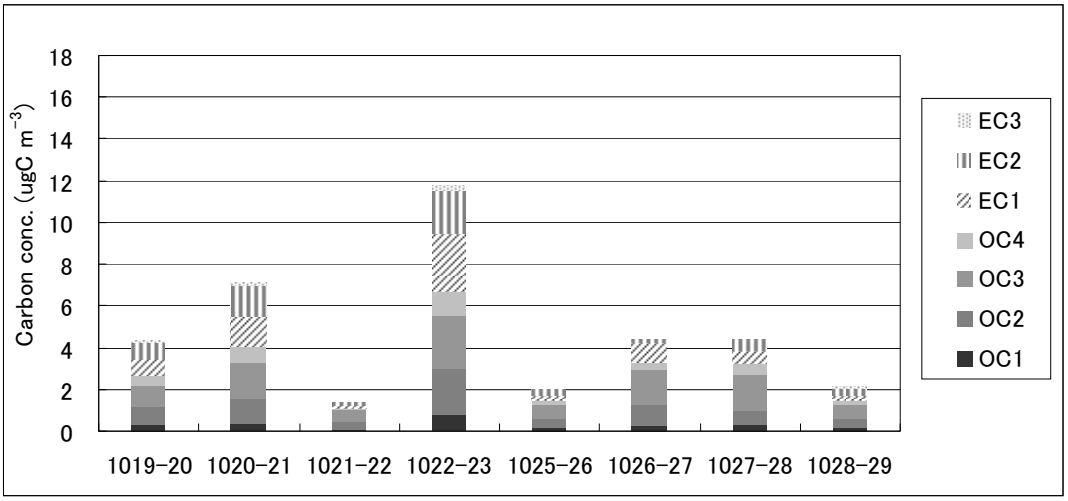

Figure 5. Carbon conc. in $PM_{2.5}$ sampled by $PM_{2.5}$ impactor at Niigata (October 2010).

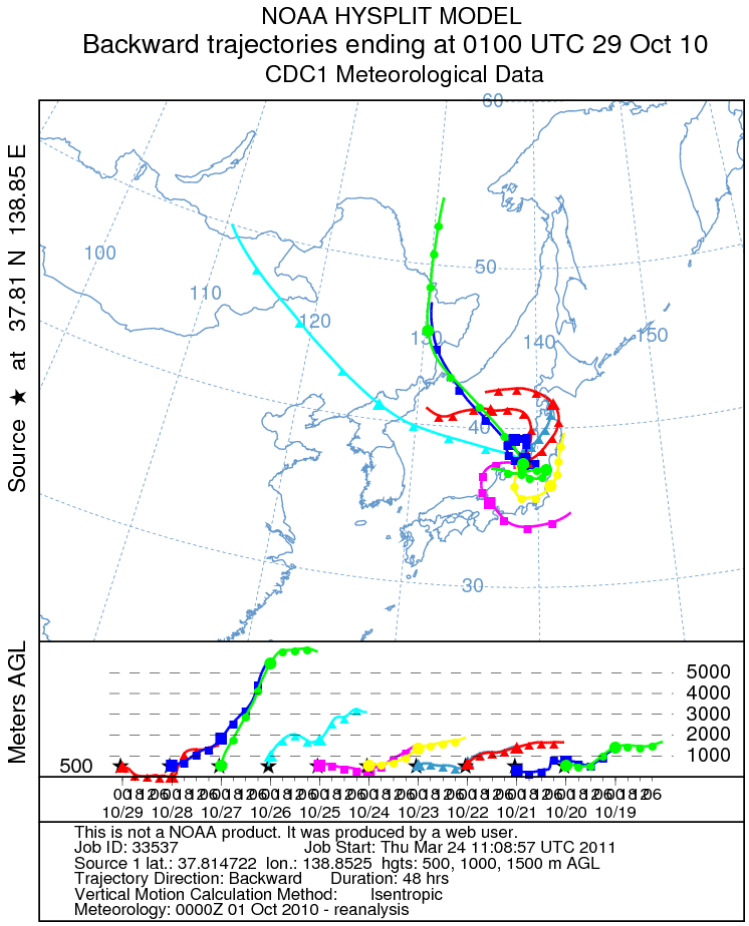

Figure 6. Daily back trajectories during 19 and 29 October, 2010 (Analysis time: 48 hours).

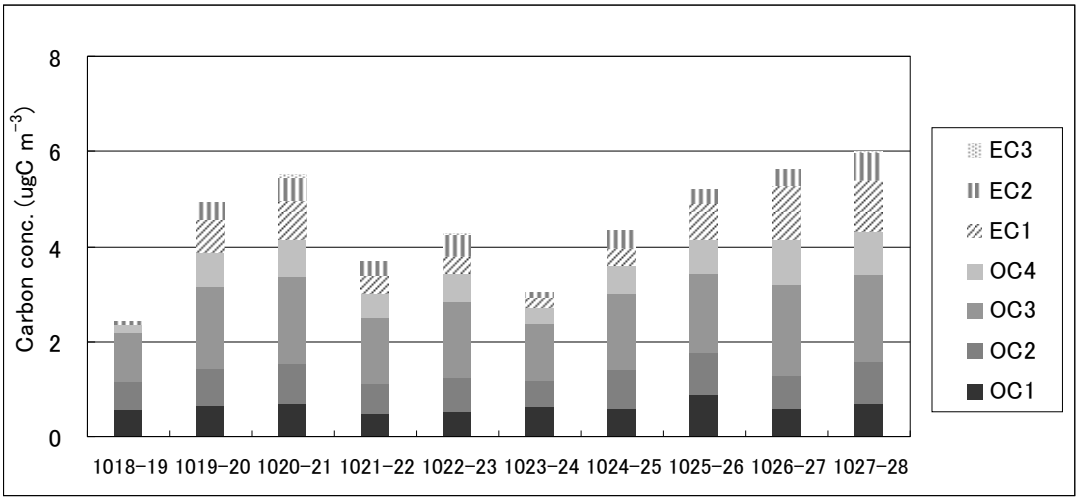

Figure 7. Carbon conc. in $PM_{2.5}$ sampled by $PM_{2.5}$ cyclone at Niigata (October 2011).

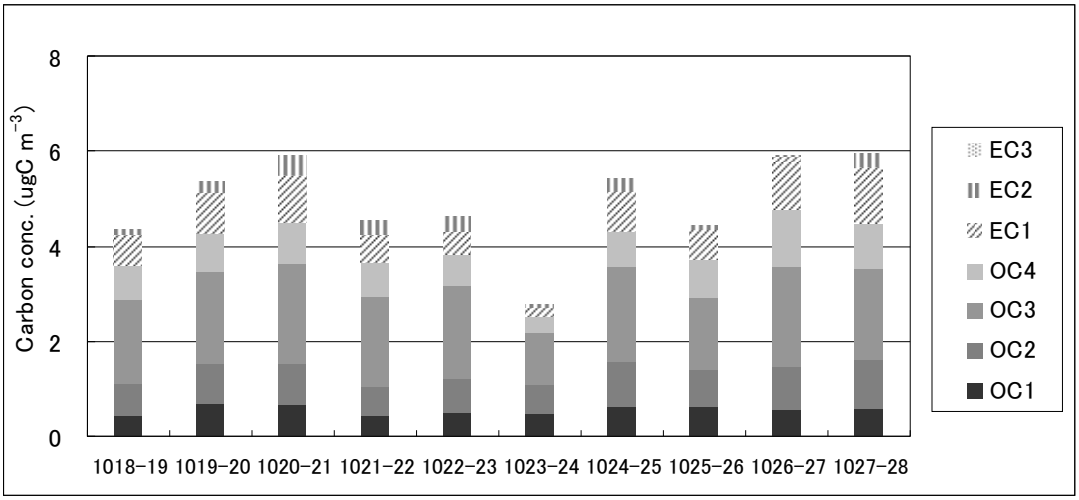

Figure 8. Carbon conc. in TSP sampled by 4 stage filter pack at Niigata (October 2011).

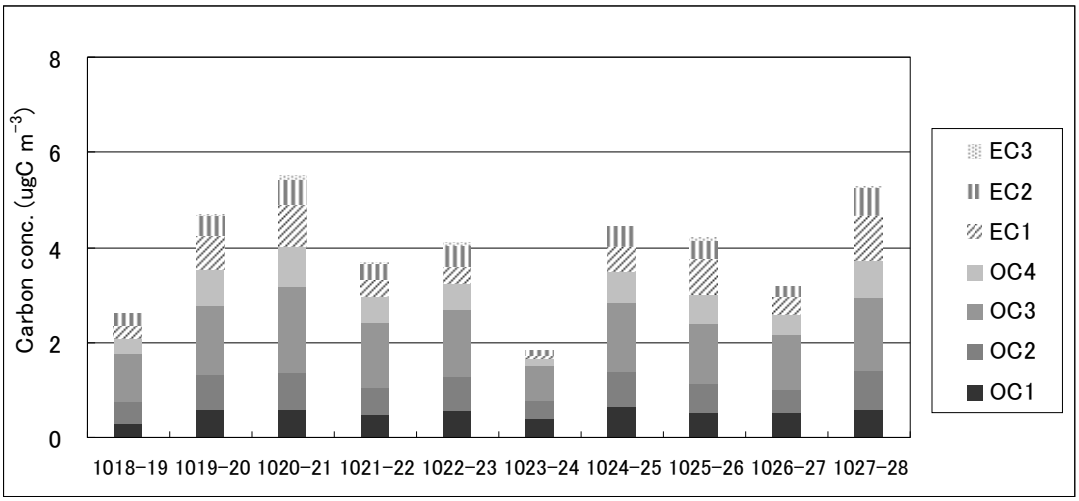

Figure 9. Carbon conc. in $PM_{2.5}$ sampled by $PM_{2.5}$ impactor at Niigata (October 2011).

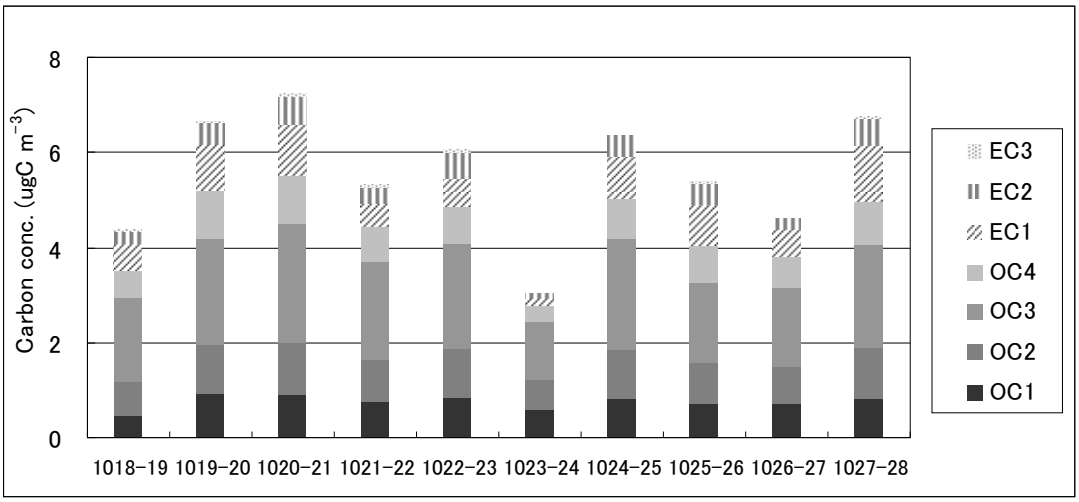

Figure 10. Carbon conc. in TSP sampled by $PM_{2.5}$ impactor at Niigata (October 2011).

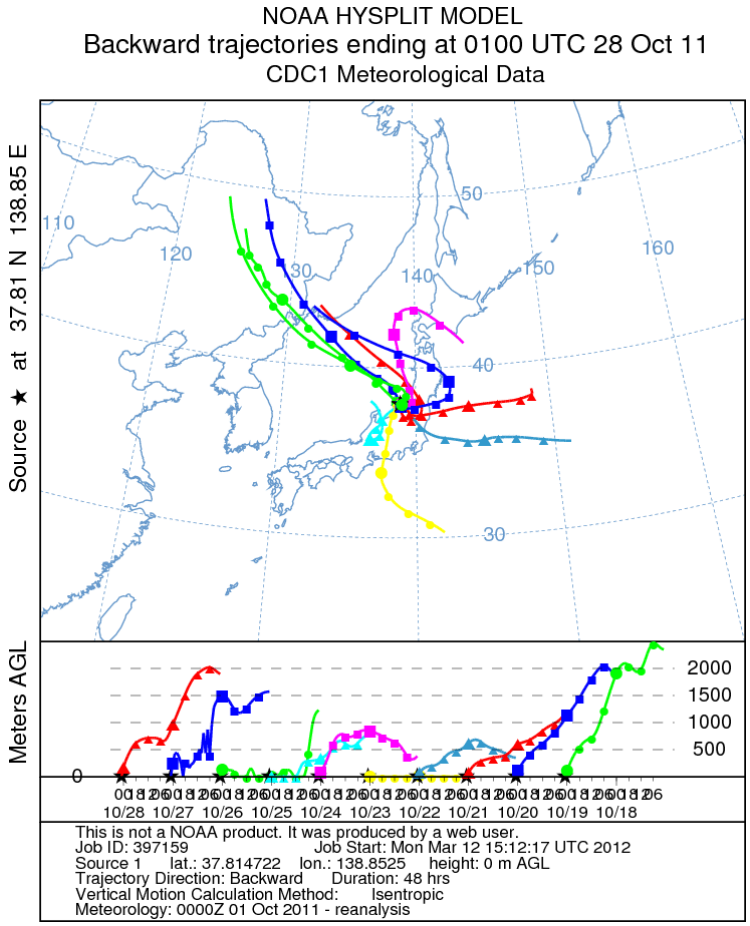

Figure 11. Daily back trajectories during 18 and 28 October 2011 (Analysis time: 48 hours).

Some peaks of carbon concentrations were observed during each monitoring period, and relationship between peak event and long range transportation of air pollutants was considered. High peaks of carbon concentrations for all types of samplers were observed at Niigata during 19-21 October and 22-23 October in 2010 and during 19-20 October and 24-28 October in 2011. From the results of back trajectory analysis shown in Figures 6 and 11, air mass was moved from central east and north east China to Niigata on the days of high carbon peaks event. Other study demonstrated high peaks of carbonaceous aerosol due to long range transportation from Asian continents were observed in Jeju Island in Korea (Kim *et al*., 2000) and remote sites in Japan (Matsumoto *et al*., 2003). It is important to detect high peaks events in monitoring at remote sites.

5. Current status and future works

Intensive monitoring during 2010 and 2012 was conducted at remote sites in Japan and Korea. After compiling all monitoring data, the data will be exchanged between NIER and the NC under the agreement between both institutes. Then, the feasibility of various types of filter pack sampler will be discussed by experts in Japan and Korea. Final the outcomes obtained in this project are planned to publish as a peer reviewed paper.

6. References

Chow, J. C., Watson, J. G., Chen, L.W.A., Arnott, W.P. and Moosmüller, H. 2004. Equivalence of Elemental Carbon by Thermal/Optical Reflectance and Transmittance with Different Temperature Protocols. Environmental Science and Technology. 38: 4414-4422.

EANET. 2003. Technical Document for Filter Pack Method in East Asia. Network Center for EANET. Acid Deposition and Oxidant Research Center, Niigata, Japan.

Kim, Y.P., Moon, K.C. and Lee, J. H. 2000. Organic and elemental carbon in fine particles at Kosan, Korea. Atmospheric Environment. 34: 3309-3317.

Matsumoto, K., Uematsu, M., Hayano, T., Yoshioka, K., Tanimoto, H. and Iida, T. 2003. Simultaneous measurements of particulate elemental carbon on the ground observation network over the western North Pacific during the ACE-Asia campaign. Journal of Geophysical Research. 108: 10.1029/2002JD002744.

Scientific and Technological Research Papers from Participating Countries

For our cooperation on research activities, we have some research papers from our participating countries that have been utilized the EANET data. Therefore, they are included in this part of the EANET Science Bulletin.

Chemical Composition of Aerosol in Atmosphere of Arid and Semi-Arid Territories of Mongolia

D. Azzaya[1,*], D. Oyunchimeg[1], E. Enkhbat[1], G.S. Zhamsueva[2], A.S. Zayakhanov[2], A.V. Starikov[2], V.V Tsydypov[2], T.S. Balzhanov[2], T.V. Khodzher[3] and L.P. Golobokova[3]

[1]Institute of Meteorology and Hydrology of Mongolia
Juulchiny gudamj-5, Ulaanbaatar-210646, Mongolia.
**corresponding author: azzaya23@yahoo.com.*
[2]Institute of Physical Materials of Science, Siberian Branch of Russian Academy of Sciences
6, Sakhyanovoy st., Ulan-Ude, 670047, Russia.
E-mail: Lrf@ipms.bscnet.ru.
[3]Limnological Institute, Siberian Branch of Russian Academy of Sciences
3, Ulan-Batorskaya st., Irkutsk, 664033, Russia.
E-mail: khodzher@lin.irk.ru

Abstract

Climate change is a global problem of concern to humanity. During recent decades, anthropogenic air pollution has been identified as a main cause of changes in the content of the atmosphere. This situation is constantly intensified by the continuing growth of air pollution in areas located near emission sources as well as in distant territories.

Aerosol samples were collected in the atmosphere of Mongolia (Sainshand and Baruun-Urt, East Gobi; Hanbogd and Dalanzadgad, South Gobi; industrial centers Ulaanbaatar and Sukhbaatar) during the summer periods of 2005-2010.

It is found that the differences in the composition and concentration of atmospheric aerosols collected at Ulaanbaatar, Sukhbaatar, Baruun-Urt, and Sainshand provide evidence of the different sources of aerosol particles in these observation locations. The transport of pollutants and the transport of terrigenous particles by wind are major factors that influence the chemical composition of aerosols in Sainshand and Baruun-Urt with undeveloped industry. Concentration of aerosol ions in these sites is 0.9-63.3 μg m^{-3}. The local emissions play an important role in the formation of aerosols composition in industrial cities of Ulaanbaatar and Sukhbaatar. The similarity of content and composition of atmospheric aerosols in Ulaanbaatar and Beijing in winter season are determined. Sum of ions concentrations amounted to 9.8-75.1 μg m^{-3}. The regional emissions associated with development of the mining industry have a strong influence on the formation of the composition of

suspended particles in the sites of South Gobi. Aerosol concentration amounted to 19.7-46.1 μg m^{-3} in winter. The main ions in the aerosols at Sainshand and Baruun-Urt are SO_4^{2-}, NO_3^-, NH_4^+, in Ulaanbaatar and Sukhbaatar - SO_4^{2-}, NO_3^-, HCO_3^-, Ca^{2+}, NH_4^+, in Hanbogd and Dalanzadgad - SO_4^{2-}, NO_3^-, NO_2^-, Cl^-, Ca^{2+}, K^+, Na^+.

Key words: Chemical composition of aerosol, PM_{10}, atmosphere, Desert Gobi

1. Introduction

Tropospheric aerosol particles play important roles in Earth's climate system and in the biogeochemical cycle. These particles affect Earth's radiation balance by scattering and absorbing solar and terrestrial radiation; they also modify the cloud properties by acting as cloud condensation nuclei and influence the tropospheric chemistry (Charlson *et al*., 1992). Atmospheric aerosols can have a marked impact on health, air quality, and visibility on both the global and regional scales. Furthermore, the role of aerosols in the global energy budget has been examined in many observational and modelling studies, and their estimated radiative forcing could be similar in magnitude to that of greenhouse gases (IPCC, 2007).

Atmospheric aerosols consist of solid or liquid particles suspended in air. The aerosols are formed as a result of wind mixing of mineral dust from Earth, evaporation from sea splashes, volcanic and anthropogenic emissions, combustion of biomass, injection of biogenic particles into the atmosphere, and chemical reactions in the air. Due to their long life expectancy in the troposphere (one or two weeks in the majority of areas on Earth), aerosol particles can be transferred over long distances (Kondratyev, 2002), and aerosol particles can have an influence on extensive territories as a result of distant transfer. The distribution of atmospheric aerosols depends on the meteorological conditions (direction and speed of air masses, precipitation), the turbulent activity in the atmosphere, and the particle sizes.

Many studies have investigated the development of dust aerosols and their transportation and deposition, but researchers are now discovering that the type and amount of dust in the atmosphere vary according to latitude, longitude, altitude, and time of year. Research on suspended particles in different geographical areas is of great importance because the properties of atmospheric aerosols form under the influence of such regional factors as a land relief, vegetative cover, prevailing weather conditions, and the existence of industrial facilities (Plaude *et al*., 2006; Wang *et al*., 2008). In particular, much attention has focused on the study of aerosols in the arid regions of Mongolia, where dust storms are often observed. Dust storms play an important role in the formation of atmospheric aerosols. At the same time, due to weak development and its distance from industrial centres, the region can be considered as providing a background level of particulate material. As a component of Central Asia, the Mongolian Gobi is of great interest for the study of atmospheric aerosols. The atmospheric aerosols in the Mongolian Gobi are less studied than those in the Chinese portion of the Gobi desert. It has been established that the Mongolian Gobi is large-scale source of dust (aeolian) aerosols (Wang *et al*., 2008). Aeolian dust has a strong impact on the climate systems and also

significantly influences the atmospheric radiation balance by scattering and absorbing various radiation components and modifying the optical properties and lifetimes of clouds (Yabuki *et al*., 2005). A particularly strong effect of dust aerosols from Central Asia is experienced in the Pacific Ocean to the Far East (Kondratyev *et al*., 2005).

Investigations in the atmosphere of Central and East Asia have found a strong influence of industrial emissions on the composition and structure of aerosols. The cities of China have been revealed as the largest anthropogenic sources of pollution in Central Asia.

Previous research has shown that China is a major contributor to global emissions of sulphur dioxide (SO_2), a sulphate (SO_4^{2-}) precursor, organic carbon (OC), and black carbon (BC) aerosols. In industrial centers of China the high concentration of SO_4^{2-}, NO_3^-, NH_4^+, Na^+, Ca^{2+}, K^+, $CH_2(COO^-)_2$, F^-, NO_2^-, PO_4^{3-} are found out in aerosols (Saikawa *et al*., 2009; Chan and Yao, 2008). Sulphates are their basic component. These aerosols result from mixtures of dust aerosols and anthropogenic emissions (Li *et al*., 2008). In China SO_2 emissions, a major air pollutant from coal combustion, reached $2.55 \cdot 10^7$ tons in 2005 (Chan and Yao, 2008).

In recent decades the problem of global and regional changes in the environment and climate have been attributed to the increase in air pollution from aerosol or particulate matter (PM). Epidemiological studies reveal that the increase in $PM_{2.5}$ (particles with an aerodynamic diameter of 2.5 μm or less) and PM_{10} (particles with an aerodynamic diameter of 10 μm or less) impact the morbidity, hospitalization and premature mortality of peoples in the affected areas are increased due to particle that penetrate into the lower respiratory tract (WHO, 2006, 2007). Most studies have focused on $PM_{2.5}$ fine aerosols due to its relatively long lifetime in atmosphere and distant transfer. Consequently, the air pollution from suspended particles is not only local but also global problem. In Zhamsueva *et al*. (2011) the daily fund data of 2008 were analysed for mass concentrations of PM_{10} and $PM_{2.5}$ in Sainshand and Zamyn-Uud. It is revealed the mean annual course of mass concentration of PM_{10} and $PM_{2.5}$ fine aerosols at Sainshand and Zamyn -Uud. The average annual concentrations of aerosols do not exceed 30 μg m^{-3} for PM_{10} and 8 μg m^{-3} for $PM_{2.5}$. The elevated monthly average PM_{10} and $PM_{2.5}$ concentrations are observed in spring and winter but minimum in autumn.

Due to different climate, topography, natural areas, the presence of densely populated and poorly developed areas, which can be viewed as the background, Mongolia is of great interest in studying the formation of the territory-specific chemical composition of aerosol under local conditions and under the influence of air mass transport from industrial regions.

This article presents the results of aerosol studies in Mongolia during 2005-2010 summer periods. The purpose of these field investigations was to determine the chemical characteristics of aerosol in the atmosphere of Mongolia and those factors that influence on their formation and dynamics.

2. Materials and Methods

2.1. Geographic and climatic characteristic of the studied areas

The territory of Mongolia is located in the centre of the Asian continent and is the farthest from the ocean, among the other countries. This country is divided into two different natural areas: the northern part is dominated by forest-steppe and steppe, which are continuation landscapes of East Siberia, and the southern part, appurtenant to the arid and semi-arid regions of Central Asia. Most of the territory is situated at an altitude of 1000-3000 m above sea level and is surrounded by mountain ranges on almost all sides. The Gobi desert is located in the south and south-eastern part of Mongolia. The Mongolian climate is notably dry, continental and cold due to distance from the sea and height elevation (Xuan *et al.*, 2004). The Mongolian average temperature -35 °C in January and temperature +20 °C - +25 °C in July. The maximum air temperatures (45...58 °C) are observed in the Gobi Desert in summer. The difference between day and night temperatures in summer can reach 20 °C. Mongolia is a major source of dust aerosol. Strong daytime heating creates unstable layer in the lower troposphere in the desert, where the dust particles are lifted at the atmosphere, and dust aerosol is formed. Mineral dust, especially alkaline and soda aerosols, absorbs contaminants under aging, including nitrates and sulphates, and actively participates in chemical reactions, thus, affecting the air composition (Stone *et al*., 2011). Several factors affects on the atmospheric aerosol in Mongolia. From one perspective, the nascent temperature inversion allows the dust aerosols (the lifetime of approximately six days) to be transported over long distances (Kondratyev, 2005). The frequent and strong winds resulting from the large change in the air temperature by tens of degrees in combination with the low relative humidity also contributes to this transport. From another perspective, the territory of Mongolia is exposed of south and south-east air masses transport that bring of pollution from the industrial regions of East China, North-East China and Central China, including the cities of Shenyang, Shanghai, Beijing (Sun *et al*., 2006; Zhang *et al*., 2010). The cyclones passage is often observed in the summertime, generally from the west and northwest directions (Dementeva, 2008). During this season Mongolia falls is under the influence of the polar (moderate) atmospheric front separating the temperate and tropical air masses, which leads to active cyclogenesis in this region. Considering the characteristics of climate, topography, natural areas, and the presence of populous areas, and less developed areas, which can be regarded as the background area, Mongolia is of great interest for studying the formation of chemical composition of aerosols on its territory, both under local conditions, and under the influence of long-range transport of air masses from industrial regions. Dust from the arid zone is a powerful factor affecting the characteristics of the radiation balance in the Far East and Pacific Ocean (Kondratyev *et al*., 2005).

2.2. Sampling sites

The samples were collected at the Sainshand station (44°54′*N*, 110°07′*E,* 1000 m above sea level) in the Gobi Desert, in Ulaanbaatar (46°56′*N*, 113°07′*E*, 1300 m above sea level), in Sukhbaatar (50°14′*N*, 106°12′*E*, 620 m above sea level), Baruun-Urt (46°41′*N*, 113°17′*E*, 980 m above sea level), Hanbogd (43°12′N, 107°12′E, 1165 m above sea level) and Dalanzadgad (43°35′N, 104°25′E, 1465 m above sea level) (Figure 1).

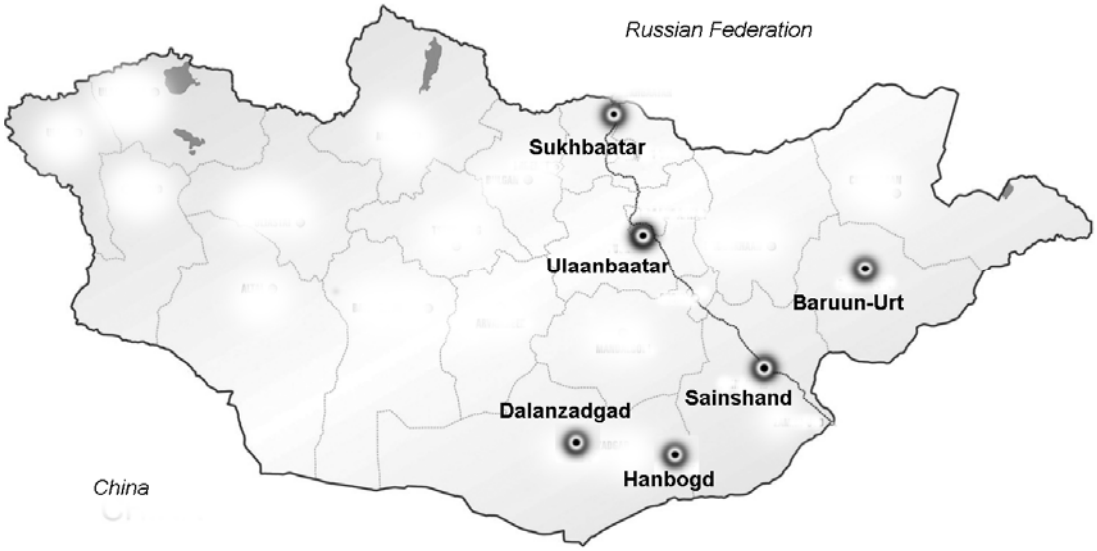

Figure 1. A map of Mongolia showing the location of sampling sites.

Table 1 shows the periods and sample sites of the observations. Ulaanbaatar is the capital of Mongolia, and is the largest industrial centre of the country. Sukhbaatar is a town in the north of the country near the Russian border, a transportation centre, large industrial city. The sampling points Sainshand and Baruun-Urt are located in outback, where there are no large sources of anthropogenic emissions. However, these areas are subject to long-range transport of pollutants. Dalanzadgad and Hanbogd are located in the South Gobi.

2.3. Methodologies

The aerosol samples were collected PM_{10} high volume sampler from Andersen instruments Inc. (USA) on to AFA-KhP and Whatman-41 filters (Zayakhanov *et al*., 2008). The ionic composition and concentration of aerosols was determined from the soluble fraction. Aerosol concentration was defined as sum of ten ions concentration in an extract solution from a filter which aerosols were collected. The sampled matter was extracted from the filters by the available volume of deionized water (0.15-0.20 μS cm^{-1}). A portion of the obtained solution was retained for pH measurements. «Expert» pH-meter (Russia) was employed. The remainder of solution was filtered through an acetate-cellulose filter with 0.2 μm pore size. Ions of NH_4^+, Na^+, K^+, magnesium (Mg^{2+}), and Ca^{2+} as well as SO_4^{2-}, NO_3^-, nitrite (NO_2^-), bromide (Br^-) hydro-carbonate (HCO_3^-), and chloride (Cl^-) ions were determined from the filtrate. The modern analytical methods of atomic adsorption and ionic chromatography were used to determine the chemical composition of the soluble fraction. These techniques are recommended for providing correlation with data obtained in other areas of the world (EMEP, 1996). Atomic adsorption spectrometer Carl Zeiss Jena (Germany), high performance fluid chromatographer «Milichrome A-02» (Russia), and ionic chromatographer ICS-3000 (Dionex, USA) were employed. Accuracy of measurements was not more than 10 %. HYSPLIT (Hybrid Single Particles Lagrangian Integrated Trajectory model) model, developed by NOAA (National Oceanic and Atmospheric Administration, USA) (URL: http://www.ready.noaa.gov/ready/hysplit4.html) was used for aerosols transfer pathways determination.

Table 1. Sampling sites and periods of observations.

Sampling site	Year	Period
Sukhbaatar	2005	14-15 July
Ulaanbaatar/Center	2005	16 July
Ulaanbaatar/Meteostation 1		25 July
Ulaanbaatar/Power plan		25 July
Ulaanbaatar/Meteostation 2		27 July
Ulaanbaatar/Meteostation 1	2006	18 July
Ulaanbaatar/Meteostation 1		29. July
Ulaanbaatar/Center	2011	14-24 December
Baruun-Urt	2006	13-15 July
	2007	24-26 July
Sainshand	2005	18-21 July
	2006	02-07 July
	2007	11-19 July
	2008	23-29 July
	2009	11-19 August
	2010	10-20 August
Dalanzadgad	2011	14-15,17 December
Hanbogd	2011	16 December

Several ions of water-soluble fraction of the atmospheric aerosol were determined during this study, namely hydrogen ions (H^+), sulphate ions (SO_4^{2-}), nitrate ions (NO_3^-), chloride ions (Cl^-), bicarbonate ions (HCO_3^-), ammonium ions (NH_4^+), calcium (Ca^{2+}), magnesium (Mg^{2+}), sodium (Na^+), potassium (K^+).

3. Results and discussion

3.1. Ions composition of aerosols in Ulaanbaatar and Sukhbaatar

The measurements in Ulaanbaatar were conducted in 2005 and 2006 and measurements in Sukhbaatar were carried out in 2005 (Table 1). The Ulaanbaatar studies in July 2005 were conducted in different parts of the city including the Institute of Meteorology and Hydrology of Mongolia in the central part of the city, near the Power station-3 and at the two meteorological stations located on the outskirts. The most heavily polluted air was observed near power station-3. The total content of ions in this point reached 34.7 μg m^{-3} compared with a maximum ions concentration in other parts of the city of 11.0 μg m^{-3}. The ratio of ions in the aerosol particles

shows that calcium bicarbonate ($Ca(HCO_3)_2$) is one of the main components of power station emissions and dominates in aerosols. Note that in the sample taken near power station 3, the pH of the solution of filtered substances was equal to 8.9 due to the presence of ash particles, compared with a pH of 6.3-6.8 in the remaining samples. The chemical compositions of the aerosols in the central part and outskirts of the city were similar in their cation content but differed in their anion content. On the outskirts of Ulaanbaatar, higher concentrations of NO_3^- and Cl^- ions and lower concentrations of SO_4^{2-} and HCO_3^- ions were observed compared with the values from the city centre. The correlation analysis showed a high correlation between the concentrations of HCO_3^- and Mg^{2+} (correlation coefficient r = 0.90), HCO_3^- and NH_4^+ (r = 0.85), and Na^+ and K^+ (r = 0.77) for the cations, and SO_4^{2-} (r = 0.80-0.90) and Cl^- are also weakly correlated for the cations (r = 0.53-0.68). The maximum correlation coefficient in Ulaanbaatar (r = 0.95) was observed between Ca^{2+} and HCO_3^-. The ion concentrations and their correlation coefficients indicate the predominance of SO_4^{2-} and HCO_3^- in the atmospheric aerosols in Ulaanbaatar, primarily $Ca(HCO_3)_2$ but also bicarbonates of Na^+, K^+, NH_4^+, and Mg^{2+}. The measurements from this city in 2006 showed similar results. The qualitative composition of aerosols in Sukhbaatar is similar to the aerosol composition in the centre of Ulaanbaatar, and the total content of ions (8 $\mu g \cdot m^{-3}$) is close to the suspended particle concentrations in the less contaminated areas of the capital.

It is established that the composition of aerosol particles in Ulaanbaatar in winter time has similarity to aerosols in Beijing [Sun *et al.*, 2004]. The ions SO_4^{2-} (47.2% from the sum of ions in Ulaanbaatar and 40.9% in Beijing), NO_3^- (9.7% and 22.2%, respectively) and NH_4^+ (13.3% and 16.3%, respectively) prevail in aerosol in this sites. The average of aerosol concentration in Ulaanbaatar winter was about half of a polluted city such as Beijing in which aerosol concentration reached 84.3 $\mu g\ m^{-3}$. That evidence testified the gravity of air pollution in the capital of Mongolia.

3.2. Ions composition of aerosols in Baruun-Urt

The investigation of chemical composition of water-soluble fraction of atmospheric aerosol in Baruun-Urt was carried out in 2006 and 2007. It was established that the chemical composition of aerosols in the Baruun-Urt is significantly different from aerosol composition in the industrial cities. Figure 2 shows the ionic concentrations for Baruun-Urt. Three ions, such as Ca^{2+}, NH_4^+ and SO_4^{2-} (16%, 25%, and 39% of aerosol concentration, respectively) are the dominant aerosol components in this town.

In the Baruun-Urt the content of Ca^{2+} in aerosols lower than in the industrial cities (Ulaanbaatar, Sukhbaatar) by a factor of 1.5, the Cl^- content is lower by a factor of three and the HCO_3^- content is lower by a factor of nine. Concentrations of Na^+, NH_4^+, Mg^{2+}, and K^+ increased by a factor 1.3-2.3 times, and the concentration of SO_4^{2-} increased by more than 3 times. The total ions content in the aerosols of Baruun-Urt ranged from 1.4 to 32.2 $\mu g\ m^{-3}$. This city is located in south-eastern part of Mongolia where there are no locally powerful sources of anthropogenic emissions into the atmosphere, and thus, the results suggest the influence of long-range air pollutant transport. For example, the analysis of aerosol was conducted the samples on 14 July 2006 and 24-26 July 2007, when the wind increasing up to 10 $m\ s^{-1}$ was observed. The total ions concentration in aerosols collected in dust storm day (14 July 2006) was 2.6 $\mu g\ m^{-3}$ that is almost 1.7 times higher than in the days when the dust storm was not observed (13 and 15 July 2006). The increase in the total ion content in the

aerosols was due to the increase in the NH_4^+, Ca^{2+}, HCO_3^-, and SO_4^{2-} ions. Evidently, the strong winds contributed to increase of terrigenous material in the air. The air masses in 24-26 July 2007 were brought from the southern and southeastern directions, from the industrialized regions of China.

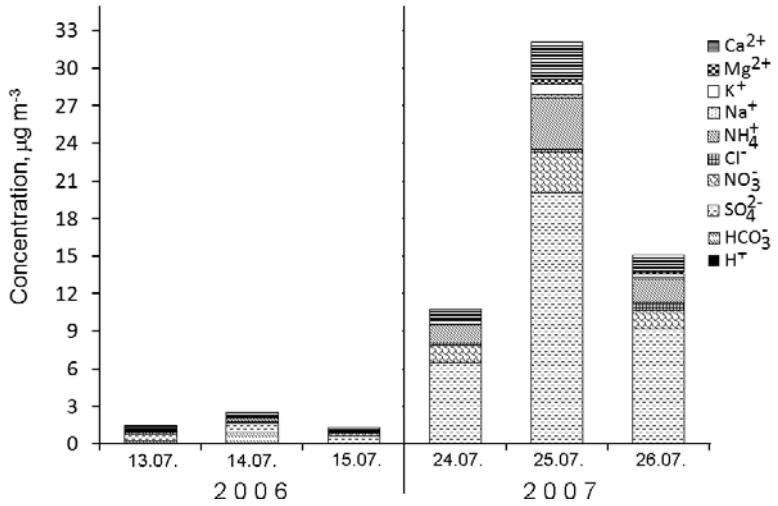

Figure 2. Temporal concentrations of soluble ions in the aerosols of Baruun-Urt.

The total content of aerosol ions reached 32.2 μg m^{-3}. High concentrations of anthropogenic ion (NO_3^-, SO_4^{2-}, Cl^-, NH_4^+) were observed at this point along with a high content of terrigenous ions (Ca^{2+}, HCO_3^-, Mg^{2+}). Analyses of air mass backward trajectory indicated that the northeast regions of Russia characterised by a low level of industrialisation were the main origin of the air mass transport back trajectories in 2006 (Figure 3).

The results were considered analysis of aerosols sampled on 13-15 July 2006 and 24-26 July 2007. On these dates, the observed average wind speed was 5-10 m s^{-1}. Analysis of the air mass transport trajectories showed that the air masses in 2006 come from the northeastern regions of Russia, an area with a low level of industrialization (Figure 3a)). However 14 July was observed air mass transport from the regions of Eastern Siberia, an area with a developed industry (Figure 3b)). The total content of ions in the aerosols on this day was 2.6 μg m^{-3}, which is almost 1.7 times higher than on the days with air masses transport from the Northeastern Siberia (13 and July 15, 2006). The increase in the amount of ions was due to the increase in the concentrations of NH_4^+, Ca^{2+}, HCO_3^- and SO_4^{2-}. At the same time the content of K^+ and Cl^- did not change significantly. On 24-26 July 2007, according to the simulation, the air masses, originated from the southern and southeastern areas of the industrialized regions of China (Figure 3c)), in most cases and the total content of ions reached 32.2 μg m^{-3}. On these dates (14 July 2006 and 24-26 July 2007), together with a high content of ions of terrigenous origin (Ca^{2+}, HCO_3^-, Mg^{2+}) observed high concentrations of anthropogenic ions - NO_3^-, SO_4^{2-}, Cl^-, NH_4^+. At this time, the chemical composition of atmospheric aerosols was formed under the influence of dust lifted from the ground and long-range transport of air masses. Evidently, the strong winds contributed to lifting of terrigenous material into the air, and the transport of air masses from the industrial regions contributes to the aerosols components of anthropogenic origin.

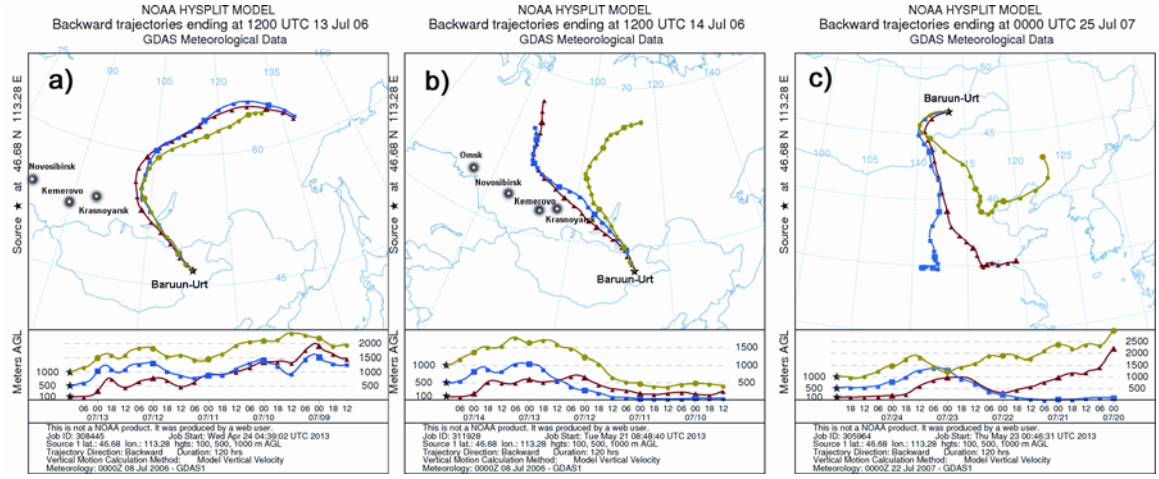

Figure 3. Backward air masses trajectories during observation period at the Baruun-Urt on the model HYSPLIT: a) 13 July 2006, b) 14 July 2006, c) 25 July 2007.

The analysis of the long-range transport of air masses demonstrate that in the episodes with a high content of suspended particles in Sainshand and Baruun-Urte were under the influence of transport from the North and East China, which have large industrial centres. This suggests that increasing of the concentration of suspended particles and a high content of anthropogenic components of aerosols in these episodes are associated with the transport of industrial pollution from China.

At the same time under influence of air masses transport from other directions, usually observed low concentrations of anthropogenic particles. These episodes of strong winds and dust storms associated with passage of fronts that increased the content of suspended particles in the air. The work of Zhang *et al*. (2010) also showed an increase in anthropogenic aerosol components in Central Asia under the influence of the transport of air masses from industrial regions.

3.3. Ions composition of aerosols in Sainshand

In the atmosphere of Sainshand and Baruun-Urt the sulphate ions, nitrate ions and ammonium ions are dominated in chemical compositions. The concentration of these ions is characteristic for industrial emissions. For all period of supervision the total concentration of water soluble ions of aerosols in 29% cases changed from 0.9 μg m^{-3} to 2.8 μg m^{-3} in 29% of the cases, from 3.0 μg m^{-3} to 10.0 μg m^{-3} in 24% of the cases, from 10.0 μgm^{-3} to 20.0 μg m^{-3} in 29% of the cases, and from above 20.0 μg m^{-3} in 19% of the cases. The highest concentrations of ions were found in 2010 (63.3 μg m^{-3}).

The average composition of the aerosols in the atmosphere of Sainshand for period of 2005-2009 period differed significantly from that of the aerosols collected in 2010 (Figure 4). The content of aerosols at Sainshand (2005-2009) was similar to the content of aerosols in Baruun-Urt and with content of aerosols in Ulaanbaatar and Sukhbaatar in 2010. In 2010 concentration of suspended particles strong increased (maximum values of concentration increased three times in comparison with previous years and measured up 63.3 μg m^{-3}, earlier was 20.3 μg m^{-3}).

The concentration range of the total ion content increased significantly and varied from 7.5 μg m^{-3} to 63.3 μg m^{-3} compared with a range of 0.9-20.3 μg m^{-3} in previous years. For the relative composition of aerosols,

the proportion of the ion compositions of HCO_3^-, Cl^-, and Ca^{2+} increased significantly, and the proportions of NH_4^+ and SO_4^{2-} ions decreased accordingly. In 2010, the content of HCO_3^- ions reached 32.2 μg m^{-3}, and the content of calcium ions reached 11.3 μg m^{-3}, compared with 0.0-1.5 μg m^{-3} and 0.1-2.1 μg m^{-3} during the 2005-2009 period, respectively. The concentrations of other ions in the aerosol particles in 2010 were also high; however, their content did not exceed their maximum values in previous years. In 2010, the maximum concentration of ions occurred in the aerosols that were selected during 12-14 August and 17-18 August. During these periods, high values of pH (7.4-8.1) were observed in the aqueous extracts of the aerosol samples, whereas on other days in 2010 and in previous years, the pH of the aerosol samples varied within the limits of 4.5-6.7 in most cases. Note that in the 2010 samples with a low content of suspended particles, the same relative concentrations of major components were observed as in the samples collected in 2005-2009. The filters used in 2010 displayed an orange colour, in contrast to the greyish samples of previous years.

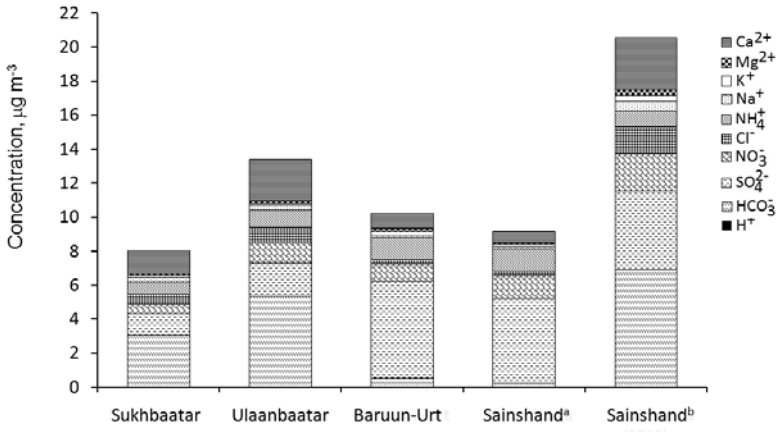

Figure 4. Comparison of average concentrations of soluble ions of aerosols from Sukhbaatar 2005, Ulaanbaatar 2005-2006, Baruun-Urt 2006-2007, Sainshand (a) 2005-2009, (b) 2010.

High concentrations of HCO_3^-, Cl^-, and Ca^+ were observed in certain 2010 aerosol samples. This observation suggests that the main influence on the formation of these ions was components of terrigenous origin.

Calculations of the backward trajectories of air mass transport show that the chemical content in 2010 was formed over the central, south, and eastern parts of Mongolia (Figure 5). Strong winds and dry hot weather in 2010 contributed to the increase in the air particles of terrigenous origin, which contained many impurities. Larger amounts of HCO_3^- ions were found in the aerosols when strong winds (10 m s^{-1}) were observed in Sainshand.

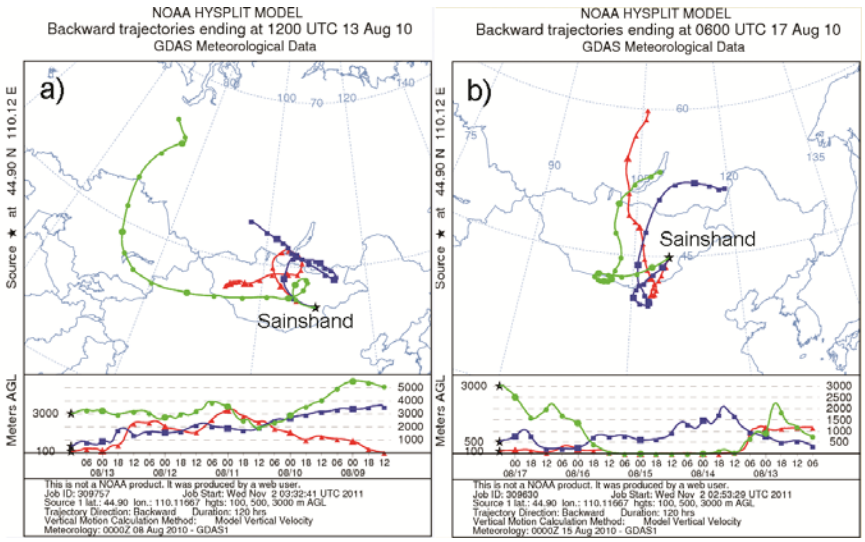

Figure 5. Backward air masses trajectories during observation period at the Sainshand on the model HYSPLIT: a) 13 August 2010, b) 17 August 2010.

Low concentrations of aerosols were observed during the periods with windless weather and also with air mass transport from the territories of Russia and Kazakhstan. The greatest contribution to the composition of these aerosols was due to NH_4^+, Ca^{2+}, SO_4^{2-}, and NO_3^- ions. The Cl^- and N^+ ion contributions were also high. High coefficients of correlation (greater than 0.9) were calculated between the concentrations of NH_4^+ and SO_4^{2-} ions and H^+ and SO_4^{2-} ions. The coefficient of correlation between the cations of Ca^{2+}, Mg^{2+}, Na^+, and K^+ metals and the Cl^- ion was 0.9. High ion concentrations predominated in the aerosols, where the chemical composition was formed in weather conditions with strong winds of up to 7-10 m s^{-1} and under the influence of air mass transfer from the Takla Makan Desert and the industrial areas of China. Dust aerosol contains sorbed pollutants from the atmosphere, especially aged particles. Together with terrigenous particles, high concentrations of SO_4^{2-} and NO_3^- also exist in the aerosols (Stone *et al.*, 2011). Large contributions to the chemical compound formation of the aerosols explain the ions of NH_4^+ and Ca^{2+} and an overall high total content of ions. In certain periods, the fraction of NO_3^- ions increased.

The salt aerosol source in Central Asia are the salt lakes and salt marshes of the North-western China (Abuduwaili *et al.*, 2008). Studies in the Northwest of China carried out at the station Aksu, which is situated with salt marshes with brown soils, showed that the local aerosols contain calcite ($CaCO_3$), halite (NaCl) and gypsum($CaSO_4 \cdot 2H_2O$) with soil origin. Prevailing ions of soluble fraction of these aerosols are SO_4^{2-}, NO_3^-, Cl^-, NH_4^+, Ca^{2+} and Na^+ (Yabuki *et al.*, 2005). These ions can have the same origin in Mongolia.

To determine the sources and chemical composition of aerosol particles coefficients of correlation (r) were calculated between sampled concentrations of the major water-soluble components of aerosols from Sainshand. The coefficient of correlation between the pairs of ions NH_4^+ - SO_4^{2-} and Ca^{2+} - HCO_3^- are equal to 0.87 and 0.97, respectively. Nitrates have good correlation with Na^+ ($r = 0.76$), K^+ ($r = 0.81$), Mg^{2+} (r = 0.77) and

Ca^{2+} (r = 0.73). Strong relationship between Cl and such metals as Ca^{2+}, Mg^{2+} , Na^{+} and K^{+} are noted (coefficients r are equal 0.75, 0.82, 0.90 and 0.85, respectively).

Analysis of the correlation coefficients of the components and concentrations of ions in the aerosols of Sainshand and Baruun-Urt allows us to assume that the local aerosols are dominated by SO_4^{2-}, carbonates, NO_3^{-}, NH_4^{+}, and Ca^{2+}, and SO_4^{2-} and NO_3^{-} are indicators of anthropogenic emissions.

In the atmosphere of Baruun-Urt, a significant amount of $Ca(HCO_3)_2$ and magnesium carbonate ($MgCO_3$) was found in the summer of 2006. Due to strong winds in this year, a significant amount of dust was picked up from the ground.

3.4. Measurements in the South Gobi

The region of the South Gobi is strong influenced from the industrial regions of China which are large sources of anthropogenic emissions. At the same time there are a lot of under populated and poor developed territories which can be considered still as background site. The Oyuu-Tolga gold-copper field and Tavan-Tolga coal field in the South Gobi actively develop in recent years. Open-pit mining in the arid regions of Mongolia, transportation of minerals by continuous truck traffic to China will lead to sharp increase of pollution of atmosphere. It will have impact on surrounding territories due to air-masses long-range transport.

The chemical composition of atmospheric aerosols in Hanbogd and Dalanzadgad located near development of fields conformed to a chemical composition of the large industrial centers atmosphere and is similar to that of the aerosols of Ulaanbaatar. The sum of the main water-soluble ions of aerosol particles in Hanbogd and Dalanzadgad ranged from 19.7 μg m^{-3} to 46.1 μg m^{-3}. The anthropogenic ions SO_4^{2-}, Cl^{-}, NO_3^{-}, and NO_2^{-} (Figure 5) prevail in aerosols of Hanbogd and Dalanzadgad. High concentrations of nitrite ions NO_2^{-} and nitrate ions NO_3^{-} in aerosols of South Gobi (concentration from 0 to 3.3 μg m^{-3} for NO_2^{-} and from 0.9 to 3.9 μg m^{-3} for NO_3^{-}) are connected with emissions of the motor transport. The average concentration of NO_2^{-} in aerosols in Dalanzadgad reached 1.8 μg m^{-3}, NO_3^{-} reached 3.0 μg m^{-3}. The concentrations of these ions in Hanbogd reached 0.4 μg m^{-3} and 3.7 μg m^{-3}, respectively. The revealed NH_4^{+} absence in the South Gobi aerosols can be connected with a small share of emissions from coal burning.

4. Conclusions

The differences in composition and concentration of atmospheric aerosols collected in Ulaanbaatar, Sukhbaatar, Baruun-Urt, and at Sainshand, testify to the different sources of aerosol particles at these observation points. Analysis of the aerosols composition and the simulation of meteorological conditions indicate that the pollutants transport to the area of research as well as the wind transport of terrigenous particles, (particularly during the dust storms) are major factor that influence on the formation of the chemical composition of aerosols in the atmosphere of Sainshand and Baruun-Urt. The local emissions play an important role in formation of aerosols composition in Ulaanbaatar and Sukhbaatar. Polluting anthropogenic components arrive in Mongolia, mainly from the southern and southeastern directions, originating in China. This observation is supported by simulations of the air mass pathways with the HYSPLIT model. The major ions in the aerosol

particles in Sainshand and Baruun-Urt are SO_4^{2-}, NO_3^-, and NH_4^+ and, in certain cases, HCO_3^- and Ca^{2+} ions as well. The SO_4^{2-}, NO_3^-, HCO_3^-, Ca^{2+}, and NH_4^+ ions are the main components of suspended particles found in Ulaanbaatar and Sukhbaatar. The concentration of suspended particles in these points in the absence of transport from the southern direction does not exceed 10.0 μg m^{-3}. The content of atmospheric aerosols at Sainshand and Baruun-Urt increases to 20.3 μg m^{-3} under the influence of the southern transport pathways, a level comparable with the concentration of aerosols in the industrial cities of Mongolia, such as Ulaanbaatar. High concentrations of sulphates indicate the anthropogenic origin of the aerosol particles. Increases in aerosols of up to 63.3 μg m^{-3} during strong wind condition are observed in Sainshand in 2010. In this time their composition was noted strong growth of the content of carbonate ions and calcium ions, making the composition of these aerosols similar to aerosols of Ulaanbaatar. The main contribution to the budget of aerosols in Mongolia is imported anthropogenic emissions and terrigenic dust.

Atmospheric aerosols research in Hanbogd and Dalanzadgad in December, 2011 showed that a major factor of formation of component structure of the aerosol particles are the regional emissions connected with the mining industry and the motor traffic. These sources leads to the high contents of terrigenous components – Ca^{2+} (1.7-6.1 μg m^{-3}), K^+ (0.8-2.0 μg m^{-3}) and Na^+ (3.4-9.1 μg m^{-3}), and also NO_2^- (0.0-3.3 μg m^{-3}) and NO_3^-(0.8-3.9 μg m^{-3}), containing in products of combustion of fuel, in aerosols. The existence of Br^- in aerosols in Dalanzadgad (0.1-2.0 μg m^{-3}) may be to connect with saline soils in this region is characteristic.

5. Acknowledgments

The work is performed at support of Presidium Program of Russian Academy of Science (Project № 4.12), Siberian Branch of Russian Academy of Science (Integrate Projects № 14).

6. References

Abuduwaili, J., Gabchenko, M.V., Xu, J. 2008. Eolian transport of salts - a case study in the area of Lake Ebinur (Xinjiang, Northwest China). Journal of Arid Environments. 72(10): 1843–1852.

Balin, Yu.S., Ershov, A.D., Penner, I.E., Makukhin, V.L., Marinaite, I.I., Potemkin, V.L., Zhamsueva, G.S., Zayakhanov, A.S., Butukhanov, V.P. 2007. Experimental and model studies of spatial distribution of the atmospheric aerosol over Lake Baikal. Atmospheric and Oceanic Optics. 20(2): 114-121.

Belan, B.D., Ivlev, G.A., Kozlov, A.S., Marinaite, I.I., Penenko, V.V., Pokrovskii, E.V., Simonenkov, D.V., Fofonov, A.V., Khodzher, T.V. 2007. Comparison of air composition over industrial cities of Siberia. Atmospheric and Oceanic Optics. 20 (5): 428- 437.

Chan, Ch.K., Xiaohong, Yao. 2008. Air pollution in mega cities in China. Atmospheric Environment. 42(2): 1–42.

Charlson, R.J., Schwartz, S.E., Hales, J.M., Cess, R.D., Coakley Jr., J.A., Hansen, J.E., Hofmann, D.J. 1992. Climate forcing by anthropogenic aerosols. Science. 255: 423–430.

Gorshkov, A.G., Marinaite, I.I., Zhamsueva, G.S., Zayakhanov, A.S. 2004. Benzopyrene isomer ratio in organic reaction of aerosols over water surface of Lake Baikal. J. Aerosol Sci. 35(2): 1059-1060.

IPCC. 2007. Climate Change 2007. The Physical Science Basis.

Kondratyev, I.I., Kachur, A.N., Yurchenko, S.G., Mezentseva, L.I., Roschupkin, G.T., Semykina, G.I. 2005. Synoptic and Geochemical aspects of abnormal dust transfer in south Primorski krai. Bulletin of the Far Eastern Branch of the Russian Academy of Sciences. 3: 55–65.

Kondratyev, K.Ya. 2002. Aerosol as climate-forming component of the atmosphere. 1. Physical properties and chemical composition. Atmospheric and Oceanic Optics. 15(2): 123-146.

Kondratyev, K.Ya. 2005. From nano- to global scales: properties, processes of formation and aftereffects of the atmospheric aerosol impacts. 6. Long-range transport and sedimentation processes. Atmospheric and Oceanic Optics. 18(4): 285-302.

EMEP. 1996. Manual for sampling and chemical analysis. EMEP Cooperative Programme for Monitoring and Evaluation of the Long-range Transmission of Air Pollutant in Europe. NILU: EMEP/CCC-Report 1/95. Reference: 0-7726.

NOAA/ARL. 1997-present, HYSPLIT 4 model (http://www.arl.noaa.gov/ready/hyslit4.html), NOAA Air Resources Laboratory, Silver Spring, MD.

Plaude, N.O., Vychuzhanina, M.V., Monakhova, N.A., Grishina, N.P. 2006. Some results of 11-year Measurements of Atmospheric Aerosol Characteristic near Moscow. Russian Meteorology and Hydrology. 1: 19-26.

Ravindra, K., Bencs, L., Wauters, E., Hoog, J. 2006. Seasonal and site-specific variation in vapour and aerosol phase PAHs over Flanders (Belgium) and their relation with anthropogenic activities. Atmospheric Environment. 40 (4): 771-785.

Saikawa, E., Naik, V., Horowitz, L.W., Liu, J., Mauzerall, D.L. 2009. Present and potential future contributions of sulphate, black and organic carbon aerosols from China to global air quality, premature mortality and radiative forcing. Atmospheric Environment. 43(17): 2814–2822.

Stone, E.A., Yoon, S.-C., Schauer, J.J. 2011. Chemical Characterization of Fine and Coarse Particles in Gosan, Korea during Springtime Dust Events. Aerosol and Air Quality Research. 11(1): 31–43.

Sun, Y., Zhuang, G., Wang. Y., Han, L., Guo, J., Dan M., Zhang, W., Wang, Z., Hao, Zh. 2004. The air-borne particulate pollution in Beijing – concentration, composition, distribution and sources. Atmospheric Environment. 38(35): 5991–6004.

Wang, X., Xia, D., Wang, T., Xue, X., Li, J. 2008. Dust sources in arid and semiarid China and southern Mongolia: Impacts of geomorphological setting and surface materials. Geomorphology. 97(3-4): 583–600.

WHO. 2006. Health risk of particulate matter from long-range transboundary air pollution. Joint WHO/UNECE Convention Task Force on the Health Aspects of Air Pollution. World Health Organisation, European Centre for Environment and Health, Bonn Office, Bonn.

WHO. 2007. Health relevance of particulate matter from various sources. WHO Workshop Report, Bonn Office, Bonn.

Xuan, J., Sokolik, I.N., Hao, J., Guo, F., Mao, H., Yang, G. 2004. Identification and characterization of sources of atmospheric mineral dust in East Asia. Atmospheric Environment. 38(36): 6239–6252.

Yabuki, S., Mikami, M., Nakamura, Yu., Kanayama, Sh., Fu, F., Liu, M., Zhou H. 2005. The Characteristics of Atmospheric Aerosol at Aksu, an Asian Dust-Source Region of North-West China: A Summary of Observations over the Three Years from March 2001 to April 2004. Journal of the Meteorological Society of Japan. 83A: 45-72.

Zhang, B., Tsunekawa, A., Tsubo, M. 2008. Contributions of sandy lands and stony deserts to long-distance dust emission in China and Mongolia during 2000–2006. Global and Planetary Change. 60(3-4): 487–504.

Zhang, W., Wang, W., Chen, J., Liu, H., Dai, T., Yang, X.-Ya., Zhang, F., Lin, J., Wang, Z. 2010. Pollution situation and possible markers of different sources in the Ordos Region, Inner Mongolia, China. Science of the Total Environment. 408(3): 624–635.

Zayakhanov, A.S., Zhamsueva, G.S., Tsydypov, V.V., Ayurzhanaev, A.A. 2008. Automated system for monitoring atmospheric pollution. Measurements Technique. 12: 1342-1346.

Zhamsueva, G.S., Zayakhanov, A.S., Tsydypov, V.V., Ayurjanaev, A.A., Golobokova, L.P., Khodzher, T.V., Azzaya, D., Oyunchimeg, D. 2009. Temporal variability of small gaseous impurities, chemical and dispersive composition of aerosol in arid territories of Mongolia. Aerosols of Siberia. 16: 70-71.

Zhamsueva, G.S., Zayakhanov, A.S., Tsydypov, V.V., Ayurjanaev, A.A., Dementeva, A.L., Azzaya, D., Oyunchimeg, D. 2011. Particularities of Formation and Transport of Arid aerosol in Central Asia. Chapter 4. In: Nejadkoorki, F. (Eds.), Advanced Air Pollution. Intech, Croatia, pp. 51-66.

Trace Gases Behavior in East Gobi Atmosphere of Mongolia

D. Azzaya[1,*], D. Oyunchimeg[1], E. Enkhbat[1], G.S. Zhamsueva[2], A.S. Zayakhanov[2], V.V. Tsydypov[2], T.S. Balzhanov[2] and A.V. Starikov[2]

[1]Institute of Meteorology and Hydrology of Mongolia, Juulchiny gudamj-5, Ulaanbaatar-210646, Mongolia.

**corresponding author: azzaya23@yahoo.com.*

[2]Institute of Physical Materials of Science, Siberian Branch of Russian Academy of Sciences, 6, Sakhyanovoy st., Ulan-Ude, 670047, Russia.

E-mail: Lrf@ipms.bscnet.ru.

Abstract

Studies of trace gases and their correlation with meteorological parameters of the atmosphere of Mongolian Gobi present a great interest. Mongolian Gobi is a remote region without trace gases monitoring stations.

The results of studies of temporal variability of surface ozone, nitrogen oxides and meteorological parameters in the atmosphere of the Gobi Desert (Sainshand station) during summer 2009 are presented.

Continuous synchronous measurements of surface ozone (O_3) and nitrogen dioxide (NO_2) concentrations were obtained using an automated measurement system. Meteorological and turbulent characteristics of the atmosphere were measured using automated ultrasonic meteorological complex. The average concentrations of ozone and nitrogen dioxide during observation period were 85 μg m^{-3} and 44 μg m^{-3}, respectively. Variations of hourly average concentrations of O_3 changed from 37 to 160 μg m^{-3}, NO_2 changed from 10 to 70 μg m^{-3}. It is established that the surface ozone and nitrogen dioxide is determined mainly by circulation processes. Under influencing of cold front of air mass the increasing of ozone concentration up to 160 μg m^{-3} and nitrogen dioxide concentration up to 70 μg m^{-3} were observed. Significant increasing of the ozone and nitrogen dioxide concentrations were noted when wind was from southerly and south-easterly directions due to the possible transport of air from polluted regions of China. The specific regime of behavior of surface ozone in the atmosphere of the arid territories with its day and night increasing is revealed.

Key words: Small gaseous impurities; Atmosphere; Turbulence characteristics; Desert Gobi.

1. Introduction

Processes of formation of spatial-temporary variability of small gaseous impurities in surface atmosphere are defined by complex interaction of natural and anthropogenous sources of impurities. Natural climatic factors of region define a specific regime of atmospheric circulation processes. Small gaseous impurities of atmosphere considerably influence on condition of surrounding environment both in regional and in global scales. Thus it is necessary to organize regular air pollution measurements, especially, in surface level (Rovinskiy and Yegorov, 1986).

Ozone plays an important role in chemistry and photochemistry processes in troposphere. The content of ozone is defined by its vertical transport from the high layers of atmosphere and formation of O_3 in the lower troposphere as a result of photochemical reactions with participation of nitrogen oxides and volatile organic compounds. Many studies focus on the formation of surface ozone due to man-made and natural factors (in densely populated areas) while air pollution and the dependence on meteorological parameters in arid territories of Central Asia and the Gobi Desert have not been investigated yet (Zvyagintsev *et al*., 1997; Zakharov *et al*., 2004; Demin *et al.*, 2004; Demin and Beloglaz, 2004).

Thus investigations of the arid territory of Mongolia (Eastern Desert Gobi) have a special interest due to absence of network monitoring station of ozone and small gaseous impurities.

In paper round-the-clock continuous synchronous measurements of concentrations of surface ozone (O_3), oxides of nitrogen (NO_x) meteorological, turbulent and radiating characteristics of atmosphere are presented.

2. Materials and Methods

2.1. Geographic and climatic characteristic of the studied areas

Desert Gobi is the territory, including the South-East part of Mongolia. It represents the high plain laying, elevation 1000 m above mean sea level. East Gobi is located not far from the coast of the Pacific Ocean as well as the East China Sea and the Sea of Japan, but some ridges of the Gobi reduce their influence to a minimum. For a year atmospheric precipitations fall less than 200 mm in the East steppe and foothill plains (Babaev *et al*., 1986).

Except of the geographical location, the circulation of air masses, the terrain and the radiant energy of the sun are influenced on the formation of climate in region. Ridges of the Altai, Khangai, Khentii and Hovsgol have a particular impact on the change in the properties of air masses and their circulation. General circulation of air masses is changed due to the influence of these ridges and often formed local circulation.

2.2. Methodologies

Since 2005 every summer measurements of the surface ozone concentration and nitrogen oxides are conducted by Institute of Physical Materials Science of Siberian Branch of the Russian Academy of Sciences and Institute of Meteorology and Hydrology of Mongolia during joint scientific expedition in the Gobi Desert.

Sample site is located in the building of the Dornogovi Hydrometeorology Service Mongolia - station Sainshand on the considerable distance from the city.

The measurements of small gaseous impurities were conducted at station Baruun-Urt during summer 2005-2006. Station Sainshand (44º 54' N, 110º 07' E) is located in arid zone of the Gobi, station Baruun-Urt (46º 56' N, 113º 07' E) is located in the Southeast of Mongolia in the semi-arid steppe zone with a poor vegetation cover. The scheme of the location of sampling stations is presented in Figure 1.

Round-the-clock continuous synchronous measurements of O_3, NO_x, meteorological, turbulence and radiation characteristics of atmosphere have been received by means of the automated operative system of registration and statistical processing of measurements. Sampling of air was carried out at 2 m above ground level. The automated operative system of registration and statistical processing of measurements includes chemiluminescent gas analyzer P-310 (NO_2, NO), chemiluminescent gas analyzer 3.02. P1 (O_3), the block of registration and processing of measurements. All gas analyzers are products of the instrument-making company "OPTEC" (Sankt-Peterburg, Russia). The relative error of chemical measurements does not exceed ±20 % (Zayakhanov *et al*., 2008). Calibration of gas analyzers is carried out automatically by means of the built-in calibrated sources of microstreams. Besides periodically calibration of gas analyzers by the external calibrator Mod. ML 8500 («Monitor Labs», USA) was made for the control of measurements accuracy of concentration O_3, NO_x. Automated ultrasonic meteorological station AMK-03 was used for measurements of instantaneous data of temperature, humidity, speed and direction of wind, turbulence characteristics of atmosphere (Azbukin *et al*., 2006).

Figure 1. A scheme of the location of sampling stations.

3. Results and discussions

Figure 2 presents diurnal variation of hourly average concentrations of ozone, nitrogen dioxide for station Sainshand (August, 2009).

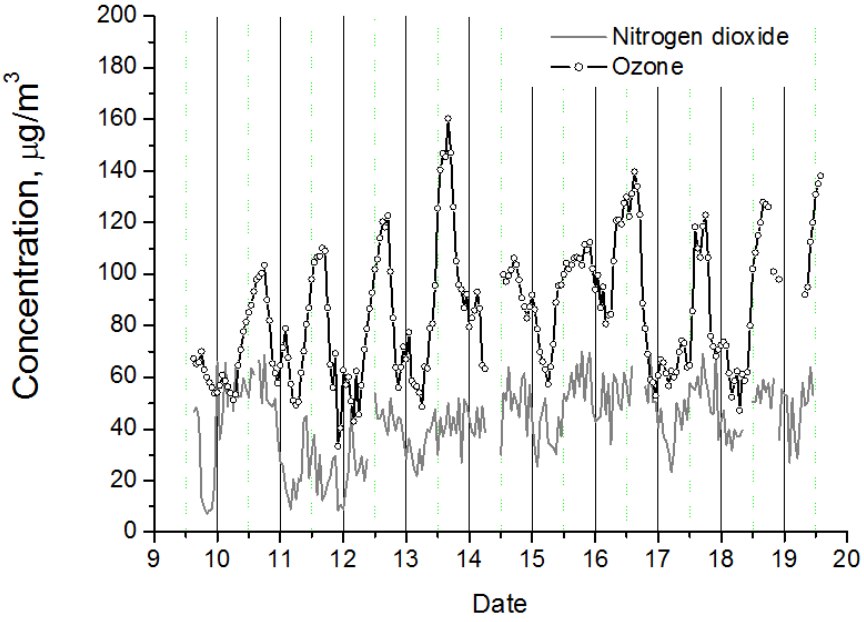

Figure 2. Average diurnal variation of concentrations of surface ozone and nitrogen dioxide for station Sainshand (August, 2009).

For all period of supervision the average concentrations of ozone and nitrogen dioxide were 85 μg m^{-3} and 44 μg m^{-3}, respectively. It is noted that in separate days in the conditions of high temperatures maximum the hourly ozone concentrations reach high values of 160 μg m^{-3} and nitrogen dioxide of 70 μg m^{-3}, the minimum average values for ozone were 37 μg m^{-3}, for nitrogen dioxide - 10 μg m^{-3}.

High concentrations of the dust aerosol and small gaseous impurities were observed when the dust storm passed (13 August 2009). Increasing of the ozone concentration reached values to 160 μg m^{-3} due to develop convection in zones of the cold front and transportation of air from overlying layers of the atmosphere with higher content of ozone. In these periods high concentrations of nitrogen dioxide (60-70 μg m^{-3}) also were observed. One of the reasons of high ozone concentration in atmosphere of the East Gobi is apparently feature of the common circulation of atmosphere between northern 30 and 45-degree latitudinal zones characterized as "desert belt". At these latitudes the circulating processes which determined the transport of air mass are characterized by interaction of warm air mass from equatorial zone (Hadley cell) and air mass from the temperate latitudes (Farrell cell). According to common circulation of the atmosphere the raised air mass above equator and raised air mass above industrial regions of Eastern Siberia dry up, cool in free troposphere then slowly descend to heated ground in the of 30-40 degree latitudes, transferring with itself tropospheric ozone from higher layers of the atmosphere.

Figure 3 shows the hourly variations of the main meteorological parameters during the measurement period. The weather was unstable, daily temperature did not exceed 30-35^{o}C. Such meteorological conditions due to increasing of turbulent exchange promote more intensive mixing of the air mass and inflow of the ozone from the high layers of the atmosphere. It is shown that during passing of the cold front (13 August 2009) the sharp decrease of the air temperature, increase in humidity and pressure decrease are observed.

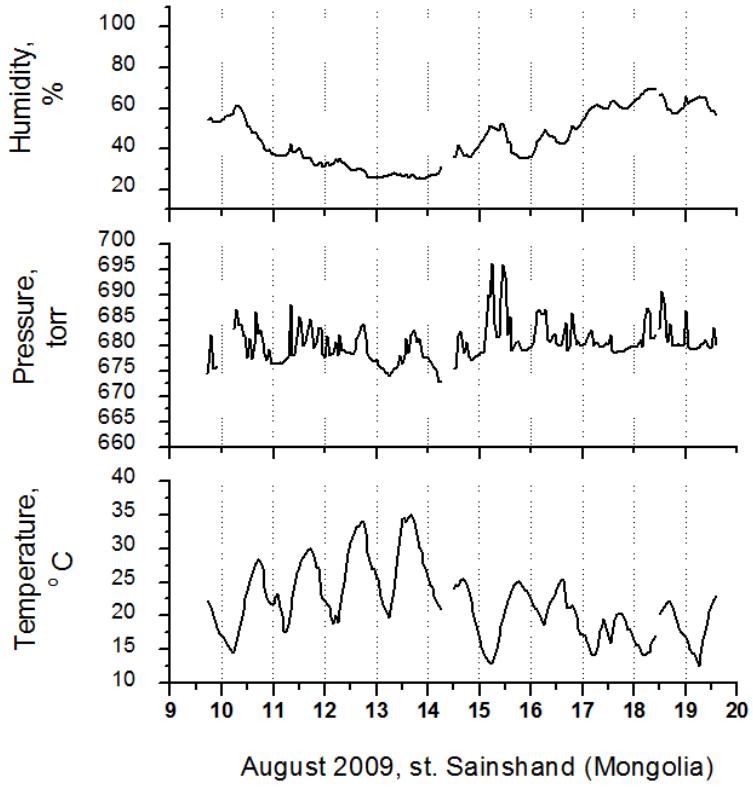

Figure 3. Temporal variation of meteorological parameters of atmosphere for station Sainshand (August, 2009).

On the following Figure 4a),b) the variations of the instant values of air temperature, horizontal and vertical components of the wind speed during dust storms on 13 and 16 August are given.

Previous researches of daily dynamics of variations of the concentration surface ozone and nitrogen dioxide have been shown, that a character of their concentration changing is coincided and is determined by mainly air circulation processes (Zhamsueva *et al*., 2008). It testifies to the common mechanism of their transfer into area of supervision and is connected, apparently, with their transport from more distant areas. In summer 2006 diurnal variation of hourly average concentration of the surface ozone has minimum equal 55 μg m^{-3} in morning (06 hour) during sunrise, and then in the afternoon the increasing of ozone up to 133 μg m^{-3} was observed. Maximum of O_3 for all period of supervision was 150-160 μg m^{-3}. At absence of anthropogenous sources of air pollution the diurnal variation of concentration of the surface ozone is caused by daily dynamics of the mixed layer and the layer of night temperature inversion near the terrestrial surface. As known at intensive vertical mixing of air, ozone which comes from free troposphere can increase a level of the surface ozone up to 100-150 μg/m^3 (Zvyagintsev *et. al*., 2002). Besides at presence photochemical active reagents in conditions of the high solar activity there is an additional photochemical formation of the surface ozone, which depends on meteorological factors and air pollution concentrations. At rather high observed concentration of the nitrogen dioxide in the atmosphere of the Desert Gobi it was necessary to expect strengthening of processes of the photo dissociation of NO_2 in the daytime with formation of atomic oxygen, then and surface ozone.

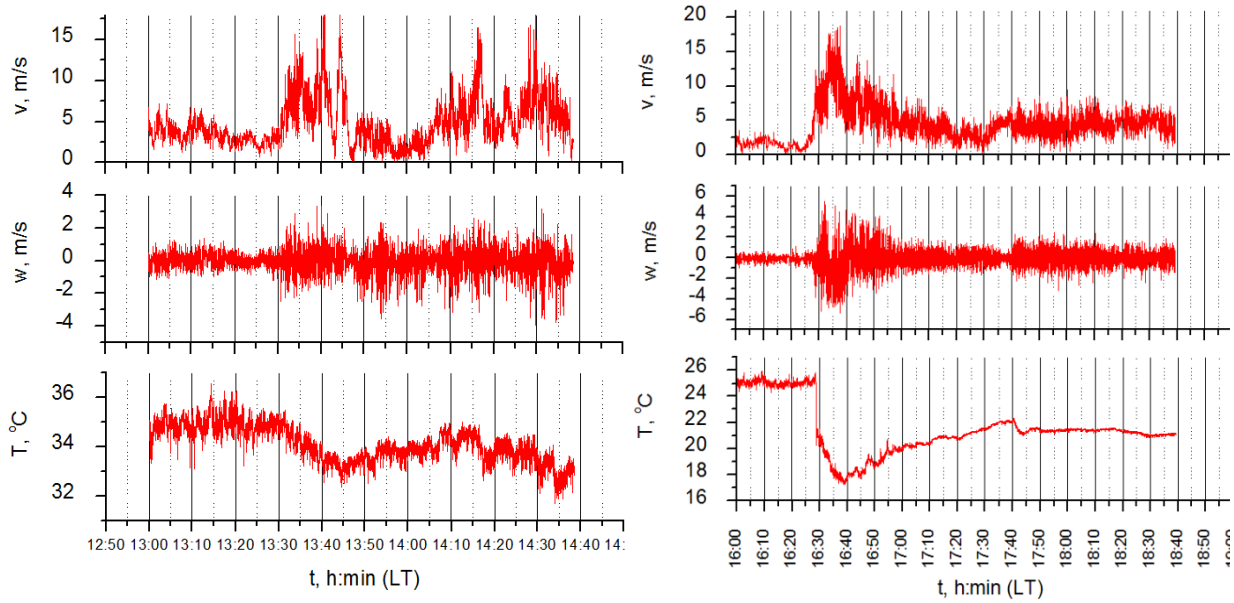

Figure 4. Temporal variation of temperature (T), horizontal (w) and vertical (v) components of wind speed: a) 13 August 2009; b) 16 August 2009.

However in our experiments a participation of the nitrogen oxides in reactions photolysis and oxidations with education or destruction of the ozone didn't manage to be found. At measurements the nitrogen oxide as an intermediate product of the reactions photolysis was not shown or his levels were lower than a threshold of registration of the gas analyzer P-310 which taking into account an error of the definition doesn't exceed 4 μg m^{-3}. It is thus possible that accumulation of the nitrogen oxides in the atmosphere doesn't happen at rather high speed of education and oxidation of the nitrogen oxide.

At night intensity of the temperature inversions considerably increases and blocks inflow of the ozone from free troposphere to surface layer. These conditions lead to decrease of the night ozone concentration and increase of chemical destruction of the ozone. High level of the surface ozone concentrations in the Gobi is testified that speed of the ozone destruction due to ozone's drainage on a terrestrial surface not so is high, as in the continental areas of the tropical and moderate latitudes with active vegetation. High levels of the night ozone concentration (55 μg m^{-3}) testify about it. The similar behavior of the weak ozone destruction in droughty areas, in particular in the Sahara Desert is also noted in work (Vassi, 1968).

According to the available publications, unfortunately, practically there are no data on concentration of others photochemical active impurities in the atmosphere of the arid territories, which necessary for comparison and the analysis of behavior of the surface ozone and other small gaseous impurities-predecessors of the ozone. Perhaps there is another source of the ozone. Ozone is generated on the surface sand by hypothetical mechanism, associated with static electricity under intense solar radiation and low wind. In the presence of the Southern and Southeast direction of a wind the significant increase of the surface ozone and nitrogen dioxide concentrations was noted. It is found based on the analysis of meteorological and synoptic processes and experimental studies

of the trace gases in the atmosphere of the Desert Gobi. Growth of concentration of impurities is also noted at the Southwest direction of a wind, but dependence less weak.

Analysis of found data of the radiosonde measurements for 3 years at the station Sainshand testifies the formation of the powerful jets in the region. If to consider 30 m/s out of the lower limit speed jet streams then the frequency of the jet streams by radiosonde data in May was 62% in June to 47% in July and 42% of the observation time. During this period, in the area 30-45ºN latitude the strong subtropical jet streams are often observed, which can lead to rupture of the tropopause and the transfer of stratospheric ozone in the troposphere.

Satellite remote sensing data for the summer months also confirm high concentrations of the tropospheric ozone at high latitudes. Herewith the high concentrations are noted in a zone of a subtropical jet current (http://acdb-ext.gsfcnasa.gov/Data_services/cloud_slice/data_archive) that is a consequence first of all of intense stratosphere-troposphere exchange in these latitudes due to the subtropical currents.

In addition, one of the reasons of the high level of gaseous concentrations in atmosphere of arid territories is low wet and dry deposition. In the summer heat ground does not allow to descending of small gaseous impurities to surface, that lead to accumulation of impurities in atmosphere.

Specific meteorological conditions play a significant role in increasing ozone in daytime. Weather conditions affect the turbulent mixing (convective and adjective processes), especially, in different climate zones. High solar radiation and as a result of high absorptive ability of a terrestrial surface in the absence of vegetation lead to rise of the turbulent processes in the afternoon. Figure 5 confirms this situation, where daily vertical heat flux variation between ground surface and atmosphere for different climate regions: arid (Sainshand), semi-arid (Baruun-Urt) and sharp continental (Boyarskiy) is shown. Station Boyarskiy (51° 83' N, 106° 06' E) is located at the Southeast coast of Lake Baikal in Russia.

Measurements of the vertical heat flux were conducted using automated ultrasonic meteorological station AMK-03 at height of 4 m. As shown in the Figure 5 maximal development of thermal turbulence (convection of surface atmosphere) is observed in daytime. At this time considerable vertical flux of heat which is directed up from earth’s ground has taken place due to intensive mixing of surface air with over-lying layer of the atmosphere.

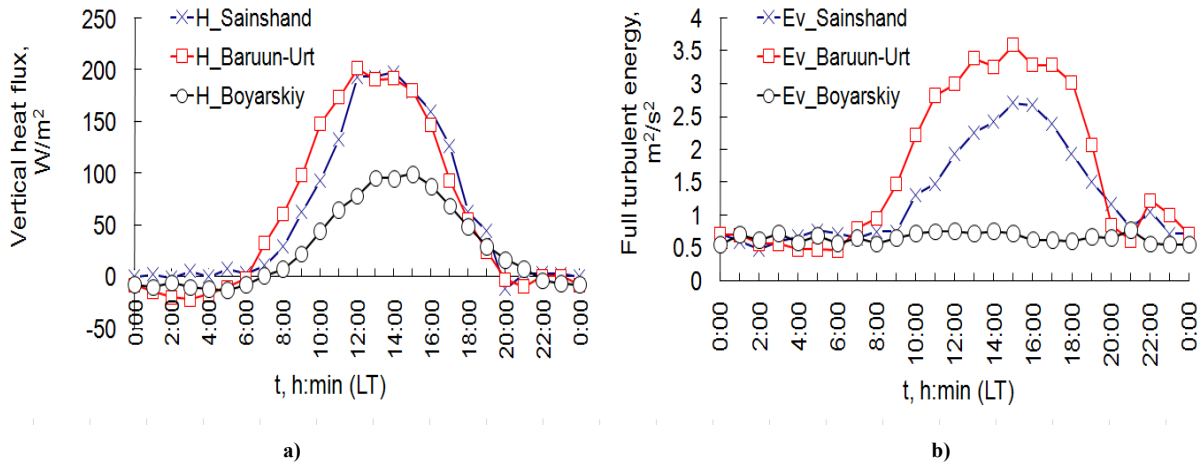

a) b)

Figure 5. Average daily variation of vertical heat flux (a) and full turbulent of energy (b) for different climate: Sainshand (arid area, 1 July 2006-8 July 2006), Baruun-Urt (semi-arid area, 10 July 2006-15 July 2006), Boyarskiy (sharp continental, 24 July 2006-30 July 2006).

In daytime intensity of the turbulent exchange in the atmosphere of the arid and semi-arid areas is 5-7 times higher than in humid climate of the Lake Baikal and reaches a maximum value of 3.5 m^2 s^{-2} at st. Sainshand and 2.5 m^2 s^{-2} at st. Baruun-Urt.

First of all the developing of turbulence in the conditions of the dry arid climate is caused by the air convection promoting to growth of kinetic energy of the pulsations. Vertical heat flux (Figure 5b)), which characterizes the convective flows, in the Gobi Desert is higher in 2-3 times than on Lake Baikal in the daytime. During high solar activity and high temperatures in the presence of photochemical active reagents the favorable conditions for the photochemical generation of the ozone are formed. As noted in Zhamsueva *et al*., 2008, the contributions of photochemical and tropospheric sources of the ozone in the 30-60ºN latitude are approximately equal, that in aggregate can provide the increasing the level of the ozone to 160 μg m^{-3} and above.

4. Conclusions

In this study, the data of the small gaseous impurities in atmosphere have been collected at station Sainshand during summer 2009. These data of the ozone were compared with data obtained previously in the summer.

High ozone and nitrogen dioxide concentrations were observed at the station Sainshand during all time of supervision. The average concentrations of ozone and nitrogen dioxide during observation period were 85 μg m^{-3} and 44 μg m^{-3}, respectively. Variations of hourly average concentrations of the O_3 changed from 37 to 160 μg m^{-3}, NO_2 changed from 10 to 70 μg m^{-3}. It is established that the surface ozone and nitrogen dioxide is determined mainly by circulation processes. Under influencing of cold front of the air mass, the increasing of the ozone concentration up to 160 μg m^{-3} and nitrogen dioxide concentration up to 70 μg m^{-3} were observed.

Further studies are needed to increase our knowledge about local atmospheric circulation and long-range transport of air mass for understanding of reason of high level of the surface ozone and nitrogen dioxide and their transformation in process of transport to region. In future we will plan to conduct experiments in different sites of the Gobi desert.

5. Acknowledgments

The authors are grateful to the Center of Hydrometeorology and Environment Monitoring of Dornogobi and Sukhbaatar images for allowing possibility to be carried out our investigations. Thanks also go to N. Enkhmaa and K. Enkhbayar for help with the fieldwork. The work is performed at support of Presidium Program of the Russian Academy of Science (Project № 4.12), Siberian Branch of Russian Academy of Science (Integrate Projects № 14).

6. References

Azbukin, A.A., Bogushevich, A.Ya., Ilyichevskiy, V.S., Korolkov, V.A., Tikhomirov, A.A., Shelevoy, V.D. 2006. Automated ultrasonic meteorological complex AMK-03. Meteorology and Hydrology. 11: 89-98.

Babaev, A.G., Drozdov, N.N., Zonn, I.S., Freykin, Z.G. 1986. Deserts. Misl. Moscow. 1-318.

Demin, V.I., Beloglazov, M.I. 2004. About influence of local circulation processes on ground ozone dynamics. Atmosphere and ocean optics. 4: 331-333.

Demin, V.I., Yelanskiy, N.F., Beloglazov, M.I. 2004. About relation of ozone ground concentration and interfusion layer altitude. Atmosphere and ocean optics. 8: 662-665.

Rovinskiy, F.Ya., Yegorov, V.I. 1986. Ozone, nitrogen oxides and sulphur in low troposphere. Hydrometeoizdat. Leningrad. 1-184.

Zakharov, I.S., Kuznetsov, G.I., Tarasova, O.A. 2004. The season variation of different processes contribution in the ground ozone variability over Europe. Report of International conference of students, aspirants and young scientists “Lomonosov-2004”. 109-111.

Zayakhanov, A.S., Zhamsueva, G.S., Tsydypov, V.V., Ayurzhanaev, A.A. 2008. Automated system for monitoring atmospheric pollution. Measurements Technique. 12: 1342-1346.

Zvyagintsev, A.M., Kruchenitskiy, G.M. 1997. About spatial-temporal relations of ozone ground concentration in Europe. Izvestiya of Russian Science Academy. Atmospheric and ocean physics. 33-1: 104-113.

Zhamsueva, G.S., Zayakhanov, A.S, Tsydypov, V.V, Ayurjanaev, A.A Azzaya, D., Oyunchimeg, D. 2008. Assessment of small gaseous impurities in atmosphere of arid and semi-arid territories of Mongolia. Atmospheric Environment. 42-(3): 582-587.

Zvyagitsev, A.M., Kuznetsova, I.N. 2002. Variability of surface ozone in surroundings of Moscow: The results of ten years regular observations. Izvestiya of Russian Science Academy. Atmospheric physics and ocean. 38(4): 486-495.

Vassi A. 1968. Atmospheric ozone. M.: Mir. 83 p.

Recent Hydrochemical Regime of the Pereemnaya River

L.M. Sorokovikova[1], V.N. Sinyukovich[1], I.V. Tomberg[1], N.V. Bashenkhaeva[1], N.P. Sezko[1],
I.N. Lopatina[1], T.V. Khodzher[1] and Tsuyoshi Ohizumi[2]

[1]Limnological Institute, Russian Academy of Science/Siberian Blanch, Irkutsk, Russia.
E-mail: lara@lin.irk.ru
[2]Asia Center for Air Pollution Research, Niigata, Japan.
E-mail: ohizumi@acap.asia.

Abstract

The EANET Program has been performed the long-term investigations and obtained new data on chemical composition and hydrochemical regime of the Pereemnaya river. The Pereemnaya river waters has been characterized by extremely low mineralization formed under the conditions of high moisture, low air temperatures, distribution of hard soluble rocks within the catchment basin and flushing regime. Analysis of the data shows that low-mineralized river waters respond to the changes of geochemical conditions in the catchment basin. The increase of sulphate and nitrate in atmospheric precipitation has caused changes of ionic ratio in the Pereemnaya river water in the recent period compared with the 1950s. Changes observed in the composition of salt-forming ions (HCO_3^-, SO_4^{2-}, Ca^{2+}, and Mg^{2+}) demonstrate that the resistance of river waters to acidification decreased over the last decades because of the input of acidified components into the river catchment basin. The results obtained have confirmed that the Pereemnaya river is an appropriate model site for the analysis of surface water conditions and testify to the necessity of further monitoring of its chemical composition within the EANET Program.

1. Introduction

Chemical composition of a river, which is formed under conditions of cold climate and over moistening, is characterized by intense inflow of dissolved substances from the alluvial soils, silica in particular, and alkaline and alkaline-earth compounds (Kondrashova *et al.*, 1977, Kuzmin, 1998, Targulyan, 1971). The most moistened area is located on the Northeastern slope of the Khamar-Daban ridge opposite the Angara river within the mountain framing of the Lake Baikal basin. Humid air flows of the prevailing NW transfer penetrate into this area via the Primorsky ridge along the Angara river valley (Astrakhantsev *et al*., 1962, Afanasyev, 1976), generating favorable conditions for the river runoff formation (Pereemnaya, Vydrinnaya and Vtoraya Shestipalikha), which are the tributaries of Lake Baikal on the Southeastern shore.

The Pereemnaya river starts near the Mount Sokhor (2,316 m a.s.l.). The river length is 42 km with the catchment area of approximately 360 km^2. The average altitude of the basin is 1,260 m a.s.l., the river slope is 34.9%. Archean rocks of the Sharyzhalgai and Slyudyanka complexes on the basin territory are composed predominantly of gneiss, crystalline schist and pegmatite (Zonov, 1966, Efremov, 1970). The major part of the basin is represented by mountainous-taiga soil zone. The lower boundary of the taiga forest begins from the lake shore, whilst its upper boundary, depending on the slope exposition, is up to 900-1,800 m (Vaskovsky, 1973). The goltsy altitudinal belt is dominated by alpine heath landscapes with herb and lichen.

The outlet of the Pereemnaya river crosses the entire system of small mountain lakes, the largest of which is Lake Kholodnoye, approximately 0.3 km wide. The lakes are located at 1,500-1,800 m a.s.l. surrounded by steep rugged slopes with rock ridges and placers on their tops. Arctic-tundra raw soils with acid reaction are formed on the slope surface under the layer of crust and laminar lichens (Martynov, 1965, Martusova, 1988).

The climate is sharp continental on this territory, and only on the lake coast the climate is marine. The winter in the mountains is severe and long. According to the data of the Khamar-Daban weather station, the average annual air temperature is 3.4°C, average annual precipitation on the coast is approximately 800 mm, whilst in the mountains 1,500 mm and more (Afanasyev, 1976, Vaskovsky, 1973).

Hydrological investigations have been performed on the Pereemnaya river only for 4 years. Average annual river runoff for the years of observation corrected from the neighboring water streams is 1,040-1,300 mm. Average evaporation value is 237 mm $year^{-1}$ (Vaskovsky, 1973). The river is fed by snow and rain waters; the highest water level is recorded in June. In the cold period (November-April), the runoff amounts to 10-15% of the annual flow (Sinyukovich and Troitskaya, 2000).

Based on the long-term observations performed on the Pereemnaya river within the EANET Program, it is described the specific characteristics of chemical water composition of the river and its runoff under conditions of high moisture and elevated anthropogenic load.

2. Materials and methods

The hydrochemical studies were started in the Pereemnaya river in 1995. Together with British scientists, it is investigated several lakes on the Khamar-Daban ridge in the zone of bald mountains, including Lake Kholodnoye (Figure 1).

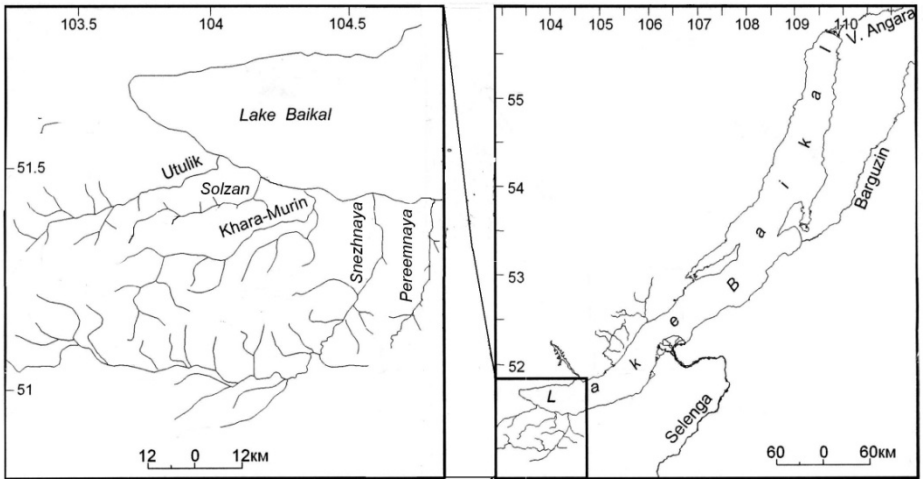

Figure 1. Geographical location of study area.

Since 1996 Limnological Institute of Siberian Branch of the Russian Academy of Sciences have been performing comprehensive investigations of chemical composition of snow and river waters in the main hydrological phases (winter low-water period, spring flood and summer-autumn low-water period). The data obtained before active economic development of this territory served as reference characteristics of chemical water composition of the studied rivers and atmospheric precipitation (Votintsev, 1954, Votintsev *et al*. 1965). To estimate pollutant input from atmosphere, snow samples were collected in the river valley before snow melting (late February-early May) over the entire height of snow cover.

In the laboratory samples with river and snow waters were filtered through a 0.45 μm membrane filter. Cations were detected by the atomic absorption method (relative error 3-5%) (Semenov, 1977, Boeva, 2009), anions were determined by high performance liquid chromatography (HPLC) (relative error 5-10%) (Baram *et al*., 1999). Phosphorus was measured with a colorimetric method using ammonium molybdate and ammonium nitrogen with Nessler's reagent (relative errors 2% and 4-5%, respectively) (Stroganov, and Buzinova, 1980, Wetzel, and Likens, 1991). The validity of the data obtained was verified by calculating the anion and cation balance (relative error 3%) as well as by regular quality control of the analyses conducted within the EANET Program on testing standard samples of "surface waters".

3. Results and discussion

Natural conditions in the Pereemnaya river basin, such as significant heights, distribution of massive crystal rocks, great amount of the atmospheric precipitation, rank and clean washed soils and low intensity of chemical weathering, predetermine the formation of the low-mineralized waters, which is characteristic of the hydrochemical regime in mountain rivers and lakes in the areas with similar natural climatic conditions (Kondrashova, *et al*., 1977, Targulyan, 1971, Turk and Norman, 1990). The first hydrochemical investigations in the Pereemnaya river were conducted in 1949-1952 (Votintsev *et al*., 1965).

3.1 Lake Kholodnoye

Lake Kholodnoye is located on the Khamar-Daban ridge in the zone of bare mountains (goltsy). It is fed by snow waters and a glacier. The research was conducted in July during intense snow melting. The water temperature was 2ºC, pH was in the range of 6.0-6.2, and concentration of dissolved oxygen in the surface water layer was 9.2-9.5 mg l^{-1} (73% enrichment). The water mineralization in Lake Kholodnoye was low (5.8 mg l^{-1}) and similar to the mineralization of snow water on the lake coast (Table 1). However, it differed in pH values (higher) and chemical composition. The lake water belonged to the hydrocarbonate class of the calcium group, whilst the snow water was of the sulphate class of the calcium group (Table 1). Unlike the lake water, snow water contained considerable amount of NH_4^+ (up to 16%) and H^+ (up to 14%). As is seen from the table, the chemical composition of atmospheric precipitation was transformed during the formation of lake water: replacement of major ions and insignificant increase of water mineralization due to weathering of underlying rocks.

Table 1. Chemical water composition in the Pereemnaya River basin, July of 1995.

Analyzed water	pH	P_{tot}, µg l^{-1}	P_{min}, µg l^{-1}	NO_3-N, mg l^{-1}	NH_4^+-N, mg l^{-1}	Si, mg l^{-1}	Σions, mg l^{-1}
Snow water	5.2	-	-	0.32	0.16	0.06	4.60
Lake Kholodnoye	6.0	7	1	0.02	0	0.31	5.84
Pereemnaya river mouth	6.5	12-30	0-3	0.20-0.31	0-20	2.18	19.2

*tot: total, min: minimum, Σions: total ions = SO_4^{2-}+NO_3^-+Cl^-+Na^++K^++Ca^{2+}+Mg^{2+}+NH_4^++HCO_3^-.

3.2 Pereemnaya river

The Pereemnaya river, as stated above, starts from the mountain lakes. Chemical composition of the lake water is affected mostly by the composition of atmospheric precipitation (Table 1). The lake water on its way to the river mouth is enriched with mineral salts that enter the river bed from the basin territory. As a result of water transformation of different genesis (surface, ground and drain), the concentration of major ions and nutrients increases in the river waters from the outlet to the mouth. In the summer of 1995, total ions (∑ions) increased up to 13 mg l^{-1} from the outlet to the river mouth (Table 1). The investigations carried out in the Pereemnaya river mouth for the past decade showed that the water was of low mineralization during the entire year: ∑ions varied from 13.6 to 34.9 mg l^{-1} with the maximum concentrations of major ions during ice period. The inflow of snow water into the river basin in April caused the decrease of mineralization to 15-16 mg l^{-1}. In May, after snow melting, water mineralization rose insignificantly (up to 19 mg l^{-1}) due to the input of mineral substances from the upper soil layer and tree waste. In June, when snow melted in the mountains, the water mineralization decreased to its minimum (11 mg l^{-1}). The ion concentration gradually increased in the months to follow. Long-term data on the chemical composition of the river water showed that, beginning from 2008, there was a trend in increasing major ion concentrations, in particular sulphates. For example, in 2004, ∑ions and sulphate concentration varied within 18.6-25.3 mg l^{-1} and 5.7-9.6 mg l^{-1}, respectively. In 2010, maximal values of ∑ions and sulphate were 34.9 mg l^{-1} and 15.4 mg l^{-1}, and in 2011, 32.9 and 14.2 mg l^{-1}, respectively (Figure

2). The rise of ion concentration is likely attributed to the low-water period, possible intense input of mineral substances from soils and increase of anthropogenic load.

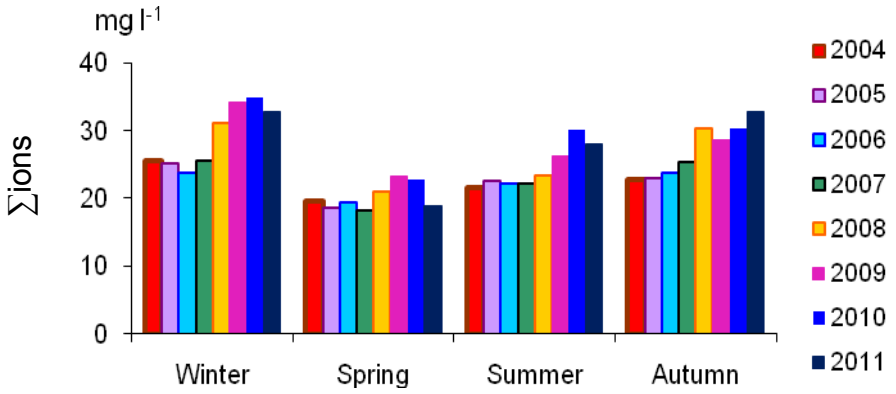

Figure 2. Seasonal fluctuations of ∑ions (mg l^{-1}) in the Pereemnaya river water in 2004-2011.

As was noted earlier (Sorokovikova *et al*., 2004), the increase of pollutant input via atmosphere onto the catchment basins of the rivers in Southern Baikal caused the rise in the concentration of chemical components in river waters. Accumulation rate of sulphate in snow cover in the mountain areas on the Northwestern slope of the Khamar-Daban ridge where the Pereemnaya river starts was 1.3 t km^{-2}, whereas on the Southern slope its amount was an order lower (Kokorin and Politov, 1991, Obolkin *et al*., 1991). Compared with the results of 1950-1980 (Tarasosa and Meshcheryakova, 1992, Votintsev *et al*., 1965), current ∑ions, nitrate nitrogen, sulphate in the Pereemnaya river water are 10-15%, 60% and 100% higher than the reference values. The Σ ion increase in the Pereemnaya water was recorded during the low-water period and floods. This is attributed to intensification of weathering processes in the catchment area which are likely associated with the rise of anthropogenic load on river waters observed for the past decades. The increase of absolute concentrations of acidifiers (sulphate and nitrogen) caused changes in the relative composition of major ions: increase in sulphate content and decrease in hydrocarbonate and calcium (Sorokovikova *et al*., 2004). Sulphate content in the relative composition increased from 36 to 61%, whereas hydrocarbonate concentration decreased from 68 to 58%.

According to (Votintsev *et al*., 1965), maximum concentrations of the nitrate nitrogen (0.36 mgN l^{-1}) in the Pereemnaya water were registered in winter. Dynamics of nutrient concentrations observed during recent years showed that their maximum was recorded in the river during snow melting in the mountains in May-June (Figure 3). In the summer-autumn period, NO_3^- concentrations decreased to their minimum.

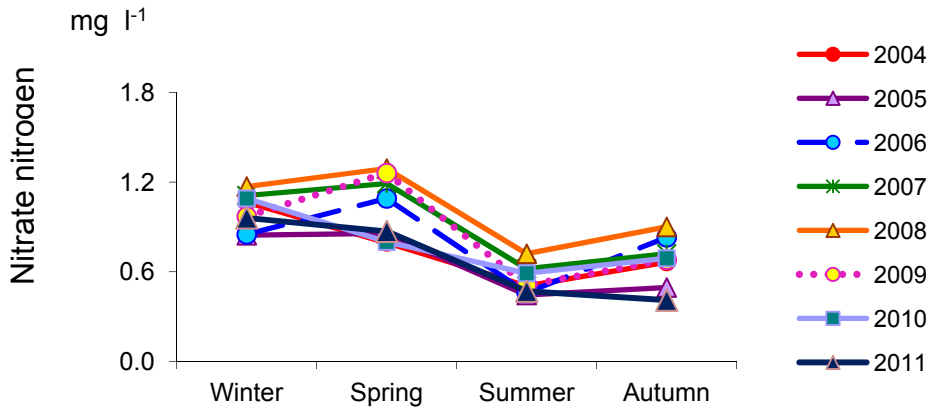

Figure 3. Seasonal variations of nitrate nitrogen (mg l^{-1}) in the Pereemnaya river water in 2004-2011.

Elevated concentrations of the ammonium nitrogen inflowing from melting snow and upper soil thawing layers were also registered in the river water during spring floods. Increased content of NH_4^+ was also recorded during summer floods. No ammonium nitrogen was registered in the river water from October till the beginning of the spring flood. Nitrite nitrogen was recorded sporadically. In recent years, the concentration of total mineral nitrogen in the river water ranges from 0.16 to 0.51 mgN l^{-1}.

Concentrations of the total and mineral phosphorus in the water were low: 2-14 and 1-4 µg P l^{-1}, respectively. The lowest content of the total phosphorus was registered in winter, whilst elevated concentrations were observed during high-water level and summer floods. Minimum and elevated concentrations of the mineral phosphorus were recorded during snow melting and in winter, respectively.

Annual dynamics of the Si concentrations as well as of the major ions was governed by seasonal changes in the river runoff, which was noted by Votintsev *et al*. (1965). The Si content increased up to 3.8 mg l^{-1}. The input of snow water with insignificant Si content (0.06 mg l^{-1}) (Votintsev and Khodzher, 1998) caused the decrease of its concentrations in the river water during high-water period.

Thus, the inflow of waters from the basin territory into the river bed, which were enriched with nutrients, caused the increase of the latter in the river water. From the river outlet to its mouth the NO_3^- content in the water increased from 0.02 (Lake Kholodnoye) to 0.25-0.51 mgN l^{-1} in the river depending on the water level. Whereas, Si, NH_4^+, and PO_4^{3-} concentration ranged from 0.31 to 1.80-3.68 mgSi l^{-1}, from 0 to 0.02 mgN l^{-1}, and from 1 to 5 µgP l^{-1}, respectively.

Organic carbon (C_{org}), bichromate and permanganate oxidation (BO and PO) were determined in the river water. BO, PO, and organic carbon concentration varied during a year from 2.4 to 4.8 mgO l^{-1}, from 0.4 to 1.9 mgO l^{-1}, and from 0.5 to 3.1 mgC l^{-1}, respectively, (Figure 4).

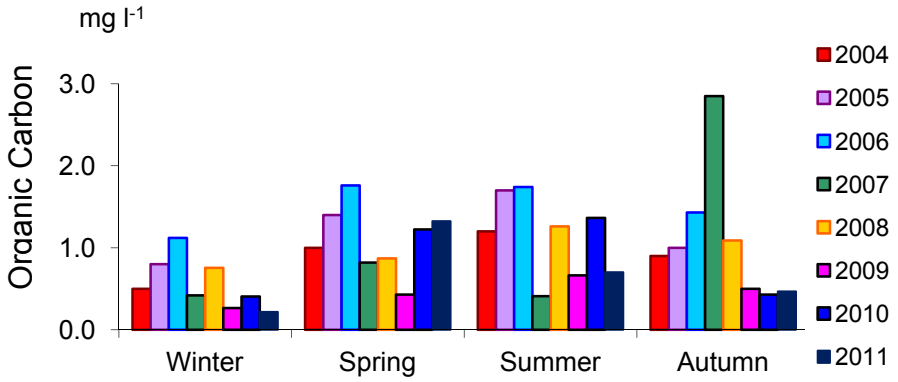

Figure 4. Dynamics of organic carbon in the Pereemnaya River water.

Ratios PO/BO and PO/C_{org} varied mainly within 11-23 and 0.6-1.0, respectively, with the dominance of fulvic acids. Elevated organic carbon concentrations were observed in the water during spring and summer floods. Ratios PO/BO and PO/C_{org} increased during these periods up to 40 and 1.5, respectively, with the rise of the humic acid.

The pH in the Pereemnaya river water, which drains acidic silicate rocks, was low (5.7-7.2). Minimal pH values were observed during floods. Low pH values were also attributed to high input of $SO_4^{2-}$and NO_3^- into the catchment territory and dominance of fulvic acids. The Pereemnaya River waters were nonresistant to acidification due to small amount of the ions and low buffer ability to neutralize acid components.

The comparison of the Acid Neutralization Capacity (ANC) data for 1955-1960 with our results showed that from 1960 to 2010 the resistance of river waters to acidification decreased as a result of input of acidified components into the river catchment from atmosphere. The ANC values in the Pereemnaya river during this period decreased from 219 μeq l^{-1} to 99 μeq l^{-1} dropping to the critical level ≤50 μeq l^{-1} during snow melting [6], the so-called "pH stress".

The runoff of the Pereemnaya river is low and its effect on chemical composition of the Lake Baikal coastal waters can be registered only in the zone of the river mouth. Nevertheless, it is necessary to take into account the amount of chemical components, in particular sulphate and nitrate nitrogen, inflowing into the lake. Analysis showed that during average water level the input of dissolved substances with the river waters into the lake is 7,580 t $year^{-1}$, including 1,200 t $year^{-1}$ of sulphate, 99 t $year^{-1}$ of nitrate nitrogen, and 860 t $year^{-1}$ of silicon. The great bulk (up to 80-90%) of analyzed chemical substances is carried by the river during the period of open water. The majority of them inflow from the soil layer, which is characteristic of the rivers that drain mountain-tundra and mountain-taiga territories composed of massive and crystal rocks (Dzhamalov *et al.*, 1996, Targulyan, 1971) .

The main characteristic of input of the ∑ions and some components is their modulus, it is in general features to characterize processes of the chemical denudation within the river basins. The neighboring rivers running from the Khamar-Daban ridge (Snezhnaya and Khara-Murin) are characterized by high modulus of the ionic input – 180-217 kg ha^{-1} (Votintsev *et al.*, 1965). According to the recent results, the modulus of ionic input is 211 kg ha^{-1} of which has already come in dissolved form with precipitation (30.5 kg ha^{-1} (Votintsev, 1954)). Therefore, the real decline of matter from the basin due to dissolution and removal of the underlying rock is

180.5 kg ha^{-1}. When the specific gravity of natural soil 2.5-3.5 kg dm^{-3} (we took 3 kg dm^{-3}), this corresponds of the volume 60.2 dm^3, or layer height 0.00602 mm. Thus, the chemical denudation in the basin of the Pereemnaya river is estimated to be 0.0060 mm $year^{-1}$. The rates of chemical denudation for the Snezhnaya river basin and the Khara-Murin River are 0.0062 mm $year^{-1}$and 0.0052 mm $year^{-1}$, whereas the modulus of the Pereemnaya river runoff is significantly higher (34l s^{-1} km^{-2}) than that in the other rivers (14.60 and 18.9l s^{-1} km^{-2}, respectively).

4. Conclusion

Long-term investigations performed within the EANET Program was obtained a new data on chemical composition and hydrochemical regime of the Pereemnaya river.

Waters of the extremely low mineralization are formed under conditions of the high moisture, low air temperatures, distribution of the hard soluble rocks within the catchment basin and flushing regime. This specific feature is clearly observed in the Pereemnaya river. Total ions in the river water amount to 34 mg l^{-1} because of its shallow river bed. Analysis of the data shows that low-mineralized river waters respond, first of all, to the changes of geochemical conditions in the catchment basin. The increase of sulphate and nitrate in atmospheric precipitation that feed the river caused changes of the ionic ratio in the Pereemnaya river water in the recent period compared with the 1950-s. Changes observed in the composition of salt-forming ions (HCO_3^-, SO_4^{2-}, Ca^{2+}, and Mg^{2+}) demonstrate that the resistance of the river waters to acidification decreased over the last decades because of the input of the acidified components into the river catchment basin. In the recent years, the ANC values in the Pereemnaya river water decreased to 99 μeq l^{-1}, and these values were even lower ≤50 μeq l^{-1} during snow melting.

The results obtained have confirmed that the Pereemnaya river is an appropriate model site for the analysis of surface water conditions and testify to the necessity of further monitoring of its chemical composition within the EANET Program.

5. References

Afanasyev, A.N. 1976. Water resources and water balance of the Lake Baikal basin. Novosibirsk. Nauka. 238 p.

Astrakhantsev, V.I., Ivanov, I.N. and Rybak, O.L. 1962. Hydrological conditions on the South-Baikal territory of mineral deposits, Materials on Hydrogeology of Mineral Deposits in East Siberia, Irkutsk. 9: 79-94.

Baram, G. I., Vereshchagin, A.L. and Golobokova, L.P. 1999. Application of microcolumn HPLC with UV detection to analysis of anions in environmental objects. Journal of Analytical Chemistry. 54: 962–965.

Boeva, L.V. 2009. A Manual for Chemical Analysis of Land Surface Waters. Hydrometeoizdat, Rostov-on-Don. 1032 p.

Dzhamalov, R.G., Zlobina, V.L., Mironenko, V.M. and Ryzhenko, B.N. 1996. Acidification impact of atmospheric precipitation on chemical balance. Field data. Thermodynamic modeling, Water Resources. 5: 556-564.

Efremov, A.I. 1970. Hydrogeology of the USSR. Nedra. 22: 1-432.

Kokorin, A.O. and Politov, S.V. 1991. Input of pollutants from atmosphere with precipitation in Southern Pribaikalye. Meteorology and Hydrology. 1: 48-54.

Kondrashova, I.A., Rabinovich, A.L., Mikhailichenko, L.A. and Gorbacheva, E.G. 1977. Conditions of chemical water composition formation in high-mountain rivers from the upper basin of the Teberda River. Hydrochemical Materials. 66: 68-72.

Kuzmin, V.A. 1998. Chemical water composition of tributaries in South-East and Southern Baikal and its dependence on natural conditions. Geography and Natural Resources. 5: 70-77.

Martusova E.G. 1988. Vegetation of the river basins Pereemnaya-Abiduy. Vegetation of the Khamar-Daban Ridge. Novosibirsk: Nauka. pp. 56-68.

Martynov, V.P. 1965. Soils of mountain Pribaikalye. Ulan-Ude. 165 p.

Obolkin, V.A., Khodzher, T.V., Anokhin, Yu, A. and Prokhorova, T.A. 1991. Acidity of atmospheric precipitation in the Baikal region. Meteorology and Hydrology. 1: 55-60.

Semenov, A. D. 1977. A Manual for Chemical Analysis of Land Surface Waters. Hydrometeoizdat, Leningrad. 534 p.

Sinyukovich, V.N. and Troitskaya, E.S. 2000. Average river runoff of the Baikal basin and its determination based on insufficient observation data. Geography and Natural Resources. pp 60-64.

Sorokovikova, L.M., Netsvetaeva, O.G. and Tomberg, I.V. 2004. Impact of precipitations onto chemical composition of riverine waters of Southern Baikal. Optika atmosfery i okeana. 5(6): 423-427.

Stroganov, N. S. and Buzinova, N.S. 1980. A Manual for Practical Hydrochemistry. Moscow State University Publishers, Moscow. 193 p.

Tarasosa, Ye. N. and Meshcheryakova, A.I. 1992. Actual state of Lake Baikal hydrochemical regime. Novosibirsk, Nauka. 140 p.

Targulyan, V.O. 1971. Soil formation and weathering in cold damp areas. Nauka. 270 p..

Turk, John M. and Norman, E. Spahr. 1990. Rocky Mountains, Acidic Deposition and Aquatic Ecosystems. New York: Springer-Verlag. pp. 471-499.

Vaskovsky, M.G. 1973. Resources of the USSR surface waters. Hydrometeoizdat. 16(3): 1-400.

Votintsev, K.K. 1954. Chemical composition of waterd of Pre-Baikal precipitations. DAN. 5: 979-981.

Votintsev, K.K. and Khodzher, T.V. 1998. Chemical water composition of tributaries in South-East and Southern Baikal and its dependence on natural conditions. Geography and Natural Resources. 5: 100-105.

Votintsev, K.K., Glazunov, I.V. and Tolmacheva, A.P. 1965. Hydrochemistry of rivers in the Lake Baikal basin. Nauka. 495 p.

Wetzel, R. G. and Likens, G.E. 1991. Limnological Analyses. Springer-Verlag, New York. 391 p.

Zonov, B.V. 1966. Hydrology of South-East Siberia. Nauka. 171 p.

First-Order Evaluation of Transboundary Pollution Fluxes in Areas of EANET Stations in Eastern Siberia and the Russian Far East

Gromov S.A.[1], Gromov S.S.[2], Zamyatina M.Yu.[3]and Trifonova-Yakovleva A.M.[1]

[1]Institute of Global Climate and Ecology (IGCE) Roshydromet and RAS, Glebovskaya 20-B, Moscow, 107258 Russia.

E-mail: gromov.igce@gmail.com, yakovleva.eanet@gmail.com

[2]Max Planck Institute for Chemistry, Hahn-Meitner-Weg 1, 55128 Mainz, Germany.

E-mail: sergey.gromov@mpic.de

[3]Lomonosov Moscow State University (MSU), Faculty of Geography, Leninskiye Gory 1, 119991 Moscow, Russia.

E-mail: maria.zamyatina.int@gmail.com

Abstract

Estimates of the climatological air mass exchange in the lower troposphere (within 3 km average sea level, a.s.l.) across two regions of the Russian border in Eastern Siberia and the Russian Far East are obtained using the long-term air sound data on mean layer winds. Using a simplified transport box-model, annual and seasonal exchange of air was calculated for the boundary segments of selected geographical regions. With the use of data from the stations of the Acid Deposition Monitoring Network in East Asia (EANET), a first-order evaluation of the transboundary pollution fluxes of sulphur- and nitrogen-compounds is made for the period of 2006-2008. Estimates of the net transport to/from Russia suggest that the export of predominantly clean air occurs over the East Siberian border, whereas the Far East territories act as a sink for Chinese transboundary pollution.

Key Words: transboundary pollution, air mass transport climatology, air exchange balance, EANET

1. Introduction

Airborne compounds containing sulphur and nitrogen play an important role in Earth atmospheric chemistry. Being capable of absorbing solar radiation at different wavelengths, they are recognized to have a certain potential to influence the climate evolution on Earth (Rovinsky and Yegorov, 1986). Current interest in studying these compounds arises due to their increased global input into the atmosphere. An equally important aspect, videlicet (*viz*.) the negative effect of these substances on human health, biota and human infrastructure, further motivates a more practical investigation of their spatial and temporal distributions.

Since sulphur dioxide and nitrogen oxides are mostly co-emitted in course of the use of fossil fuel, the increasing consumption of the latter in recent decades (assuming invariable non-anthropogenic sources) promoted a steady growth of the atmospheric load of these compounds, hence concomitant environment deterioration. In as much as gases and aerosols are transported with the air flow, the observed changes in concentrations of pollutants over an area occur due to existence of short- and long-range transport of air masses susceptible to direct emission. A transboundary drift of pollutants, in turn, may have a significant impact on the ecological situation of the neighboring territories. Few earlier studies examining the environmental monitoring data (Izrael *et al*., 1987) found out the interrelation of the changes in pollutant concentrations over the territory and the direction and velocity of the air flow. The objective of this study is to evaluate a potential transboundary air transport and related pollutant fluxes by using a relatively facile technique of estimating with the first-order application of available meteorological and monitoring data.

We apply our method to the detailed geographically concerned evaluation of the transboundary air pollution exchange in the region of Eastern Siberia and the Russian Far East. The anticipated concomitant growth of industrial emissions causes further importance of the task of conducting this study. Below, we therefore focus on the brief description of the method and input data used, followed by the application to calculating the air mass and air pollutant exchange in the lower troposphere over two part of Asian border of Russia.

2. General Description of Method and Data Used

The applied approach represents an indirect assessment of the pollutant transport reckoned proportional to the horizontal transport of air enclosed in the lower troposphere, and to the concentration of a given pollutant this air mass contains. The horizontal transport component is evaluated as the air transition efficiency ($m^3\ s^{-1}$) in a given direction or eventually over the individual transects of the border of interest. We thereby assume that the amount of air transferred in particular direction is proportional to the corresponding mean layer wind velocities and their climatological recurrence observed at the nearest air sounding station. The domains of interest are the

following segments of the Russian border: Irkutsk (IR) corresponding to the EANET air quality monitoring site Mondy, Dalnerechensk (DR) and Vladiviostok (VL), corresponding to the EANET site Primorskaya ().

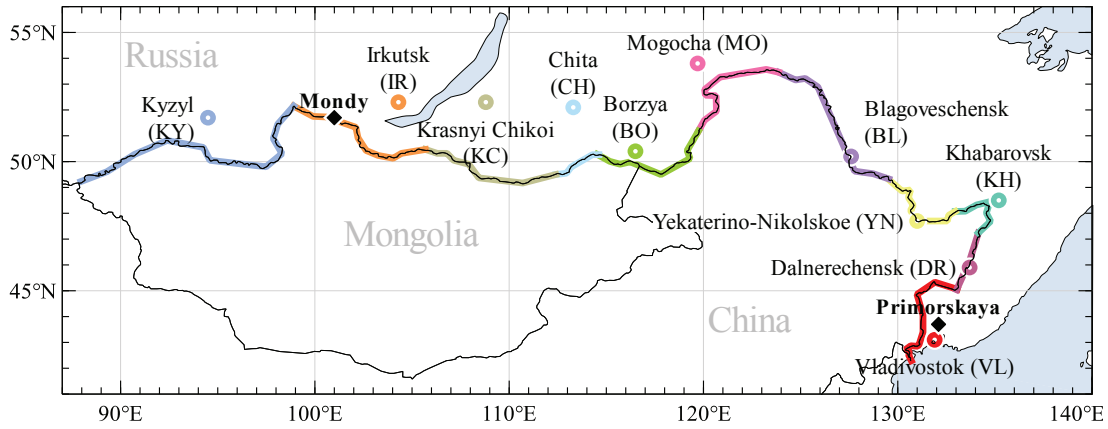

Figure 1. Locations of the selected aerological (air sounding balloon) stations and EANET monitoring stations (diamonds) along the Asian border of Russia. Colors distinguish the segments pertaining to particular stations.

As wind data input we use the results of Research Institute of Hydrometeorological Information – World Data Centre (RIHMI-WDC) climatological data processing (Brukhan, 1984) conducted for the atmospheric soundings at aerological stations located along the continental border of East Asian territory of Russia. Data covers the 10-year period 1961−1970 selected through the highest number of operating stations and observation acquisition rate. The data provides long-term averages and statistics on the wind meteorological regime (*e.g.*, mean vector/scalar velocities, direction, standard vector deviation, and steadiness) in a set of given altitude ranges; owing to the long-term regular measurements, the series used are expected to be representative up to date. The results of the numerical integration procedure (Brukhan, 1983) were used to transfer aerological statistics into the eight-rhumb[2] wind speed and recurrence distributions (climatic wind roses) at station for every month. Wind roses essentially provide the rhumb-integrated values of the wind speed and recurrence that would result from the normally (2D-circular) distributed probability densities of the velocities and directions matching the averages and vector deviation of the observed winds. The climatic wind roses derived for two air sounding stations, Irkutsk and Vladivostok, obtained among others is given in .

[*] **Note:** *Hereinafter the term "rhumb" is equivalent to "wind direction". The eight-rhumb distributions thus represent the N, NE, E, SE, S, SW, W and NW directions, respectively* (see, *e.g.*, Crutcher, 1956).

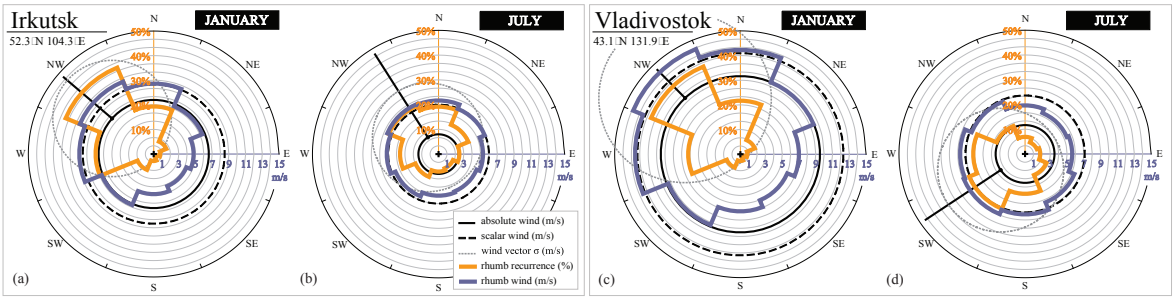

Figure 2. Eight-rhumb climatic wind roses at Irkutsk (Baikal area) and Vladivostok (Primorye) derived from the aerological climatic wind data within a 3 km layer (see text). Left (a, c) and right (b, d) panels refer to January and July, respectively. Thick contours represent the average wind speed (blue) and recurrence (orange) in respective rhumbs. The solid black circles refer to the average wind magnitude (radial lines indicate wind direction); the remaining circles denote the average wind standard vector deviation (dotted) and scalar wind magnitude (dashed). Note that the rhumb data are the result of numerical processing, as opposed to the input actual statistical data. The reader is referred to the literature (*e.g.*, Crutcher, 1956) for supplementary information on the properties of the wind rose plots.

The distributions shown in highlight similar speed and opposite turn variations in winds typically observed in the south of Eastern Siberia (Baikal area) and Primorye (Primorsky Krai), respectively. The wind regimes are commonly influenced by alternation of seasonal atmospheric action centers determining the climate characteristics of the respective regions (Khromov and Petrosyants, 2006). For instance, winter winds are largely caused by the Siberian anticyclone, favoring stable and strong north-west winds with recurrence rates of nearly 40%. In contrast to that, summer conditions driven by the Asian summer depression are characterized by markedly lower wind stability and recurrence. In the case of coastal Vladivostok (and generally, at the most of Far East areas), seasonal wind shear is further enhanced by Asian Monsoon circulation, whereas winds inside continent merely show diminished variation.

Evidently, seasonal alterations in wind regime in combination with the complexities and irregularities of the borderline directions render the task of transboundary flux calculations somewhat intricate. To avoid ambiguous formulations, we declare the transport of air removal from Russian territory as *positive*, and, conversely, the influx of air masses from the neighboring territories into Russia as *negative*. It enables to estimate the integral transport terms over each border element (BE) in both directions, as well as their sum yielding the net transport term for selected periods. The calculation procedure (for terseness omitted here) computes the cross-boundary-relevant (*i.e.*, orthogonal to the line of the direction) wind components for every rhumb and appoints them an appropriate sign. The relevant wind components are subsequently multiplied by horizontal length and specific air layer height associated with a selected to yield the air volumetric transfer velocity ($m^3\ s^{-1}$). The specific layer heights are assigned equal to the residue between the height of the upper transport layer

boundary in lower troposphere (see below) and the average surface elevation (a.s.l.) of the respective s. Finally, the three *air transport* terms (AT, in units of volume per period), *viz.* positive, negative and net, are derived by integrating with respective transfer velocities over the given period, in this case of one month.

Setting transport upper boundary with 3 km a.s.l. is caused by retaining the highest possible representativeness of our results with regard to the input wind data used, as well as with respect to the assumptions on pollutant abundances made from published observations. For instance, lowermost climatic wind values granted by used data source (Brukhan, 1984) typically refer to layer averages reckoned for the range between the surfaces and matching 3 km (a.s.l.); it is unfeasible to make any inferences on the average wind properties below this altitude. On the other hand, evaluations of the vertical distributions in the atmosphere of the compound of interest (e.g., SO_x or NO_x) suggest this layer to contain the highly dominant part of their atmospheric content and, as more important, to have seasonal variations pertained to the domain below the top of this layer (Rovinsky and Yegorov, 1986).

Unfortunately, the monitoring data we possess is limited to the near-surface concentrations of sulphur and nitrogen compounds. Also there are no any supplement results for these regions to be capable to provide near-real information on air pollutant vertical profiles. Although more sophisticated approaches might be available (we consider applying them in subsequent studies) for this study we adopt the zero-order approximation, taking the surface concentrations at the nearest monitoring station as representative for the entire segment length and up to the top of layer. The ultimate result, the three *pollutant transport* terms (PT, in units of mass) are thus derived by combining correspondent terms and the average concentrations observed in respective months.

Noteworthy, the applied method is likely to overestimate the absolute terms, because concentrations are typically found to decline with height, being chiefly influenced by the surface processes (*e.g.*, emission and deposition). The *net* s, however, are the result from the subtraction of the respective absolute terms, which cuts a large part of the absolute error out and mainly emphasizes the seasonal variations in concentrations. We notice that the uncertainty of derived net grows proportionally to term magnitude, as opposed to the absolute / terms.

3. Results

The calculation results are aggregated in . Panel (a) shows the detailed estimates of over the several parts of the continental Asian Russian border extended in front of operating EANET atmospheric deposition monitoring sites. Geographical layout (in particular, mountains) of IR segment (see abbreviations introduced in) renders monthly AT values be sensitive at least to the changes in the local wind regime. There are marked variations in net for DR and VL segments. These are mainly driven by the changes in wind shear and stability, judging by variations in total of ±31% for these prominent segment cases. Deeper insight into these results denotes total to be proportional to the scalar wind speed, *i.e.* the absolute air transition intensity in the vicinity of air sounding station. The steadiness of the wind (*i.e.*, the ratio of its mean vector and scalar velocities), in turn, demonstrates

how largely the wind is scattered around its direction. If steadiness is low, there are comparable contributions of more equally distributed wind directions to the absolute terms thus substantially attenuating the net transport. Higher sensitivities are pinpointed by larger difference in the ratio between the positive and negative terms from unity, respectively.

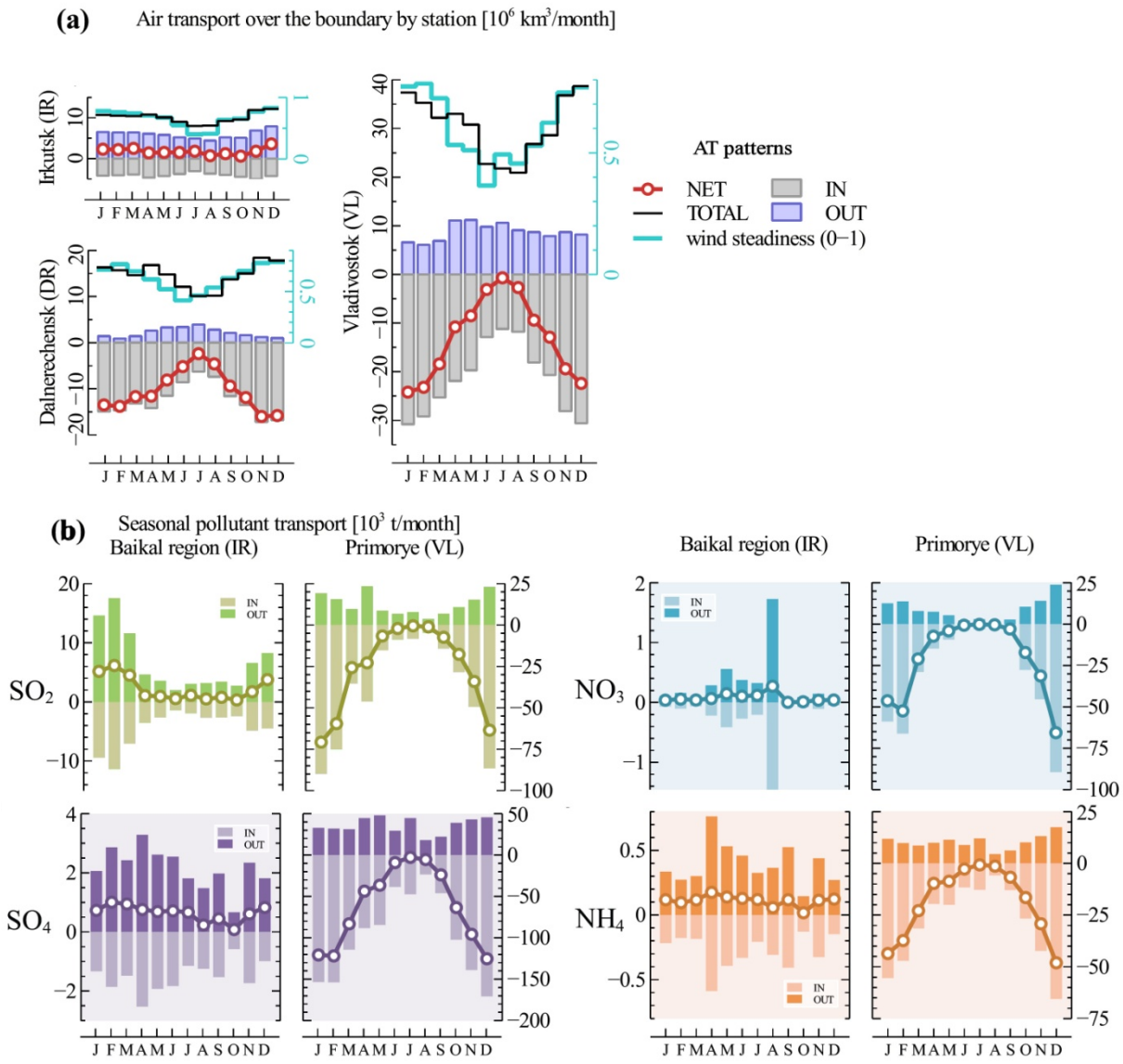

Figure 3. Calculation results of air mass (a) and pollution (b) transport across the border of Asian Russia at Baikal (IR) and Primorye (VL) areas (see text). Note the varying axis scales in panel (b).

The application of the calculation results to estimating pollutant transfer (in the form of PT) were done for two study regions where air concentration monitoring data are obtained. The latter are available from the regular long-term observations at the sites of the Acid Deposition Monitoring Network in East Asia (EANET)

operating within Baikal area (at remote station Mondy corresponding to the IR segment) and in Primorye (regional station Primorskaya, segment VL) in the Asian territory of Russia (EANET, 2009). For the current evaluation we used the observational data on sulphur (SO_2, SO_4) and nitrogen (NO_3, NH_4) compounds for 2006−2008, guided by the similarity in the seasonal profiles and annual averages of the observed concentrations in this period (Khodzher *et al*., 2011). The monthly "climatological" averages were compiled from the multi-year Filter pack sampling measurements (Figure 4). As expected, they show the stark difference in seasonal variation registered in the regional (*i.e.* more susceptible to pollutant transport from distant industrial sources) and remote conditions. Notably, the net patterns for VL segment conform the evident seasonal air pollution variations at Primorskaya, suggesting these are being driven by the regional pollution transport. Indeed, a linear regression of corresponding average concentrations with respect to (*w.r.t.)* the terms yields high correlation coefficients of 0.79−0.91 (at R^2=0.62−0.82) for inward and net transport, as opposed to the much lower values for outward flows (correlations of 0.41−0.67, R^2=0.17−0.45). The variations of pollutants at Mondy are generally not linked to (average R^2 ~ 0.12 for all terms), with an exception of SO_2 that moderately correlates with the positive. That implies the likely presence of a regional SO_2 source to the north-northeast of site, *i.e.* contrariwise to the main outflow direction at the IR segment (a plausible emission area would be the industrial region of Irkutsk oblast).

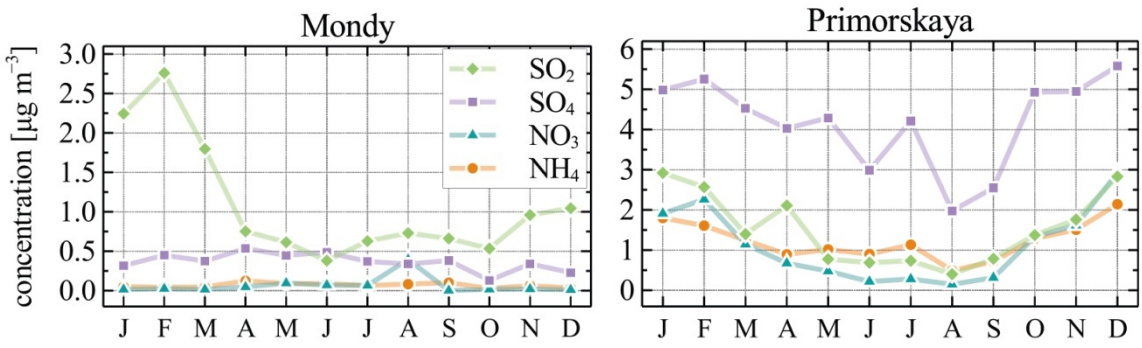

Figure 4. Intra-annual multi-year average variation of pollutant concentrations observed in 2006−2008 at two EANET monitoring stations used as input data. Note the varying axis scales.

Panel (b) in presents the seasonal evolution of the calculated terms for the segments for these two regions. The intra-annual dynamics at Primorye shows clear concomitance of them with the net over VL where pollutant transfer rates reach tens of thousand tons per month across about 540 km of this border segment. Whilst winter season provides 50−66% of the annual mass, diminished net and declining concentrations furnish its summer share at negligible 1−2%. Unlike that case the variations in net at Baikal region are much less in range being mainly propelled by the changes in pollutant abundances. Overall at IR segment the net is positive (*i.e.*, outward Russia) but comprises extremely lower total values for the comparable segment length of ~580 km (see Table 1). The dynamics of relative contribution of monthly net is similar to VL results for SO_2 only with winter and summer totals account for 57% and 8% of the annual transport, respectively.

The evaluation results suggest that about 400 thousand tons of S (around 10^6 tons of oxidized sulphur compounds) are being transported annually across the VL segment of state border into the Russian territory, with maximum fluxes occurring in cold season. The amount of transferred N ($233 \cdot 10^3$ tons) in this area is less than that of S, with the predominance of reduced nitrogen in the form of aerosol ammonium (Table 1). The fluxes of S and N compounds across the IR border segment are evidently smaller than that estimated for Primorye (by at least two orders of magnitude).

Table 1. Estimated seasonal and annual net pollutant transboundary transport across western (Baikal area) and eastern (Primorye) segments (IR/VL) for 2006−2008 (10^3 tons)†

Species	DJF	MAM	JJA	SON	Annual
SO_2	15.1 / −193.8	6.5 / −55.1	2.2 / −3.7	2.8 / −59.2	26.6 / −311.8
SO_4	2.6 / −367.8	2.4 / −163.2	1.6 / −17.3	1.1 / −183.2	7.7 / −731.5
NO_3	0.1 / −164.3	0.3 / −32.4	0.5 / −1.3	0.1 / −51.4	0.9 / −249.4
NH_4	0.3 / −129.0	0.4 / −41.2	0.3 / −4.8	0.3 / −52.5	1.3 / −227.5

† Positive and negative values denote fluxes outward and inward Russia, respectively.

4. Conclusions

With a simple yet robust approach we evaluate that the net lower tropospheric air transport over the Russian territories conterminous with East Asian countries has a clear seasonal behavior favoring strongest air mass exchange disequilibrium in winter. The peculiar geographical layout turns individual border line segments into net entry or exit ports for the air masses, depending on seasonal changes in wind patterns. We estimate that annually Russia exports a relatively small amount of air over the western part of the East Siberian border (e.g. neighbouring Mongolia), but imports an amount more than 1.5 times exceeding that across the border segments in Far East. Furthermore, as the observations suggest, imported air is substantially more polluted, hence the Russian East territories are likely to act as a sink for transboundary air pollution. The net cross-boundary flux of airborne sulphur in Primorye region is estimated to be of several hundred thousand tons annually, with the major contribution pertaining to the winter-spring season. An extrapolation for the entire border extension along the Russian Far East suggests doubling to quadrupling of these values.

5. References

Brukhan, F.F. 1983. Climatological Processing and Analysis of Aerological Data (ed. Kornjushina O.G.). Gidrometeoizdat, Moscow (in Russian).

Brukhan, F.F. 1984. Aeroclimatic Characteristics of the Mean Winds over USSR (ed. Ignatjushina E.N.). Gidrometeoizdat, Moscow (in Russian).

Crutcher, H.L. 1956. On the standard vector-deviation wind rose. J. of Meteor. 14: 28-33.

EANET. 2009. Second Report for Policy Makers – Clean Air for a Sustainable Future. Acid Deposition Monitoring Network in East Asia (EANET), Bangkok, Thailand.

Khodzher, T.V., Obolkin, V.A., Potemkin, V.L. 2011. National assessment of the state of acid deposition monitoring of Russia. Second Periodic Report on the State of Acid Deposition in East Asia. Part II-National Assessments. EANET, UNEP/RRC.AP, 205-239.

Khromov, S.P., Petrosyants, M.A. 2006. Meteorology and Climatology. "Nauka", Moscow.

Rovinsky, F.Y., Yegorov, V.I. 1986. Ozone, Nitrogen and Sulphur Oxides in the Lower Troposphere. Gidrometeoizdat, Leningrad (in Russian).

EANET Science Bulletin

Thailand

Network Center for EANET
Acid Deposition Monitoring Network in East Asia (EANET)
Asia Center for Air Pollution Research (ACAP)
1182 Sowa, Nishi-ku, Niigata-shi, 950-2144, Japan
Tel: (+81) 25-263-0550
Fax: (+81) 25-263-0566
EANET website: http://www.eanet.asia